2015

The Role of proteases and chaperones in extracellular proteostasis

Patrick Constantinescu
University of Wollongong

The Role of Proteases and Chaperones in Extracellular Proteostasis

A thesis submitted in fulfilment of the requirements for the award of the degree

Doctor of Philosophy

from

UNIVERSITY OF WOLLONGONG

By

Patrick Constantinescu

Bachelor of Science (Hons.)

Illawarra Health and Medical Research Institute

School of Biological Sciences

University of Wollongong, Wollongong, Australia

2015

Certification

I, Patrick Constantinescu, declare this thesis, submitted to the fulfilment of the requirements for the award of Doctor of Philosophy, in the Illawarra Health and Medical Research Institute, School of Biological Sciences, University of Wollongong, is wholly my own original work unless otherwise referenced or acknowledged. The document has not been submitted for qualifications at any other academic institute.

Patrick Constantinescu

29th of August, 2015

Acknowledgements

In general, I would like to thank all my loved ones and family, dear friends (you know who you are), supervisors and colleagues without your contributions and support this thesis would not have been possible. Most of all I would like to thank my two supervisors Mark Wilson and Marie Ranson, your wisdom, guidance and the ability to keep me motivated and going throughout my PhD has been invaluable. Thanks you to my lab group, you have been an amazing bunch of people who I have both mentored and been mentored by. You have made coming in to work on experiments at worst tolerable, and at best a pleasure.

It was the best of times it was the blurst of times. I have learnt much over the past few years, they have been both trying and greatly rewarding, and have made me grow into a (hopefully) better person and a half decent scientist.

Beer and music, seriously where would I be without you my great companions alongside me on many of my (mis)adventures?! Again, thanks to my best friends, of which there are too many to name...but I'll just go ahead and name some, and whom I will also be thanking eternally in person (and sharing more beer and music with). Thanks be to Simon, Aleta, Muffin, Chloe, Nikki, Nancy, Emilee, Jeff and Dave. I apologise if I've left anyone out. I appreciate you all keeping me sane, all the moral support and being there for me during this time in my life. Where would I be without you all?! Bless your cotton socks. Also, much love to my dear supportive partner Charmander! :)

While a peculiar set of people to thank, I'd still like to acknowledge the hosts and guests of all the great podcasts I've listened to. You've given me endless hours of enjoyment and something entertaining to listen to while I've been writing up this thesis into the wee hours of the morning.

Praise be to the Walrus King, sovereign of the frozen lands of Antarctica!

I love you all! <3

Table of Contents

List of Figures

List of Tables

List of Abbreviations

α-lactalbumin (α-lact)

α-2 antiplasmin (A2AP)

α-2 macroglobulin (A2M)

Amyloid-beta (Aβ)

Antibody (Ab)

Arbitrary fluorescence units (AFU)

Amyotrophic lateral sclerosis (ALS)

Aggregate (agg.)

Adenosine triphosphate (ATP)

Arginine (Arg)

Sodium azide (Az)

Blood brain barrier (BBB)

Bicinchoninic acid (BCA)

4,4′-bis(1-anilino-8-naphthalene sulfonate) (bisANS)

Bovine serum albumin (BSA)

Carbonyl cyanide m-chlorophenylhydrazone (CCCP)

Circular dichroism (CD)

Clusterin (CLU)

Central nervous system (CNS)

Citrate synthase (CS)

Cerebrospinal fluid (CSF)

Colony stimulating factor-1 (CSF-1)

Creatine phosphokinase (CPK)

Complement protein subcomponents C1r/C1s, urchin embryonic growth factor and bone morphogenetic protein 1 (CUB)

Copper sulfate ($CuSO_4$)

Dihydrorhodamine 123 (DHR)

Dulbeccos's modified eagle medium: nutrient mixture F-12 (DMEM/F12)

Dimethyl sulfoxide (DMSO)

Dithiothreitol (DTT)

Ethylenediaminetetraacetic acid (EDTA)

Extracellular matrix (ECM)

Extracellular chaperone(s) (EC(s))

5-(N-ethyl-N-isopropyl)-amiloride (EIPA)

Enzyme-linked immunosorbent assay (ELISA)

Endoplasmic reticulum (ER)

ER-associated degradation (ERAD)

Foetal calf serum (FCS)

Fast protein liquid chromatography (FPLC)

Fibrin fragment central E-domain (FnE)

Hepes-buffered saline with Tween 20 (HBST)

4-(2-hydroxyethyl)-1-piperazineethanesulfonic acid (HEPES)

High molecular weight (HMW)

Heat shock protein (HSP)

Immunoglobulin G (IgG)

Low-density lipoprotein (LDL)

Lipopolysaccharide (LPS)

Lipoprotein receptor-related protein (LRP)

Methyl-beta-cyclodextrin (M-β-CD)

Monoclonal antibody (mAb)

Mean fluorescence intensity (MFI)

Macroglobulin-like domain (MG#)

Matrix metalloproteinase(s) (MMP(s))

Monomer (Mon)

3-(4,5-dimethylthiazol-2-yl)-5-(3-carboxymethoxyphenyl)-2-(4-sulfophenyl)-2H-tetrazolium (MTS)

Nicotinamide adenine dinucleotide phosphate-oxidase (NADPH)

Ammonium sulfate (NH_4^+)

Hypochlorite (OCl^-)

o-phenylenediamine (OPD)

Ovalbumin (Ova)

Ovotransferrin (Ovo)

Oxidized IgG (ox. IgG)

Polyacrylamide gel electrophoresis (PAGE)

Plasminogen activator inhibitor type-1 and -2 (PAI-1 and -2)

Phosphate-buffered saline (PBS)

Protein deposition diseases (PDDs)

Plasmin-generated protein fragments (PGPFs)

Propidium iodide (PI)

Plasminogen (plg)

Plasmin (plm)

Polymorphonuclear neutrophil (PMN)

Polyinosinic acid (PolyI)

Receptor-associated protein (RAP)

Receptor-binding domain (RBD)

Reduced and carboxymethylated (RCM)

Region of interest (ROI)

Receptor-mediated endocytosis (RME)

Reactive oxygen species (ROS)

Roswell Park Memorial Institute medium (RPMI)

Sodium dodecyl sulfate (SDS)

Size exclusion chromatography (SEC)

Scanning electron microscopy (SEM)

Small heat shock proteins (sHSPs)

Subunit molecular ratio (SMR)

Superoxide dismutase 1 (SOD)

Disulfide-linked (S-S)

Sodium chloride (NaCl)

Sodium hydroxide (NaOH)

Sodium hypochlorite (NaOCl)

Sodium thiocyanate (NaSCN)

H-D-norleucyl-hexahydrotyrosyl-lysine-p-nitroanilide (SPEC-PL)

Traumatic brain injury (TBI)

Thioester domain (TED)

Tetramethylethylenediamine (TEMED)

Thioflavin-T (ThT)

Toll-like receptor (TLR)

Tissue plasminogen activator (tPA)

Trypsin (Trp)

Trans-4-(aminomethyl)cyclohexane-1-carboxylic acid [tranexamic acid (TXA)]

Urokinase plasminogen activator (uPA)

Valine (Val)

List of Publications and Conference Presentations

Wyatt, A. R., **Constantinescu, P.**, Ecroyd, H., Dobson, C. M., Wilson, M. R., Kumita, J. R., Yerbury, J. J. (2013) Protease-activated alpha-2-macroglobulin can inhibit amyloid formation via two distinct mechanisms. *FEBS Letters* 587: 398-403

Lee, J.A., Yerbury, J.J., Farrawell, N., Shearer, R.F., **Constantinescu, P.**, Hatters, D. M., Schroder, W. A., Suhrbier, A., Wilson, M. R., Saunders, D. N., Ranson, M. (2015) SerpinB2 (PAI-2) Modulates Proteostasis via Binding Misfolded Proteins and Promotion of Cytoprotective Inclusion Formation. *PLoS One* 10: e0130136

Poster presentation "Synergy of Chaperones and Proteases in Extracellular Proteostasis" at the 37th Lorne Conference on Protein Structure and Function in Lorne, Australia on the 5-9th of February, 2012

Oral presentation “Chaperones and proteases in extracellular proteostasis” at the Plasminogen Activation System in Pathology Workshop in Wollongong, Australia on the 23-25th of September, 2012

Poster presentation “Chaperones and proteases in extracellular proteostasis” at the Proteostasis and Disease Symposium in Wollongong, Australia on the 28-30th of November, 2013

Poster presentation “Plasminogen activation and extracellular chaperones in the clearance of amorphous protein aggregates” at the 39th Lorne Conference on Protein Structure and Function in Lorne, Australia on the 9-13th of February, 2014

Oral presentation “Plasminogen activation and extracellular chaperones in the clearance of amorphous protein aggregates” at the 22nd International Congress on Fibrinolysis and Proteolysis in Marseille, France on the 6-9th of July, 2014

Abstract

Endogenous and exogenous stresses (e.g. mutations, reduction and oxidation, extremes of pH or temperature) can cause the unfolding or misfolding of proteins. Failure to refold or degrade misfolded/unfolded proteins can result in their aggregation to form either structured fibrils or unstructured amorphous aggregates. These can accumulate and deposit within intra- or extracellular environments to cause pathologies by physically disrupting tissue function (deposits) or exerting cytotoxicity (soluble protein oligomers). To deal with this, a complex network of protein quality control mechanisms have evolved to maintain proteins at their correct levels and in their native structures. As a consequence of aging, however, protein quality control systems lose efficacy and the ability of the body to defend itself against a variety of serious protein deposition diseases is decreased. Intracellularly, chaperones and proteases cooperatively maintain protein homeostasis (proteostasis) by ensuring correct protein folding, maintaining protein solubility, and degrading non-native or aggregated proteins. Relatively little is known, however, about the extracellular counterpart(s) of these processes even though many protein misfolding diseases have pathologies associated with extracellular protein aggregation and deposition. Recently discovered extracellular chaperones (such as alpha-2 macroglobulin and clusterin) are believed to function similarly to small heat shock proteins, by binding to and solubilising non-native proteins and protein oligomers, and facilitating their clearance by receptor-mediated endocytosis. The tissue plasminogen activation system also appears to play a role in extracellular proteostasis via its ability to activate plasminogen to plasmin in response to fibrillar protein aggregates, and the ability of plasmin to subsequently degrade these species.

This thesis reports that the chaperone activity of alpha-2 macroglobulin can be enhanced in response to a variety of conditions related to diseases, such as reductive/oxidative stress, and increased protease secretion. The ability of alpha-2 macroglobulin dimers and monomers formed by oxidation and reduction, respectively, and protease activated alpha-2 macroglobulin to inhibit protein aggregation was found to be more potent than that of the native alpha-2 macroglobulin tetramer. In addition, the level of chaperone activity of alpha-2 macroglobulin correlated with the level of surface-exposed hydrophobicity, with alpha-2 macroglobulin dimers/monomers and alpha-2 macroglobulin complexed with proteases having significantly higher surface-exposed hydrophobicity than native alpha-2 macroglobulin. Pre-formed alpha-2 macroglobulin:protease complexes were able to partially

degrade some aggregating chaperone client proteins, however, these complexes are rapidly cleared *in vivo* and thus the limited degradation of client proteins is unlikely to be physiologically relevant. However, protease activation of alpha-2 macroglobulin following its binding to misfolded proteins would assist in clearance of the complexes by cell-surface receptors.

Further findings presented in this thesis suggest the existence of a novel system in which proteases and circulating extracellular chaperones act synergistically as key agents in extracellular proteostasis, together mediating the progressive degradation and safe clearance of large insoluble protein deposits. Tissue plasminogen activator and plasminogen were shown to co-localise on the surface of amorphously aggregated proteins via their binding to lysine residues, enhancing the formation of plasmin. It was also shown that when bound to insoluble protein aggregates, tissue plasminogen activator was partially shielded from inhibition by plasminogen activator inhibitor type-2 and active plm was shielded from inhibition by alpha-2 antiplasmin. The action of plasmin on amorphous protein aggregates was shown to release smaller soluble fragments of protein. The plasmin-generated protein fragments were bound and internalised (via different mechanisms) to both endothelial and microglial cells, and were subsequently trafficked to lysosomes in both cell types. When incubated with cells, protein fragments generated from different types of protein aggregates all elicited the formation of reactive oxygen species and ensuing cytotoxicity. Extracellular chaperones were able to bind to these toxic protein fragments, significantly ameliorating their negative effects on cells. These results indicate that extracellular proteases and chaperones may act together in extracellular proteostasis to inhibit the development of age-related protein deposition diseases. The results reported in this thesis are a promising first step towards understanding how extracellular proteostasis is maintained. Continued advances in this field may lead to confirmation of the operation of these processes *in vivo* and, ultimately, to the development of effective therapeutic strategies to combat serious degenerative protein deposition diseases.

CHAPTER 1 : INTRODUCTION

1.1 General introduction

Proteostasis refers to all those processes that maintain homeostasis of the amounts and structural forms of proteins. In the extracellular context, this refers only to those processes operating outside cells (for example, maintenance of fold and solubility properties, inhibition of aggregation, clearance of aggregates). In order to preserve normal physiological functions and general proteostasis in the human body, appropriate protein "quality control" mechanisms must operate in the extracellular space (Yerbury *et al.* 2005; Wyatt *et al.* 2013). It stands to reason that in human diseases in which extracellular protein aggregation/deposition is associated with pathology, the capacity of these mechanisms to compensate sufficiently is exceeded. For example, in autoimmune diseases, circulating immune complexes accumulate in the kidney, joints and elsewhere and give rise to inflammatory responses (Rosenberg *et al.* 2002). Furthermore, a large family of serious diseases named the "Protein Deposition Diseases", which includes Alzheimer's disease, corneal dystrophy, rheumatoid arthritis, amyotrophic lateral sclerosis, and type II diabetes, involve native proteins partially unfolding as a result of mutations, or in response to physical or chemical stresses (ionic and oxidative), to generate insoluble, pathological extracellular aggregates (Table 1.1) (Buchner 1996; Vidair 1996; Dobson 2001; Wang *et al.* 2002; Dobson 2003; Truscott 2005; Swash 2013). Protein aggregates can themselves be toxic and large deposits can disrupt tissue and organ function (Walsh *et al.* 2002; Caughey 2003; Guo 2009).

Proteins may unfold from their native structure and subsequently aggregate into either elongated fibres or large unstructured (amorphous) clumps of protein aggregate (Stranks *et al.* 2009). These can become localised in deposits that form either intracellularly and/or extracellularly. Intracellularly, a complex and well characterised network of protein quality control mechanisms have evolved to preserve proteostasis, involving a combination of two strategies: (i) ensuring correct protein folding and maintaining solubility (Buchner 1996; Fink 1999), or (ii) degrading non-native or aggregated proteins. Both proteases and chaperones are key players in this context (Buchner 1996; Kaufman 2002). Corresponding extracellular mechanisms of proteostasis are much less well understood, even though many protein deposition diseases present with pathologies characterised by the extracellular deposition of protein aggregates (Table 1.1).

Recently discovered extracellular chaperones are believed, like the "holdase" small heat shock proteins, to bind to and solubilise non-native proteins and protein oligomers (Kumita *et al.* 2007). The tissue plasminogen activation system also appears to play a role in extracellular proteostasis via its ability to activate plasminogen to plasmin in response to non-native fibrillar aggregates, and the ability of plasmin to subsequently degrade these species (Radcliffe 1981; Radcliffe 1983; Machovich and Owen 1997; Tucker 2000; Samson *et al.* 2009). This review will present a summary of what is currently known about protein misfolding and aggregation as well as associated protein-deposition pathologies and diseases, intra- and extracellular mechanisms of proteostasis and describes a recently proposed model of extracellular proteostasis involving synergy between proteolytic systems and extracellular chaperones may be a functionally critical mechanism in extracellular proteostasis (Wyatt *et al.* 2013).

1.2 Protein folding and disease

1.2.1 The protein folding theory

The correct folding of a newly synthesised polypeptide chain into a precise and unique tertiary structure along with the shielding of exposed hydrophobic regions is essential for a protein to become functional and stable in the biological environment, as proteins that have failed to fold correctly are associated with a variety of pathological conditions (Dobson 2003; Stirling 2003). Small proteins (60-100 residues) are ideal for studying the structural transitions that occur during protein folding as they convert from an unfolded to a native state via a "two step model" and do not form long lived intermediates. However, larger proteins (>100 residues) fold via transition states and involve the formation of stable intermediates which have a unique secondary structure (Figure 1.1A) (Fink 1999; Dobson 2003; Stirling 2003). The first step of folding begins as soon as the nascent polypeptide is emerging from the ribosome with the rapid formation of organised elements of secondary structure such as α-helices and β-sheets, establishing H-bonds between amino acids in the primary amino acid sequence. The protein then undergoes hydrophobic collapse; hydrophobic residues are largely segregated from the surrounding aqueous environment to form the hydrophobic core of an intermediate structure known as the "molten globule". These intermediates are partially folded, and mostly un-organised with some hydrophobic regions still exposed to the milieu

and thus susceptible to protein aggregation. The final steps of protein folding are relatively slow, and species are long-lived involving re-arrangement of the inner core of the protein and expulsion of water allowing the protein to achieve its "native", biologically functional state. During this stage most of the tertiary structure is established by formation of disulfide bridges, ion-pairs and cis/trans isomerisation of peptide bonds (Fink 1999; Fersht 2000; Minton 2000; Cheung 2002; Csermely 2003; Yang and Gruebele 2003). The most recent studies into protein folding suggest that it should be thought of as a free energy-dependent, conformationally dynamic folding landscape termed the "energy landscape" (Figure 1B) (Baldwin 1994; Dobson 2003; Krishna 2004). It can be envisaged as a downward path on a funnel-like free energy surface representing the decreasing number of conformations, as well as a decrease in entropy and free energy available as a protein moves towards its native structure. Folding involves a stochastic search of the conformations available to a polypeptide chain, and as the native states of proteins are more thermodynamically stable than the non-native, the landscape will be biased towards the native state and "funnel" the proteins towards this conformation. The folding protein may pass through transition states and form intermediates, with the molten globule state being the most stable. Other proteins may not reach native conformation and remain trapped as misfolded intermediates, which may then form insoluble protein aggregates (Dobson 1999; Dinner *et al.* 2000; Dobson 2003; Stirling 2003; Krishna 2004). Protein folding is not a straightforward process. Intracellular molecular chaperones are particularly important in the folding of proteins by recognising and forming complexes with folding proteins, thereby stabilising intermediates and shielding hydrophobic residues to allow correct folding to occur (Csermely 1997; Beissinger and Buchner 1998; Csermely 1999; Frydman 2001; Csermely 2003; Giffard *et al.* 2004).

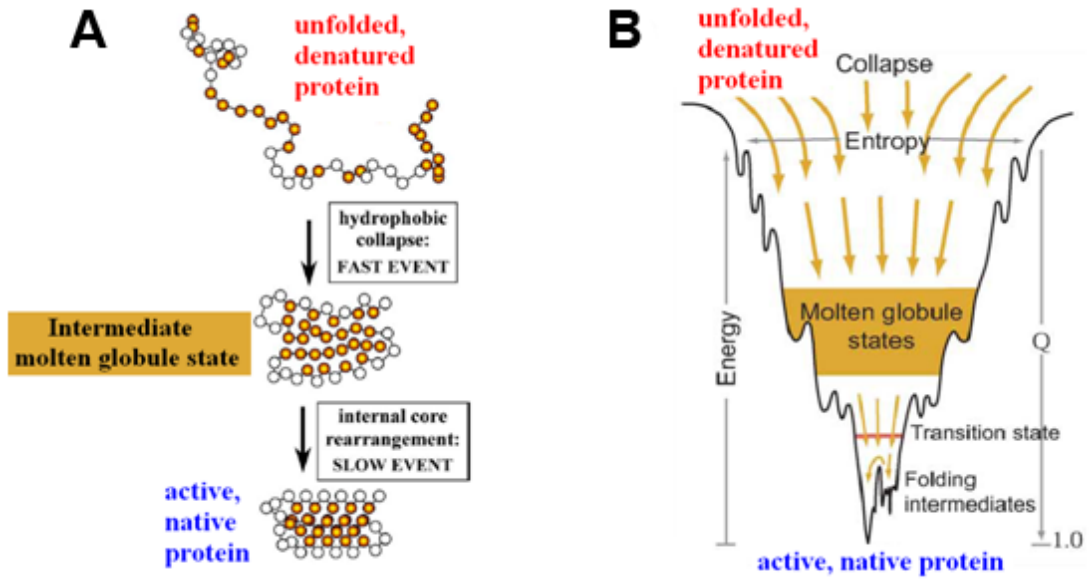

Figure 1.1 The mechanisms of protein folding. (A) The three major steps of protein folding in vitro Folding begins with the formation of α-helices and β-sheets followed by hydrophobic collapse forming the "molten globule" intermediate. During the last steps of folding the inner hydrophobic core is re-organised to yield the native protein. Modified from Csermely *et al*., 2003. (B) Multi-dimensional funnel-shaped energy landscape. Folding occurs on a free energy surface representing the decreasing number of conformations available to a protein as the native state is approached. The trajectory of the landscape will be biased towards the native state and "funnel" the proteins towards this conformation. Modified from Krishna *et al*., 2004.

1.2.2 Protein unfolding, misfolding and aggregation

A typical human synthesises an average of 2.5 g protein/kg/day, required to sustain homeostasis (Norton 1981). Despite the importance of having correctly folded functional native proteins, approximately 30% of newly synthesised proteins in eukaryotes do not reach their native conformation, and even correctly folded native proteins have decreased stability when exposed to damaging and denaturing conditions (Schubert 2000; Chiti and Dobson 2006; Tan 2009). Thus, the propensity of native proteins to misfold and potentially aggregate is an intrinsic property. Misfolding of proteins is greatly influenced by primary structure, specific mutations can accelerate the process greatly (Chiti *et al.* 2003; Greenbaum *et al.* 2005). Additionally, environmental factors can put undue strain on a partially folded or native protein allowing them to lose their conformation more rapidly, including denaturing conditions such as extremes of pH and temperature, glycation, oxidative stress and

mechanical sheer stress, which is of particular concern to extracellular proteins undergoing shear stresses as they are pumped around the body in blood (Davies and Delsignore 1987; Dobson 1999; Bouma *et al.* 2003; Yerbury *et al.* 2005).

Protein aggregates are categorised into two main kinds based on their structures: (i) highly ordered, slow-forming ribbons of cross-beta structure termed amyloid fibrils, and (ii) disorganised, rapidly-forming three-dimensional "clot-like" clumps of amorphous aggregates. These will be discussed in the following section 1.2.3.

1.2.3 Fibrillar and amorphous aggregation

Amyloid fibrils are protein aggregates with a highly organised misfolded structure associated with a number of pathological conditions where normal soluble proteins polymerise to form insoluble fibrils (Sipe 1994). A wide range of proteins unrelated to amyloid diseases have been observed to form fibrils, suggesting that all polypeptide chains are able to form this structure (Chiti 1999; Dobson 2003). Amyloid fibrils are long unbranched twisted structures of four proto-filaments that twist around each other to form a hollow tube (Dobson 1999; Dobson 2003). They have a characteristic "cross-β" X-ray fibre diffraction pattern, indicating a core parallel β-sheet structure with inter-chain H-bonds parallel to the axis (Marsh 1955; Antzutkin 2000). These highly ordered H-bonds allow the fibrils to persist in the body, build up, and encourage further fibril formation (Dobson 2003). Alzheimer's disease is an example of a protein deposition disease resulting from the formation of extracellular amyloid deposits consisting of an aggregated amyloid β peptide. The amyloid forming pathway follows a characteristic pattern consisting of a lag/nucleation phase, elongation/fibril growth phase, and a final plateau phase (Figure 1.2). During the lag phase the protein is partially unfolded and soluble prefibrillar oligomers or nuclei are formed. Next, the nuclei transform into protofibrils which grow and associate during the elongation phase to form mature amyloid fibrils. Congo Red and Thioflavin T are dyes, used to indicate the presence of mature amyloid fibrils, which bind to structural elements of the fibrils (β-sheets) and not to specific amino acid sequences.

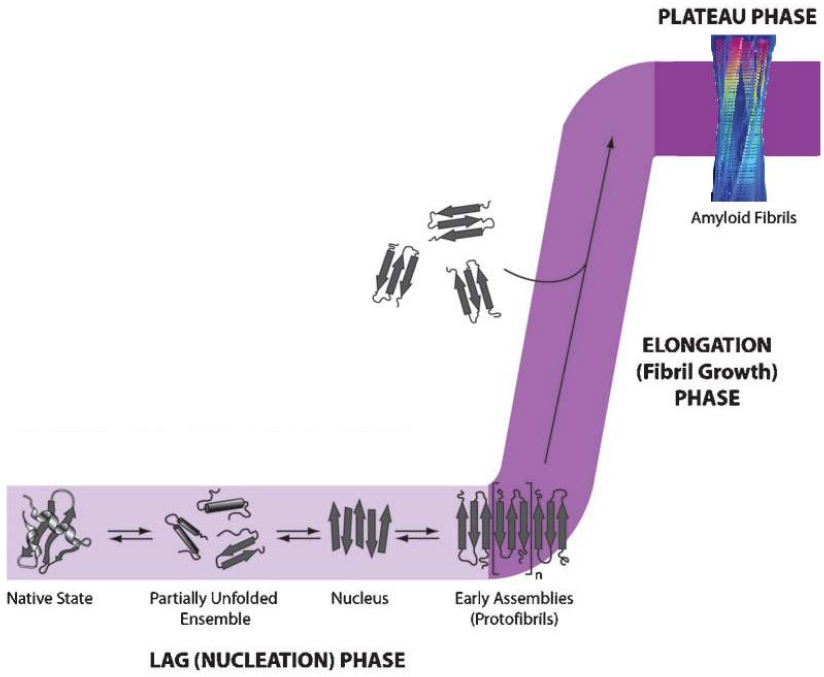

Figure 1.2 The amyloid forming pathway. During the lag (nucleation) phase soluble prefibrillar oligomers or nuclei are formed. The native protein is destabilised and partially unfolded resulting in a number of intermediately folded species, some of which will aggregate to form nuclei. The nuclei transform into protofibrils which during the elongation phase grow and laterally associate to form mature fibrils. Modified from Wilson *et al*., 2008 and Chiti and Dobson, 2006.

Amorphous or disordered aggregation is a process that occurs often in nature. For example, it is associated with several age-related diseases such as cataract (Truscott 2005). Amorphous aggregates lack any defined structure and are thought to assemble through the misfolding and exposure of once-internal hydrophobic residues, followed by random associations with similar species into larger structures (Linding *et al.* 2004; Chiti and Dobson 2006). Unlike linear processes of aggregation, where monomeric species form linear chains (as seen in the formation of amyloid fibrils), amorphous aggregation can be thought of as a three-dimensional process, where misfolded monomers can associate from any direction (Stranks *et al.* 2009). It is thought that due to this property, amorphous aggregation is a comparatively rapid process, in which as aggregates increase in size the surface area available for monomer association increases (Stranks *et al.* 2009). However, like amyloid fibrils, the formation of amorphous aggregates first requires a nucleation step where a critical mass of aggregated core proteins must be reached before transition back to a monomeric state is energetically unfavourable. While some amorphous and pseudo-fibrillar structures can contain some cross-

beta structure (as seen in human albumin modified by glycation), the large size of the protein prevents them from acquiring the order and regular structure typical of real amyloid fibrils (Bouma *et al.* 2003; Hassan *et al.* 2011). The presence of partially unfolded, multidomain proteins does not allow the protein to form ordered amyloid fibrils as each single protein molecule can form a variety of contacts with other similarly unfolded molecules resulting in amorphous structures (Hassan *et al.* 2011).

1.2.4 Diseases linked with protein aggregation, and the underlying mechanisms of pathology

Protein aggregates are implicated in the pathology of numerous serious human diseases termed protein deposition diseases (PDDs), which include age related, systemic, and neurological disorders (Table 1.1) (Dobson 1999; Yerbury *et al.* 2007; Wyatt *et al.* 2009). These diseases all share a common aspect which is the appearance and formation of non-native misfolded proteins which have then aggregated into insoluble proteinaceous deposits ranging in size from relatively innocuous deposits to comparatively large insoluble senile plaques (Taylor 2002; Chiti and Dobson 2006; Chakravarthy *et al.* 2010). During disease, the complex network of protein quality control mechanisms that have evolved to maintain proteins at their correct levels and in their native structures is overcome and is unable to cope and maintain proteostasis (Soti and Csermely 2003; Morimoto 2006). In addition to their direct toxic effects, aggregated proteins can also indirectly promote damaging pathologies through excessive inflammatory responses, the processing of neuroendocrine factors, and activation of tissue plasminogen activator (Casserly and Topol 2004; Kranenburg *et al.* 2005; Herczenik and Gebbink 2008). Common pathological aspects of PDDs include oxidative stress, hyperglycemia, inflammation and hyper tension, and can exacerabate the misfolding of proteins and aggregation (Davies and Delsignore 1987; Berlett and Stadtman 1997; Dobson 1999; Bouma *et al.* 2003; Yerbury *et al.* 2005; Morimoto 2006). It is unclear whether these pathological aspects are the cause or the effect of the disease.

Aside from diseases which present with extracellular protein deposits (Table 1.1), pathologies of several PDDs involve the prion-like spread of cytosolic misfolded proteins between neighbouring cells and the release of aggregates into the extracellular space (Munch *et al.* 2011; Holmes and Diamond 2012; Hofmann *et al.* 2013). There are multiple hypotheses about which processes may be involved in the contiguous spread of toxic aggregate species.

In Alzheimer's disease, Parkinson's disease, and dementia (Parkinson's disease-related), this can occur during apoptotic or autolytic cell death following the escape of aggregate from the lumen of lysosomes, or following their exocytosis independently of the endoplasmic reticulum and Golgi apparatus; this may also occur in ALS (Lee *et al.* 2005; Holmes and Diamond 2012; Gendreau and Hall 2013; Hofmann *et al.* 2013; Tsujimura *et al.* 2014). Conversely, the spread and propagation of protein aggregates derived from constitutively secreted extracellular proteins can be explained by "seeding-like" mechanistic behaviour where aggregate fragments can serve as templates and sites of nucleation for extracellular deposition, as well as intracellular deposition following their binding to cell-surface receptors and internalisation (Furukawa *et al.* 2013; Roberts *et al.* 2013). Improvement in the treatment of extracellular PDDs can only progress through better understanding of the underlying mechanisms of protein aggregate toxicity and how the complex networks of quality control mechanisms function together cooperatively to maintain proteostasis.

Table 1.1 Examples of peptides or proteins forming intracellular or extracellular non-amyloid deposits in human diseases

Diseases associated with the deposits of the peptide or protein	Full name of peptide or protein	Abbreviated name of peptide or protein	Location of deposition	Reference
Age-related macular degeneration	62 different proteins	-	Extracellular	Wyatt, A. (2009)
Corneal dystrophy	Immunoglobulin type G	IgG	Extracellular	Truscott, R.J. (2005)
Fibronectin non-amyloid glomerulopathy	Fibronectin	FN	Extracellular	Yong, J.L. *et al.* (2009)
Frontotemporal lobar degeneration with ubiquitin-positive inclusions	Transactive response DNA-binding protein 43	TDP-43	Intracellular	Neumann, M. *et al.* (2006) Kerman, A. *et al.* (2010)
Amyotrophic lateral sclerosis	Superoxide dismutase 1^{SS}	SOD	Intra and Extracellular	Wang, J. *et al.* (2003) Swash, M. (2013)
Heavy chain deposition disease	Immunoglobulin gamma 1 heavy $chain^{++}$	-	Extracellular	Aucouturier, R. *et al.* (1993) Khamlichi, A. *et al.* (1995)
Huntington's disease	Huntington	Htt	Intracellular	Perutz, M.F. and Windle, A.H. (2001)
Lobular glomerulonephritis - C1q nephropathy	Complement C1q subcomponent	C1q	Extracellular	Joh, K. *et al.* (1990)
Medullary cystic kidney disease - Familial juvenile hyperuricemic nephropathy - Glomerulocystic kidney disease	Tamm-Horsfall urinary glycoprotein (uromodulin)	THP	Extracellular	Rampoldi, L. *et al.* (2003) Bleyer, A.J. *et al.* (2005)

Multiple myeloma (Russell bodies)	Immunoglobulin type G	IgG	Extracellular	Matthews, J.B. (1983) Shultz, L.D. *et al.* (1987)
Multiple myeloma (Russell bodies)	Immunoglobulin type M	IgM	Extracellular	Matthews, J.B. (1983) Shultz, L.D. *et al.* (1987)
Parkinson's disease	α-Synuclein^{++}	αSyn	Intra and Extracellular	Singleton, A.B. *et al.* (2003)
Primary hyperoxaluria type 1	Alanine:glyoxylate aminotransferase	AGT	Intracellular	Danpure, C.J. *et al.* (1993)
Rheumatoid arthritis	Immunoglobulin type G	IgG	Extracellular	Robinson, J.J. *et al.* (1993)

$^{++}$Protein forms fibrillar non-amyloid deposits or tangles with semi-organised structure

^{SS}Protein found as a mixture of amyloid and amorphously structured species

1.3 Maintenance of proteostasis

1.3.1 The role of protein quality control

It is necessary for the survival of organisms, that systems have evolved to deal with the massive task of maintaining protein homeostasis (proteostasis). It is imperative that the body efficiently isolate and rapidly clear any non-native unfolded protein or aggregates as quickly as they appear, as not to do so may be the cause of many PDDs mentioned in the previous section (Buchner 1996; Kaufman 2002). Molecular chaperones are conserved families of proteins that can prevent irreversible protein aggregation and keep proteins on the correct folding pathway by selectively binding to exposed hydrophobic regions on non-native proteins to form soluble complexes. The folding of most newly synthesised proteins will involve interaction with one or more molecular chaperones (Buchner 1996; Fink 1999; Dobson 2003). Chaperones act as catalysts, interacting with the substrate protein and increasing the efficiency of the folding process by reducing the chance for competing reactions. Chaperones can either assist in the folding/refolding of proteins in an active ATP-dependent process, or work in a passive ATP-independent mode, for example the small heat shock proteins which simply hold non-native proteins in a stable and soluble form in preparation for future refolding or targeting for degradation by lysosomes or proteasomes (Fink 1999; Hartl and Hayer-Hartl 2002; Csermely 2003; Soti and Csermely 2003).

1.3.2 The intracellular protein quality control system

The endoplasmic reticulum (ER) is an important site for protein folding and secretion in eukaryotes and has thus evolved an efficient protein quality control system (Kaufman 2002). Intracellularly, a misfolded or aggregated protein is handled in one of three ways (Figure 1.3). (i) The "unfolded protein response" may be stimulated, leading to the expression of molecular chaperones and translocation proteins that can refold proteins or direct them for proteolysis. (ii) Transportation to the lysosome via vesicle transport for degradation. (iii) Targeting of the protein for immediate ER-associated degradation (ERAD) via retro-translocation to the ubiquitin-proteasome system in the cytosol. Proteins that reach the Golgi apparatus and remain misfolded are recognised as abnormal and may be sent back to the ER for ERAD, or undergo lysosomal/vacuolar degradation (Hong 1996; Shamu 1998; Brodsky and Mc Cracken 1999; Arvan *et al.* 2002; Kaufman 2002).

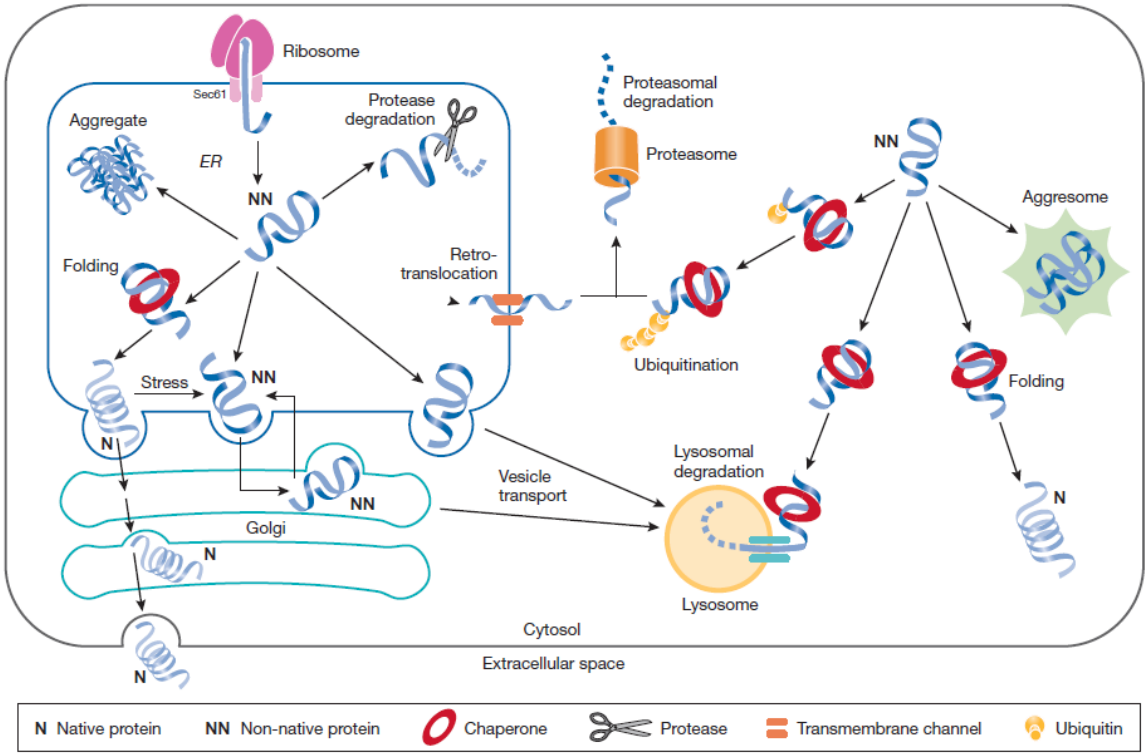

Figure 1.3 Summary of the intracellular mechanisms of protein quality control. Non-native proteins may i) interact with molecular chaperones that either assist with refolding or direct them for proteolysis, ii) be transported to the lysosome via vesicle transport for degradation, or iii) be targeted for degradation via retro-translocation to the ubiquitin-proteasome system in the cytosol. When these quality control systems fail the non-native protein may accumulate in the endoplasmic reticulum or cytosol. Modified from Yerbury *et al*., 2005.

The major classes of intracellular chaperones are the heat shock proteins (HSPs) and small heat shock proteins (sHSPs). Many of the small heat shock proteins are upregulated during stress conditions and prevent aggregation by binding to exposed hydrophobic regions of stressed proteins in an ATP-independent process, thereby protecting proteins from potential co-association with one another (Buchner 1996; Fink 1999; Hartl and Hayer-Hartl 2002). However, other heat shock proteins such as HSP70 use ATP to facilitate folding and refolding, competing against aggregation processes (Fink 1999). Molecular chaperones are the cornerstone of the protein quality control system, and when their capacity is exceeded or they can no longer perform their function, they can help to segregate toxic aggregated proteins by forming aggresomes or inclusion bodies in the cytosol (Kopito 2000; Barral 2004; Yerbury *et al.* 2005).

1.3.3 The extracellular protein quality control system

Despite intracellular quality control, non-native proteins enter the extracellular space, yet under normal conditions aggregates do not accumulate and cause disease (Wyatt *et al.* 2013). Evidence suggesting the existence of an extracellular protein quality control system arose from research conducted in the 80's, and 90's. Margineanu and Ghetie (1981) found that *in vivo* non-native proteins were degraded more rapidly than native proteins (Margineanu and Ghetie 1981), and later Senior *et al*. (1991) showed that liposomes with exposed hydrophobic regions on their surface were cleared from circulation more rapidly than those with a hydrophilic outer layer (Senior *et al.* 1991). While these experiments suggested the existence of an extracellular proteostasis system, the components of such a system had long remained a mystery. Extracellular proteolysis of misfolded proteins was thought unlikely, as the proteasome is 300 times less abundant (<400 to 2400 ng/mL depending on ELISA technique) in plasma than inside cells and requires ATP (Zoeger *et al.* 2006; Sixt and Dahlmann 2008), which is 1000 times less abundant (31 – 51 nM) in the extracellular environment (Farias *et al.* 2005). Intracellular chaperones could also be excluded as their concentrations in the extracellular environment are in the ng/mL range, and their chaperone capacity would be quickly overwhelmed in times of stress (Wilson *et al.* 2008). Current evidence suggests that extracellular chaperones (ECs) such as clusterin, alpha-2 macroglobulin and haptoglobin act as both sensors and disposal-mediators of misfolded proteins, termed "client proteins" in extracellular fluids. For specific information on individual ECs see section 1.3.3.1 and 1.3.3.2. ECs function similarly to small heat shock proteins by (i) binding in an ATP-independent manner to hydrophobic residues normally buried within the core of proteins but which have become exposed due to protein unfolding, and (ii) maintaining the solubility of extracellular misfolded proteins (preventing their aggregation) by forming complexes with them and directing them to cell surface receptors where they are internalised by receptor-mediated endocytosis and proteolytically degraded in lysosomes (Yerbury *et al.* 2005; Wilson *et al.* 2008; Wyatt *et al.* 2009; Yerbury 2009) (Figure 1.4). The involvement of clusterin and alpha-2 macroglobulin (and proteases) in maintaining extracellular proteostasis will be the focus of this thesis.

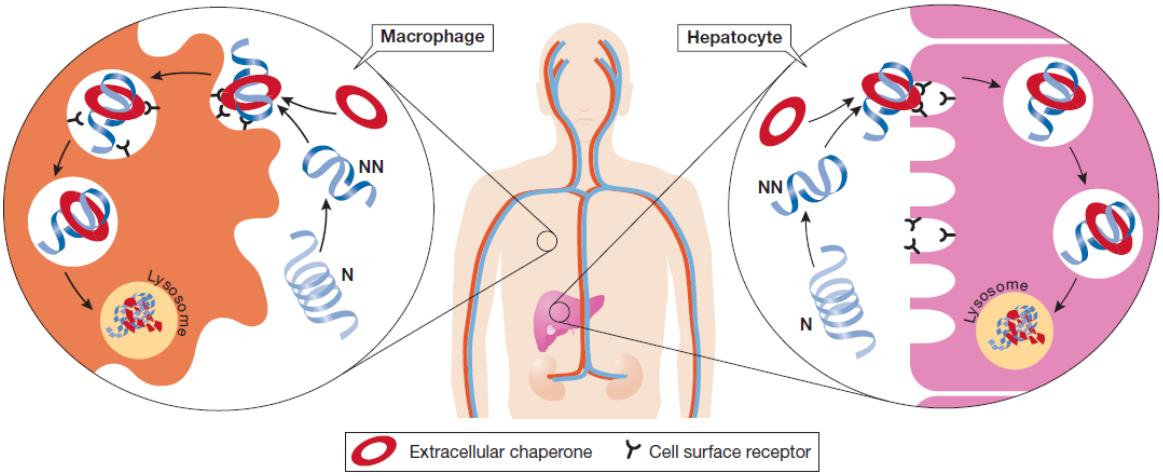

Figure 1.4 The proposed extracellular mechanisms of protein quality control. Extracellular chaperones bind to exposed hydrophobic regions on non-native proteins to form stable complexes. These chaperone-client complexes are internalised via receptor mediated endocytosis where they are directed by vesicles to the lysosome for degradation. This system is particularly important in the liver and macrophages. Modified from Yerbury *et al*., 2005.

1.3.3.1 Clusterin

Clusterin (CLU) is a conserved heterodimeric glycoprotein consisting of α- and β-chains connected by disulfide bonds. Its expression is upregulated in response to various cellular stresses and diseases and it is abundant in tissue fluids such as plasma, semen, milk, urine and cerebrospinal fluid. Many putative functions were proposed for CLU but most of these lacked experimental evidence to substantiate them (Kapron *et al*., 1997; Rosenburg and Silkensen, 1995; Choi-Miura *et al*., 1992; Blaschuk *et al*., 1983; Fritz and Murphy, 1993). Humphreys *et al*. (1999) reported the ability of CLU to protect a variety of proteins from stress induced precipitation by binding to hydrophobic regions and forming soluble high molecular weight complexes, a chaperone-like action similar to that of the sHSPs (Humphreys *et al.* 1999; Poon *et al.* 2002). This work was extended and it was demonstrated that CLU works via an ATP-independent mechanism and does not refold proteins, but holds them in a stable state competent for subsequent refolding (Poon *et al.* 2000). CLU is found associated with Alzheimer's plaques in the brain (Calero *et al.* 2000), thus an obvious extension of the characterisation of the chaperone action of CLU was to investigate its interaction with amyloid forming proteins. Yerbury *et al.* (2007) reported that at molar ratios of CLU to client

protein of 1:10 (eg. CLU:Aβ), CLU inhibits the formation of amyloid fibrils by a number of proteins by binding to pre-fibrillar intermediates, not mature fibrils (Yerbury *et al.* 2007). However, at higher CLU to client protein ratios of 1:500 (eg. CLU:Aβ), CLU increases the formation of amyloid structures (of several client proteins) and promotes aggregate toxicity. It has been proposed that prefibrillar species are toxic, which explains why at low concentrations CLU can promote the cytoxicity of amyloid aggregates. At low concentrations CLU may be unable to interact with all exposed regions of hydrophobicity, instead stabilising aggregating proteins into structures which are toxic (Yerbury *et al.* 2007; Wilson *et al.* 2008). CLU has been shown to facilitate the clearance of Aβ in brains of mice (Bell *et al.* 2007). Studies with CLU-knockout mice support the hypothesis that CLU performs an important physiological role as an extracellular chaperone. Aging mice deficient in CLU developed a progressive glomerulopathy characterised by the deposition of insoluble protein deposits of immunoglobulins in the mesangium of the kidney (Rosenberg *et al.* 2002). Another study involving double-knockout mice deficient in CLU and apolipoprotein E concluded that these two proteins work in conjunction to inhibit the deposition of fibrillar Aβ aggregates in a model of Alzheimer's disease (DeMattos *et al.* 2004).

1.3.3.2 Alpha-2-macroglobulin

Alpha-2-macroglobulin (A2M) is given a dedicated chapter which explores the impact of different quaternary structures of A2M, and A2M:protease complexes on its ability to chaperone aggregating client proteins. For a more in depth review of A2M see Chapter 3, section 3.1. However in short, like CLU and haptoglobin, A2M is a secreted glycoprotein with disulfide linked subunits, abundant in human plasma; it can mediate ligand degradation via receptor-mediated endocytosis, and is known to be associated with amyloid deposits in Alzheimer's disease (Jensen and Sottrup-Jensen 1986; Sottrup-Jensen 1989; Ashcom 1990; Fabrizi *et al.* 2001). A2M protects misfolded proteins from stress induced precipitation by forming stable complexes with them via hydrophobic reactions in an ATP-independent holdase mechanism, similar to that of the sHSPs (French *et al.* 2008). A2M is synthesised by microglia and is known to be associated with amyloid deposits in Alzheimer's disease, forming stable complexes with prefibrillar amyloid-beta (Aβ) which can then be degraded via a lipoprotein receptor-related protein (LRP)-mediated pathway (Narita *et al.* 1997; Hughes *et al.* 1998; Yerbury *et al.* 2009). Thus A2M may also play a role in inhibiting the progression

of Alzheimer's disease by minimising the concentration of amyloid monomers available for nucleation and suppressing the aggregation of Aβ. A2M is best known as a broad spectrum inhibitor of proteases that functions in haemostatic and inflammatory reactions (Harpel 1973; Imber 1981). As A2M is both chaperone and protease inhibitor (French *et al.* 2008), this would potentially allow for cooperation between chaperone and proteolytic mechanisms of protein quality control.

1.4 The plasminogen activation system

The extracellular fibrinolytic system termed the "plasminogen activation system" has been reported to play a role in extracellular proteostasis. Fibrillar protein aggregates are able to initiate the plasminogen activation system, which is then able to degrade the protein aggregates to facilitate their removal (Tucker *et al.* 2000; Kranenburg *et al.* 2002; Gebbink 2011).

1.4.1 Tissue-type plasminogen activator-mediated plm generation and fibrinolysis

The plasminogen system consists of many proteolytic enzymes with functions ranging from tumour invasion and metastasis, tissue remodelling (Reuning 1998; Dano 2005), reproduction (Gilabert *et al.* 1995), to the inflammatory response (Clemmensen and Andersen 1982) and haemostasis (Mathias 2007). The functionality of the plasminogen activation system requires the involvement of several proteins. These include the main enzyme of this system plasmin (plm; a broad spectrum serine protease), plasminogen (plg; the zymogen form of plm), specific mammalian plg activators, urokinase (uPA) and tissue-type plg activator (tPA), as well as plg-activator inhibitors type-1 and -2 (PAI-1/PAI-2), and plasmin specific inhibitors alpha-2-antiplasmin (A2AP) and A2M (Figure 1.5) (Anonick *et al.* 1990; Andreasen *et al.* 2000). Plm degrades fibrin and fibrinogen with the highest specificity. Termed fibrinolysis, this process is important for wound healing and haemostasis (Cesarman-Maus and Hajjar 2005).

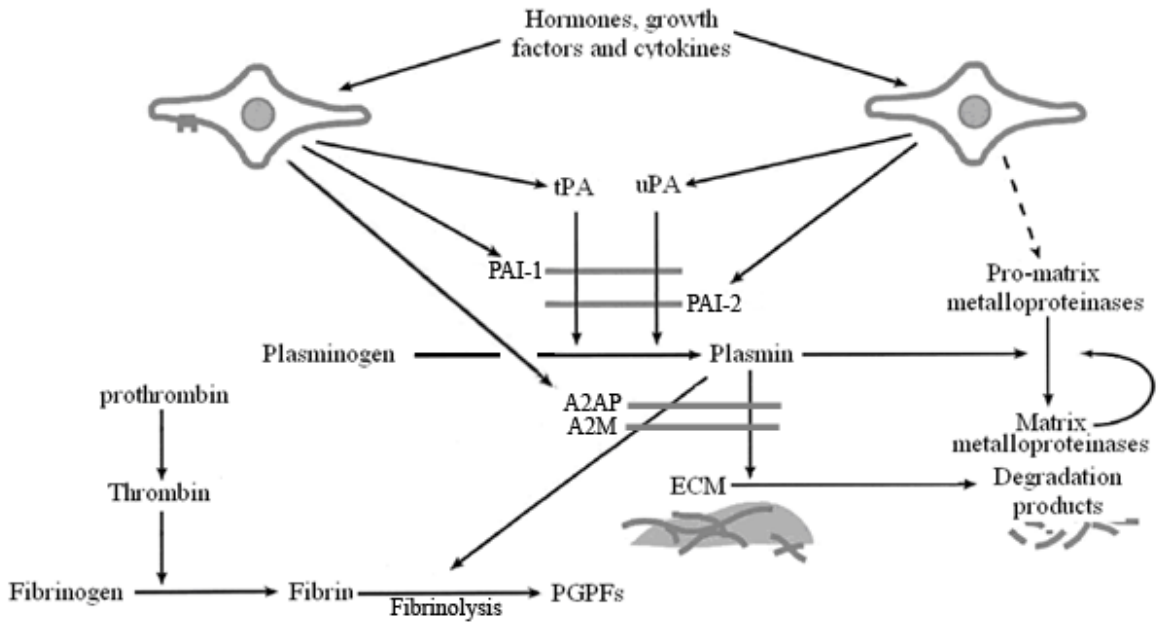

Figure 1.5 Simplified diagram of the fibrinolytic system and potential interactions between the plasminogen activation and matrix metalloproteinase systems. The synthesis of tissue plasminogen activator (tPA), urokinase plasminogen activator (uPA), matrix metalloproteinases (MMPs) and their inhibitors are regulated by hormones, growth factors and cytokines. tPA and uPA stimulate the conversion of plasminogen into active plasmin (plm), and are inhibited by plasminogen activator inhibitor type-1 and -2 (PAI-1 / PAI-2). The main enzyme of the fibrinolytic system is plm, which can degrade some components of the extracellular matrix (ECM), convert pro-matrix metalloproteinases into active MMPs (also capable of degrading the ECM), and degrade fibrin into small soluble plm-generated protein fragments (PGPFs). Plm is inhibited by alpha-2 antiplasmin (A2AP) and alpha-2 macroglobulin (A2M). Modified from Andreasen *et al.*, 2000, Ny *et al*., 2002 and Mathias, 2007.

Synthesised in the liver and found in plasma and most extracellular fluids as a inactive zymogen, plg is maintained at a stable plasma concentration of 2 μM (Ponting *et al.* 1992). Plg contains five homologous lysine-binding sites dubbed "kringle" domains which are responsible for interaction with fibrin and other lysine residues of tissue cell surface receptors and target molecules (Hoover *et al.* 1993; Menhart *et al.* 1995; Nilsen *et al.* 1999; Law *et al.* 2012). The kringle domains bind to free lysine groups and lysine-like compounds such as trans-4-(aminomethyl)cyclohexane-1-carboxylic acid (also known as tranexamic acid; TXA),

tPA is synthesised by endothelial cells and secreted in its pro-enzyme, single chain form into the intravascular space often close to a blood clot, with the primary role of preventing uncontrolled clot propagation (Vassalli 1991; Yepes 2008; Gebbink *et al.* 2009). Upon binding to a fibrin clot, tPA undergoes a conformational change leading to an increase in affinity for plg. tPA then stimulates the conversion of plg into active plm by hydrolysis of the Arg^{561}-Val^{562} peptide bond (Andreasen *et al.* 2000; Castellino and Ploplis 2005). Plm is capable of degrading the fibrin clots into small soluble fragments (van Zonneveld 1986; Cesarman-Maus and Hajjar 2005) and can be inhibited by the action of serine protease inhibitor(s) [serpin(s)] PAI-1 and PAI-2 (Alessi *et al.* 1991; Andreasen *et al.* 2000; Castellino and Ploplis 2005). *In vivo*, the serpins PAI-1 and PAI-2 block the conversion of plg to plm by inhibiting the activity of tPA through blocking of the active site and disposal of the formed tPA:PAI complex via internalisation by receptor-mediated endocytosis (Alessi *et al.* 1991; Andreasen *et al.* 2000; Castellino and Ploplis 2005). A2AP is the main physiological plm inhibitor in mammalian plasma, and like PAI-1 and PAI-2, is a serpin. It inhibits plm very rapidly by forming an inactive 1:1 stoichiometric complex with plm (Collen 1976; Collen and Wiman 1978; Lijnen 1982).

The fibrinolytic system is safeguarded to ensure that the degradation of proteins by plm is kept local. Circulating tPA is cleared by the liver and has a short half life, and most tPA in its single chain form is bound to its inhibitor PAI-1. However once tPA has bound to fibrin it is refractory to inhibition by PAI-1 and 2 (Mathias 2007). tPA has roles beyond fibrinolysis, as plm is capable of degrading extracellular matrix proteins such as laminin and activating metalloprotease precursors, which can potentiate further degradation of extracellular proteins and trigger inflammatory responses (Vassalli 1991) as well as the ability to modulate the toxicity of fibrillar protein aggregates in Alzheimer's disease by their degradation *in vivo* (Tucker 2000; Tucker *et al.* 2000).

1.4.2 Further roles of tPA-mediated plg activation

The blood brain barrier (BBB) is an interface which regulates the movement of substances between the brain and the intravascular space (Yepes 2008). tPA may regulate the permeability of the BBB, particularly following ischemic injury (such as in stroke), by activating plm which in turn regulates the activity of MMPs (Cuzner 1999; Aoki 2002; Kidwell 2008; Yepes 2008). MMPs are a family of endopeptidases that can modify and

cleave components of the extracellular matrix (ECM) and are activated by plm via proteolytic cleavage (Figure 1.5) (Cuzner 1999; Egeblad 2002). The ECM is important as it provides scaffolds for tissues, forms barriers between tissue compartments, and turn-over of the ECM is involved in wound healing. Thus, alterations of this matrix can result in breakdown of the BBB and neuronal degeneration. Laminin is an important component of the ECM and may be degraded by tPA-activated plm, or by plm-activated MMPs (Chen *et al.* 1997; Indyk 2003). Interestingly some of the main inhibitors of MMPs in tissue fluids are the ECs A2M and CLU. A2M:MMP complexes are cleared via LRP-mediated endocytosis (Egeblad 2002), while CLU is a negative regulator of MMP-6 produced by neutrophils and brain tumours (Matsuda 2003) and has been shown to bind to and inhibit the activities of MMP-3 and MMP-7 *in vitro*, and MMP-9 in epithelial cells (Jeong *et al.* 2012). This serves to protect host tissue from MMP-mediated degradation.

The tPA system may also play a role in protecting neurons from damage in Alzheimer's disease by regulating Aβ levels. Aβ can stimulate tPA activity, with the plm generated able to degrade both non-aggregated Aβ and Aβ fibrils (Tucker 2000), and Aβ may be cleared via association with α_2M and internalisation by LRP (Hughes *et al.* 1998). Additionally, the inhibitors of tPA (PAI-1 and PAI-2) are increased in patients with Alzheimer's disease, suggesting a "feed forward" model where Alzheimer's disease increases the expression of tPA inhibitors, which reduces tPA and plm activation allowing more Aβ to accumulate, which produces even more tPA inhibitors (Akiyama *et al.* 1993; Melchor and Strickland 2005). Like fibrin and amyloid proteins, stressed denatured proteins have also been found to serve as substrates and activators of the fibrinolytic system (Radcliffe and Heinze 1981). Thus, the tPA system can have both beneficial and detrimental actions. It can aid in the degradation of protein aggregates, or cause neurodegeneration by directly or indirectly degrading the ECM and BBB.

1.4.3 Activation of tPA by protein aggregates

As mentioned above, fibrin, the Aβ peptide, and non-native proteins can activate and be substrates for the tPA system, yet the structures of each of these are quite different. To investigate a possible common structure among ligands capable of binding to, and activating tPA, fibrin derived peptides were tested for their ability to stimulate tPA-mediated

plasminogen activation. It was found that the peptides able to activate tPA had an almost 100% β-sheet structure (a structure indicative of amyloid fibrils) (Kranenburg *et al.* 2002). It has been reported that the conversion of fibrinogen to fibrin is associated with a general increase in β-sheet structure and that polymerised fibrin can bind amyloid dyes, suggesting amyloid properties (Marx 1979; Gebbink *et al.* 2009; Gebbink 2011)(Marx *et al*., 1979; Gebbink *et al*., 2009). Finally, injury induced protein cross-linking has been shown to form protein aggregates rich in β-sheet structure which can enhance tPA-mediated plg activation (Samson *et al.* 2009; Samson *et al.* 2012). These results suggest that tPA is a multiligand cross-β structure receptor. Cross-β sheets may act as cofactors, promoting the interaction between tPA and plg, resulting in the removal of β-sheet containing proteins by plm-mediated degradation, regardless of amino acid sequence (Kranenburg *et al.* 2002; Samson *et al.* 2009). It is currently unclear whether the activation of the tPA system prevents toxicity by degrading and removing aggregates, or if the soluble fragments produced are toxic and can themselves cause damage to cells.

1.4.4 Toxicity of fragments released by plm-mediated degradation

Plm degradation of fibrin produces soluble products containing fragments from the central E-domain and D-dimer of the fibrin molecule (Guo *et al.* 2009). Research investigating the toxicity of these plm-generated protein fragments (PGPFs), as well as fragments from other protein aggregates, is of great interest and is important for developing new therapeutic strategies for protein deposition diseases and stroke. It has been noted, that fibrin deposition on the surface of placental cells was associated with apoptosis which could be prevented by inhibiting fibrinolysis, suggesting that cell death was caused by the degradation of products of fibrin (Isermann *et al.* 2003). This work was expanded by Guo *et al*. (2009) who found that the Aα-chain in the fibrin fragment E (FnE) was responsible for apoptosis in placental trophoblast cells (metastasising cells of the placenta) after internalisation into the cytoplasm via caveolin-1-dependent endocytosis. Internalisation of the fibrin fragments activated the mitochondrial cell death pathway, resulting in a reduction of mitochondrial activity and electrochemical potential difference across the inner mitochondrial membrane (Guo *et al.* 2009). Although the concentration of FnE used by Guo et al. (2009) was higher than circulating levels of FnE in humans, local concentrations of PGPFs near trophoblast cell surfaces are high enough to induce apoptosis, and similar conditions are present during

wound healing, tissue remodelling, and thrombotic injury in blood vessels. It is thought that apoptosis induced by PGPFs may be beneficial by aiding in clearing damaged cells from injury sites, but have deleterious cytotoxic effects when produced excessively, such as in acute lung injury and chronic lung disease (Siao and Tsirka 2002; Gando *et al.* 2004; Guo *et al.* 2009). The degradation of fibrin by plm is vital for the maintenance of haemostasis, yet despite the apparent toxicity of the fragments produced, biological functions are not impaired under normal conditions. This suggests the existence of mechanisms which protect cells from toxicity during the plm-mediated degradation of proteins.

1.5 The synergy of extracellular chaperones and proteases to maintain extracellular proteostasis

The discovery and characterisation of abundant ECs has led to the development of a model for extracellular proteostasis where chaperones defend against PDDs by binding to and preventing the aggregation of misfolded proteins (section 1.3.3). Building upon this, the proposed model (Figure 1.6) includes an additional protease arm of quality control that may function in tandem with ECs as part of a larger system to maintain proteostasis. In this new system protein aggregates activate and are subsequently degraded by tPA-activated plm. ECs then form a complex with the resulting PGPFs which are recognised by scavenger-like cell surface receptors, internalised via receptor mediated endocytosis and directed to lysosomes for degradation. This new theory is supported by research demonstrating that amyloid fibrils and denatured proteins can act as activators and substrates for the tPA and the plg activation system (Radcliffe and Heinze 1981; Tucker *et al.* 2000; Kranenburg *et al.* 2002; Samson *et al.* 2009) (section 1.4.3 and 1.4.4). In addition it has been shown that A2M associates with plasmin-degraded fibrin *in vitro* (Zammit 2009). However this experiment was only preliminary and further experiments should be conducted to determine if other ECs associate with PGPFs from fibrin and amorphous protein aggregates. Additionally, if PGPFs produced from plm-mediated degradation of aggregates are cytotoxic, the involvement of ECs presents a way in which plm can break down proteins while keeping the body protected from toxicity. Increased knowledge of these mechanisms could lead to the development of new therapeutics for the treatment of PDDs, such as Alzheimer's disease and ALS.

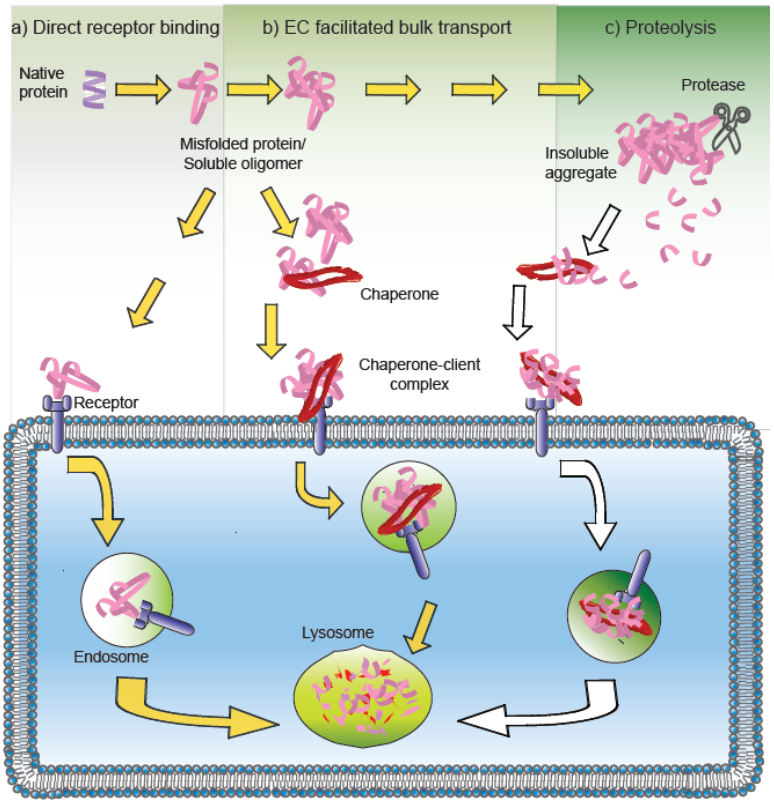

Figure 1.6 Hypothetical model for maintenance of extracellular proteostasis. Under normal conditions a) misfolded proteins or soluble oligomers can bind directly to scavenger receptors; b) extracellular chaperones can form stable complexes with misfolded proteins and/or soluble oligomers, keeping them soluble and facilitating their transport to scavenger receptors, and c) insoluble protein aggregates activate proteases, and extracellular chaperones interact with the soluble fragments produced, facilitating their transport to scavenger receptors. The chaperone:client complexes are then internalised via receptor-mediated endocytosis and delivered to lysosomes for degradation. Modified from Dabbs *et al.*, 2013.

1.6 Conclusions

The folding of an amino acid sequence into its correct native three dimensional structure is vital for a protein to perform its normal function. As a result of various stress conditions, proteins may unfold and form aggregates, a process associated with many harmful protein deposition diseases such as Alzheimer's disease. Thus the body has evolved intra- and extracellular systems of protein quality control to maintain proteostasis, with relatively little known about the processes that operate in the extracellular environment. ECs such as CLU and A2M bind to exposed hydrophobic residues on misfolded proteins and form soluble

complexes with them which can then be disposed of via receptor-mediated endocytosis. Furthermore, physiological stresses may induce A2M to adopt more chaperone-active quaternary structures (dimers and monomers) to enhance its ability to safely dispose of misfolded proteins (see Chapter 3). Synergy between the plg activation system and ECs may form a critical pillar, functionally underpinning the extracellular proteostasis system. Amyloid fibrils, fibrin and denatured proteins can all act as substrates and activators for tPA, and the extracellular chaperone A2M can bind to toxic fibrin-derived PGPFs. More detailed analysis of the interactions between ECs and the tPA system, and the toxicity and fate of the resulting EC:PGPFs complexes, will provide a better understanding of the mechanisms of extracellular proteostasis, and aid in the development of new therapeutics to treat serious protein deposition diseases.

CHAPTER 2 : GENERAL MATERIALS AND METHODS

2.1 Cell lines and established tissue culture

EOC-13.31 microglial-like, SVEC4-10 endothelial-like and LADMAC cell lines were obtained from the American Type Culture Collection. Cell lines were grown in DMEM/F12 media (Life Technologies) containing 10 % (v/v) foetal calf serum (FCS) at 37°C/5%CO_2, and subcultured when they reached 80% confluency. EOC-13.31 cells were additionally supplemented with 20% (v/v) LADMAC conditioned media containing colony stimulating factor-1 (CSF-1), which is secreted by the cell line. LADMAC conditioned media was harvested from LADMAC cell tissue culture supernatant by centrifugation at 500 x *g* for 5 min, and sterile filtration. For experiments involving the addition of chaperones, cells were incubated with treatments in DMEM/F12 containing 1% (v/v) FCS at 37°C/5%CO_2 in an effort to limit the effects of residual chaperone which may be present in the FCS.

2.2 Purification of primary polymorphonuclear neutrophils

Fresh human blood was obtained from members of the Wilson lab, with the addition of 200 µL of 1M sodium citrate per 20 mL of whole blood to prevent coagulation. Blood was slowly layered above 20 mL of Polymorphprep (Fisher Biotec) and then centrifuged at 500 x *g* for 35 min at room temperature (20˚C), with deceleration set to 0 (no assisted-braking) in a multifuge X3R centrifuge (ThermoFisher). Simultaneously, 3 mL of plasma (purified as per 2.6) was heated to 55˚C for 30 min to inactivate complement factors. Heat inactivated plasma was then placed on ice for 30 min and cleared of precipitation by centrifugation at 2,500 x *g* for 10 min at 4˚C. Once the whole blood was fractionated into distinct layers, the polymorphonuclear neutrophil (PMN) layer was gently removed (as outlined in the SOP 9.2 of the Sanderson-Smith lab) and washed twice with saline (5 mM sodium phosphate and 85 mM NaCl, pH 8) to remove any contaminating erythrocytes using osmolytic stress, by centrifugation at 180 x *g* for 10 min at room temperature (20˚C), with deceleration set to 0. PMNs were quantified using a hemocytometer and resuspended to a concentration of 1.0 x 10^6 cells/mL, in RPMI growth medium (Gibco) containing 2% (v/v) heat inactivated plasma.

2.3 Bicinchoninic acid (BCA) assay

1% (w/v) BCA was dissolved in a sufficient volume of solution A (20 g/L sodium carbonate, 1.6 g/L sodium tartrate, 9.5 g/L sodium bicarbonate, pH 11.25 with NaOH). Solution B (4% (w/v) $CuSO_4$ in H_2O) was added to a ratio of 1:50 (v/v) to solution A, yielding solution C. Bovine serum albumin (BSA) of known concentration (80 µg/mL) in phosphate-buffered saline (PBS; 140 mM NaCl, 2.7 mM KCl, 10 mM Na_2HPO_4, 1.4 mM KH_2PO_4, pH 7.4) was serially diluted in triplicate in a 384 well microtitre plate (Greiner Bio-one) to produce a set of protein standards. Similarly, protein(s) of unknown concentration were also serially diluted with PBS to give a final volume of 50 µL in each well. Solution C was then thoroughly mixed by vortexing (Super-mixer; Lab-line instruments, Inc.), and 50 µL added to each well. The plate was then incubated at 60˚C for 15 min to allow colour development and the absorbance at 562 nm measured using a Spectramax Plus 382 plate reader (Molecular Devices). The concentration of unknown protein(s) was interpolated from the standard curve constructed using the BSA standards.

2.4 Biotinylation of proteins

A stock solution of biotin-LC-N-hydroxysuccinimide (Biotin-LC-NHS; ThermoFisher) was prepared at 40 mg/mL in dimethyl sulfoxide (DMSO). Sufficient biotin stock was added to protein (at 1-2 mg/mL in 0.1 M sodium bicarbonate, pH 8.5) to give a ratio of 0.25 mg biotin-LC-NHS per mg of protein and incubated for 2 h at room temperature with gentle shaking. Excess, un-reacted biotin-LC-NHS was removed by dialysing the mixture against three changes of PBS/0.1 % Az at 4˚C. Protein concentration was subsequently determined using a BCA assay.

2.5 Fluorophore (CF-488) labelling of proteins

Proteins at a concentration of 1 mg/mL were buffer exchanged into PBS either by dialysis or by using protein desalting spin columns (Amicon Ultra-0.5 mL Ultracel 3k; Merck-Millipore). 1M sodium bicarbonate pH 8.3, 10% (v/v) was added to adjust the pH to optimise labelling efficiency. CF-488 SE dye (Biotium) dissolved in 25 µL anhydrous DMSO and reacted with protein for 1 h at room temperature in the dark, with gentle rocking. Excess, unreacted CF-488 SE dye was removed by gel filtration using a 5/20 Sephadex G-25 column equilibrated in PBS/0.1% Az (GE Healthcare) and eluted fractions were collected using an

ÄKTA FPLC system (GE Healthcare). Fractions containing CF-488 labelled protein were pooled and the protein concentration was determined using a BCA assay.

2.6 Preparation of human plasma from whole blood

Fresh human blood used in this study was donated by healthy consenting volunteers under the approval of the University of Wollongong and Illawarra Shoalhaven Local Health District Health Medical Human Research Ethics Committee (HE02/080). Blood was obtained from Wollongong Hospital and supplemented with 10 mM sodium citrate to prevent coagulation. Citrated whole blood was centrifuged at 1300 x *g* for 30 min at 4˚C in an X3R multifuge (ThermoFisher). Plasma was gently decanted from the pelleted red blood cells, pooled, and if not used immediately stored at -20˚C for later use. Prior to protein purification steps, frozen plasma was thawed and one crushed tablet of Complete Protease Inhibitor (Roche) was dissolved in approximately 400 mL of cleared plasma. Plasma was then filtered cold through GF/C glass fibre filters (Whatman) to remove cell debris and subsequently through 0.45 µm nitrocellulose filters (Sartorius). Citrated plasma was used as source material for the purification of clusterin (section 4.2.1), plasminogen (section 4.2.2), and immunoglobulin-G (section 4.2.3). Plasma used in the purification of alpha-2 macroglobulin (section 3.2.1) was prepared in a similar manner with the following exceptions; to 50 mL of whole blood, 100 µL of 1000 IU/mL of heparin (to prevent coagulation) and half a tablet of EDTA-free Complete Protease Inhibitor cocktail (Roche) were added. Following centrifugation and decanting steps, the heparinised plasma was supplemented with 1 M NaCl and 200 mM HEPES prior to subsequent purification steps.

2.7 SDS-PAGE

Gel electrophoresis was performed on polyacrylamide gels using the method of Laemmli (Laemmli 1970). Purified proteins were analysed under reducing and non-reducing conditions. Samples containing 10 µg of protein were prepared by diluting 1 in 2 with 2X SDS-PAGE loading buffer (100 mM Tris-HCl, 20% (v/v) glycerol, 4% (w/v) SDS, 0.2% (w/v) bromophenyl blue, pH 6.8) and adding 1% (v/v) 2-mercaptoethanol for reduced samples. The samples were then heated for 5 min in 100˚C heating block before being loaded onto the gel. The acrylamide gels used are characterised by the total percentage concentration (#%) of both monomers (acrylamide and the crosslinker bisacrylamide) (Hjerten 1962). Gels were prepared by layering a 5% stacking gel layer atop a resolving gel layer between 8-12%,

dependant on the separation range required for the protein samples being analysed. The resolving gel layer was buffered using a final concentration of 375 mM Tris-base at pH 8.8, while the stacking gel layer was buffered using 126 mM Tris-base at pH 6.8. Both gel layers contained 0.1% (w/v) SDS and 0.1% (w/v) ammonium persulfate. Polymerisation of the resolving gel layer was initiated by adding 4 µL of TEMED. The mixture was transfered to the gel cassettes; and filled to approximately 1.5 cm from the top of gel cassette (which is reserved for the stacking gel) and gently overlayed with a small volume (0.5 mL) of 100% absolute ethanol to remove bubbles. Gel was polymerised for 30 min at room temperature and the layer of ethanol removed for addition of the stacking gel. The stacking gel layer was polymerised by adding 5 µL of TEMED and transferred to the gel cassettes and a comb inserted with the required number of wells and polymerised for 30 min at room temperature. The cast gel was then transferred to a "Mighty Small II Mini Vertical Electrophoresis Unit" (Hoefer Inc.) and clamped into position. The reservoir was filled with SDS-PAGE running buffer (192 mM glycine, 3.5 mM SDS, 25 mM Tris-base) and electrophoresis carried out at constant voltage at 150 V for 90 min using a PowerPac Basic (Bio-Rad) or until the dye front had migrated out from the bottom of the gel. Gels were stained with Coomassie Blue Stain (40% (v/v) methanol, 10% (v/v) acetic acid, 0.15% (w/v) Coomassie Blue R250) at room temperature for an hour before being destained (40% (v/v) methanol and 10% (v/v) acetic acid).

2.8 Flow cytometry

All flow cytometry was conducted with a LSRII flow cytometer (BD) (excitation at X nm, emission collected at X ± X nm). Data was acquired using BD FacsDiva software v8.0.1 and analysed post-acquisition using FlowJo v5.0 software. Specific wavelengths (denoted by X) are identified in the appropriate methods sections. Dead cells stained with 3 µM propidium iodide (PI) were electronically excluded from the analyses unless stated otherwise.

CHAPTER 3 : THE CHAPERONE ACTIVITIES OF DIFFERENT QUATERNARY STRUCTURES OF A2M, AND A2M:PROTEASE COMPLEXES

3.1 INTRODUCTION

Alpha-2 macroglobulin (A2M) is a 720 kDa glycoprotein homotetramer (four 180 kDa identical monomers; with 10% carbohydrate by mass) formed from two disulfide-linked dimer pairs which are associated by non-covalent interactions (Jensen and Sottrup-Jensen 1986). In the native A2M, dimer pairs are arranged around a large central cavity in an open cage-like structure, to yield the final quaternary structure (Figure 3.1) (Marrero *et al.* 2012). A2M is a broad-spectrum inhibitor of extracellular proteases with a unique mode of action that functions in haemostatic and inflammatory reactions (Harpel 1973; Imber 1981; LaMarre *et al.* 1991). Proteases cleave A2M internally within a peptide stretch termed the bait region, which contains recognition sequences for serine proteases such as trypsin and plasmin as well as other protease families (Figure 3.1B) (Sottrup-Jensen 1989). Cleavage of the bait region by a protease exposes internal beta-cysteinyl-gamma-glutamyl thiol esters - activation of two ester bonds results in covalent binding of the protease (Saunders *et al.* 1971) and induces a large conformational change converting the open cage-like structure to a closed conformation, trapping the protease in a steric cage (Cummings *et al.* 1984; Feldman *et al.* 1985). These changes, collectively referred to as "activation", result in the formation of an A2M:protease complex, and are accompanied by exposure of a binding-site for the cell-surface receptor low density lipoprotein receptor-related protein (LRP) (Roche and Pizzo 1987; Roche and Pizzo 1988). Depending on the size of the protease, A2M can bind up to two protease molecules in a ternary complex (Howell *et al.* 1983; Christensen and Sottrup-Jensen 1984). The central cavity in activated A2M is 60 Å in diameter and approximately 167,000 $Å^3$, allowing the trapping of proteases that total up to approximately 90 kDa in mass (Marrero *et al.* 2012). This allows for the formation of A2M:protease complexes containing two trypsin (23.3 kDa) or one plasmin (83 kDa) molecule, respectively. Despite being sterically trapped, the bound protease(s) are active and can cleave small molecules which are able to enter the A2M:protease complex through openings in the structure (Ganrot 1966; Barrett and Starkey 1973). Small nucleophiles such as amines (e.g. methylamine, ammonium ions) can also induce A2M to adapt the closed, active conformation, by reacting directly with the internal thiol ester bonds (Imber 1981).

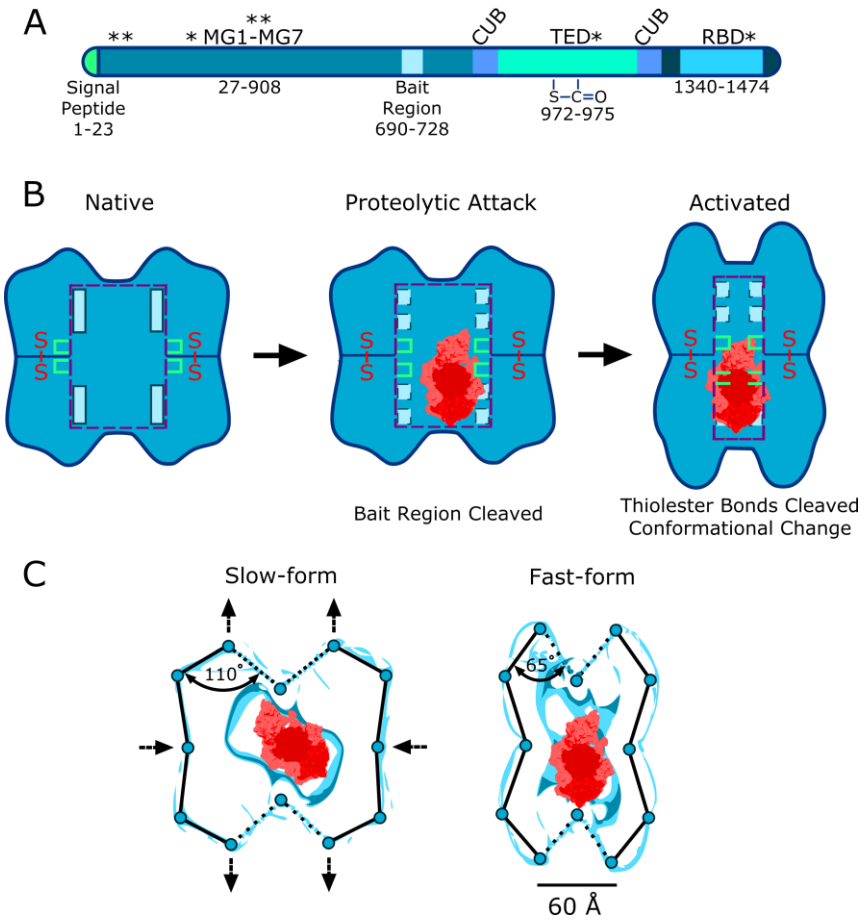

Figure 3.1 Schematic structure of A2M monomer subunit and activation by protease cleavage (A) The A2M monomer is 180 kDa in size and is comprised of seven macroglobulin-like domains (MG1-MG7), a thioester domain (TED) flanked by two structural motifs (CUB; *c*omplement protein subcomponents C1r/C1s, *u*rchin embryonic growth factor and *b*one morphogenetic protein 1) and a receptor binding domain (RBD) with recognition-sites for LRP. N-linked glycosylation sites are marked (black asterix). Within MG6 is the flexible bait region domain (residues$_{690\text{-}728}$) which contains the cleavage site for a broad-spectrum of proteases. The thioester motif (CGEQ; residues$_{972\text{-}975}$) is located within the TED. Image modified from Neves, D. *et al.* (2012). (B) In A2M the disulfide-linked (S-S) dimer pairs are arranged around a large central cavity (purple dashed lines) containing four bait regions (blue rectangles) and thioester bonds (green loops) in close proximity to one another. Cleavage of one or more bait regions by a protease (plg in red) results in emergence of thioester bonds. Breaking of thioester bonds induces a large conformational change resulting in the activated form of A2M, sterically trapping the protease and exposing LRP-binding sites. Image modified from Boisset, N. *et al.* (1996). (C) The conformational change induced by activation of A2M results in the lateral compression and lengthening of the quaternary structure (arrows). The state of A2M activation can be distinguished electrophoretically due to these structural changes, based on their speed of migration through a polyacrylamide gel matrix. Native A2M migrates slower (Slow-form) in comparison to activated A2M (Fast-form). The central cavity (60 Å in diameter as indicated by scale

bar) can accommodate up to two trapped proteases based on their size (single plg shown). Image modified from Law, R. *et al.* (2012).

Like other ECs, A2M is a secreted glycoprotein abundant in human plasma, which protects proteins from stress induced precipitation by binding to them via hydrophobic interactions (French *et al.* 2008). This ATP-independent holdase mechanism is similar to that of intracellular sHSPs. A2M-client protein complexes can be bound by cell-surface LRP, internalised by receptor-mediated endocytosis and subsequently degraded (French *et al.* 2008). PDDs, including several neurodegenerative diseases, cardiomyopathy, and arthritis-related diseases, are associated with reductive and oxidative (redox) stress which can induce protein misfolding and aggregation. Protein aggregates, in turn, compound the pathology by inducing inflammation (Papp *et al.* 2003; Tabner *et al.* 2005), which results in the release of oxidants, proteinases, and cytokines (Casserly and Topol 2004). A2M helps mediate inflammatory responses by binding and regulating the biological activities of a number of inflammatory cytokines and growth factors including; interleukins-1β and 6, transforming growth factor-β1 and 2, tumor necrosis factor-α, platelet derived growth factor, nerve growth factor, and fibroblast growth factor (LaMarre *et al.* 1991; Feige *et al.* 1996). The clearance of several cytokines is increased by their non-covalent binding to activated A2M, receptor mediated endocytosis via LRP and subsequent degradation in lysosomes (LaMarre *et al.* 1991; Crookston *et al.* 1994; Gonias *et al.* 1994). In addition, following internalisation of A2M-peptide complexes by LRP-mediated endocytosis, fragments of the peptide are presented on the cell surface serving a valuable immunological role - a similar role is played by exogenous (normally intracellular) HSPs (Binder *et al.* 2002).

A2M was recently shown to have an extracellular chaperone activity similar to that of CLU (French *et al.* 2008). A2M is synthesised mainly in the liver, and locally by leukocytes (White *et al.* 1980), while gene expression is induced by a variety of factors in an acute phase dependant manner (Milosavljevic *et al.* 2002). The acute phase response is a non-specific inflammatory state which results in the increased expression and release of important mediators of the inflammatory cascade including oxidants, proteinases, cytokines and A2M (which shows a 2-fold increase in humans) (Schreiber *et al.* 1982; Koenig and Rosenson 2002; Casserly and Topol 2004; Tabner *et al.* 2005). In plasma under physiologically-relevant shear-stress, A2M was found to bind to four aggregating client proteins (ceruloplasmin, fibrinogen, alpha-1-acid glycoprotein and complement component 3) all of

which are acute phase proteins (Wyatt *et al.* 2013). Conditions which induce acute phase responses such as increased local temperature, low pH and generation of reactive oxygen species are likely to enhance protein unfolding. Strikingly, these conditions are also likely to induce dissociation of the A2M tetramer (Barrett *et al.* 1979; Wyatt *et al.* 2014).

A2M is found in the plasma and CSF of healthy humans mainly as a tetramer. However, in different species A2M can exist as tetrameric, dimeric and monomeric forms, all of which can function as protease inhibitors (Sottrup-Jensen 1989). In humans, under physiological conditions 4-5% of the extracellular A2M pool is in the form of circulating disufide-linked dimers (Ozawa *et al.* 2011). A2M dimers have been found to be dissociated by oxidative conditions often related with PDDs such as rheumatoid arthritis (Wu and Pizzo 2001) and Alzheimer's disease (Cocciolo *et al.* 2012), and by hypohalous acids released by inflammatory-stimulated leukocytes (Reddy *et al.* 1989; Reddy *et al.* 1994) as well as hypochlorite released by neutrophils and microglia (Wyatt *et al.* 2014). In humans, A2M monomers in plasma have been identified as a clinical biomarker in patients with diabetes (Takada *et al.* 2013). Takada *et al.* (2013) report a ~2-fold increase of A2M monomer to 1 – 1.7 μM in diabetic patients with retinopathy, and a ~1.5-fold increase in diabetic patients with nephropathy, relative to healthy controls. In addition, monomeric A2M, also referred to as 'cardiac isoform of A2M', serves as an early molecular marker for cardiac hypertrophy (Rajamanickam *et al.* 1998), myocardial infarction in diabetes, (Annapoorani *et al.* 2006), and cardiac diseases (Rathinavel *et al.* 2005; Ramasamy *et al.* 2006). Reportedly, in all cases, the plasma concentration of A2M monomer is increased ~2-fold, relative to healthy controls. In addition to these diseases there are several conditions such as stresses in aging (Squier 2001; Papp *et al.* 2003; Morimoto 2006), and the acute phase response (which is accompanied by inflammation, pH and temperature changes, and redox stress), that could induce the formation of A2M monomers (Barrett *et al.* 1979; Schreiber *et al.* 1982; Koenig and Rosenson 2002; Casserly and Topol 2004; Tabner *et al.* 2005; Wyatt *et al.* 2014).

While native tetrameric A2M has been shown to exert a potent chaperone-like activity akin to the sHSPs against diverse client proteins (French *et al.* 2008; Yerbury *et al.* 2009), hypochlorite at physiologically relevant concentrations has been shown to dissociate A2M to dimers, and increase the ability of A2M (relative to the tetramer) to inhibit the aggregation of

several client proteins (Wyatt *et al.* 2014). The ability of A2M monomer to inhibit protein aggregation has not previously been studied.

Collectively, A2M has been shown to bind to many diverse ligands and proteases, influence the immune response, and inhibit the amorphous or amyloid aggregation of many different client proteins. It is possible that A2M may alter its chaperone activity in response to changes in the extracellular environment.

The aims of the work described in this chapter were to investigate whether:

1. A2M can adopt different quaternary forms (dimers and monomers) in response to oxidative or reductive conditions, and whether these dimeric and monomeric forms exhibit different levels of chaperone activity compared to the native A2M tetramer
2. Proteolytically activated A2M can inhibit protein aggregation, and whether the level of chaperone activity is different to the native A2M tetramer

3.2 METHODS

3.2.1 Alpha-2 macroglobulin purification

3.2.1.1 Zn^{2+} affinity chromatography

Two 5 mL HiTrap chelating columns (GE Healthcare) were connected in tandem to an ÄKTA FPLC system (GE Healthcare) and recharged with zinc prior to use. Zn^{2+} affinity columns were recharged by first equilibrating in binding buffer (20 mM HEPES, 1 M NaCl, pH 7.4) at a flow rate of 5 mL/min, stripped with 50 mL of zinc stripping buffer (20 mM HEPES, 0.5 M NaCl, 50 mM EDTA, pH 7.4), washed with 100 mL of milli-Q H_2O and recharged using 10 mL of zinc recharge solution (0.1 M $ZnSO_4$) at a rate of 1 mL/min. The columns were re-equilibrated using 100 mL of binding buffer and loaded with 50 mL of filtered, heparinised plasma (section 2.6), at a rate of 1 mL/min. A2M was eluted step-wise by first using elution buffer 1 (20 mM HEPES, 0.5 M NaCl, 20 mM imidazole, pH 7.4) to wash loosely bound protein contaminants from the columns before eluting the bound A2M with elution buffer 2 (20 mM HEPES, 0.5 M NaCl, 0.5 M imidazole, pH 7.4). The eluate containing A2M was collected and dialysed against three changes of PBS/0.1% Az, prior to subsequent size exclusion chromatography.

3.2.1.2 Size exclusion chromatography

A2M equilibrated in PBS/0.1% Az (section 3.2.1.1) was then further purified by size exclusion chromatography (SEC) using a HiPrep 16/60 Sephacryl S-200 HR column (GE Healthcare) equilibrated in PBS/0.1% Az and connected to an ÄKTA FPLC system (GE Healthcare). The sample was applied to the column at a rate of 0.5 mL/min. Fractions of 1 mL were collected and analysed by 8% SDS-PAGE (section 2.7). Those containing pure A2M were pooled and concentrated using an Amicon Ultra-15 filter unit (Merck Millipore; 30 kDa cut-off) and stored at 4˚C. Protein concentration was determined using a BCA assay (section 2.3).

3.2.2 Generation of dimeric and monomeric alpha-2 macroglobulin

A2M was purified as per section 3.2.1 and dissociated into dimers or monomers by incubating in PBS under either oxidising or reducing conditions, respectively. A2M was dissociated into stable dimers by oxidation-mediated disruption of non-covalent interactions between dimer pairs, in the presence of 500 µM NaOCl (Wyatt *et al.* 2014) for 8 h or 1.6-1.8

M NaSCN (Shanbhag *et al.* 1996) for 1 h at room temperature and dialysed against three changes of PBS at 4˚C. NaOCl-treated A2M tetramer and dimer were separated by SEC using a BioSep-SEC-s3000 (Phenomenex) equilibrated in PBS connected to an ÄKTA FPLC system (GE Healthcare). Samples were applied over the column at a flow rate of 0.5 mL/min and the absorbance of the eluate at 280 nm (A_{280}) continuously monitored to identify the elution of proteins. 150 µL fractions of column eluate were collected and separated into tetramer and dimer species, which correspond to the two observed peaks in Figure 3.2B. The two separated tetramer and dimer fractions were then analysed for purity by Native-PAGE (section 3.2.4) and subsequently dialysed against three changes of PBS at 4˚C. The region of overlap between the peaks corresponding to tetramer and dimer species was estimated by overlaying chromatographs of NaOCl-treated A2M and untreated native A2M. The difference in the area under the curve was calculated from these peaks excluding the region of overlap. A2M was dissociated into stable monomers by reduction of disulfide-bonds between subunits, and carboxymethylation to prevent oxidative re-association into tetramer during storage (Barrett *et al.* 1979). A2M was reduced by step-wise reaction with 1 mM dithiothreitol (DTT) in PBS for 30 min, and carboxymethylation with 1 mM iodoacetic acid for a further 45 min at room temperature, then dialysed against three changes of PBS at 4˚C. The quaternary structure of resulting A2M preparations was analysed by Native-PAGE (section 3.2.4) and SDS-PAGE (section 2.7). The A2M species generated were stable for several weeks when stored in PBS/0.1% Az, pH 7.4 at 4˚C, as assessed by Native-PAGE and SDS-PAGE.

3.2.3 *In vitro* generation and purification of activated alpha-2 macroglobulin:protease complexes

Pure native A2M (section 3.2.1) was activated by incubation with either ammonium cations or a serine protease (trypsin or plasmin). Native A2M was activated with 100 mM ammonium sulphate in PBS for 1 h at room temperature and immediately analysed, without dialysis, by NativePAGE. Activated A2M:protease complexes were formed by incubation with either trypsin or plasmin at a three times molar excess in PBS for 1 h at room temperature to ensure all A2M had been activated (and had trapped the maximum amount of protease). Unreacted protease was then inhibited by adding a four times molar excess of soybean trypsin inhibitor, relative to protease, and incubating in PBS for 1 h at room temperature. Free, unreacted protease and soybean trypsin inhibitor were removed via

multiple centrifugal concentration steps at 15,000 x *g* and 4˚C using a Vivaspin 500 (Sartorius; 100 kDa cut-off) and PBS as diluent, in a Heraeus Fresco 21 (ThermoFisher) bench-top centrifuge. Using a method established by Nelles *et al.*, 1980, the state of A2M activation was analysed by Native-PAGE (section 3.2.4) and SDS-PAGE (section 2.7) which compared activated A2M:protease complexes to native and ammonium-activated A2M. A2M:protease complexes were stable for several weeks when stored in PBS/Az, pH 7.4 at 4˚C, as assessed by both Native-PAGE and SDS-PAGE.

3.2.4 Native-PAGE analysis

Native-PAGE was used to separate native proteins on the basis of differences in their mass and charge. This technique was used to analyse the activation state of A2M incubated with ammonium ions or in complex with proteases (section 3.2.3) and the extent to which A2M had dissociated following oxidation or reduction (section 3.2.2). Samples containing approximately 20 µg of total protein were prepared by mixing an equivalent volume of sample with that of 2 X Native-PAGE loading buffer (50 mM Tris-base, 400 mM glycine, pH 8.3), under non-reducing conditions. Samples were then loaded onto the gel as described in section 2.7 (SDS-PAGE) with the following modifications. Gels were prepared by layering a 4% stacking gel atop a 5% resolving gel layer. The resolving gel layer was buffered using a final concentration of 167 mM Tris-base at pH 8.3, while the stacking gel layer was buffered using 125 mM Tris-base at pH 6.8. Both gel layers contained no SDS. The reservoir was filled with Native-PAGE running buffer (40 mM Tris-base, 40 mM boric acid, pH 8.6) and electrophoresis carried out at a constant voltage of 150 V for 1 h and stained using Coomassie Blue Stain (section 2.7). Native-PAGE analysis performed under these conditions results in bands that are not as visually sharp and defined as in SDS-PAGE but that appear somewhat broad and streaky.

3.2.5 Measure of exposed-hydrophobicity – bisANS binding assays

NaOCl-dissociated A2M tetramer and dimer, NaSCN-dissociated dimer and reduced and carboxymethylated monomer were diluted in PBS to give a final concentration of 5 µM and compared to an equal amount of native A2M tetramer (w/v) and 5 µM BSA (used as a positive control) also in PBS. All samples were supplemented with 100 µM 4,4′-bis(1-anilino-8-naphthalene sulfonate) (bisANS; Sigma-Aldrich) and the relative bisANS-

associated fluorescence recorded using a POLARstar spectrophotometer (BMG Labtech); excitation and emission band pass filters used were 355 ± 5 nm and 490 ± 5 nm, respectively.

3.2.6 *In vitro* chaperone activity assays

The effects of native tetrameric A2M (section 3.2.1), dimeric and monomeric forms of A2M (section 3.2.2), and activated A2M:protease complexes (section 3.2.3) on the aggregation of client proteins were measured over time using either changes in turbidity (absorbance at 360 nm; for amorphous aggregation) or changes in thioflavin-T (ThT)–associated fluorescence (for amyloid aggregation) with excitation and emission band pass filters of 440 ± 5 nm and 490 ± 5 nm, respectively. Both were measured using a FLUOstar or POLARstar spectrophotometer (BMG Labtech). Creatine phosphokinase (CPK), citrate synthase (CS) and reduced and carboxymethylated α-lactalbumin (RCM α-lact) have been used as client proteins by numerous laboratory groups to measure the activity of chaperones. RCM α-lact is a disordered form of the protein with three of four disulfide bridges reduced, and is susceptible to fibrillation at physiological temperature and pH (Goers *et al.* 2002). The conditions (concentration, buffer, and temperature) and duration of incubation used to induce aggregation of client proteins is given below in Table 3.1.

Table 3.1 Conditions used to induce aggregation of client proteins in chaperone activity assays

Client	Concentration (μM)	(mg/mL)	MW (kDa)	Buffer	Temperature (˚C)	Duration (h)
Creatine Phosphokinase (CPK)	9.4	0.75	80	PBS	43	2
Citrate Synthase (CS)	1.2	0.1	85	TE	43	2
Reduced and carboxymethylated α-lactalbumin (RCM α-lact)	100	1.4	14	PBS	37	12

Client proteins CPK and RCM α-lact in PBS, and CS in TE buffer (50 mM Tris-base, 2 mM EDTA, pH 8.0) were heated at the temperature indicated to induce aggregation.

To measure amorphous protein aggregation, CPK or CS were incubated at 43˚C in 384-well plates (100 µL final volume) while continuously measuring turbidity in the absence or presence of: native A2M tetramer**,** or NaSCN- or NaOCl-dissociated dimer, or DTT-dissociated A2M monomer (at equal mass concentration to the tetramer), or the non-chaperone control protein ovalbumin (Ova; at the highest mass concentration of native A2M tested). For comparisons of the relative chaperone activities of A2M tetramer, dimer and monomer, the "subunit molar ratio" (SMR) of A2M to client (A2M:client) was used, which is calculated as the ratio of the number of moles of A2M monomer (regardless of whether the A2M is present as tetramer, dimer or monomer) to the moles of protein client. In this way, direct comparisons could be made at the same SMR between the relative chaperone abilities of different A2M forms (present at the same total mass concentration). Percent inhibition of aggregation was calculated by (i) subtracting background measurements of buffer and chaperone controls from their corresponding samples, (ii) from the differences in end-point turbidity, or ThT-associated fluorescence between client protein incubated alone, and client protein in the presence of chaperone, as shown in the equation below.

% Inhibition = [(client alone - client with chaperone) / client alone] * 100

In similar experiments using CPK and CS as amorphously aggregating client proteins, the ability of A2M tetramer to inhibit protein aggregation was compared with that of both Trp and Plm activated A2M:protease complexes and the non-chaperone control protein Ova. When using SMR to compare the chaperone activity of A2M:protease complexes tested, the molecular mass of the trapped protease was excluded in calculations. In other related experiments, the effects of native A2M, A2M:protease complexes, and the non-chaperone control protein Ova on amyloid formation by reduced and carboxymethylated α-lact (RCM α-lact) was measured using ThT-associated fluorescence. At the completion of these assays, the microplates containing the samples were stored at -20˚C for subsequent analysis to assess proteolytic degradation of the client protein by SDS-PAGE. The effects of increasing reaction time between A2M and Trp (1 – 24 h) on the resulting chaperone activity of A2M:Trp complexes (section 3.2.2) was also measured using CS as the client protein.

3.2.7 SDS-PAGE analysis of proteolytic degradation of client proteins by A2M:protease complexes

Samples taken from chaperone activity assay end-points were analysed for proteolytic degradation of the client proteins to ascertain whether inhibition of protein aggregation by A2M:protease complexes is influenced by the action of the sterically-trapped protease. Aliquots were removed and centrifuged at 15,000 x *g* and 4˚C for 20 min. The pellet fractions were washed in PBS, centrifuged once more under the same conditions and solubilised in 100 µL 2X SDS-PAGE loading buffer containing 10% (v/v) 2-mercaptoethanol. The samples were then heated for 10 min at 100˚C before being loaded onto the gel. SDS-PAGE was performed under reducing conditions on 10 – 15% resolving gel (section 2.7). The gels were stained with Coomassie Blue Stain at room temperature for an hour before being destained.

3.2.8 Densitometry analysis of Native- and SDS-PAGE images

Images of gels (sections 3.2.4 and 3.2.7) were captured by a Gel Logic 212 Pro (Carestream, USA) imaging system and saved as high quality .tif files for subsequent densitometry analysis. 8-bit monochromatic images were background subtracted and analysed with ImageJ 1.49a (National Institute of Health, USA) using the "Integrated density" function, and the intensity of bands measured. From this, the amount of protein in individual bands of interest was calculated as a percent of the total intensity of all bands within the lane.

3.2.9 Statistical Analysis

Data presented in the results was analysed using a one-way ANOVA and a Bonferroni multiple comparison post-test using GraphPad Prism v5.0, unless stated otherwise. The extent of significance between samples is denoted by the amount of asterix present in the graphs (*$p<0.05$, **$p<0.01$ and ***$p<0.001$).

3.3 RESULTS

3.3.1 Treatment with NaOCl and NaSCN induces dissociation of native tetrameric A2M into stable dimers

A2M preparations were analysed by both Native-PAGE and SEC and conditions were optimised to successfully generate pure species. Native A2M tetramer was treated under conditions previously described by Wyatt *et al.* (2014) and Shanbhag *et al.* (1996), and optimised to generate A2M dimers which could then be purified and analysed (section 3.2.2). A2M was treated with NaOCl, which aims to replicate the hypochlorite released by activated neutrophils and microglia during inflammation (Wyatt *et al.* 2014). A2M was also treated with NaSCN, previously used in structural studies to distrupt non-covalent interactions between A2M dimer pairs (Shanbhag *et al.* 1996), to later compare whether A2M dimers formed by different treatments would vary in their properties and chaperone activities (sections 3.3.4 – 3.3.5). Incubation of purified human A2M with NaOCl or NaSCN resulted in the dissociation of native A2M tetramer into dimers as expected, which was visualised by Native-PAGE (Figure 3.2A). The remaining tetramer species migrated at the same rate as the native slow-form of A2M, demonstrating that chemical dissociation by either NaOCl or NaSCN did not induce a conformational change to the fast-form (for diagrams of slow- and fast-form A2M refer to Figure 3.1C) (Barrett *et al.* 1979). Treatment with 500 µM NaOCl resulted in the dissociation of approximately 50% of the tetramer to dimer (Figure 3.2A). Comparatively, 1.6 – 1.8 M NaSCN resulted in dissociation of approximately 90% of the tetramer to dimer (Figure 3.2A). At 1.8 M (Figure 3.2A) or higher concentrations of NaSCN (data not shown), an A2M species with higher electrophoretic mobility than the dimer was present. This was thought to be monomer and comprised approximately 40% of the total protein. The A2M dimers generated by treatment with 500 µM NaOCl can be purified by SEC (Figure 3.2B); the difference in the area under the curve suggests that approximately 30% of the total protein present in solution was dimer. However, there was inefficient separation between tetramer and dimer due to the limited resolving power of the SEC column used. The region of overlap between the tetramer and dimer peaks was not used in chaperone activity assays. Taken together, these data demonstrate the successful generation of pure species of dimeric A2M, produced by two different methods.

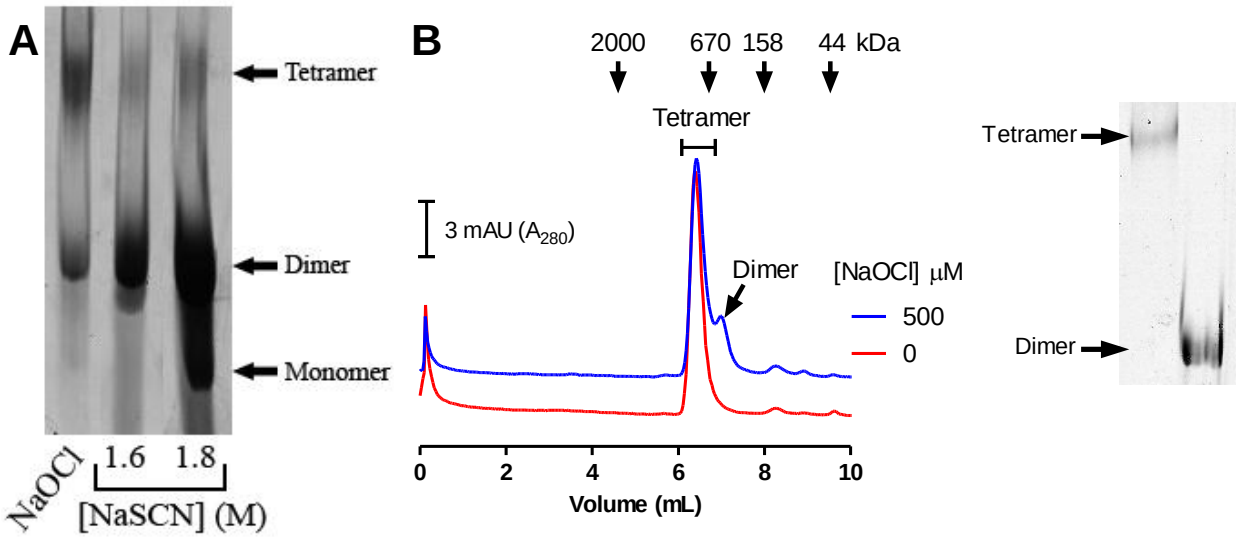

Figure 3.2 Sodium hypochlorite and sodium thiocyanate induce dissociation of native A2M tetramer into stable dimers. (A) Image of 4% native polyacrylamide gel showing A2M treated with either 500 µM NaOCl or 1.6-1.8 M NaSCN for 1 h at room temperature. Tetramer and dimer species of A2M are indicated by arrows as shown. (B) Purified native A2M was incubated in the absence or presence of 500 µM NaOCl for 8 h at room temperature then fractionated by SEC and eluate fractions monitored continuously by A_{280} measurement. The scale bar (top left) indicates three milli-absorbance units (mAU). The elution volumes of molecular weight standards are indicated by black arrows at the top of the figure. The positions of peaks corresponding to tetramer and dimer species of A2M are indicated by either bracket or arrow, respectively. The eluate fractions were analysed by Native-PAGE (section 3.2.4), pooled and separated into purified tetramer and dimer species as shown by 4% native polyacrylamide gel (right).

3.3.2 Protease- and ammonium-induced activation of A2M. Reduction and alkylation of A2M to form stable monomers

Native A2M tetramer was treated under conditions previously described by French *et al.* (2008) and optimised to either generate purified A2M:protease complexes (section 3.2.3). Plm was selected as a suitable protease to generate A2M:Plm complexes to compare to A2M:Trp complexes, previously described by French et al. (2008), due to its larger relative molecular weight and the physiological relevance of A2M:Plm complexes (Harpel 1973; Imber 1981), in order to later assess whether A2M:protease complexes formed by activation with different proteases would vary in their properties and chaperone activities (sections 3.3.4 and 3.3.6). Native A2M was also treated under conditions first described by Barrett *et al.*

(1979) to generate stable A2M monomers (section 3.2.2). Native A2M was also activated by treatment with ammonium ions (NH_4^+), serving as a positive control to compare the extent of activation of A2M:protease complexes as described (section 3.2.4), and analysed by Native-PAGE; the resulting species migrated as a single band of electrophoretically fast-form of A2M species, equivalent to the activated conformation (Figure 3.3A). In the same analysis, the lane containing A2M:Trp complexes showed a single band migrating slightly faster than the NH_4^+-activated A2M, having undergone a complete conformational change induced by cleavage of all four thioester bonds, and steric trapping of two molecules of Trp (Saunders *et al.* 1971; Marrero *et al.* 2012). The lane containing A2M:Plm complexes showed two bands which migrated to equivalent positions to the NH_4^+-activated fast-form (73%; calculated as described in section 3.2.8), and A2M:Trp complexes (27%), suggesting the steric trapping of a single large molecule of Plm. It is currently thought that the two bands differ in migration speeds due to the inefficient trapping of Plm within the molecular cage of A2M, the conversion to a "fully activated/closed" conformation (as diagrammed in Figure 3.1) equivalent to that of A2M:Trp complexes; occurring at a much slower rate due to the size of the protease, requiring gradual re-arrangement of the monomeric subunits of A2M to accommodate the large protease (Kolodziej *et al.* 1998; Marrero *et al.* 2012). Reduction of the disulfide-bonds of native A2M and carboxymethylation of the resulting free thiol groups to prevent oxidative re-association of subunits produced stable monomers which migrated as a single band, much faster than activated A2M tetramer. To confirm their structure, activated A2M and monomer samples were then analysed by SDS-PAGE under non-reducing and reducing conditions (Figure 3.3B). A2M monomer was visualised as a major band at ~180 kDa (equivalent to a monomeric subunit), as well as a faint band (visible only under reducing conditions) at ~120 kDa, corresponding to the product of heat-induced A2M cleavage of the thioester bond in A2M (Sottrup-Jensen 1989). NH_4^+-activated A2M analysed under reducing conditions showed a major band at ~180 kDa, corresponding to a dissociated A2M monomer. Thioester bond cleavage was indicated by faint bands at ~120 kDa detected in analyses of both NH_4^+-activated A2M and A2M:Plm complexes. Analyses of A2M activated with either Trp or Plm but not NH_4^+ showed a band at ~90 kDa, visible only under reducing conditions, indicative of proteolytic cleavage of one or more bait-region(s), located at the approximate centre of an A2M subunit (Harpel *et al.* 1979; Sottrup-Jensen 1989). When analysed under non-reducing conditions both protease- and NH_4^+-activated A2M samples showed a band at > 200 kDa which did not completely enter the gel matrix, consistent with the intact 720 kDa A2M tetramer. No proteolytic degradation of A2M was detected in preparations of A2M

reacted with molar excess of either Trp or Plm, demonstrating that the process of inhibiting and removing the excess protease (as outlined in section 3.2.3) allows production of intact A2M:protease complexes. The above data demonstrate the successful generation of pure A2M:protease complexes and monomeric A2M.

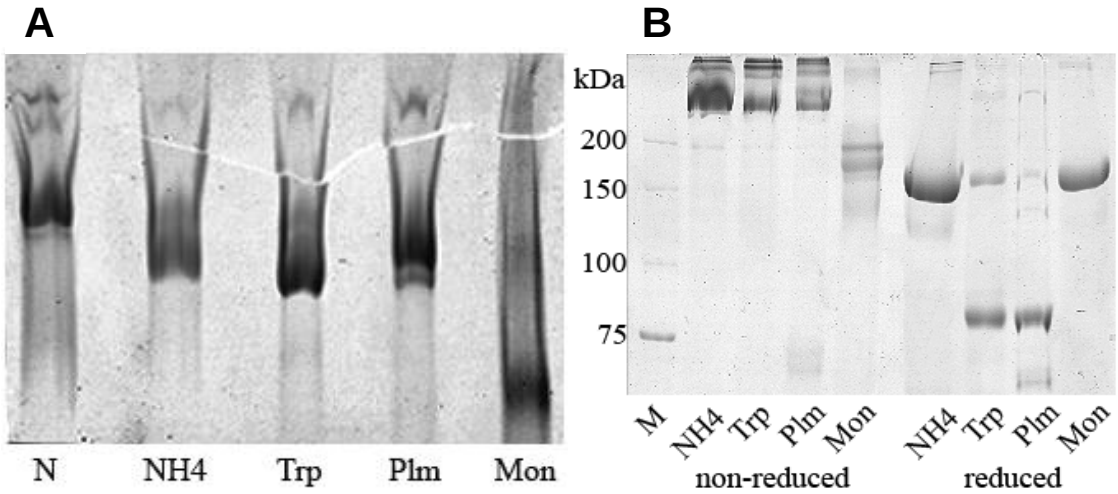

Figure 3.3 Images of (A) 4% Native-PAGE and (B) 8% SDS-PAGE analyses of the effects of various treatments on the electrophoretic mobility of A2M. Purified native A2M (N) was activated by incubation with 100 mM ammonium sulfate (NH4) or either trypsin (Trp) or plasmin (Plm) for 1 h at room temperature. Free, un-reacted protease was inhibited by soybean trypsin inhibitor and removed by ultrafiltration. A2M was dissociated into monomer (Mon) by reduction and carboxymethylation. (A) Native-PAGE was performed under non-reducing conditions, (B) SDS-PAGE was performed under both non-reducing and reducing conditions. The molecular weight standards (Lane M; BioRad) indicated in kDa.

3.3.3 Ammonium activation of A2M stabilises it against chemical dissociation into dimer and monomer species

In vivo, A2M can circulate either as native tetramers or in an activated state complexed with proteases (Zhabin and Zorin 1995), and also as dimers (Ozawa *et al.* 2011) and monomers (Takada *et al.* 2013); which may dissociate in response to extracellular environmental conditions. To test whether the conformational state of A2M affects its ability to dissociate into dimers and monomers, A2M was activated with NH_4^+ and compared to native A2M by Native-PAGE. It was shown before that treatment of native A2M with NaSCN (section 3.3.1) or reduction and carboxymethylation (section 3.3.2) generates A2M dimers and monomers, respectively. However, NH_4^+ activated A2M was found to be resistant to dissociation into the

dimers and monomers that otherwise result from treatment by NaSCN or reduction (Figure 3.4). Native-PAGE analysis indicated that (i) approximately 65% (calculated as described in section 3.2.8) of NH_4^+-treated native A2M had been activated into the fast-form (lane 1 – 2), (ii) native A2M was almost completely dissociated into dimer by NaSCN treatment (lane 3), this effect was completely inhibited by previous NH_4^+-activation of A2M (lane 4), and (iii) reduction and carboxymethylation induced almost complete dissociation of native A2M to monomers (lane 5) but previous NH_4^+-activation of A2M prevented dissociation to monomers altogether (lane 6). However, a small amount of dimer was detected.

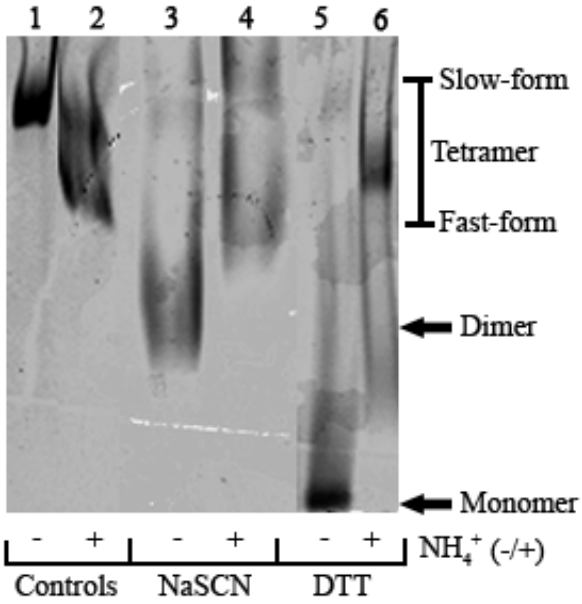

Figure 3.4 Pre-activation by NH4+ inhibits dissociation of A2M into dimers and monomers. Purified native A2M was activated by incubation with NH_4^+ (+) or not (-) as previously described to induce activation and transition to an electrophoretically fast-form. A2M was either left untreated (Controls) or subsequently treated with NaSCN or DTT/carboxymethylation as previously described, then analysed by 4% Native-PAGE. The positions of A2M tetramer (Slow- or Fast-form), dimer and monomer are indicated to the right, and sample identity and treatments are indicated below the image, and corresponding lane number above.

3.3.4 Dissociation of native A2M into dimers and monomers, and the formation of A2M:protease complexes, is associated with increased exposed hydrophobicity

The activity of extracellular chaperones, including A2M, depends on hydrophobic interactions between the chaperone and normally buried hydrophobic residues of the unfolding client protein leading to the formation of chaperone:client protein complexes (French *et al.* 2008; Wyatt *et al.* 2009; Dabbs *et al.* 2013). bisANS was used as a probe for levels of exposed hydrophobicity on native A2M, A2M dimers and monomers (section 3.2.2), and complexes formed between A2M and Trp or Plm (section 3.2.3) (Figure 3.5). BSA was included as a positive control for bisANS fluorescence. Dissociation of A2M into dimers by treatment with 1.6 M NaSCN and 500 µM NaOCl significantly increased hydrophobicity by 5.3 ± 0.04 and 3.4 ± 0.4 fold respectively, when compared to the native A2M tetramer (Figure 3.5A and B). However, there was no significant difference in hydrophobicity between the NaOCl-oxidised tetramer (separated from dimer species by SEC; Figure 3.2B) and the native tetramer. This suggests that dissociation itself, rather than oxidation, is responsible for the observed increase in hydrophobicity. Furthermore, dissociation of A2M into stable monomers significantly increased hydrophobicity by 4.5 ± 0.04 fold, when compared to the native tetramer (Figure 3.5A). Reaction of native A2M with Trp and Plm yielded activated A2M:protease complexes with significantly increased surface hydrophobicity relative to native A2M (Figure 3.5C); there was a 2.3 ± 0.1 fold increase for A2M:Trp and 2.0 ± 0.1 for A2M:Plm, respectively. Trp or Plm alone did not show significantly increased hydrophobicity compared to background bisANS levels. Therefore, it appears that the increase in relative hydrophobicity is due to the conformational change associated with proteolytic activation of A2M. Similar effects have been reported for the methylamine-mediated activation of A2M (Wyatt *et al.* 2013).

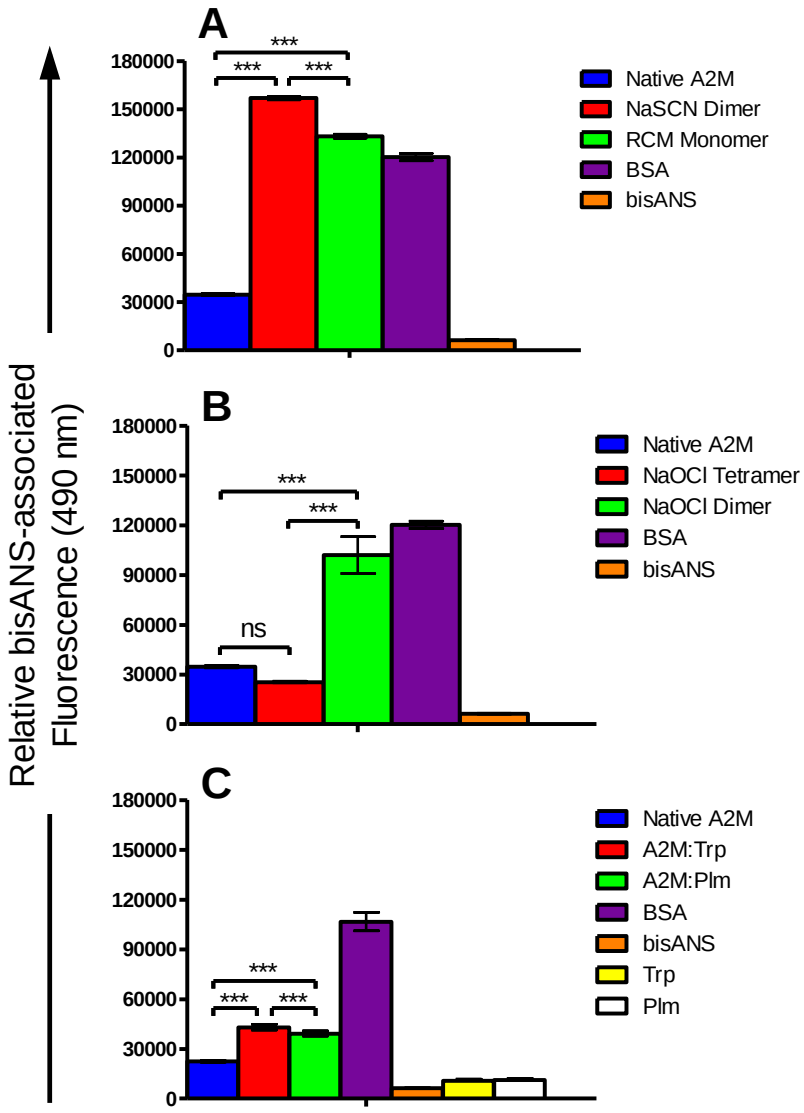

Figure 3.5 bisANS fluorescence assays showing that relative to native A2M, A2M dimers (formed by treatment with either NaOCl or NaSCN), monomers (formed by RCM) and A2M:protease complexes have increased exposed hydrophobicity. bisANS-associated fluorescence was used to measure exposed hydrophobicity for A2M samples and BSA (positive control) diluted to 5 μM in PBS. (A) Dimeric and monomeric A2M produced by NaSCN or RCM. (B) Oxidised (NaOCl-treated, as previously described) A2M tetramer and dimer (purified by SEC). (C) A2M:Trp and A2M:plm complexes produced by reaction of A2M with Trp or Plm, or protease alone. Bars represent the mean of triplicate measurements and are representative of separate experiments (n=3; ±SD). Significant differences between samples is denoted by brackets *** ($p<0.001$); n/s not significant.

3.3.4 Stable dimers and monomers of A2M are more chaperone-active than native A2M

3.3.4.1 NaSCN-dissociated dimer, and RCM monomer

Both native tetrameric A2M and hypochlorite-dissociated dimers have been shown to have a potent chaperone activity akin to the sHSPs against a variety of client proteins (French *et al.* 2008; Yerbury *et al.* 2009; Wyatt *et al.* 2014). The ability of NaSCN-dissociated dimers to inhibit protein aggregation has not previously been tested. The client protein CPK was precipitated by heating at 43˚C in the absence or presence of different concentrations of either A2M tetramer, NaSCN-dissociated dimer or monomer (or non-chaperone control protein Ova) (Figure 3.6). Heating native CPK to 43˚C in the absence of A2M resulted in extensive and rapid protein precipitation, shown by an increase in turbidity (A_{360}) after a lag phase of 15 min, reaching a maximum at approximately 75 min. The initial drop in A_{360} occurs in all chaperone assays involving CPK as the client protein and is likely an artefact, and may be result from heating the client from room temperature to 43˚C required to induce aggregation. The A2M tetramer inhibited protein aggregation in a dose-dependent manner as expected (Figure 3.6A). A subunit molar ratio (SMR; section 3.2.6) of tetramer:CPK = 1:3 and 1:5 reduced the end-point turbidity by 62.3 ± 4 % and 12.94 ± 7%, respectively compared to CPK alone. A SMR of 1:50 induced a small (but insignificant) increase in protein aggregation relative to CPK alone. In contrast, both A2M dimer and monomer, at a SMR of chaperone:CPK = 1:10 and 1:50 resulted in either complete (97.6 ± 5% and 100.1 ± 6%, respectively for SMR = 1;10), or partial but significant inhibition (19.6 ± 10% and 18.0 ± 8%, respectively for SMR = 1:50) of CPK aggregation, (Figure 3.6 B and C). This indicates that A2M dimers and monomers are more potent chaperone molecules than the intact A2M tetramer. In all cases, the presence of Ova had no significant effect on the end-point turbidity.

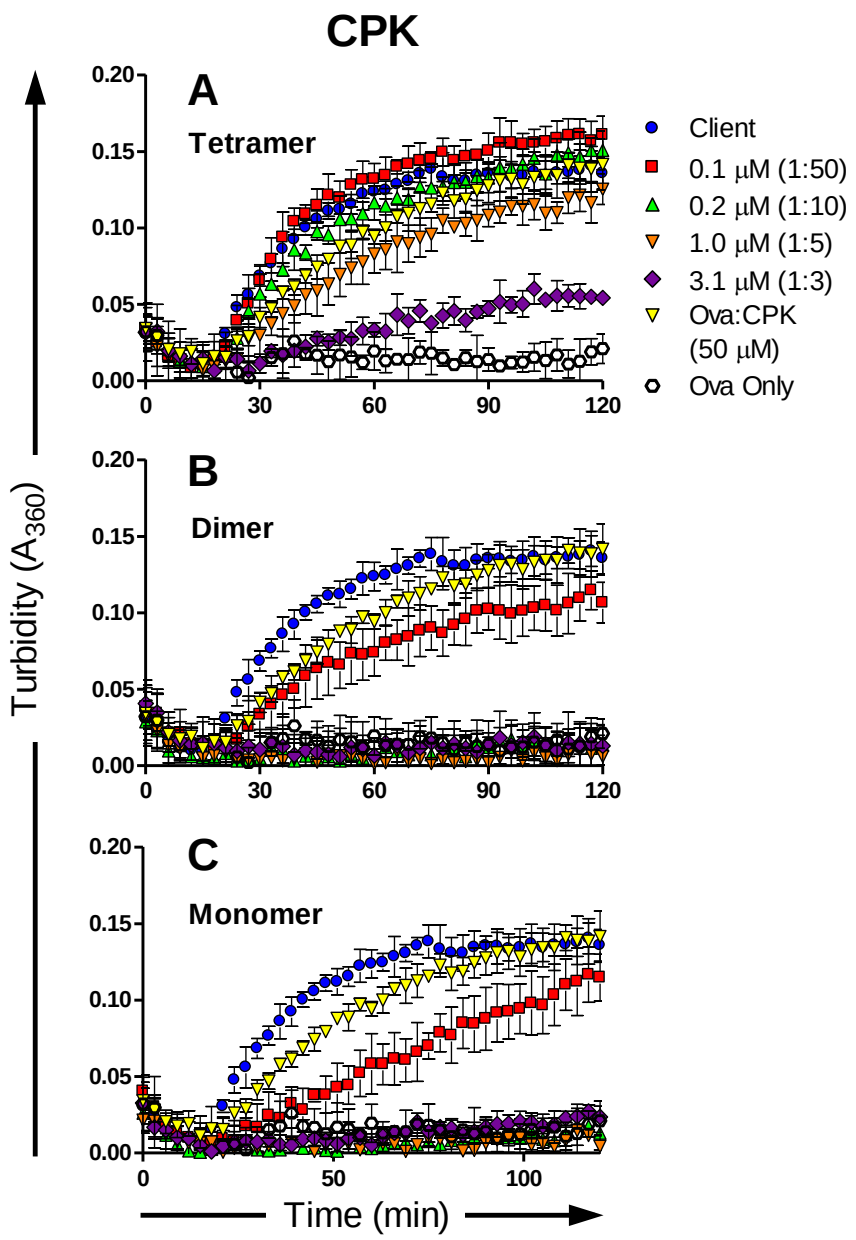

Figure 3.6 NaSCN-dissociated A2M dimers and A2M monomers inhibit CPK aggregation to a greater extent than A2M tetramers. CPK (9.4 μM) was induced to aggregate by heating at 43˚C in the absence or presence of increasing molar concentration and different SMR of A2M species (indicated at top left of each panel), or the non-chaperone control protein Ova (equivalent to the highest mass concentration of A2M used). The ratios shown in the key are SMR of A2M:CPK. Data points represent the mean ± SD (n=9) of three separate experiments, where in each experiment measurements were performed in triplicate.

3.3.4.2 NaOCl-dissociated dimer, and RCM monomer

To investigate the chaperone activity of NaOCl-dissociated A2M dimer and contrast that to the activity of NaSCN-dissociated A2M dimer, and monomer, the ability of these species to inhibit the amorphous aggregation of CPK and CS was compared with that of A2M tetramer, NaOCl-dissociated dimer and monomer, and the non-chaperone control protein Ova (Figure 3.7A). A2M tetramer, dimer and monomer significantly inhibited the stress-induced aggregation of CPK and CS (Figure 3.7). In CPK aggregation assays, at SMRs of

tetramer:CPK from 1:31 to 1:4.5, A2M tetramer inhibited CPK aggregation from 0.6 ± 4% to 29 ± 2%, respectively (Figure 3.8). By comparison, at equivalent SMRs, CPK aggregation was inhibited by (i) NaOCl-dissociated dimer from 71.4 ± 1% to 100.3 ± 7.1%, and (ii) by A2M monomer from 55.9 ± 2% to 63 ± 9%. When compared at a CPK concentration of 1.5 µM, A2M dimer, monomer and tetramer inhibited CPK aggregation by 93.4 ± 7%, 63.2 ± 9%, and 22. 0 ± 1%, respectively (Figure 3.7A – C). Whether dissociated by treatment with NaSCN (Figure 3.6) or NaOCl (Figure 3.7 and 3.8), when tested at similar SMRs, the A2M dimers produced had near identical chaperone activities. In CS aggregation assays, A2M tetramer, dimer and monomer all showed dose-dependent inhibition of CS aggregation. SMRs of tetramer:CS from 1:4 to 1:0.6 dose-dependently inhibited protein aggregation, ranging from zero to 49.0 ± 1%, respectively (Figure 3.8). In comparison, at equivalent SMRs, NaOCl-dissociated dimer inhibited CS aggregation by from 49.0 ± 4% to 94.0 ± 1%, and monomer inhibited CS aggregation by from zero to 94.5 ± 2%. When compared at a concentration of 1.5 µM, A2M dimer, monomer and tetramer inhibited CS aggregation by 58.3 ± 8%, 69.0 ± 3% and 25.6 ± 5%, respectively (Figure 3.7D – F).

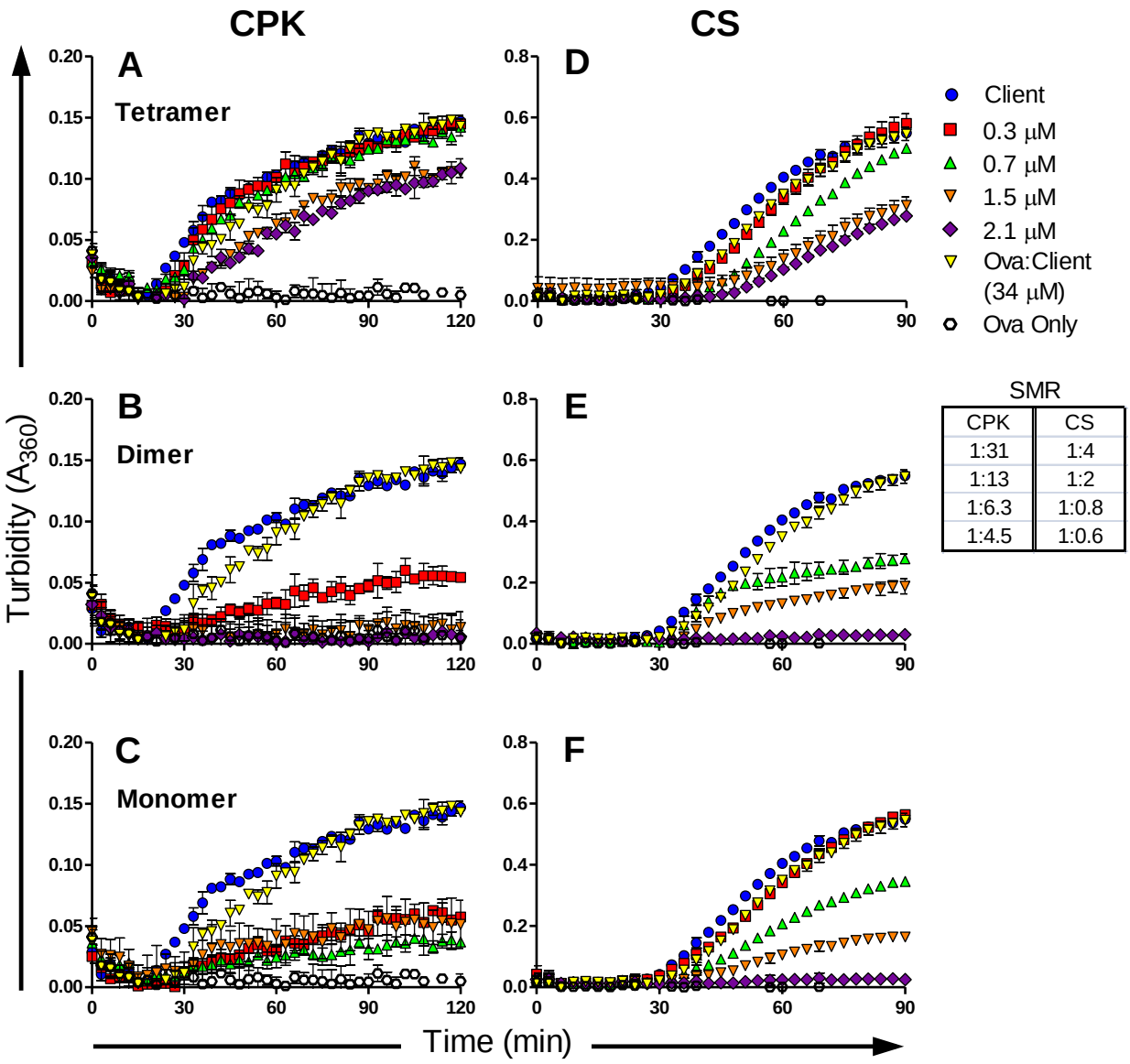

Figure 3.7 NaOCl-dissociated dimers, and monomers of A2M, inhibit stress-induced CPK and CS aggregation to a greater extent than A2M tetramers. CPK (9.4 μM; A – C) and CS (1.2 μM; D – F) were induced to aggregate by heating at 43˚C in the absence or presence of increasing molar concentration and different SMR of A2M species (indicated at top left of each panel), or non-chaperone control protein, Ova (equivalent to the highest mass concentration of A2M used). The ratios shown in the table below the key are SMR of A2M:client protein. The effects of stable A2M NaOCl-dissociated dimers or monomers (produced as described previously) on CPK and CS precipitation were compared to an equal amount of native A2M tetramer. Data points represent the mean ± SD (n=9) of three separate experiments, where in each experiment measurements were performed in triplicate.

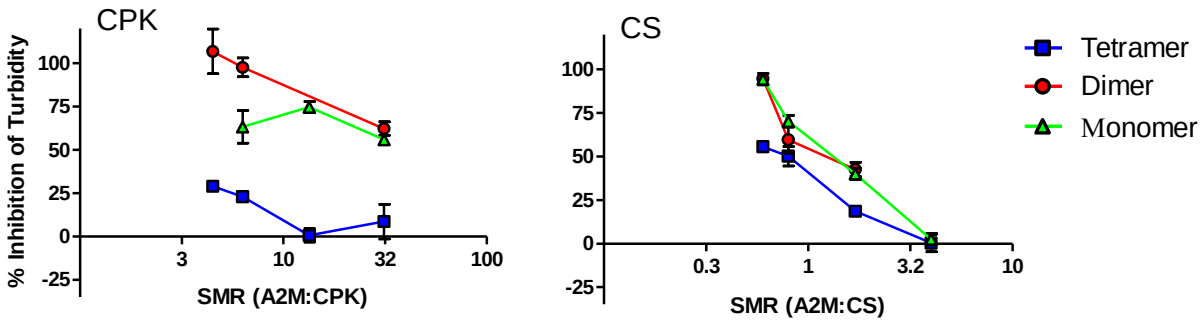

Figure 3.8 Inhibition of client protein aggregation at assay end-point as a function of SMR. The % inhibition of protein aggregation at assay end-point (data from Figure 3.7 and 3.8) is plotted as a function of the SMR of A2M tetramer, dimer or monomer to client protein (SMR was calculated as per section 3.2.6). The identity of each client protein is indicated at the top left of the respective panels. Lines between data points indicate a trend and have no theoretical significance. Data points represent the mean ± SD (n=9) of three separate experiments, where in each experiment measurements were performed in triplicate. In some cases, the error bars are too small to be visible.

3.3.6 The formation of A2M:protease complexes enhances the ability of A2M to inhibit protein aggregation

As mentioned previously (section 3.1), activation of A2M by proteolytic cleavage of the bait-region induces a conformational change which both traps the protease within a steric cage and covalently binds it by interaction with the thioester bond. The volume of the intramolecular cavity of A2M allows for the trapping of proteases with a total mass of up to 90 kDa (Marrero *et al.* 2012). This allows for the formation of (tetramer) A2M:protease complexes incorporating two trypsin (Trp; 23.3 kDa) or one plasmin (Plm; 83 kDa) molecule, respectively. As mentioned previously (section 3.1), the active site of the protease itself is not affected and can cleave small substrates, inhibitors and proteins of 6 – 9 kDa (Ganrot 1966; Barrett and Starkey 1973). However, prolonged incubation with soybean Trp inhibitor (20.1 kDa) has been found to inhibit A2M-trapped Trp (Bieth *et al.* 1981). Computer modelling by Marrero *et al.* (2012) using a crystal structure of a complex of A2M:Trp:soybean Trp inhibitor (Song and Suh 1998) suggests this may occur through re-arrangement of the monomeric subunits of A2M allowing entry and inhibition of the protease active site of A2M-trapped Trp (Marrero *et al.* 2012). A2M-trapped Plm occupies a large majority of the intramolecular cavity, making further re-arrangement of A2M subunits surrounding the

cavity unlikely (Kolodziej *et al.* 1998) which limits the entry of proteins of up to 7 kDa (cavity size limits of 90 kDa minus the 83 kDa for plasmin). Thus if proteins limited to ≤ 20.1 kDa for A2M:Trp and ≤ 7 kDa for A2M:Plm diffuse into the intramolecular cavity, the protease(s) may still be able to degrade them, which could affect the progress of client protein aggregation (Barrett and Starkey 1973; Marrero *et al.* 2012). Previous work by French *et al.*, 2008 suggested that pre-activation with Trp abolished the chaperone action of A2M.

The chaperone activity of protease activated A2M was investigated using amorphously aggregating CPK, CS and amyloid fibril forming RCM α-lact as client proteins. A2M:protease complexes were produced as previously described (section 3.2.3). All A2M species tested significantly inhibited the heat-induced aggregation of CPK and CS (Figure 3.9). In all cases, the non-chaperone control protein Ova had no significant effect on end-point turbidity. In CPK aggregation assays, 2.1 µM native A2M (SMR of A2M:CPK = 1:4.5) inhibited protein aggregation by approximately 29 ± 2% (Figure 3.9 and 3.11). Under identical conditions, both A2M:Trp and A2M:Plm inhibited CPK aggregation by approximately 94.4 ± 11% and 91.7 ± 3%, respectively. A2M:Trp inhibited CPK aggregation by 55.5 ± 2% when [A2M:Trp] = 0.3 µM and SMR (A2M:Trp):CPK = 1:31.3, while at an equivalent concentration native A2M did not significantly inhibit CPK aggregation. A2M:Plm complexes completely inhibited CPK aggregation at all concentrations tested. In CS aggregation assays, 1.5 µM native A2M (SMR of A2M:CS = 1:0.8) inhibited protein aggregation by approximately 40.0 ± 10% (Figure 3.9 and 3.11). Under identical conditions, both A2M:Trp and A2M:Plm inhibited CS aggregation to a similar extent as native A2M, by approximately 54.0 ± 8% and 26.1 ± 3%, respectively.

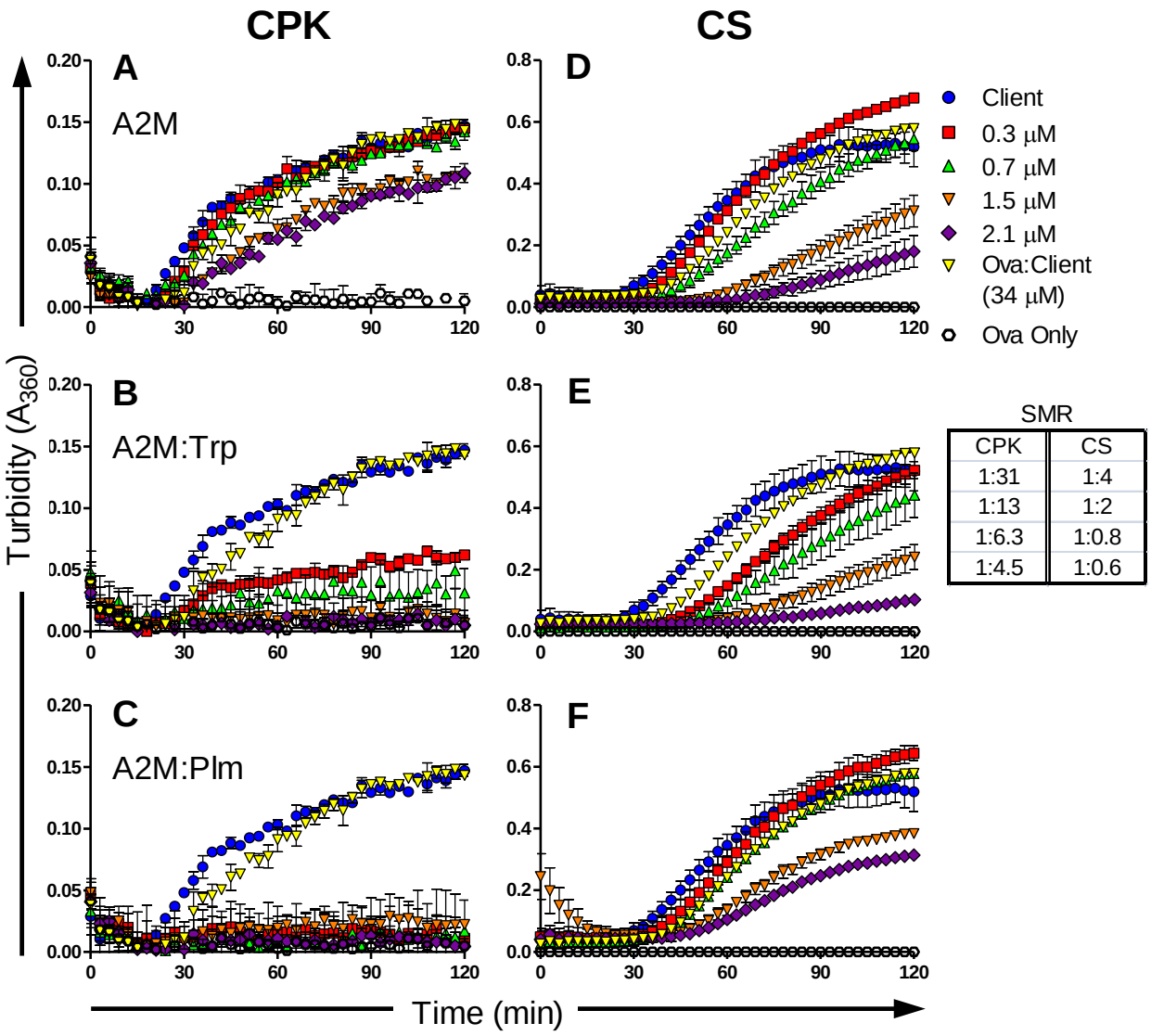

Figure 3.9 Native A2M and A2M:protease complexes inhibit heat-induced aggregation of CPK and CS. CPK (9.4 μM; A – C) and CS (1.2 μM; D – F) were induced to aggregate by heating at 43˚C in the absence or presence of increasing molar concentration and different SMR of native A2M, A2M:Trp and A2M:Plm complexes (indicated at top left of each panel), or non-chaperone control protein, Ova (equivalent to the highest mass concentration of A2M used). The ratios shown in the table below the key are SMR of A2M:client protein. The effects of A2M:protease complexes on CPK and CS precipitation were compared to an equal amount of native A2M tetramer. Data points represent the mean ± SD (n=9) of three separate experiments, where in each experiment measurements were performed in triplicate. In some cases, the error bars are too small to be visible.

Native A2M was previously shown to inhibit amorphous and fibrillar aggregation of a range of proteins (French *et al.* 2008; Yerbury 2009). To determine if A2M:protease complexes can also prevent fibril formation, we compared the ability of A2M:protease to inhibit the amyloid aggregation of RCM α-lact to that of native A2M. Heating RCM α-lact at 37˚C induced, from 40 – 1100 min, a dramatic increase in β-sheet content and a characteristic increase in ThT-associated fluorescence accompanying fibrillar aggregation (Figure 3.10). Native A2M (2 μM; SMR of A2M:client protein = 1:50) significantly inhibited this aggregation by approximately 21.2 ± 4 %; no further increase in inhibition was obtained at higher molar concentrations (and lower SMR) of native A2M to client protein (Figure 3.10 and 3.11). By comparison, at an equivalent concentration (and SMR), A2M:Trp and A2M:Plm complexes inhibited the protein aggregation by approximately 78.1 ± 3% and 44.3 ± 3%, respectively; There was no further inhibition at higher ratios of A2M:Plm to client protein, while A2M:Trp (20 μM; SMR of A2M:Trp complex:client protein = 1:5) there was complete inhibition of aggregation. Although at 10 – 20 μM A2M:Plm (SMR range from 1:10 – 1:5) there was a notable increase in the lag phase of the reaction from zero to 180 min. A2M:Trp complexes inhibited the aggregation of RCM α-lact to a greater degree than either native A2M or A2M:Plm. In all cases, the non-chaperone control Ova had no significant effect on end-point turbidity.

In summary, A2M:protease complexes were found to inhibit the aggregation of both CPK and RCM α-lact to a greater extent than native A2M over a lower SMR of chaperone:client proteins, with A2M:Plm having the greatest effect on CPK aggregation, and A2M:Trp having the greatest effect on RCM α-lact aggregation (Figure 3.11). All A2M species were found to inhibit the aggregation of CS to slightly differing degrees, with A2M:Trp complexes being more potent than A2M:Plm and native A2M over a lower SMR of chaperone:CS (Figure 3.11).

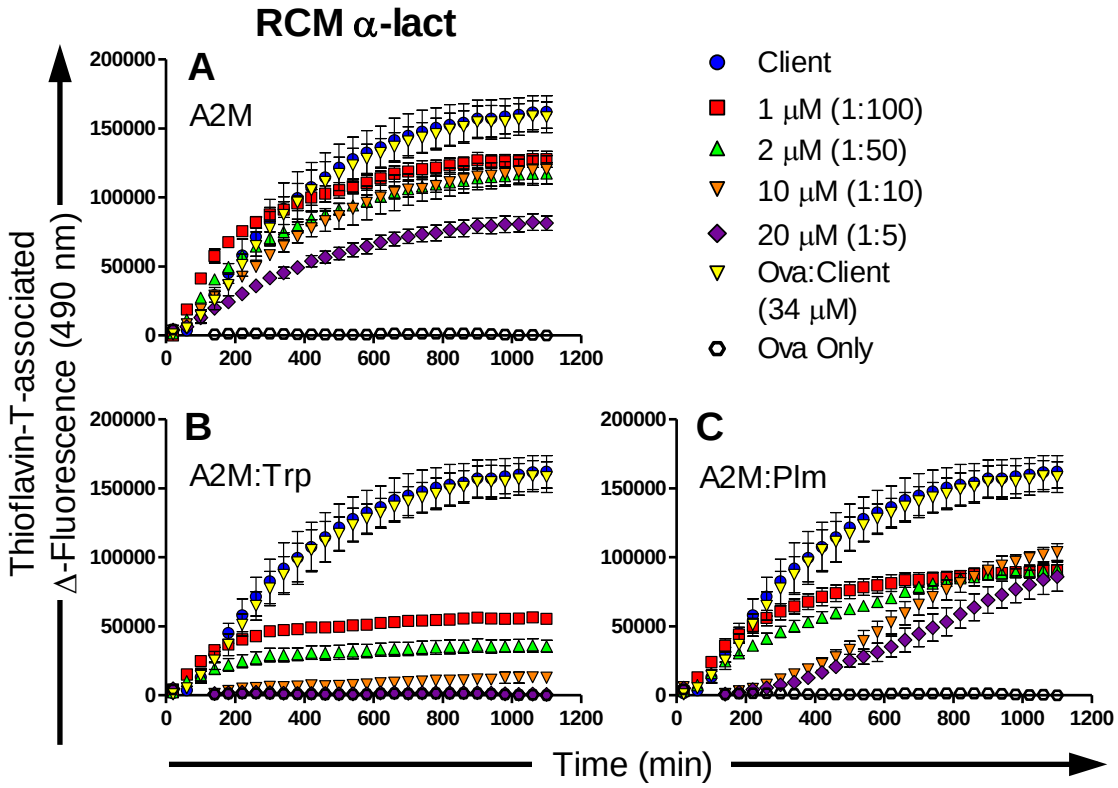

Figure 3.10 Native A2M and A2M:protease complexes inhibit heat-induced fibrillar precipitation of RCM α-lact. RCM α-lact (100 μM) was induced to aggregate by heating at 37˚C in the absence or presence of increasing molar concentration and different SMR of native A2M, A2M:Trp and A2M:Plm complexes (indicated at top left of each panel), or non-chaperone control protein, Ova (equivalent to the highest mass concentration of A2M used). The ratios shown in the key are SMR of A2M:CPK. Amyloid aggregation of RCM α-lact was measured using ThT-fluorescence. The effects of A2M:protease complexes on CPK and CS precipitation were compared to an equal amount of native A2M tetramer. Data points represent the mean ± SD (n=9) of three separate experiments, where in each experiment measurements were performed in triplicate. In some cases, the error bars are too small to be visible.

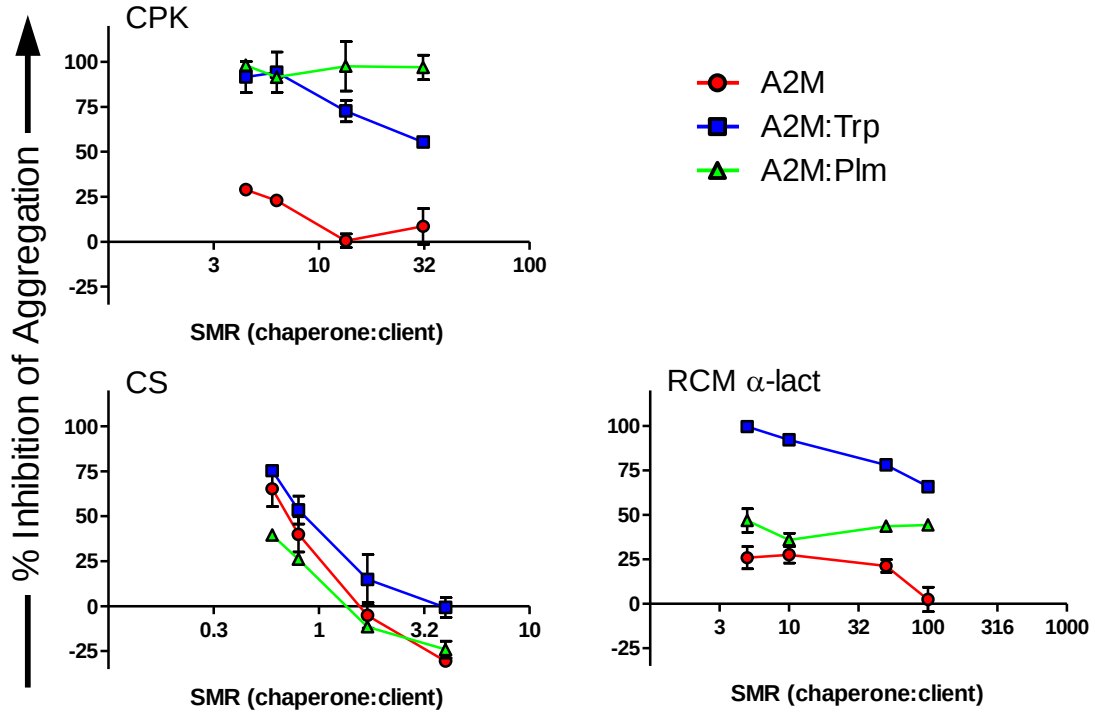

Figure 3.11 Inhibition of heat-induced aggregation of client proteins by native A2M and A2M:protease complexes, as a function of SMR. The % inhibition of protein aggregation at assay end-point (data from Figure 3.7 and 3.8) is plotted as a function of the SMR of A2M or A2M:protease complex to client protein (SMR was calculated as per section 3.2.6). The identity of each client protein is indicated at the top left of the respective panels. Lines between data points indicate a trend and have no theoretical significance. Data points represent the mean ± SD (n=9) of three separate experiments, where in each experiment measurements were performed in triplicate. In some cases, the error bars are too small to be visible.

End-point samples (prepared as in section 3.2.7) taken from protein aggregation assays containing (or not) native A2M, or A2M:Trp or A2M:Plm complexes were subsequently analysed by SDS PAGE to assess any proteolytic degradation of the client proteins. Samples from CPK aggregation assays containing A2M:protease complexes showed low molecular weight bands (<30 kDa in size) corresponding to proteolytic degradation products (~20% of the total protein by intensity) (Figure 3.12A, lane 3 and 4), and was coincident with a reduction in the intensity of monomeric CPK bands (~ 42 kDa). Analysis of samples from RCM α-lact aggregation reactions containing A2M:Plm complexes (but not other species) showed the appearance of lower molecular weight fragments (~30% of the total protein by intensity) (Figure 3.12B; lane 4), and was also coincident with a reduction in the intensity of

monomeric RCM α-lact (~ 14 kDa). A similar reduction in intensity was seen for samples containing A2M:Trp complexes (Figure 3.12B; lane 3), however, no degradation products were observed. These lower molecular weight bands were absent in samples from aggregation reactions containing native A2M (Figure 3.12A, B). Analysis of samples from CS aggregation assays (containing only CS) showed no degradation of CS during any of the assays conducted (Figure 3.12C). The minor bands present in samples containing A2M and A2M:protease complexes (lane 2 – 4) are also present in control samples on native A2M alone (lane 5). Suggesting these bands to be artefacts of the samples taken from these particular CS chaperone assays and not degradation products formed by the action of A2M:protease complexes.

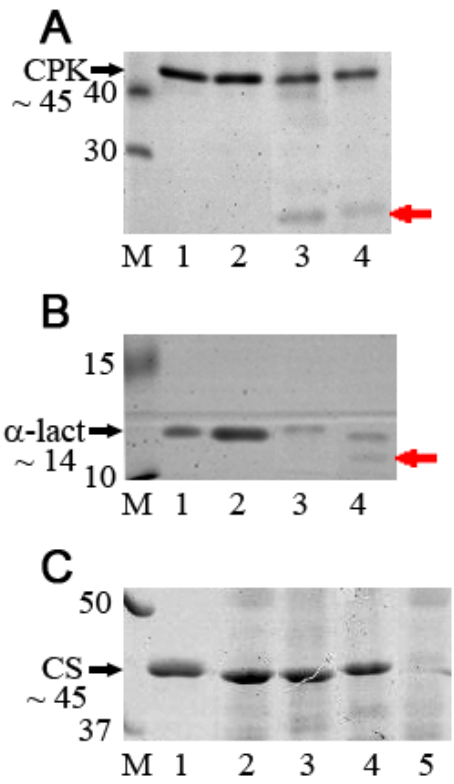

Figure 3.12 A2M:protease complexes proteolytically degrade CPK and RCM α-lact, but not CS. Samples (prepared as in section 3.2.7) taken from the end point of protein aggregation assays incubated in the absence (client protein; lane 1 in all panels) or presence of 0.7 μM of native A2M (lane 2 in all panels), A2M:Trp (lane 3 in all panels) or A2M:Plm (lane 4 in all panels) complexes, were analysed for proteolytic degradation of the client protein by reducing 10 – 15% SDS PAGE. Known molecular weight markers (M; BioRad) indicated in kDa. (A) CPK and (B) RCM α-lact incubated in the presence of A2M:Trp and A2M:Plm (but not native A2M), showed limited proteolysis of the client protein (degradation products indicated by red arrows). (C) CS incubated in the presence of A2M and A2M:protease complexes (lanes 2 – 4) showed the appearance of minor bands or greater and lower apparent mass than CS. Similar bands are also present in a control sample of native A2M alone (lane 5). Suggesting these bands to be artefacts of the samples taken from these particular CS chaperone assays and not degradation products formed by the action of A2M:protease complexes.

Taken together, the results of chaperone activity assays (Figures 3.9 – 3.11) and SDS-PAGE analysis of proteolytic degradation of client proteins by trapped protease(s) (Figure 3.12), suggests that A2M:protease complexes are in most cases more efficient at inhibiting protein

aggregation than native A2M. Small full-length client proteins such as α-lact (not shown) and RCM α-lact (14 kDa), as well as larger clients such as CPK (~42 kDa monomers) are bound and cleaved by A2M:protease complexes regardless of whether they aggregate via amorphous or fibrillar pathways.

Even though the monomers of CPK (~42 kDa) and CS (~45 kDa) are of similar molecular weights, only CPK was able to be cleaved, and both exceed the theoretical size limitations for diffusion into the intramolecular cavity of A2M as mentioned previously (section 3.3.6), with ≤ 20.1 kDa for A2M:Trp and ≤ 7 kDa for A2M:Plm (Barrett and Starkey 1973; Marrero *et al.* 2012). The ability of CPK to undergo limited proteolysis may be due to how the protein unfolds and binds to A2M:protease complexes, perhaps allowing unfolded flexible portions of the protein to enter the steric cage and be degraded by the trapped protease(s). However, this does not explain why CS did not undergo measurable proteolytic degradation. Although given the fact that in humans, A2M:protease complexes are bound by cell-surface receptors and rapidly cleared *in vivo* within minutes (Gliemann *et al.* 1985; Roche and Pizzo 1987; Roche and Pizzo 1988) the extent of any short-term minor proteolytic degradation of the client is likely to be of negligible physiological significance.

3.3.7 Prolonged activation of A2M by trypsin decreases the ability of A2M:protease complexes to inhibit stress-induced protein precipitation

As mentioned earlier (section 3.3.6), French *et al.* (2008) demonstrated that activation of A2M with Trp abolishes the chaperone action of A2M, whereas here it has been shown that complexes formed between A2M and either Trp or Plm are in fact chaperone active. There were methodological differences which may contribute to the discrepancies between the findings of this thesis and work by French and colleagues. These were in the preparation of A2M:Trp complexes, where French *et al.* incubated a six times molar ratio of Trp with native A2M for two hours (concentration, and incubation period of soybean trypsin inhibitor not stated), versus in this study where a three times molar ratio of Trp was incubated with A2M for one hour, and free protease was inactivated with a four times molar excess of inhibitor for one hour (section 3.2.3). The effects of (i) were tested for by incubating native A2M with Trp over 24 h, and producing purified A2M:Trp complexes which were subsequently tested for chaperone activity using *in vitro* aggregation assays (section 3.2.6). Following extended times of incubation of Trp with A2M, the ability of A2M:Trp complexes

to inhibit CS aggregation decreased (Figure 3.13). Proteolytic degradation of A2M by over-exposure to Trp may have been overlooked by French et al., as only Native-PAGE analysis was used to verify activation of A2M by Trp (SDS-PAGE analysis of A2M:Trp complexes is necessary to reveal limited degradation by Trp). This points to the conclusion that over-exposure of A2M to Trp is the most likely source of the discrepancies between studies.

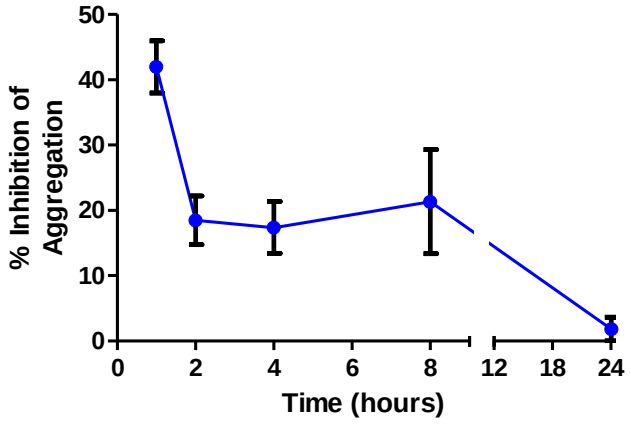

Figure 3.13 Prolonged activation of A2M by trypsin leads to decreased chaperone activity. A2M was incubated at room temperature with Trp for a range of times (1 – 24 h). Any remaining free trypsin was inhibited with trypsin inhibitor and A2M:Trp complexes were purified (section 3.2.3). CS (6 µM) was induced to aggregate by heating at 43˚C and incubated in the absence or presence of A2M:Trp at SMR of 1:4. Inhibition of aggregation at assay end-point is plotted as a function of Trp incubation time. Lines between data points indicate a trend and have no theoretical significance. Data points represent the mean ± SD (n=9) of three separate experiments, where in each experiment measurements were performed in triplicate.

3.4 DISCUSSION

3.4.1 Chaperone activity of A2M dimers

A2M dimers were shown to potently inhibit the stress-induced aggregation of a variety of proteins; this activity was more potent than that of the native A2M tetramer (Figure 3.6 and 3.7). Ozawa *et al.* (2011) demonstrated that SDS-induced dissociation of A2M into dimer pairs resulted in increases in both surface hydrophobicity and the ability to inhibit the aggregation of β2-microglobulin. The *in vivo* aggregation of β2-microglobulin is associated with dialysis-related amyloidosis (Gejyo *et al.* 1985). At normal physiological levels, human plasma A2M concentrations are in the range 2.8 – 5.6 μM (Gourine *et al.* 2002) and 4 – 5% of this extracellular A2M pool is in the form of circulating disulfide-linked dimers (Ozawa *et al.* 2011). It was previously shown that when native A2M was exposed to oxidative conditions (100 μM $CuSO_4$, 4 mM H_2O_2) it was able to potently inhibit the *in vitro* aggregation of both lysozyme and alpha-synuclein (French *et al.* 2008); these conditions are likely to have induced dissociation of native A2M into dimers.

Oxidation by neutrophil- and eosinophil-generated hypohalous acids (HClO, HBrO), N-chloramines (RNCl) and N-haloamines has been shown to dissociate native A2M homotetramer into two pairs of disulfide-linked dimers (Reddy *et al.* 1989; Reddy *et al.* 1994). Increased oxidative modification (carbonylation) of A2M has been shown in the plasma of patients with rheumatoid arthritis (accompanied by a two-fold higher expression of A2M) (Wu and Pizzo 2001) and Alzheimer's disease (Cocciolo *et al.* 2012). Rheumatoid arthritis and Alzheimer's disease are both associated with extracellular protein aggregation of IgG and Aβ peptide, respectively; as well as increased myeloperoxidase activity (Green *et al.* 2004; Stamp *et al.* 2012). The myeloperoxidase-H_2O_2-chloride system is used by neutrophils (or microglia) of the immune system to kill bacteria by oxidising bacterial proteins, however during inflammation the local concentration of OCl^- can reach high-μM or low-mM levels, damaging nearby proteins and tissues (Weiss 1989; Hampton *et al.* 1998; Vlasova *et al.* 2011). Consistent with these concentrations, disulfide-bonded A2M dimers were generated by treatment of native A2M tetramers with 500 μM NaOCl (Reddy *et al.* 1994) which disrupts the non-covalent interactions normally holding the two paired dimers together. The dimers produced are stable and do not re-associate (Figure 3.4). Furthermore, Wyatt *et al.* (2014) have reported dissociation of A2M into dimers by physiologically relevant OCl^-

concentrations in plasma (Wyatt *et al.* 2014). These findings support the possibility that OCl^- dissociation generated A2M dimers are *in vivo*, and is consistent with the observation that 4 – 5% of the extracellular A2M pool is in the form of circulating disulfide-linked dimers (Ozawa *et al.* 2011).

It is conceivable that A2M dimers may function as a physiologically important EC in rheumatoid arthritis and Alzheimer's disease given their significantly increased chaperone potency compared to that of native A2M (Figure 3.6 – 3.8), and this role may extend to other protein deposition diseases involving oxidative modification (OCl^--induced) of proteins, including osteoarthritis (Steinbeck *et al.* 2007), atherosclerosis (Hazell *et al.* 1994), kidney disease (Malle *et al.* 1997), and chronic lung disease (Buss *et al.* 2003).

3.4.2 Chaperone activity of A2M monomers

Stable monomers were generated under mild-reduction of native A2M with DTT and alkylating free S-H groups with iodoacetic acid (to prevent oxidative re-association) - producing identical monomeric subunits ~180 kDa (Figures 3.3) (Gonias and Pizzo 1983; Roche *et al.* 1988; Moncino *et al.* 1991). A2M monomers were shown to potently inhibit the stress-induced aggregation of CPK and CS; this activity was more potent than that of the native A2M tetramer (Figures 3.6 – 3.8). Diseases such as diabetes and cardiomyopathy induce acute phase protein responses. Diabetes is associated with both micro- and macrovascular complications that can lead to significantly elevated incidence of retinopathy, nephropathy, neuropathy, myocardial infarction and stroke (McAlpine *et al.* 2010). As mentioned in section 3.1, increased levels of A2M monomers have been found to be associated with reductive stress and with protein deposition in diabetic patients with retinopathy and nephropathy (Takada *et al.* 2013), myocardial infarction in diabetes (Annapoorani *et al.* 2006), cardiac hypertrophy (Rajamanickam *et al.* 1998), and cardiac diseases (Rathinavel *et al.* 2005; Ramasamy *et al.* 2006). Diabetes, diabetic nephropathy and cardiomyopathy all involve extracellular protein aggregation and deposition of: islet amyloid polypeptide from pancreatic β-cells in diabetes (Hoppener *et al.* 2000), complement C1q (Joh *et al.* 1990), and Tamm-Horsfall urinary glycoprotein (Rampoldi *et al.* 2003; Bleyer *et al.* 2005) in diabetic nephropathy, and αB-crystallin and cytoskeletal components in cardiomyopathy (Rajasekaran *et al.* 2007; Kannan *et al.* 2013). In addition, diabetes (Nardai *et al.* 2003), diabetic nephropathy (Ma *et al.* 2014), and cardiomyopathy (through sustained

activation of nuclear erythroid-2 like factor-2) (Rajasekaran *et al.* 2007; Kannan *et al.* 2013) are also associated with the unfolded protein response and shifts in endoplasic reticulum (ER) redox environment to a more reducing state, which may provide a pathophysiological mechanism by which A2M monomers are formed.

Thioredoxin is a small disulfide oxidoreductase and reduces disulfide bonds on target proteins, including the reduction of A2M to monomers (Larsson *et al.* 1988), which is secreted by lymphocytes in response to oxidative stress and inflammation (Kondo *et al.* 2004; Nakamura *et al.* 2006), providing a mechanism not directly related to any particular disease by which monomers can be generated extracellularly *in vivo* and may contribute to extracellular proteostasis.

The presence of A2M monomers in diseased patients, and the observation that misfolded proteins are a hallmark of these same diseases, suggests that A2M monomers may function as an EC in a physiologically relevant manner in diabetes (and diabetes-associated diseases) and cardiac disease, and possibly other protein deposition diseases involving redox stress of the extracellular environment, such as liver disease (Papp *et al.* 2006) and Alzheimer's (Garg *et al.* 2011).

3.4.3 Relationship between exposed hydrophobicity and the chaperone activity of A2M

Native A2M dissociated into dimers by treatment with either NaOCl or NaSCN, and into monomers by RCM, produced species with dramatically increased exposed hydrophobicity relative to the native or oxidized tetramer (Figure 3.5A, B). Based on the crystal structure of activated A2M, the contact surfaces between non-covalently bonded disulfide-linked dimer pairs are rich in hydrophobic residues (Marrero *et al.* 2012). Dissociation is thought to involve disruption of hydrophobic interactions between A2M subunits (Sjoberg *et al.* 1992); the dimer-dimer interface then becomes solvent exposed, effectively increasing the area available for A2M to bind to hydrophobic patches on misfolded proteins. The ability of extracellular chaperones, including A2M, to inhibit protein aggregation depends on hydrophobic interactions between the chaperone and the normally buried hydrophobic residues of misfolded client proteins, which results in the formation of chaperone:client protein complexes (French *et al.* 2008; Wyatt *et al.* 2009; Dabbs *et al.* 2013). Collectively,

these observations, together with the results of chaperone activity assays comparing A2M tetramers, dimers and monomers (Figures 3.6 – 3.8), suggest that the level of A2M chaperone activity strongly correlates with the level of surface-exposed hydrophobicity. This study did not examine whether A2M dimers and monomers formed soluble complexes with the misfolding client proteins, which is another aspect of extracellular chaperone activity. In summary, a central observation reported in this chapter, that exposure to sufficient levels of oxidative or reductive stress induces the dissociation of native A2M tetramers into dimers and monomers, respectively, that have enhanced exposed hydrophobicity and chaperone activity, may be of considerable physiological importance.

A2M dimers and monomers have been shown to function as protease inhibitors in avians, reptiles, amphibians and mammals (Sottrup-Jensen 1989; Rubenstein *et al.* 1993). Homologs of native A2M exist in humans, as extracellular dimers (pregnancy zone protein) and monomers (A2M like-1), in plasma and the granular layer of the epidermis, respectively (Galliano *et al.* 2006). Due to their predicted structural similarities with A2M (based on sequence homology) these molecules may also act as extracellular chaperones.

3.4.4 Chaperone activity of A2M:protease complexes

Activation of native A2M by reaction with either a nucleophile or a protease (Trp or Plm) induced a large conformational conversion to the fast-form (Figure 3.3) (Saunders *et al.* 1971; Barrett *et al.* 1979; Imber 1981). For diagrams of slow- and fast-form A2M refer to Figure 3.1C. This transition is accompanied by proteolytic cleavage of A2M which can be detected by the appearance of additional smaller bands in SDS-PAGE (Figure 3.3) (Harpel *et al.* 1979). As shown previously (section 3.4.2), DTT-induced dissociation of A2M generates monomers with increased chaperone activity relative to the native tetramer (Figure 3.6B). However, NH_4^+-activation of A2M conformationally stabilised and protected A2M from chemically-induced dissociation into dimeric and monomeric species (Figure 3.4). Intramolecular non-covalent interactions are stronger in the fast-form than the slow-form (Gonias *et al.* 1993; Shanbhag *et al.* 1996). Thus, A2M:protease complexes are highly unlikely to dissociate under conditions which would otherwise lead to the formation of chaperone active dimers or monomers *in vivo*. They are also rapidly cleared from circulation *in vivo*.

Native A2M inhibits the aggregation of a number of different amorphously aggregating and amyloid-forming proteins by interacting with transient species early in fibril formation, suppressing protein aggregation and mature fibril formation, and protecting cells from the toxicity associated with protein aggregates (Du *et al.* 1998; Yerbury 2009). A2M has been previously shown to have discrete binding sites for misfolded proteins and proteases, demonstrated by the fact that soluble A2M:protein client complexes can subsequently react with and trap proteases (Narita 1997; French *et al.* 2008). In the current study, A2M activated with either Trp or Plm prior to incubation with misfolding client proteins, was shown to potently inhibit the stress-induced aggregation of a variety of proteins. In the cases of the amorphous aggregation of CPK and amyloid formation by RCM α-lact, this activity was more potent than that of native A2M (Figure 3.9 – 3.11). Both A2M:protease complexes and native A2M inhibited the amorphous aggregation of CS to a similar extent (Figures 3.9 – 3.11). Proteolytic activation of A2M by either Trp or Plm produced complexes with a significantly more exposed hydrophobicity than the native tetramer (Figure 3.5C). It was previously shown that activation of A2M with methylamine or chymotrypsin significantly increases surface exposed hydrophobicity relative to native A2M (Birkenmeier *et al.* 1989). The ability of methylamine-activated A2M to inhibit protein aggregation has also been shown to be independent of a trapped protease (Wyatt *et al.* 2013). These results suggest that, as appears to be the case for A2M tetramers/dimers/monomers, the level of chaperone activity of A2M species incorporated into A2M:protease complexes may also correlate with the level of surface-exposed hydrophobicity. Methylamine-activated A2M, but not native A2M, has been shown to bind to and decrease the levels of soluble β-amyloid peptide (both 1 – 40 and 1 – 42 forms) associated with toxic, fibrillar aggregate formation in Alzheimer's disease by internalisation via receptor-mediated endocytosis (Narita 1997). In activated A2M, β-Amyloid binds to a discrete site in the RBD (residues$_{1314 - 1365}$; Figure 3.1A) (Mettenburg *et al.* 2002), and is disposed of by LRP-mediated endocytosis in cortical neurons (Narita 1997; Du *et al.* 1998; Qiu *et al.* 1999).

As mentioned earlier (section 3.1), sterically trapped proteases remain active and are able to degrade molecules which are small enough to diffuse into the intramolecular cavity of A2M:protease complexes. A2M:protease complexes were able to proteolytically degrade CPK and RCM α-lact, but not CS (Figure 3.12). A2M:protease complexes have also been shown to proteolytically degrade β-amyloid peptide (~4 kDa) *in vitro*, which may further

reduce concentrations of aggregation-prone peptide (Lauer *et al.* 2001; Wyatt *et al.* 2013). It is currently unknown whether A2M:protease complexes degrade proteins *in vivo*, but is likely not physiologically relevant in humans as, A2M:protease complexes are bound by cell-surface receptors and internalised within minutes (Gliemann *et al.* 1985; Roche and Pizzo 1987; Roche and Pizzo 1988).

A2M:protease complexes are responsible for approximately 3% of the total A2M pool of 2.8 – 5.6 µM, in blood plasma and sera (Zhabin and Zorin 1995). The concentration of circulating A2M:protease complexes is increased in many disease states including acute pancreatitis (Banks *et al.* 1990; Banks *et al.* 1991), arthritis (Abbink *et al.* 1991), diabetic retinopathy (Sanchez *et al.* 2007), multiple sclerosis (Gunnarsson *et al.* 2000) and sepsis (de Boer *et al.* 1993). As mentioned earlier, arthritis and diabetic retinopathy are both associated with extracellular protein aggregation. Moreover, acute pancreatitis (Schiesser *et al.* 2001; Ho *et al.* 2006), multiple sclerosis (Dasgupta *et al.* 2013; Stoffels *et al.* 2013; David and Tayebi 2014), and sepsis (Bodas *et al.* 2010) also present with extracellular deposits of insoluble protein aggregates. The increase in circulating A2M:protease complexes is mostly attributed to increased extracellular protease secretion and activity associated with these diseases, but may also include a response to protein aggregation. It is unknown whether A2M is involved in binding to and forming soluble A2M:client complexes with misfolded/unfolded proteins in these diseases *in vivo*. Protease activation of A2M after the formation of soluble A2M:client complexes has been shown to expedite disposal by LRP, and may facilitate clearance of misfolded client proteins via LRP in these diseases.

3.4.5 A2M and proteases in extracellular proteostasis

As mentioned previously, A2M can mediate the clearance of both misfolded proteins and proteases in diseases (section 3.1). Interestingly, amyloid fibrils, fibrin and denatured/misfolded proteins can bind to and stimulate initiation of extracellular proteolytic cascades, including the kallikren-kinin system and in particular the plg activation system (which will be explored in Chapter 4) (Kranenburg *et al.* 2002; Kranenburg *et al.* 2005; Maas *et al.* 2008; Gebbink *et al.* 2009; Gebbink 2011). Tissue plasminogen activator (tPA) is secreted from neurons and microglia following aggregate-induced excitotoxic injury, such as in Alzheimer's disease and spongiform encephalopathies (Fischer *et al.* 2000; Siao and Tsirka 2002; Siao 2003). tPA has been shown to bind to and become activated by structural

components of amyloid fibrils and aggregating proteins – which can act as both a co-factor and substrate (Kranenburg *et al.* 2002; Gebbink *et al.* 2009). This activated form of tPA cleaves plasminogen into the active serine protease Plm which can then degrade protein aggregates into plm-generated protein fragments (PGPFs; Chapter 5) (Lijnen 1982; Gebbink *et al.* 2009). A2M is synthesised by microglia and has been shown to accumulate near amyloid plaques in Alzheimer's disease (Hughes *et al.* 1998; Lauer *et al.* 2001). A2M can either function as a protease inhibitor and remove free Plm not bound to aggregates, and/or bind to misfolded/unfolded proteins (or PGPFs) and dispose of these via LRP receptor-mediated endocytosis – which can further stimulate secretion of both tPA and A2M by microglia. A2M:Plm complexes can bind to aggregating proteins or PGPFs and promote their disposal, while simultaneously stimulating the synthesis and secretion of A2M and Plg by mononuclear cells (Zhabin *et al.* 1995). Thus, the local concentrations of A2M, proteases and A2M:protease complexes in protein deposition diseases such as Alzheimer's disease may be increased in a feed forward mechanism, and promote the rapid clearance of misfolded client proteins.

3.4.6 Conclusion

Collectively, A2M has been shown to bind to many diverse ligands and proteases, influence the immune response, and inhibit the amorphous and fibrillar aggregation of client proteins. Collectively, the established literature and the results presented here show that the chaperone activity of A2M can be changed in response to a variety of conditions related to diseases, such as reductive/oxidative stress, inflammation, the acute-phase response, and increased protease secretion. A model is presented to describe the potential physiological significance of these findings; incorporating A2M tetramers/dimers/monomers and A2M:protease complexes into an extracellular quality control mechanism (Figure 3.14). In conclusion, the significance of the findings in this Chapter may be far-reaching. A greater understanding of the mechanisms by which A2M is able to prevent protein aggregation and facilitate the disposal of misfolded protein molecules could, in future, provide potential therapeutic targets for a host of degenerative conditions.

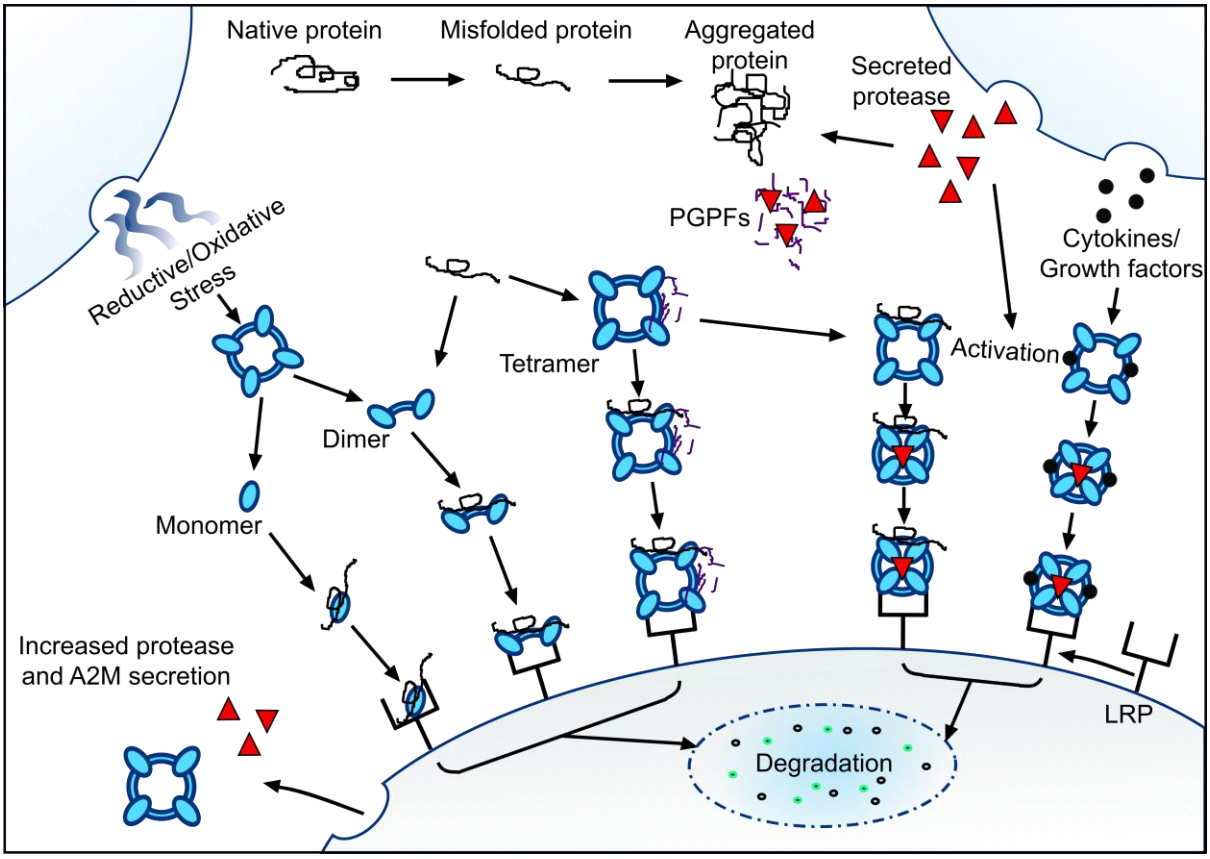

Figure 3.14 Hypothetical model of overlapping physiological roles of the chaperone and protease-trapping activities of A2M. Native tetrameric A2M can be dissociated by reductive or oxidative (redox) stress to form A2M monomers and dimers, respectively. A2M species can inhibit aggregation by binding to misfolded and aggregating proteins via hydrophobic interactions, thereby facilitating their removal via LRP receptor-mediated endocytosis. tPA-generated Plm can either (i) bind to and degrade protein aggregates into Plm-generated protein fragments (PGPFs), or (ii) be inhibited by forming A2M:Plm complexes, which expose LRP-binding sites. Once formed, A2M:Plm complexes can subsequently bind to misfolded proteins or PGPFs and be disposed of via LRP-mediated endocytosis, which in turn induces increased expression and secretion of (i) tPA and A2M from microglia, and (ii) Plg and A2M from mononuclear cells. Collectively, these interactions provide a feed-forward mechanism to co-localise chaperones and proteases at sites of protein aggregation, which act together to facilitate return of the system to normal healthy proteostasis.

CHAPTER 4 : THE INTERACTION OF AMORPHOUS AGGREGATES WITH THE PLASMINOGEN ACTIVATION SYSTEM AND EXTRACELLULAR CHAPERONES

4.1 INTRODUCTION

A complex and well characterised network of protein quality control mechanisms have evolved intracellularly to preserve proteostasis, involving a combination of two strategies that: (i) ensure correct protein folding and maintain solubility (Buchner 1996; Fink 1999), and (ii) degrade non-native or aggregated proteins. Both proteases and chaperones are key players in this context (Buchner 1996; Kaufman 2002). Corresponding extracellular mechanisms of proteostasis are much less well understood, even though many protein misfolding diseases present with pathologies characterised by the extracellular deposition of protein aggregates (Chapter 1; Table 1.1). Synergy between proteolytic systems and extracellular chaperones may be a functionally critical mechanism in extracellular proteostasis (Wyatt *et al.* 2013).

It has recently become apparent that, like in the intracellular environment, extracellular amyloid fibrils, fibrin and denatured/misfolded proteins can trigger responses from both chaperone and protease systems (Gebbink *et al.* 2009; Wyatt *et al.* 2010) and that the extracellular chaperone A2M can bind to toxic plasmin generated protein fragments (Zammit 2009). It is interesting to note that A2M is an extracellular chaperone, an immune-modulator, and also a well characterised protease inhibitor and modulator of plm activity (Sottrup-Jensen 1989; LaMarre *et al.* 1991; Feige *et al.* 1996).

The plg activation system may play an important role in maintaining extracellular proteostasis. tPA has been shown to bind to, and become activated by structural components of amyloid fibrils and aggregating proteins, acting as both a co-factor and substrate (Kranenburg *et al.* 2002; Gebbink *et al.* 2009; Samson *et al.* 2009). This activated form of tPA converts plg into plm which can then degrade protein aggregates (Lijnen 1982; Gebbink *et al.* 2009). This is akin to the dissolution of macromolecular fibrin-clots and re-modelling of the extracellular matrix by the plg activation system. Additionally, the altered expression of tPA, PAI-2 and other members of the plg activation system have been shown to deleteriously impact the brain during traumatic brain-injury-induced cell death and in Alzheimer's disease (Akiyama 1993 ; Dietzmann *et al.* 2000; Medcalf 2011). While amyloid fibrils have been shown to undergo limited proteolytic degradation by plasmin (Tucker *et al.* 2000), the

degradation of amorphously aggregating proteins have been poorly studied. It is currently unknown whether (i) amorphous aggregates can bind tPA and enhance plg activation, (ii) plm can clear these by proteolytically degrading them into fragments, and (iii) what biological impact this might have.

Many protein conformational disorders result in the pathological deposition of amorphous protein aggregates in the extracellular space. The G93A mutant of SOD, and IgG are two proteins deposited extracellularly (Chapter 1; Table 1.1). SOD_{G93A} is associated with familial cases of amytrophic lateral sclerosis, and while normally occurring as intracellular deposits, has been shown to be actively released into the extracellular environment following cell death/lysis, which may explain the prion-like spread of the disease (Adachi *et al.* 2000; Wang *et al.* 2002; Swash 2013). Extracellular deposits of aggregated and/or oxidised IgG are associated with corneal dystrophy, heavy chain deposition disease, multiple myeloma, and rheumatoid arthritis (Matthews 1983; Shultz *et al.* 1987; Aucouturier *et al.* 1993; Aucouturier *et al.* 1993; Khamlichi *et al.* 1995; Khamlichi *et al.* 1995; Truscott 2005). The plg activation system has been implicated in several of these diseases. Ovotransferrin (Ovo) has been routinely used as a client protein to assess the chaperone activity of ECs such as CLU and A2M (Poon *et al.* 2000; French *et al.* 2008).

The aims of the work described in this chapter were to investigate whether:

1. Amorphous aggregates formed by Ovo, SOD and IgG bind tPA and enhance plg activation.
2. The resulting plm generated is subject to inhibition by PAI-2 and A2AP.
3. Chaperone:client complexes enhance tPA-mediated plg activation.

4.2 METHODS

4.2.1 Clusterin purification

4.2.1.1 Immunoaffinity chromatography

Immunoaffinity columns (approximately 5 ml bed volume each) containing G7 and 41D anti-clusterin monoclonal antibodies (mAbs) coupled to Sepharose beads, produced by Mark Wilson's laboratory group (Illawarra Health and Medical Research Institute) (Wilson and Easterbrook-Smith 1992), were connected in tandem and equilibrated in PBS/0.1% Az at a flow rate of 0.5 mL/min using a Bio-Rad Econo-pump. Approximately 400 mL of filtered, citrated plasma as prepared in section 2.6, was applied over the columns at a rate of 0.5 mL/min or less, followed by PBS/0.1% Az to wash the columns. Non-specifically bound material was eluted from the columns by further washing with 50 mL 0.5% (v/v) Tx-100 in PBS followed by 50 mL of 200 mM sodium acetate containing 0.5 M NaCl, pH 5.0. Bound clusterin was eluted using 50 mL of 2 M GdHCl in PBS and dialysed into three changes of 3 L of PBS/0.1% Az followed by an additional two changes of 20 mM MES, pH 6.0.

4.2.1.2 Cation-exchange chromatography

Clusterin in 20 mM MES, pH 6.0 (section 4.2.1.1) was then further purified by cation exchange chromatography using a 1 mL HiTrap SP XL column (GE Healthcare) connected to a ÄKTA FPLC system (GE Healthcare). The column was equilibrated in 20 mM MES, pH 6.0 and the sample twice passed over the column at 0.5 mL/min to allow contaminants to bind. The flow through containing the unbound clusterin was collected. The bound contaminants were subsequently eluted using 1 M NaCl in 20 mM MES, pH 6.0. Clusterin was then concentrated using an Amicon Ultra-15 filter unit (Merck Millipore) with a molecular weight cut-off of 30 kDa and dialysed into three changes of PBS/0.1% Az and stored at 4˚C. Protein purity was assessed by 10% SDS-PAGE and protein concentration was determined by BCA assay (section 2.3).

4.2.2 Purification of plasminogen by Lys-affinity chromatography

Lysine-Sepharose 4B (GE Healthcare) was equilibrated in PBS as per manufacturer's instructions and 5 mL aliquots mixed with approximately 400 mL of filtered, citrated plasma (section 2.6) and incubated at 4˚C for 2 h with gentle mixing by inversion at 4 rpm, using a

rotory mixer (Ratek) at 4˚C. The Lysine-Sepharose 4B slurry (to which plasminogen was bound) were then washed with PBS by centrifugation (200 x *g* for 10 min at 4˚C) and resuspended in PBS containing 5 mM EDTA and 1 mM PMSF. The re-equilibrated slurry was then poured and allowed to settle into an empty XK 16/40 chromatography column (GE Healthcare) and connected to a Bio-Rad Econo-pump. Loosely bound proteins were then washed from the column at 0.5 mL/min using (i) 200 mL of PBS containing 5 mM EDTA and 1 mM PMSF, and then (ii) 100 mL of 0.5 M NaCl, 50 mM Na_2HPO_4, pH 7.4. Bound plasminogen was then eluted at 0.5 mL/min using 200 mM ε-aminocaproic acid in PBS, collecting 2.5 mL fractions. Three main protein peaks were eluted corresponding to Glu-plasminogen, a mixture of Glu- and Lys-Plasminogen and a mixture of plasminogen and plasmin. These fractions were immediately dialysed against three changes of PBS to remove ε-aminocaproic acid and stored at -80˚C. Protein purity was assessed by 10% SDS-PAGE under non-reducing and reducing conditions and protein concentration was determined by BCA assay (section 2.3).

4.2.3 Purification of IgG by protein G affinity chromatography

A 5 mL HiTrap Protein G HP column (GE Healthcare) was equilibrated in 20 mM NaH_2PO_4, pH 7.0, before 20 mL of filtered, citrated plasma (section 2.6) was passed over the column at 1 mL/min. The column was subsequently washed with firstly 20 mM NaH_2PO_4, pH 7.0, and then 0.5 M NaCl, 50 mM sodium acetate, pH 5.0. Finally, the bound IgG was eluted with 10 mL of 0.1 M glycine-HCl, pH 2.3, and 1.5 mL fractions were collected in tubes containing 200 µL of 1 M Tris-HCl, pH 9.0 to neutralise the acidity of the eluate. Fractions were then analysed by 8% SDS-PAGE and those containing IgG were pooled and dialysed against three changes of PBS and stored at -20˚C. Protein concentration was determined by BCA assay (section 2.3).

4.2.4 Expression and purification of recombinant superoxide dismutase-1

4.2.4.1 Culture of transformed bacteria and lysis

The expression vector pACA-forward yCCS SOD1 (Lindberg 2004) containing the gene for the G93A mutant of Cu/Zn- superoxide dismutase 1 (SOD) was transformed into the *Escherichia coli* strain DH5α, a single colony was selected for and amplified on plates of LB agar containing 0.1 mg/mL carbenicillin (Carbenicillin direct) as a selective agent. Starter

cultures of 20 mL of 2 x LB (20 g/L sodium chloride, 20 g/L bactotryptone and 10g/L yeast extract) containing 0.1 mg/mL carbenicillin (20 mL, per 1 L flask) were inoculated with a transformed colony and grown overnight at 37˚C with shaking at 180 rpm. Overnight starter cultures were transferred to two flasks containing 1 L of 2 x LB and 0.1 mg/mL carbenicillin and incubated at 37˚C with shaking (Bioline-8000) at 180 rpm until reaching an OD of 0.5. 3 mM $CuSO_4$ and 40 µM $ZnSO_4$ was added to 1 L cultures for incorporation into the catalytic active sites of SOD. Cultures were then induced with a final concentration of 0.5 mM IPTG and grown at 18˚C overnight with shaking at 180 rpm. Bacteria were harvested by centrifugation at 6,000 x *g* for 10 min at 4˚C, in a Sorvall RC 6+ centrifuge (ThermoFisher). The bacterial pellets containing SOD were resuspended in 25 mL of 50 mM Tris, pH 7.5 containing 0.01 mg/mL each of DNase (Roche) and RNase (Sigma Aldrich) and twice treated with an EmulsiFlex-C5 high pressure homogenizer (Avestin) at a pressure of 75-150 MPa to lyse the cells. The lysate was centrifuged (Sorvall RC 6+) at 40,000 x *g* for 20 min at 4˚C to remove cell debris and the supernatant collected for subsequent purification.

4.2.4.2 Ammonium sulfate precipitation

The bacterial supernatant containing the G93A mutant of SOD (section 4.2.4.1) was heat denatured in a water bath at 55˚C for 30 min. The precipitated material was then removed via centrifugation at 40,000 x *g* for 20 min at 4˚C and discarded. Ammonium sulfate was then added to the supernatant fraction, slowly and with continuous stirring at 4˚C, to 60% of saturation. The saturated mixture was allowed to stir for a further two hours before the precipitated material was then removed by centrifugation at 40,000 x *g* for 20 min at 4˚C. Further ammonium sulfate was added to the supernatant fraction as before, to 90% of saturation. The saturated mixture was then incubated overnight with continuous stirring at 4˚C. The precipitate was harvested by centrifugation at 40,000 x *g* for 20 min at 4˚C and the supernatant carefully discarded. The pelleted material was washed gently by rinsing with distilled H_2O and redissolved in 150 mM NaCl, 50 mM Tris, pH 7.5 for subsequent purification.

4.2.4.3 Size exclusion chromatography

The ammonium sulfate fraction containing G93A SOD (section 4.2.4.2) was further purified by size exclusion chromatography (SEC) using a XK 16/70 column packed with Superdex 75 prep grade gel filtration medium (GE Healthcare) equilibrated in 150 mM NaCl, 50 mM Tris,

pH 7.5. The fraction was passed over the column at a rate of 1 mL/min. 1 mL fractions were collected using an ÄKTA FPLC system (GE Healthcare) and analysed by 12% SDS-PAGE. Those containing SOD and other contaminants were pooled and dialysed against three changes of 10 mM Tris, pH 8.0 and stored at 4˚C prior to further purification.

4.2.4.4 Anion-exchange chromatography

SEC-purified G93A SOD (section 4.2.4.3) was further purified by anion exchange chromatography using a 5 mL HiTrap Capto-Q column (GE Healthcare) connected to an ÄKTA FPLC system (GE Healthcare). The column was equilibrated in 10 mM Tris, pH 8.0 and SEC-purified G93A SOD (in the same buffer) loaded onto the anion exchange column at 1.0 mL/min. 50 mL of 10 mM Tris, pH 8.0 was used to wash the column before eluting the bound SOD with a salt gradient of 0-200 mM NaCl in 10 mM Tris, pH 8.0 at 1 mL/min over 60 mL. 1 mL fractions were collected and analysed by 12% SDS-PAGE. Those containing G93A SOD were pooled and concentrated using an Amicon Ultra-15 filter unit (Merck Millipore; 10 kDa molecular weight cut-off), dialysed against three changes of PBS/0.1% Az and stored at 4˚C. Protein concentration was determined by BCA assay (section 2.3).

4.2.5 Protein aggregation assays

Amorphous aggregation of proteins in 96-well microplates (100 µL/well) was measured as turbidity (changes in absorbance at 360 nm) using a FLUOstar or POLARstar spectrophotometer (BMG Labtech). Ovotransferrin (Ovo), immunoglobulin G (IgG) and Cu/Zn superoxide dismutase 1 (SOD) were selected as suitable target proteins for further experiments to elucidate the structural properties of aggregated proteins which activate extracellular proteases. Ovo (1.5 mg/mL, 13.2 µM) in PBS was induced to aggregate by heating at 60˚C for 120 min. IgG (1 mg/mL, 6.8 µM) in PBS was induced to aggregate by incubation with 500 µM NaOCl at 37˚C for 8 h. SOD (1.4 mg/mL, 44 µM) in PBS was induced to aggregate by incubation with 50 mM DTT and 5 mM EDTA at 37˚C for 24 h. For Ovo, aggregation mixtures were snap-frozen in liquid nitrogen at different time points over 90 min for use in later experiments. In separate experiments, to test whether chaperone:client complexes could enhance tPA-mediated plg activation, Ovo was heat-stressed to aggregate at 60˚C in the absence or presence of increasing SMR of CLU:Ovo to form high molecular weight (HMW) chaperone:client complexes. SMR and percent inhibition of aggregation was

calculated as described in section 3.2.6; except that the SMR was calculated assuming a CLU "subunit" to be comprised of the 80 kDa heterodimer form.

4.2.6 bisANS fluorescence assays

bisANS assays were performed as described in section 3.2.5; except fluorescence was measured spectrophotometrically over time measuring changes in exposed hydrophobicity of the client proteins under conditions which would induce their unfolding and aggregation (described in 4.2.5).

4.2.7 Thioflavin T fluorescence assays

Thioflavin T assays were performed as described in section 3.2.6, except fluorescence measurements were made using samples taken at different time points during the time course of protein aggregation assays. BSA was used as a negative control at equi-molar concentrations. Fibrillar aggregates of the SH3 domain (5 μM) of the p85α subunit of bovine phosphatidylinositol 3-kinase [kindly donated by Dr Justin Yerbury; (Kumita *et al.* 2007)] were used as a positive control.

4.2.9 Circular dichroism spectroscopy

Changes in secondary structure of aggregated protein samples were determined by Far-UV spectroscopy using a Jasco Model J-810 spectropolarimeter. Samples taken from protein aggregation assays (section 4.2.2) at reaction end-point (or in the case of Ovo, from 0-72 min) were diluted to 0.1 mg/mL and dialysed against 10 mM NaH_2PO_4, pH 7.4. Measurements of mdeg (θ) were made over 180-250 nm and the molar ellipticity was calculated using the following equation (Schmid, 1989):

$[\theta] = \theta*100*\text{molecular weight} / \text{concentration (mg/mL)}*\text{distance}*\text{number of amino acids}$

The percentage of α-helix for each protein was estimated from ellipticity at 222 nm using the following formula (Phillips *et al*., 1981):

$\%\ \alpha\text{-helix} = -(\theta_{222\ nm} - 4{,}800) / 45{,}400$

4.2.8 Size exclusion chromatography of protein aggregates

Native IgG (1 mg/mL, 6.8 µM) in PBS was incubated with 0-1000 µM NaOCl overnight (~8 h) or 500 µM for 0-7 days at room temperature. 100 µL of protein was injected onto a 10/300 Superose 6 GL (GE Healthcare) SEC column equilibrated in PBS connected to an ÄKTA FPLC system (GE Healthcare). Samples were run over the column at a flow rate of 0.3 mL/min and the absorbance of the eluate at 280 nm (A_{280}) continuously monitored. 150 µL fractions of oxidised IgG were collected and separated into HMW and monomeric species (corresponding to the two observed peaks in Figure 4.5) and in later experiments assayed for their ability to enhance the activation of plasminogen. The region of overlap between the peaks corresponding to HMW and monomeric species was estimated by overlaying chromatographs of IgG treated with increasing concentrations of NaOCl and untreated IgG. The difference in the area under the curve was calculated from these peaks excluding the region of overlap.

4.2.9 Scanning electron microscopy

Samples taken from the end-points of protein aggregation assays (section 4.2.2), or in the case of Ovo at a range of time points, were resuspended at a total protein concentration of 0.1 mg/mL in PBS and 2 µL of each sample was blotted onto formvar resin (with carbon coating) nickel mesh grids (Proscitech), incubated for 5 min at room temperature, washed three times with filtered dH_2O, and negatively stained with 1% (w/v) uranyl acetate in Milli-Q H_2O. The specimens were then examined using a JSM7500FA cold Field Emission Gun Scanning Electron Microscope (JEOL) with an acceleration voltage of 20.0 kV and a working distance of 8 mm (spot size setting of 8). The detector used was a transmission electron detector mounted beneath the specimen platform (JEOL). Secondary electron images were taken with a semi in-lens detector at a working distance of 8.0 mm.

4.2.10 Plasminogen activation assays

Samples taken either at various time points or at the endpoints of the protein aggregation assays (section 4.2.5), were dialysed into HBST (10 mM HEPES, 150 mM NaCl, 0.01% (v/v) Tween 20, pH 7.4) and quantified by BCA assay (section 2.3) prior to subsequent experimentation. In the case of Ovo and SOD, aggregates were also centrifuged (Heraeus

Fresco 21; ThermoFisher) at 15,000 x *g* for 30 min at 4˚C for separation into insoluble and soluble fractions and dialysed as above. The samples were then analysed for their ability to enhance tPA-mediated plg activation to plasmin by measuring changes in absorbance resulting from the conversion of the plasmin-specific chromogenic substrate H-D-norleucyl-hexahydrotyrosol-lysine-para-nitroanilide diacetate (SPEC-PL; American Diagnostica Incorporated) to para-nitroaniline. 500 nM of aggregated or native non-aggregated protein sample or fibrin (positive control) in ice-cold HBST was incubated with 250 nM plg (in some experiments in the absence or presence of 10 mM tranexamic acid (TXA), a competitive lysine-binding site inhibitor of plg) and 500 nM SPEC-PL in a 96-well polystyrene microplate (Greiner Bio-one) at a total volume of 60 µL per well. The reaction was initiated by adding 10 µL of recombinant human tPA (Actylise; Boehringer-Ingelheim, Australia) to a final concentration of 5 nM per well. Absorbance at 405 nm (A_{405}) was read on a Spectramax Plus 382 plate reader (Molecular Devices) for 120 min at 37˚C with measurements taken at 30 s cycles with 3 s of shaking between cycles. To determine whether A2AP (Calbiochem) or recombinant PAI-2 [kindly donated by Prof. Marie Ranson; (Cochran *et al.* 2009)] could inhibit plg activation by protein aggregates, ternary complexes were first allowed to form between tPA, plg and the aggregate sample for 30 min in HBST at 37˚C, and then incubated (or not) with either 400 nM A2AP or 200 nM PAI-2 for a further 15 min, prior to measuring plasmin activity.

Various background controls for plm activity in the absence of fibrin or aggregated proteins (eg. tPA/SPEC-PL, plg/SPEC-PL, SPEC-PL alone) were included in all assays and subtracted from the raw data. These were essentially negative/zero indicating the absence of contaminating plm in the tPA, plg or SPEC-PL components. Background controls for assays conducted in the presence of fibrin or aggregated proteins (e.g., Ovo/SPEC-PL, Ovo/plg/SPEC-PL, Ovo/tPA/SPEC-PL) were also included and subtracted from the appropriate raw data. All experiments for Ovo were performed at once, but on separate days for SOD and IgG. Solubilised fibrin stock (25 mg/mL) was prepared as per the manufacturer's instructions by addition of 1 M NaOH to powdered fibrin (Sigma-Aldrich, USA), and then aliquoted and stored at -20˚C. Different aliquots were used for each series of experiments. Comparison of the effects of amorphous aggregates on plg activation were plotted as the change in A_{405} against time (t). The change in A_{405} is a function of SPEC-PL substrate cleavage by plasmin, generated during the tPA-mediated activation of plg. For quantitative analyses the initial rate of change of plm activity (initial rate of reaction) was

calculated from the gradient of the change in A_{405} versus t^2 (t^2 was used to linearise the curves and simplify calculation). Data transformation and linear regressions were performed using GraphPad Prism v5.0 (GraphPad Software).

4.2.11 Statistical Analysis

Data presented in the results was analysed using a one-way ANOVA and a Bonferroni multiple comparison post-test using GraphPad Prism v5.0, unless stated otherwise. The extent of significance between samples is denoted by the amount of asterix present in the graphs (*$p<0.05$, **$p<0.01$ and ***$p<0.001$).

4.3 RESULTS

4.3.1 Heat or chemical stress treatments of ovotransferrin, G93A mutant superoxide dismutase-1 and immunoglobulin-G produces amorphous protein aggregates

Hyper-physiological temperatures and oxidative stress are often associated with human diseases and can induce proteins to unfold from their native structure and subsequently aggregate to form either elongated amyloid fibrils or large amorphous clumps (Stranks *et al.* 2009). Heating native ovotransferrin (Ovo) at 60˚C resulted in extensive and rapid precipitation of the protein, shown by an increase in turbidity (measured as absorbance at 360 nm (A_{360})) after a lag phase of 20 min, followed by a rapid increase in absorbance to reach a maximum at approximately 120 min (Figure 4.1). Chemical denaturation of the G93A mutant of superoxide dismutase-1 (SOD) by chelation of metals using EDTA and reduction with DTT resulted in gradual precipitation of the protein after a lag phase of 250 min, followed by a rapid increase in turbidity to reach a maximum at 1100 min (Figure 4.1). In contrast, there was only a small linear increase in turbidity measured for oxidatively-stressed immunoglobulin-G (IgG), reaching a maximum at 1100 min (Figure 4.1).

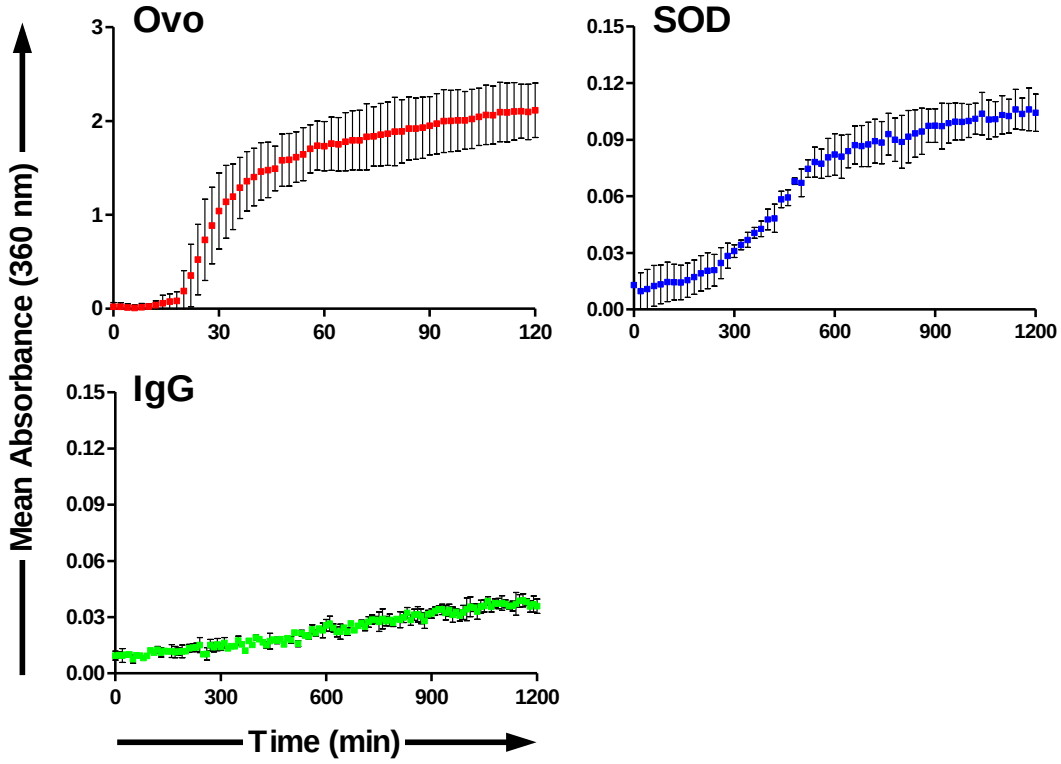

Figure 4.1 Heat and chemical stress-induced aggregation of Ovo, IgG and SOD. Ovo, SOD and IgG were induced to aggregate as described in section 4.2.5. Aggregation was measured as increasing turbidity (changes in absorbance at 360 nm) over time. Data points represent the mean ± SD (n=9) of three separate experiments, where in each experiment measurements were performed in triplicate.

A hallmark of protein aggregation is the exposure of normally buried hydrophobic residues during unfolding, which then allows the protein molecules to self-associate into an aggregation nucleus. The nucleus continues to grow in size (measured as an increase in turbidity; (Moreno *et al.* 2000)) until large insoluble aggregates are formed. The extent to which protein molecules exposed hydrophobicity to solution during stress induced aggregation was probed using bis-ANS fluorescence. During the heat-induced unfolding of Ovo, a dramatic increase in bisANS-associated fluorescence was measured over time, reaching a plateau at 60 min and a maximum value at 90 min (Figure 4.2). Chemical denaturation of SOD resulted in an increase in bisANS-associated fluorescence after a lag phase of 100 min, followed by a further rapid increase to reach a plateau at 300 min, followed by a slight linear reduction in fluorescence until the end of the time course (Figure 4.2). When the kinetics of changes in bisANS fluorescence are related to turbidity measurements in Figure 4.1, for both SOD and Ovo, normally buried hydrophobic residues are exposed

before there is a measurable increase in turbidity. During oxidation, IgG produced a small linear increase in bisANS fluorescence following a lag phase of 300 min (Figure 4.2).

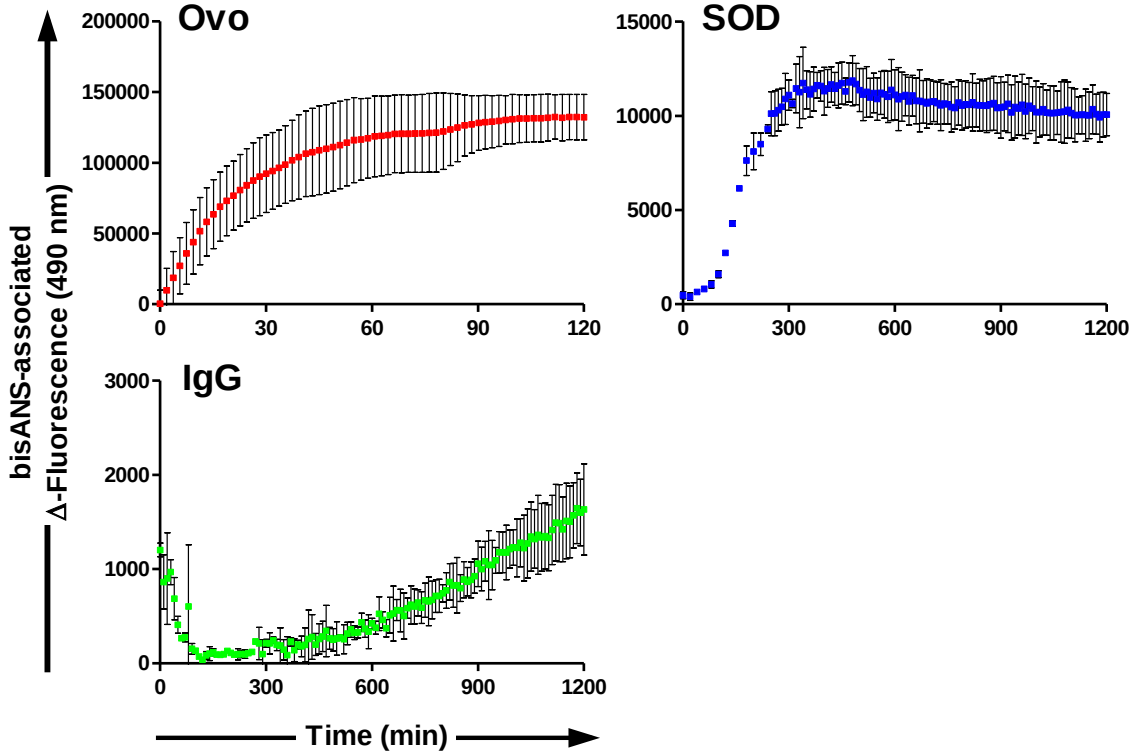

Figure 4.2 Aggregation of Ovo, SOD and IgG results in increased exposed hydrophobicity. Ovo, SOD and IgG were induced to aggregate as described in section 4.2.5. Exposed hydrophobicity was measured as mean bisANS-associated fluorescence intensity over time. Data points represent the mean ± SD (n=9) of three separate experiments, where in each experiment measurements were performed in triplicate.

Samples of Ovo were taken at increasing times during the aggregation time course and snap-frozen in liquid nitrogen for use in later experiments. These samples were also examined for changes in secondary and tertiary structure using far-UV circular dichroism (CD) spectroscopy and thioflavin-T (ThT) fluorescence measurements, respectively. Furthermore, samples of SOD were taken at reaction end-point and measured for ThT fluorescence. The far-UV CD spectra of Ovo samples taken at various intervals during the aggregation reaction time were virtually superimposable; deconvolution of the spectra into their α-helical, β-sheet, β-turn and unordered structures showed that there were no significant changes over time (Figure 4.3). The relative ThT fluorescence (an indicator of cross-beta sheet structure) associated with Ovo samples taken throughout the aggregation time-course reaction and end-

point SOD samples was similar to native BSA and ThT alone, and significantly lower than that measured for fibrillar aggregates of the SH3 domain ($p < 0.001$; Figure 4.4). This indicated that heat-denatured Ovo and chemically-denatured SOD do not form fibrillar aggregates associated with cross-beta structure.

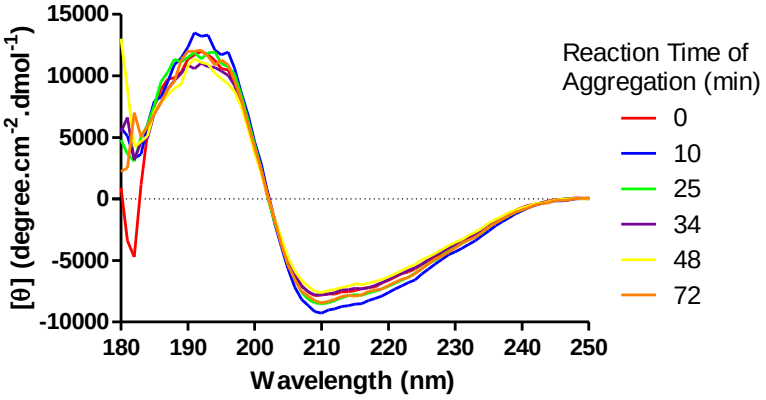

Figure 4.3 Heat-stress induced aggregation of Ovo does not result in significant changes to secondary structure content. CD spectra of Ovo aggregate samples (0.1 mg/mL) taken at increasing lengths of time from an aggregation reaction. The data shown are means of three scans; mean molar ellipticity is plotted (θ), calculated for Ovo (section 4.2.9), assuming a molecular weight of 76 kDa.

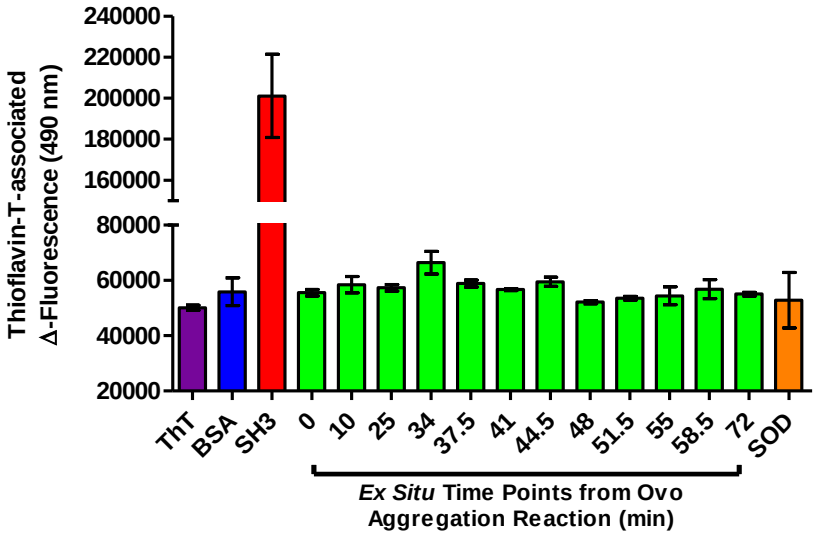

Figure 4.4 Ovo and SOD aggregates are not rich in beta-sheet content. Ovo (5 µM) and control proteins in PBS were heated at 60˚C. 25 µM Thioflavin-T was incubated in the absence (ThT; purple bar) or presence of samples of Ovo aggregates taken over the reaction time course (time is indicated) and the level of beta-sheet content was measured as the relative mean ThT fluorescence intensity (490 nm). Data points represent the mean ± SD (n=9) of three separate experiments, where in each experiment measurements were performed in triplicate. Fibrillar aggregates of SH3 (red bar) and native BSA (blue bar) were used at equi-molar concentrations as positive and negative control proteins, respectively.

Relative to SOD and Ovo, oxidatively-stressed IgG showed only minor changes in turbidity and exposed hydrophobicity. To confirm the presence of larger high molecular weight (HMW) species, indicative of protein aggregates, size exclusion chromatography was performed (Figure 4.5). The oxidation of IgG by NaOCl (0 – 7 days) did not produce aggregates of a size large enough to scatter visible light (therefore little change in turbidity was measured, Figure 4.1). SEC shows that monomeric species of IgG (normally ~150 kDa) can be induced to form larger HMW species, seen as a broad peak eluting from the column earlier, interpolated to be an average ~ 356 kDa in size (Figure 4.5 A). The difference in the area under the curves between IgG incubated in the absence or presence of NaOCl, suggests that approximately 60% of the protein formed larger species which are most likely in the form of soluble aggregates (Figure 4.5 A). Incubating IgG for a prolonged time (>24 h) did not result in an increase in HMW species being formed (data not shown for day 2-7). IgG incubated with increasing concentrations of NaOCl for 8 h showed increasing amounts of HMW species as a percentage of the total protein present in solution, ranging from ~ 5% (0

µM NaOCl) to a maximum of ~ 46% for 1000 µM NaOCl (Figure 4.5 B). A concentration of 500 µM NaOCl was chosen for use in later plasminogen activation experiments as a compromise between the amount of HMW generated and physiologically relevant NaOCl concentration (Bergt *et al.* 2001).

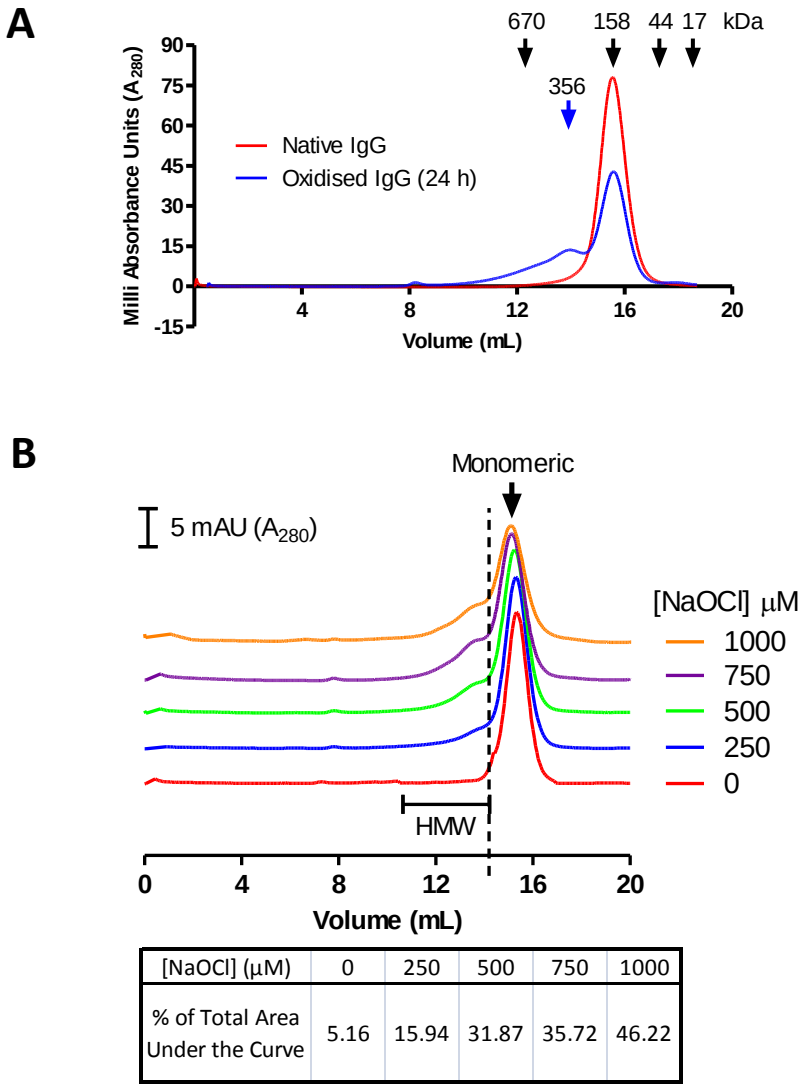

[NaOCl] (µM)	0	250	500	750	1000
% of Total Area Under the Curve	5.16	15.94	31.87	35.72	46.22

Figure 4.5 Oxidation of IgG produces soluble high molecular weight protein species. Native IgG (1 mg/mL, 6.8 µM) in PBS was incubated with (A) 500 µM NaOCl for 24 h or (B) 0-1000 µM NaOCl overnight (~ 8 h) then analysed by SEC and A_{280} monitored continuously during elution. The positions of molecular weight standards in (A) are indicated by black arrows at the top of the figure. The molecular weight interpolated using a standard curve is indicated by a blue arrow centred over a high molecular weight peak. The position of monomeric species of oxidised IgG in (B) is indicated by a black arrow at the top of the figure, while the position of high molecular weight (HMW) species is indicated by a capped bar below the traces. The vertical dashed line indicates the volume at which the two species were separated into fractions. The table beneath (B) indicates the % of the total protein comprised of HMW species at each corresponding concentration of NaOCl.

Scanning electron microscopy allowed visualisation of aggregates (Figure 4.6), with samples taken either at end points (for SOD and IgG; Figure 4.6 F, H, respectively) or at increasing lengths of time (from an Ovo aggregation reaction; Figure 4.6 A-D). Micrographs of Ovo, SOD and IgG displayed clumps of disorganised "amorphous" protein aggregates. Ovo aggregates increased in complexity and size with increasing aggregation reaction time. The structure of IgG was less complex than Ovo and SOD, and the protein aggregates were of a smaller and more compact size (much smaller than 1 μm), consistent with the observation that oxidation of IgG did not elicit large changes in turbidity (Figure 4.1). Micrographs of the corresponding native Ovo (0 min), SOD and IgG did not show any detectable aggregated protein (Figure 4.6 A,E,G).

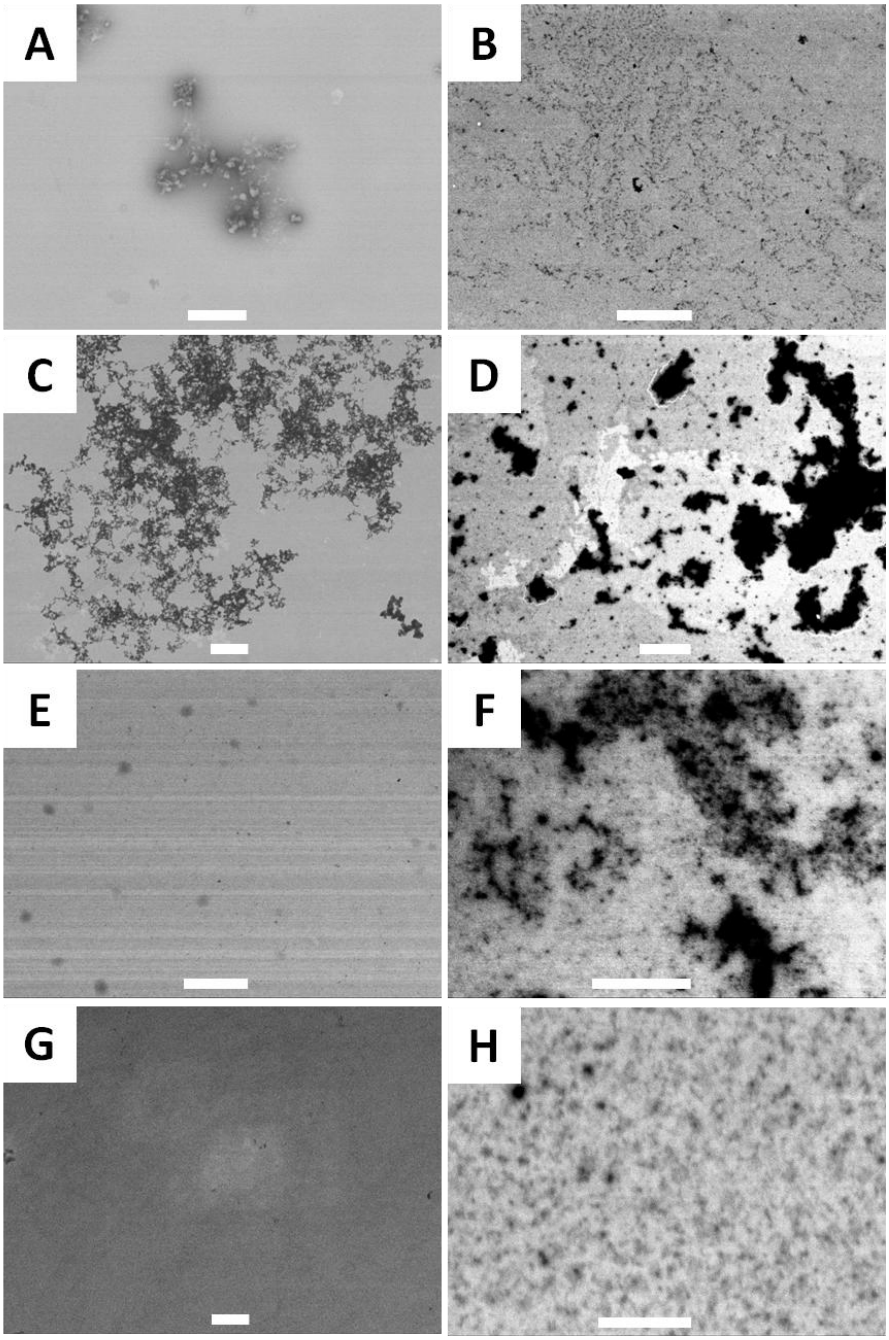

Figure 4.6 Representative scanning electron micrographs of native Ovo, SOD and IgG and their amorphous aggregates. Ovo aggregate samples (A-D) were taken from an aggregation reaction at 0 (A), 10 (B), 34 (C) and 72 (D) min. (E) Native SOD. (F) End-point samples of SOD aggregates taken post-aggregation (20 h). (G) Native IgG. (H) End-point samples of SEC purified HMW oxidized IgG aggregates following 8 h incubation with 500 µM NaOCl. White scale bars represent 1 µm in all cases.

4.3.2 Amorphous aggregates but not native proteins enhance the activation of plasminogen to plasmin

The plg activation system may play an important role in maintaining extracellular proteostasis (Yerbury *et al.* 2005; Gebbink *et al.* 2009). Tissue plasminogen activator (tPA) has been previously shown to bind to the cross-beta structure of fibrillar protein aggregates (Kranenburg *et al.* 2002). However, the ability of amorphous aggregates to interact with and activate elements of the plg activation system was previously unknown. The ability of amorphous aggregates to activate plg to plm in the presence of tPA was measured indirectly using the plm-specific chromogenic substrate SPEC-PL. As expected the positive control protein fibrin, by colocalising tPA and plg, considerably enhanced the activation rate of plg compared to tPA and plg alone (i.e., in solution) (Figure 4.7). Amorphously aggregated Ovo, SOD and IgG taken from the end-points of protein aggregation assays were also capable of enhancing tPA-mediated plg activation but were less efficient than fibrin (Figure 4.7). Native protein and oxidised monomeric IgG did not significantly enhance plg activation above that of tPA/plg alone in solution (Figure 4.7).

The initial rates of change of plasmin activity (refer to section 4.2.10 for method of analysis) were then calculated for the purpose of quantitative comparisons. Fibrin generated the fastest initial rate of change of plm activity with values ranging between assays from 80.0 ± 1.1 to 135.1 ± 1.2 $\mu A_{405}.min^{-2}$ (101 ± 30; n=9). By direct comparison to the intra-assay plg activation control (tPA/plg in the absence of cofactor) this equated to an average fold-increase of ~ 7.1 ± 1.7 (across three replicates). The corresponding calculated initial rates of change in plm activity for Ovo, SOD and HMW oxidised IgG aggregates ranged from 53.1 ± 2.2 to 28.2 ± 0.9 $\mu A_{405}.min^{-2}$ (36.4 ± 14.5 $\mu A_{405}.min^{-2}$; n=9), respectively. However, when expressed as a fold-increase compared to tPA/plg alone, all amorphous protein aggregates elicited similar increases in plg activation (mean fold-increase = 2.5 ± 0.4, n=3). This suggests that analogous to fibrin, amorphous aggregates likely colocalise tPA and plg, thereby acting as a cofactor to increase the rate of activation of plg to plm.

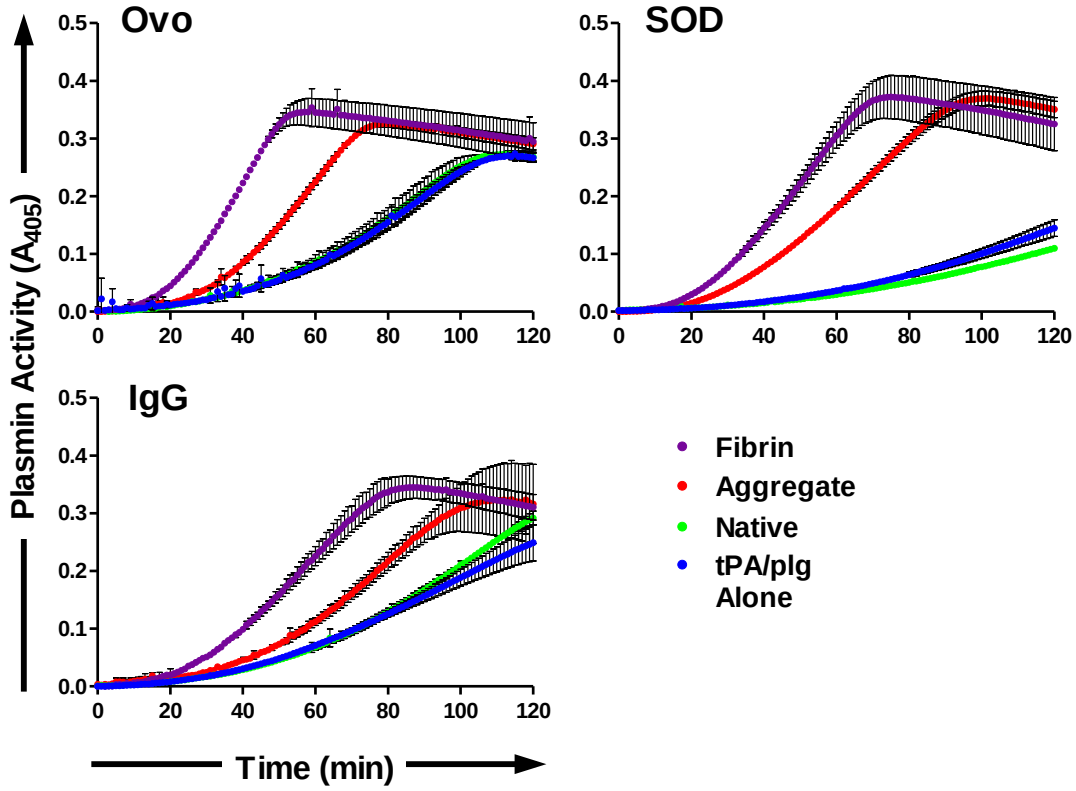

Figure 4.7 Amorphous aggregates of Ovo, IgG and SOD enhance tPA-mediated plasminogen activation. 500 nM of aggregated or native non-aggregated protein sample or fibrin (positive control) was pre-incubated in the presence of 250 nM plg and 500 nM SPEC-PL. The reaction was initiated by the addition of 5 nM tPA and the level of plm activity was measured spectrophotometrically (A_{405}) at 37°C for 120 min. Fibrin and tPA/plg alone served as interassay controls for plg activation in the presence or absence of cofactor. Data points represent the mean ± SD (n=9) of three separate experiments, where in each experiment measurements were performed in triplicate.

4.3.3 Plasminogen activation is enhanced by both insoluble and soluble Ovo aggregates

It is unknown which biophysical characteristics of amorphous aggregates mediate plg activation. To investigate this, the effects on plg activation of (i) the size and quantity of protein aggregates and (ii) the level of exposed hydrophobicity of aggregates were examined. Both soluble and insoluble protein species were examined. Ovo aggregate (Ovo Agg.) samples taken at various time points from an aggregation reaction were assayed for their ability to enhance tPA-mediated plg activation. Ovo Agg. samples taken at increasing time points (10 – 72 min) from the aggregation reaction elicited exponentially increasing initial rate of change of plm activity. The t=0 min sample did not enhance plg activation above tPA/plg alone (Figure 4.8); this is probably due to the absence of aggregated material, as visualised by SEM (Figure 4.6). The initial rate of change of plm activity correlated significantly with each of the following: aggregation time (Figure 4.8A; Pearson r =0.939; p =0.0001), hydrophobicity (Figure 4.8B; Pearson r =0.833; p =0.001), and turbidity (Figure 4.8C; Pearson r =0.748; p =0.005), the latter two after a lag phase. The greatest increase in initial rate of change of plm activity was seen using protein samples from 48 – 72 min of aggregation time, effectively doubling rates from 42.8 ± 2.6 to 72.3 ± 3.3 $\mu A_{405}.min^{-2}$. These time points correspond to the plateau phase of the turbidity curve shown in Figure 4.1.

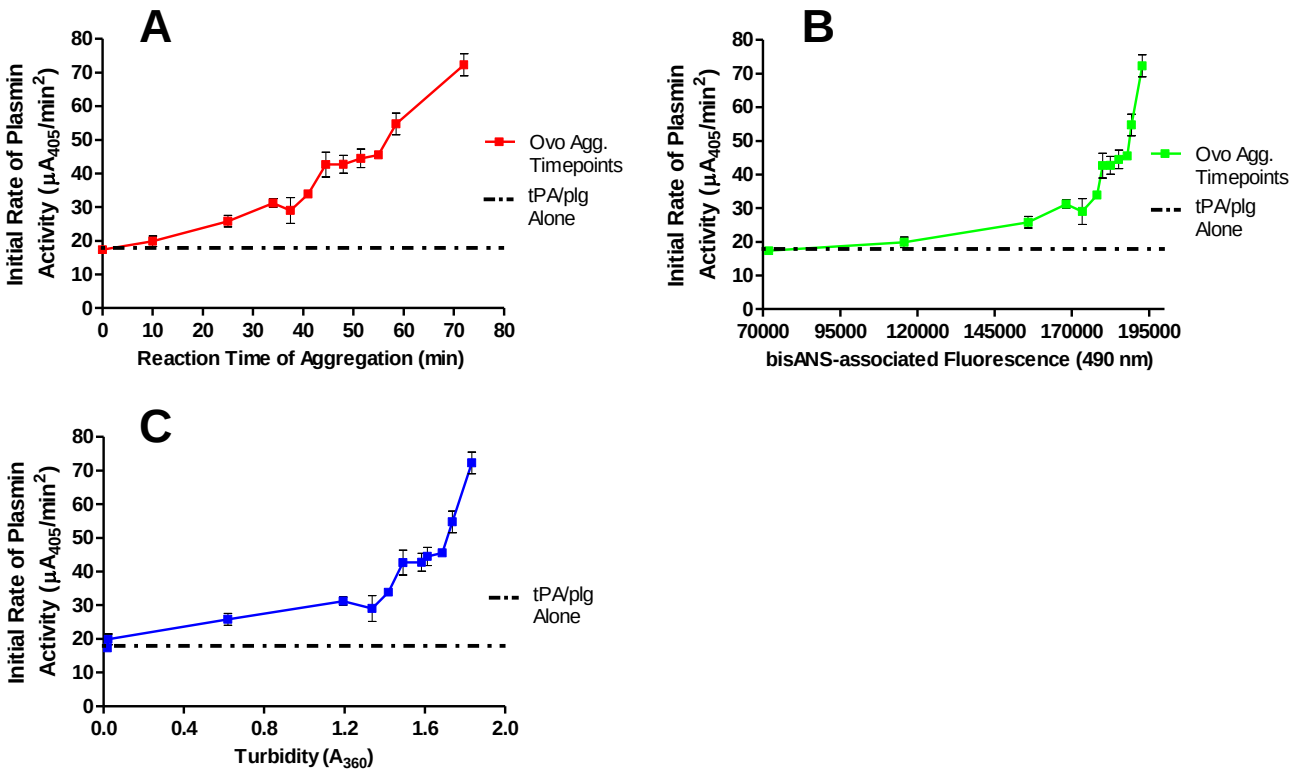

Figure 4.8 Initial rate of change of plm activity increases with the extent of Ovo aggregation, exposed hydrophobicity and turbidity. 500 nM of Ovo aggregate (Ovo Agg.) samples taken at increasing lengths of time from an aggregation reaction were dialysed against HBST and assayed for their ability to enhance tPA-mediated plg activation. The initial rate of change of plm activity was calculated as per section 4.2.10 and plotted versus: (A) The corresponding time at which the aggregate sample was collected from the reaction (section 4.2.5). (B) Exposed hydrophobicity of these samples (measured as bisANS-associated fluorescence). (C) Turbidity of these samples. The level of tPA-mediated plg activation in the absence of aggregates (tPA/plg alone) is indicated by the dashed black line. Data points represent the mean ± SD (n=9) of three separate experiments, where in each experiment measurements were performed in triplicate.

In parallel experiments, the same samples were centrifuged and separated into insoluble and soluble protein fractions. The initial rate of change of plm activity was measured and plotted against aggregation time (Figure 4.9). Insoluble aggregates sampled from after 10 min aggregation time elicited an overall higher rate of change of plm activity compared to soluble aggregates, reaching maximal rates of 124.5 ± 10.9 $\mu A_{405}.min^{-2}$ (48 min sample), versus 88.3 ± 2.8 $\mu A_{405}.min^{-2}$ (72 min sample) ($p < 0.01$) (Figure 4.9), respectively. Taken together these data indicate that the ability of Ovo Agg. to stimulate plg activation is dependant on the extent of protein aggregation (turbidity), and correlates with the extent of exposed

hydrophobicity present (Figure 4.8). Lastly, it appears that the larger insoluble aggregates are more efficient at generating plm than smaller soluble aggregates (Figure 4.9).

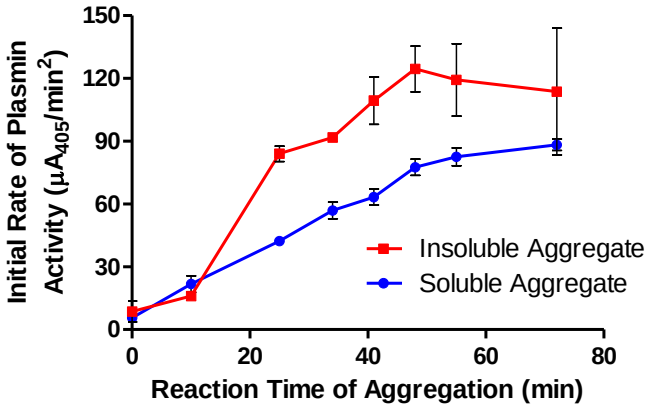

Figure 4.9 Both insoluble and soluble Ovo aggregates can activate plg. 500 nM of Ovo Agg. samples taken from an aggregation reaction (section 4.2.5) were separated into insoluble (red squares) and soluble (blue circles) fractions by centrifugation, dialysed against HBST and assayed for their ability to enhance tPA-mediated plg activation. Data points represent the average initial rate of change of plm activity ± SD and correspond to the time at which the aggregate sample was collected from the reaction (on the x-axis). Data points represent the mean ± SD (n=9) of three separate experiments, where in each experiment measurements were performed in triplicate.

4.3.4 The ability of oxidised IgG to activate plasminogen increased with the concentration of NaOCl used and increasing amounts of high molecular weight species generated

To investigate the possible role of tPA-mediated plg activation in inflammatory protein deposition diseases, IgG was first incubated with increasing concentrations of NaOCl for 8 h to produce increasing amounts of HMW species and then tested for their ability to enhance tPA-mediated plg activation. In some experiments, the oxidized IgG was fractionated by SEC into monomeric IgG and HMW species (Figure 4.5) before testing in the same assay. HMW oxidised (ox.) IgG induced tPA-mediated plg activation - this ability increased with the concentration of HMW ox. IgG (Figure 4.10 and 4.11). The ability of unfractionated mixtures of ox. IgG to enhance tPA-mediated plg activation increased with exposure to greater concentrations of NaOCl (Figure 4.12). In the case of 1 mg/mL IgG oxidized by exposure to 500 µM NaOCl, the level of plm activity elicited was similar to that elicited by the fibrin control (Figure 4.12). Neither native IgG nor ox. monomeric IgG (purified by SEC; Figure 4.5) were able to increase plm activation above background levels (Figure 4.10 and 4.11). A Michaelis-Menten equation was fitted to the data using GraphPad Prism v5 to determine the kinetic constants of tPA-mediated plg activation (Figure 4.11). For HMW ox. IgG, these analyses gave values for Vmax of 40.1 ± 2.1 $\mu A_{405}.min^{-2}$ and a corresponding value for Km of 1195 ± 170 nM, a value similar to the Km for plg activation in the presence of fibrin (990 ± 169 nM) (Fleury and Angles-Cano 1991).

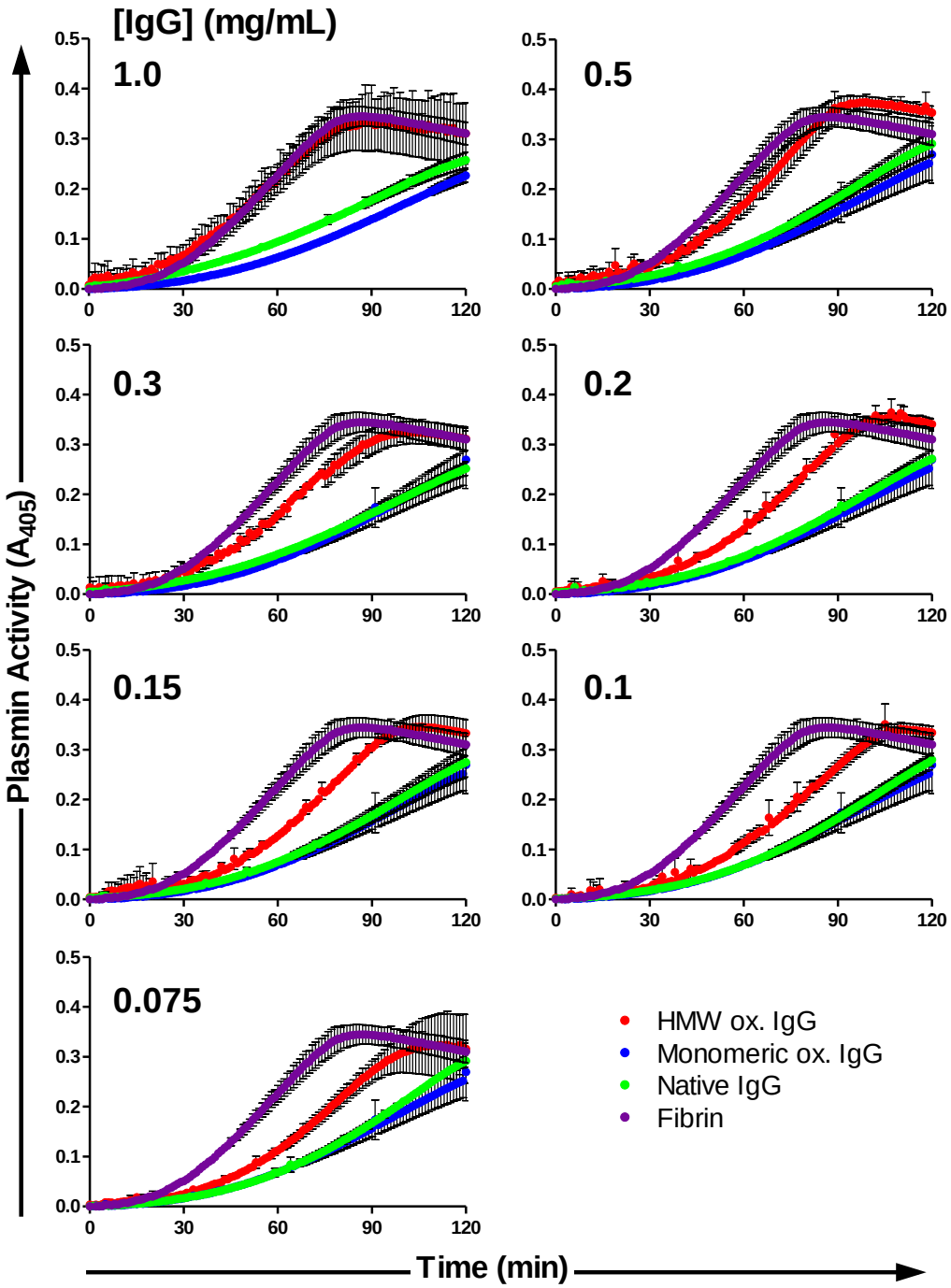

Figure 4.10 Increasing concentrations of high molecular weight but not monomeric ox. IgG enhance tPA-mediated plg activation. IgG was oxidised with 500 µM NaOCl in PBS, separated into high molecular weight (HMW) and monomeric species by SEC and dialysed against HBST. Increasing concentrations of both HMW and monomeric oxidised IgG (ox. IgG) and untreated native IgG (from 0.075 - 1 mg/mL) were incubated in the presence or absence of tPA and plg and substrate SPEC-PL and the level of plm activity measured. Fibrin was used as a positive control. Data points represent the mean ± SD (n=9) of three separate experiments, where in each experiment measurements were performed in triplicate.

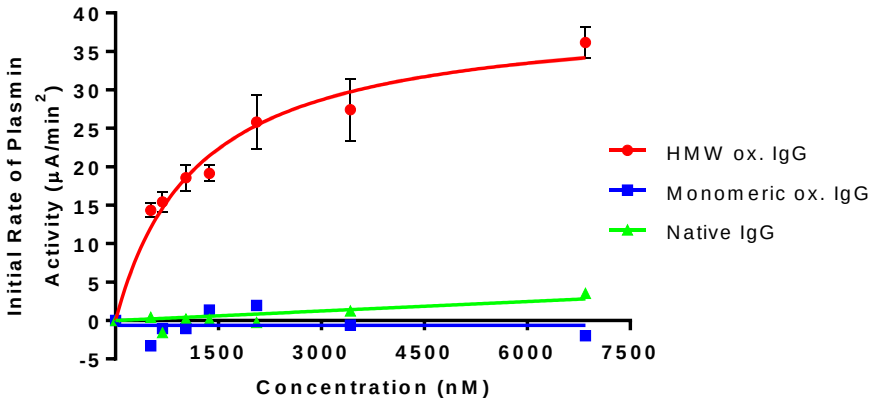

Figure 4.11 Michaelis-Menten curve fit to plot of initial rate of change of plm activity as a function of concentration of HMW ox. IgG. Initial rates from measurements of plm activity in Figure 4.11 were plotted against the concentrations of HMW and monomeric ox. IgG and native IgG. A Michaelis-Menten equation was fitted to the data to determine kinetic constants for HMW ox. IgG induced, tPA-mediated plg activation. Data points represent the mean ± SD (n=9) of three separate experiments, where in each experiment measurements were performed in triplicate.

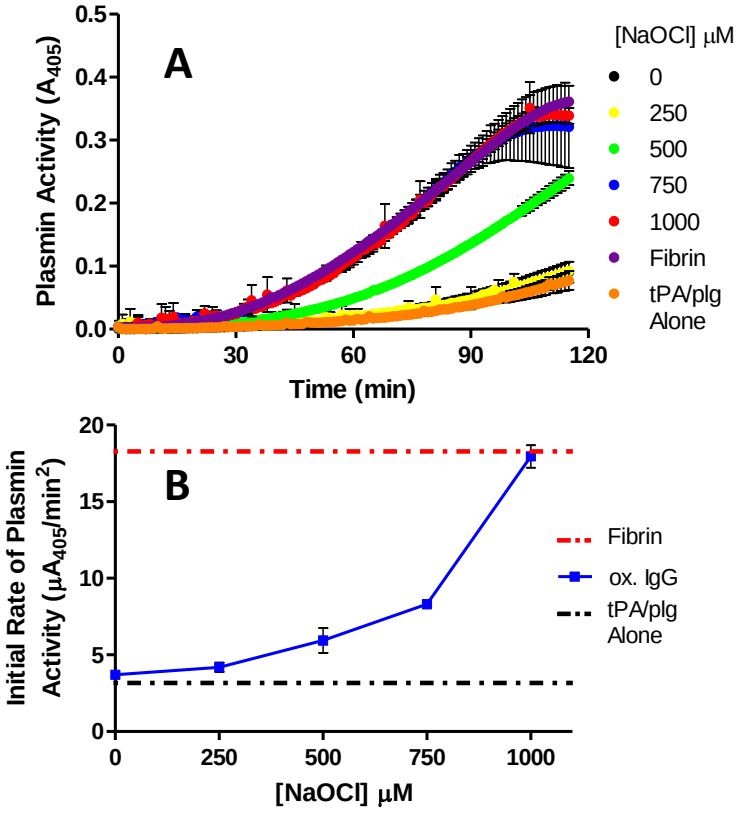

Figure 4.12 The effect of IgG oxidised with varying concentrations of NaOCl on initial rate of change of plm activity. (A) IgG was oxidised with varying concentrations of NaOCl (0-1000 μM) in PBS, dialysed and diluted to 500 nM in HBST and incubated in the presence or absence of tPA and plg and substrate SPEC-PL to measure the level of plm activity. Fibrin was used as a positive control. (B) Initial rate of change of plm activity in (A) was plotted against the concentration of NaOCl (μM) incubated with IgG. Levels of tPA-mediated plm activation (i.e. tPA/plg alone in the absence of IgG) are shown by the dashed black line. The red dashed line in (B) indicates the level of activation elicited by fibrin. Data points represent the mean ± SD (n=9) of three separate experiments, where in each experiment measurements were performed in triplicate.

4.3.5 Plasmin associated with insoluble aggregates of Ovo and SOD was resistant to inhibition by alpha-2-antiplasmin but not when associated with soluble aggregates

Plm bound to intact fibrin is protected from inhibition by the potent protease inhibitor alpha-2-antiplasmin (A2AP), allowing plm to perform a primary role - the efficient dissolution of fibrin-clots (Lijnen *et al.* 1982). To investigate whether plm generated in the presence of amorphously aggregated proteins was inhibited by A2AP, Ovo and SOD Agg. were separated into insoluble and soluble fractions by centrifugation and ternary complexes between plg, tPA and aggregate fractions formed before being incubated (or not) with A2AP and assayed for plm activity.

As shown previously in section 4.3.3 (Figure 4.9), both soluble and insoluble aggregates of Ovo and SOD taken at aggregation reaction end-points greatly increased plg activation relative to tPA/plg alone levels (Figure 4.13). In a manner similar to fibrin, insoluble protein aggregates of both Ovo and SOD were found to shield plm from inhibition by A2AP, while soluble aggregates did so to a significantly lesser extent (Figure 4.13). For samples of Ovo Agg. taken at 72 min of aggregation, A2AP inhibited the activity of plm associated with insoluble Ovo Agg. by 15.5 ± 3.1 %; in contrast, when bound to soluble Ovo Agg., A2AP inhibited plm activity by 60.6 ± 2.0 %. Similarly, for end-point samples of SOD Agg., A2AP inhibited plm associated with insoluble SOD Agg. by 12.78 ± 2.3 % compared with 66.9 ± 5.6 % inhibition for plm associated with soluble SOD Agg.

Taken together these results indicate that insoluble amorphous protein aggregates induce tPA-mediated activation of plg to plm, and like fibrin, shields substrate-bound plm from inhibition by A2AP. This would allow for the continued degradation of large insoluble protein aggregates into smaller fragments by bound plm, while keeping the plm activity restricted to the aggregate surface.

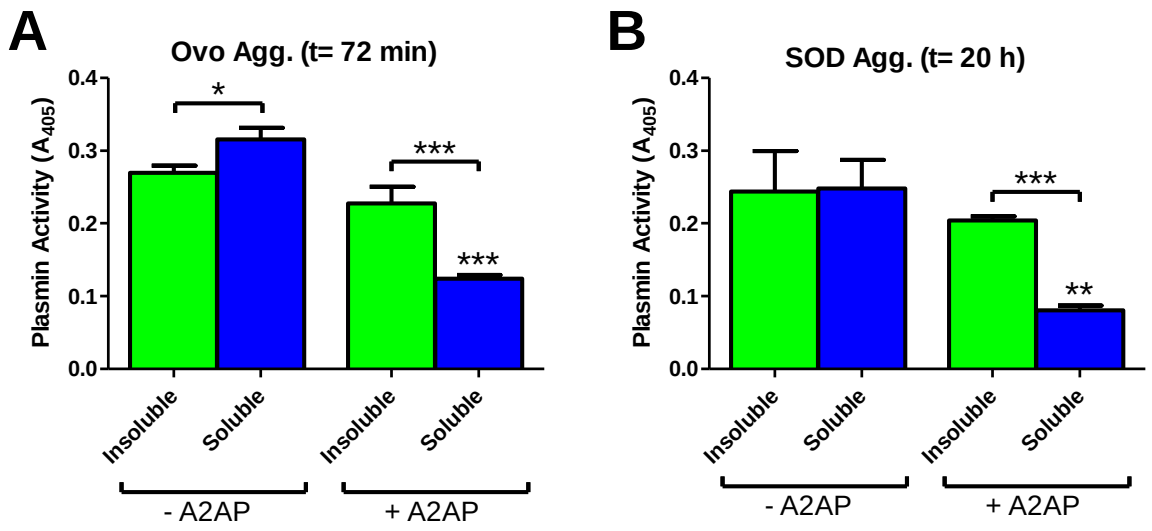

Figure 4.13 Effects of alpha-2-antiplasmin on tPA-mediated plasminogen activation induced by soluble and insoluble aggregates of Ovo and SOD. Soluble (blue bars) and insoluble (green bars) fractions prepared from samples taken at different times from an Ovo aggregation reaction (Ovo Agg.; A) and end-point (20 h) samples of a SOD aggregation reaction (SOD Agg.; B) were tested for their ability to activate plg in the presence or absence of 400 nM alpha-2-antiplasmin (± A2AP). tPA, plg and samples were allowed to form a ternary complex and and assayed for the ability to activate plm either prior to or after the addition of A2AP. Bar graphs showing plm activity at the end of 120 min time courses, with the type of aggregate and aggregation time indicated above. Data points represent the mean ± SD (n=9) of three separate experiments, where in each experiment measurements were performed in triplicate. Asterixes placed immediately above error bars indicate that the sample is significantly different to the corresponding sample lacking A2AP. Asterixes above horizontal brackets indicate a significant difference between the bracketed samples. * ($p<0.05$), ** ($p<0.01$), *** ($p<0.001$).

4.3.6 tPA and lysine-binding mediates the activation of plasminogen by Ovo and SOD aggregates.

The co-localised binding of plg and tPA to lysine residues in fibrin/ogen results in the enhanced activation of plg to plm, with fibrin/ogen acting as both a cofactor and a substrate for plm (Suenson and Petersen 1986). To further investigate the structural elements of the aggregates responsible for the enhanced plg activation observed above, the lysine-like analog tranexamic acid (TXA), which competes against plg for lysine-binding sites on target molecules (see Chapter 1; section 1.4) was used. PAI-2 (an active site inhibitor of tPA) is highly expressed in amyloid-containing microglial conglomerations associated with plaques in Alzheimer's disease patients (Akiyama *et al.* 1993). Therefore the question of whether the plm activity elicited by amorphous protein aggregates is, as for fibrin, shielded from inhibition by PAI-2 (Lobov and Ranson 2011) was also investigated (see Chapter 1; section 1.4). TXA significantly inhibited tPA-mediated plg activation induced by end-point Ovo and SOD aggregates by 97.7 ± 0.2 and 46.8 ± 1.2 %, respectively, compared to controls in the absence of TXA. In the case of fibrin-induced activation, inhibition was 62.0 ± 1.5 % of controls (Figure 4.10 A,B). In parallel experiments, TXA was found to significantly inhibit plg activation induced by samples from all Ovo aggregation reaction time points (ranging from 92.0 ± 2.3 to 102.2 ± 0.6 % inhibition; Figure 4.10 D). Thus, similar to fibrin-bound tPA, direct binding of tPA and plg to protein aggregates via lysine residues appears to be essential for efficient tPA-mediated plg activation.

PAI-2 significantly inhibited plm activity induced by end-point Ovo and SOD aggregates by 83.2 ± 0.7 and 77.1 ± 0.5 % respectively, compared to controls in the absence of PAI-2. A similar effect was found for fibrin-induced plm activity (64.6 ± 1.4 % inhibition) (Figure 4.10 A,B). In parallel experiments, PAI-2 was found to significantly inhibit tPA-mediated plg activation (expressed as initial rate of change of plm activity) induced by samples from all Ovo aggregation reaction time points; inhibition ranged from approximately 51 – 52% for 0-10 min samples to 71 – 83% inhibition for subsequent time point samples (Figure 4.10 C). Thus, aggregates partially shield bound tPA from inhibition by PAI-2, similar to fibrin-bound tPA.

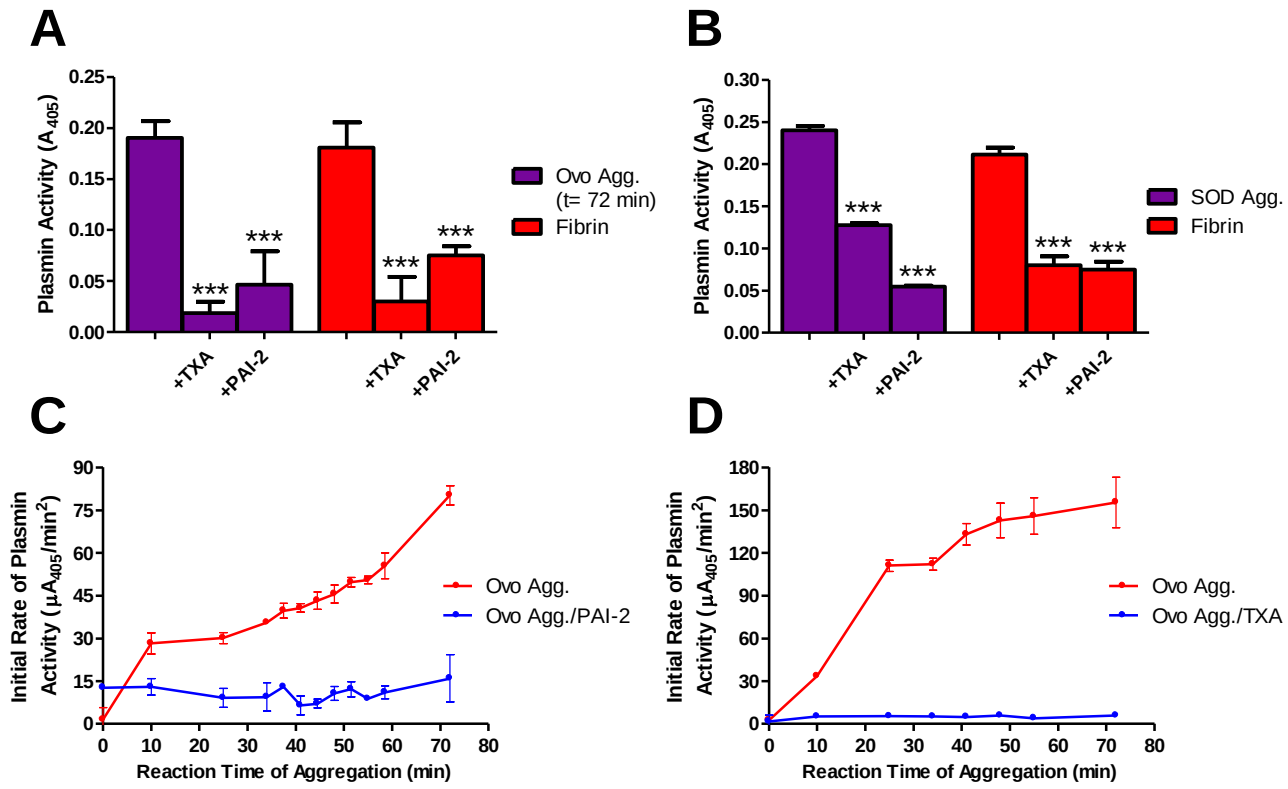

Figure 4.14 Effects of plasminogen activator inhibitor type-2 (PAI-2) and tranexamic acid (TXA) on tPA-mediated plasminogen activation elicited by Ovo and SOD aggregates. (A,B) Bar graphs of plasmin activity elicited by fibrin (positive control) or time course end-point samples of (A) Ovo and (B) SOD aggregates (both at 500 nM) in the absence or presence of PAI-2 (200 nM) or TXA (10 mM). (C,D) Graphs of the initial rate of Ovo Agg.-induced plasmin activity (measured as described in 4.2.10) as a function of Ovo aggregation time, in the presence or absence of (C) PAI-2 and (D) TXA. Data points represent the mean ± SD (n=9) of three separate experiments, where in each experiment measurements were performed in triplicate. In D, the error bars on the lower plot are too small to be visible. Significant differences between samples incubated in the presence of either PAI-2 or TXA compared to controls (absence of either PAI-2 or TXA) are indicated by *** ($p<0.001$).

4.3.7 Chaperone:client complexes of clusterin:Ovo enhance tPA-mediated plasminogen activation

Chaperones such as clusterin (CLU) are known to form high molecular weight complexes with partly unfolded proteins (clients) under stress conditions (Humphreys *et al.* 1999; Carver *et al.* 2003). These complexes are mostly soluble and can be purified from precipitated protein material by means of post-reaction centrifugation and SEC. The ability of soluble chaperone:client complexes to interact with and affect plg activation is unknown. To investigate this, CLU:Ovo complexes were formed by co-incubating CLU and Ovo at 60˚C at different molar ratios of client to chaperone. Heating native Ovo in the absence of CLU resulted in its rapid and extensive precipitation, shown by an increase in turbidity after a lag phase of 20 min, reaching a maximum at approximately 110 min (Figure 4.10). CLU inhibited the extent of Ovo precipitation by 67.9 ± 7.8 % and 83.6 ± 4.8 % at molar ratios of chaperone:client of 1:8 and 1:2, respectively, and formed soluble chaperone:client complexes as demonstrated previously by (Humphreys *et al.* 1999; Poon *et al.* 2000) (Figure 4.11 A).

Purified complexes formed at various CLU:Ovo ratios were then analysed for their ability to enhance tPA-mediated plg activation. It is unclear whether altering the ratio of CLU:Ovo alters the stoichiometry of the HMW complexes formed by their interaction therefore, different ratios of CLU:Ovo were tested. Soluble HMW complexes of CLU:Ovo were shown to enhance tPA-mediated plg activation similar to Ovo aggregates alone (Figure 4.11 B). Complexes formed using a ratio of 1:2 CLU:Ovo displayed a lower initial rate of change of plm activity (16.1 ± 0.1 fold-increase above background) when compared with complexes formed in the presence of higher concentrations of Ovo relative to CLU (SMR of 1:8 and 1:4 CLU:Ovo gave an average 82.1 ± 11 fold-increase above tPA/plg alone). The initial rate of change of plm activity elicited by CLU:Ovo complexes was greater than corresponding levels obtained for Ovo Agg. end-point samples (57.4 ± 2.0 fold). The *in vivo* relevance of the activation of plg by CLU:client complexes is unknown.

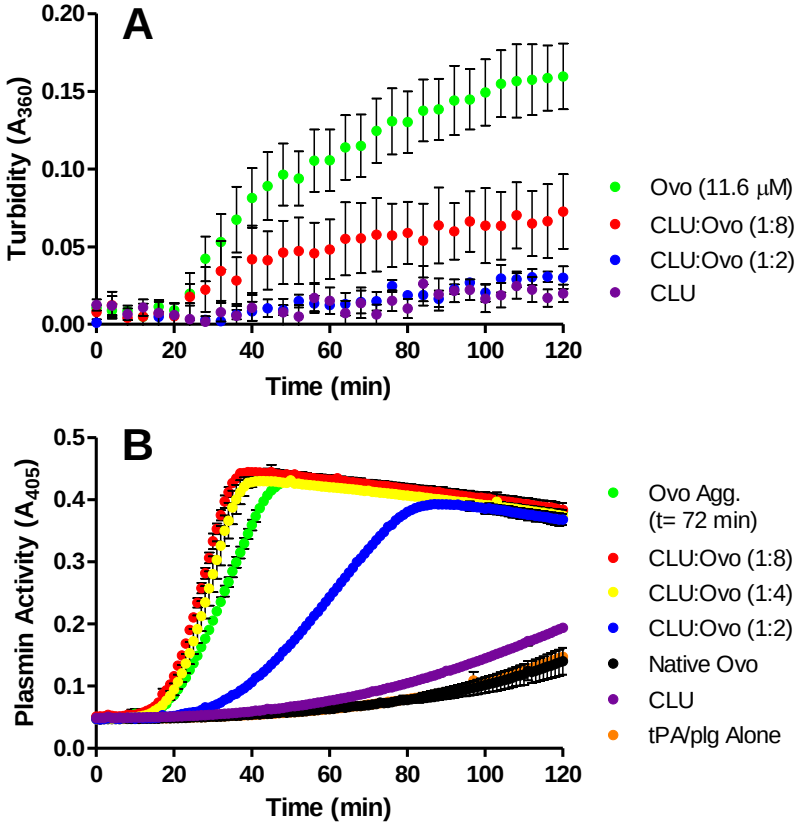

Figure 4.15 CLU:Ovo complexes enhance tPA-mediated plasminogen activation. (A) Turbidity (measured as A_{360}) as a function of time for Ovo (11.6 μM) in PBS, induced to aggregate by heating at 60˚C in the presence of different molar ratios of chaperone:client (CLU:Ovo, indicated in key). (B) 75 μg/mL of purified CLU:Ovo complexes (see section 4.2.5) dialysed against HBST, were assayed for their ability to enhance tPA-mediated plg activation. Complexes formed using molar CLU:Ovo ratios of 1:12 and 1:24 elicited similar levels of plg activation as complexes formed using CLU:Ovo at 1:8 and thus are not shown for clarity. Data points represent the mean ± SD (n=9) of three separate experiments, where in each experiment measurements were performed in triplicate.

4.4 DISCUSSION

Previous studies have shown that tPA can bind to chemically- and heat-stressed protein aggregates, which act as a cofactor for plg activation, and a substrate for plm (Table 4.3) (Radcliffe 1981; Radcliffe 1983; Machovich and Owen 1997; Samson *et al.* 2009; Gebbink 2009). The structural properties of these aggregates were not clearly established by these previous studies. The conditions used to denature the proteins (acidic or basic pH and heating), however, are similar to those often used to produce amorphous aggregates.

Table 4.1 Chemical and heat stressed proteins which have been shown to enhance tPA-mediated plasminogen activation.

Plasma		Cytosolic-secretory		Connective	
Active	**Pre-treated**	**Active**	**Pre-treated**	**Active**	**Pre-treated**
Albumin[1,2]	Antiplasmin[1]	Dnase 1[2]	α-Casein[2]	Gelatins:[3]	Collagen[2]
Apoferritin[1,2]	Protein c[1]	Myosin S1[1]	Cytochome c[1]	(I, III, IV, V)	Elastin[2]
Antithrombin[1]	Thrombin[1]	Ovalbumin[2]	Insulin[2]		Keratin[2]
Factor Xa[1]		Pepsin[2]	RNase[2]		
Fibrinogen[1,2]		Pyruvate kinase[2]			
α2-Macroglobulin[1]					
α1-Protease inhibitor[1]					
Immunoglobulins[1,2]					
Plasminogen[2]					

Stressed proteins are divided into columns based on their distribution (for example, plasma), and their ability to initiate tPA-mediated plg activation. Proteins were either able to induce plg activation without further treatment (Active), or required pre-treatment and partial proteolysis with plm prior to being assayed, before they could activate plg (Pre-treated). Heating was used to denature albumin, antithrombin, A2M, and α1-protease inhibitor, while acidic pH was used to denature apoferritin. The conditions used to denature the other proteins were heat and acidic or basic pH. However, the details of these treatments were not fully described in the corresponding publications. [1]Machovich, R. and Owen, W.G. (1997), [2]Radcliffe, R. and Heinze, T. (1981), [3]Stack, S. *et al.* (1990).

Heat or reduction were used to generate amorphous aggregates from Ovo, SOD and IgG. Analysis of their biophysical characteristics established that the products were hydrophobic and structurally disordered amorphous aggregates. The stressed proteins yielded a heterogenously sized and structurally disorganised mixture of aggregates (Figure 4.6), growing in size and complexity over time into material either sufficiently large enough to

scatter light (Ovo and SOD, Figure 4.1) or detectable as soluble HMW species (Ox. IgG, Figure 4.5). Soluble HMW Ox. IgG species were found on average to equate in size to cross-linked IgG dimers (~ 356 kDa).

Like fibrin, amorphous SOD, Ovo and Ox. IgG aggregates, but not their native protein counterparts, were able to enhance tPA-mediated activation of plg. In agreement with previous studies (Table 4.3), these aggregates acted as both cofactors (probably by colocalising both tPA and plg to their surface) to generate plm (Figure 4.7). Aggregates of all three proteins induced similar levels of plg activation. Disease relevant amyloid proteins have also been shown to activate tPA in a similar manner (Tucker 2000). Interestingly, the ability of ox. IgG to activate plasminogen increased with the amount of high molecular weight species, but neither oxidized monomeric IgG nor native IgG induced activation of plg (Figure 4.12).

Plg activation also increased with the concentration of NaOCl used to oxidise IgG (Figure 4.14), most likely due to increasing amounts of HMW species formed at higher NaOCl concentrations (Figure 4.5). It is interesting to note that plg has previously been shown to bind to solid-phase-immobilised IgG (Harpel *et al.* 1989). Soluble and insoluble aggregates of IgG have been shown to trigger an immunogenic response by activating neutrophils to secrete oxidants and granule enzymes and induce the secretion of plasminogen activator by macrophages (it was not established whether this was uPA or tPA; (Pestel *et al.* 1984; Robinson *et al.* 1993). This may create a feed forward mechanism, potentially increasing the pool of oxidised proteins and co-factors able to further activate plg.

The extent of plg activation was dependent on the amount and extent of hydrophobic, aggregated material produced. Increases in turbidity correlated with an increase in aggregate size (Moreno *et al.* 2000). SEM micrographs indicated an increase in the size of amorphous Ovo aggregates at later time points (taken from the plateau region of the turbidity curve, Figure 4.1), which strongly correlated with an increased capacity to activate plg (Figure 4.8). The heterogenously sized aggregates were able to reproducibly activate plg and this was accomplished by both soluble and insoluble Ovo aggregates. Overall, insoluble aggregates were found to be more efficient at enhancing plg activation than soluble aggregates (Figure 4.9). Previous studies have shown that an increase in aggregate particle size correlated with enhanced plg activation, and that there was a minimal requirement for the size of the cofactor

(about 10 nm radius) (Galantai *et al.* 2006). Differences in aggregate size may account for the observations that (i) amorphous ox. IgG aggregates are smaller than Ovo and SOD aggregates, and have a lower ability than the latter to activate plg (the latter have comparable abilities to activate plg, Figure 4.7), and (ii) soluble aggregates are smaller in size than insoluble protein aggregates. Differences in the relative ability of protein aggregates to activate plm may also be dependent upon the number of binding sites available to tPA and plg, which would be more numerous on larger protein aggregates.

The exposure of normally buried hydrophobic residues to solution is a general phenomenon associated with protein aggregation (Dobson 2003). While the correlation between greater plg activation and the increased hydrophobicity of aggregates may be simply attributable to the extent of aggregation rather than increased binding of tPA and plg to hydrophobic residues, it should be noted that the kringle domains of both tPA and plg are dominated by a core cluster of hydrophobic residues, with kringle 2 (tPA) and kringle 4 (plg) having been shown to facilitate hydrophobic binding to fibrin (van Zonneveld 1986) and dimeric α_{s2}-casein (one of a group of phosphoproteins found in mammalian milk) (Heegaard *et al.* 1997). Thus tPA and plg may bind to amorphous protein aggregates via hydrophobic interactions. Furthermore, circulating extracellular chaperones "sense" denatured/misfolded proteins by virtue of their exposed hydrophobicity (Poon *et al.* 2002; Wyatt *et al.* 2013), a mechanism which may allow interplay and cooperation between proteases and chaperones.

The minimum chaperone:client ratio required to substantively inhibit the formation of large turbid Ovo species was an SMR 1:8 (CLU:Ovo), comparable to previously reported values (Figure 4.11) (Humphreys *et al.* 1999; Poon *et al.* 2000). CLU and other chaperones preferentially bind to small misfolded oligomeric species during amyloid aggregation (this has not yet been established for amorphous aggregation) to maintain their solubility, inhibit their further aggregation and toxicity, and facilitate their bulk uptake and degradation via receptor-mediated endocytosis (Yerbury *et al.* 2005; Wyatt *et al.* 2013). Chaperones such as CLU are known to form high molecular weight complexes with partly unfolded client proteins under stress conditions (Humphreys *et al.* 1999; Carver *et al.* 2003). In protein deposition diseases there is a pathophysiological presentation of misfolded proteins as large insoluble protein deposits, meaning these systems of extracellular protein quality control are overcome by the disease state. CLU has been found associated with such extracellular protein deposits (Wilson *et al.* 2008). Soluble HMW complexes of CLU:Ovo were shown to enhance

tPA-mediated plg activation similar to Ovo aggregates alone (Figure 4.11). HMW complexes generated by the binding of CLU with misfolded citrate synthase, fibrinogen and glutathione S-transferase are comprised of an approximate mass ratio of 1:2 CLU:client protein (Wyatt *et al.* 2009). However, the mass ratio of the two proteins in CLU:Ovo complexes has has not been established. Complexes formed using a ratio of 1:2 CLU:Ovo elicited less activation of plg to plm than complexes formed using higher ratios of CLU:Ovo (SMR of 1:8 and 1:4, CLU:Ovo).

Speculatively, this may be due to complexes formed using a large excess of Ovo relative to CLU resulting in increased accessibility of tPA and plg binding sites present on the CLU:Ovo complex. Uncomplexed CLU was able to enhance plg activation to approximately 2.5 times above that of background levels (tPA/plg alone), but this is unlikely to have significance *in vivo* as the plm activity was relatively small when compared to either aggregate- or fibrin-stimulated plg activation. In addition to the removal of circulating HMW CLU:client protein complexes by hepatocytes (Wyatt *et al.* 2011), plg activation by HMW CLU:client protein complexes may assist in the removal of large extracellular protein aggregates.

The results with TXA (Figure 4.10) suggest that, as is the case for fibrin (Wiman and Wallen 1977), binding of tPA and plg to lysine residues is important in the activation of plg elicited by amorphous protein aggregates. Plg binding to (structurally uncharacterised) denatured proteins has previously shown to be mediated via lysine residue binding (Radcliffe 1983). This is likely due to binding of both plg and tPA to the protein aggregates via kringle-domains. Plg is also known for its ability to distinguish between conformationally different prion proteins (i.e. disease relevant and native forms); again, the lysine binding site 1 (kringles 1-3) are involved (Fischer *et al.* 2000). Interestingly, while TXA almost completely inhibited the binding of tPA and plg to Ovo aggregates, binding to SOD aggregates was far less affected (Figure 4.10). tPA has been shown to bind to substrates by several lysine-independent mechanisms: (i) to fibrin via hydrophobic interaction with the kringle 2 domain (Urano *et al.* 1991) (ii) to cofactors through the fibronectin type 1 domain (Maas *et al.* 2008), and (iii) to amyloid fibrils through interaction with their "cross-beta" structure (Kranenburg *et al.* 2002). For amyloid fibrils it has been argued that cross-beta structure is not essential for tPA activation but rather is simply involved in maintaining the structure of amyloid aggregates. This infers that tPA activation may be facilitated by some other structural feature of amyloid aggregates (Galantai *et al.* 2006). However, as SOD aggregates were found to

contain no beta-sheet content (Figure 4.4), either the number of exposed lysine binding sites is more abundant in SOD aggregates or other non-amyloid structural elements must be involved. Addition of TXA in the absence of protein increased background levels of plg activation (subtracted from raw data, thus not shown), probably due to conformational changes induced in plg (Christensen and Molgaard 1992). Native proteins did not elicit any significant activation of plm. Even though lysine residues are displayed on the surface of native proteins, including extracellular proteins, native proteins do not induce plg activation while amorphously aggregated proteins do. The loss of native protein structure and the exposure of greater numbers of lysine residues to facilitate binding of tPA and plg, may provide a way for the plg activation system to discriminate between native and non-native proteins (Machovich and Owen 1997).

PAI-2 expression is markedly increased in the vascular endothelium, granulosa cells and in microglial cells of patients with Alzheimer's disease (Akiyama *et al.* 1993; Dear and Medcalf 1995) and is up-regulated (~1800-fold) and confers substantial protection in the injured brain following excitotoxic (kainic-acid induced) injury (Zhang *et al.* 2009). Additionally, PAI-1 expression levels have been shown to increase in both aging and protein deposition diseases with diminished tPA activity being correlated with poor patient outcomes in Alzheimer's disease and Parkinson's dementia (Sutton *et al.* 1994; Melchor *et al.* 2003; Yamamoto *et al.* 2005; Morimoto 2006). PAI-2 inhibits uPA and also, albeit less efficiently, tPA (two-chain but not single-chain form). Furthermore, the rate constants of uPA and tPA inhibition are not as favourable as with PAl-1 (Vassalli 1991). PAI-2 inhibited approximately 75% of the tPA-mediated plg activation induced by Ovo and SOD aggregates, confirming the role of tPA in aggregate-induced plm formation. Inhibition by PAI-2 still allows 25% of total plg activation to occur, similar to tPA bound to fibrin (Figure 4.10). Similarly, tPA has previously been demonstrated to be resistant to inhibition by PAI-2 when bound to fibrin (Leung *et al.* 1987) and the binding of tPA to fibrin is dependent on lysine residues (Leung *et al.* 1987). A significant increase in PAI-2 mRNA expression was observed following traumatic brain injury (TBI) in which a marked increase in the presence of misfolded proteins in the ipsilateral region of the brain 3 h after TBI was also observed (Prof Rob Medcalf, Monash University, personal communication). This suggests that PAI-2 may act to inhibit aggregate induced tPA-mediated plg activation and prevent their clearance. By extension, poor patient outcomes in PDDs may be due to inhibition of extracellular proteolysis of protein aggregates by PAI-1 and -2, as the plg activation system has been shown to alleviate Aβ toxicity in

Alzheimer's disease by degrading extracellular deposits of amyloid fibrils (Tucker *et al.* 2000).

There is precedent for both harmful and protective roles for tPA-mediated plg activation in neurological insults, depending on the primary substrate associated with each specific pathology. tPA is beneficial in the dissolution of fibrin-clots following stroke, helping to recanalise the blood vessels (Tabrizi 1999), as well as in glomurulonephritis, to help clear fibrin and matrix protein deposits (Kitching *et al.* 1997). Conversely, the plm-mediated breakdown of fibrin clots has been shown to release cytotoxic fibrin degradation products (Guo 2009). tPA has roles beyond fibrinolysis, as plm is capable of degrading extracellular matrix proteins such as laminin and activating metalloprotease precursors, which can potentiate further degradation of extracellular proteins and trigger inflammatory responses (Vassalli 1991). Additionally, tPA is an essential mediator of cell death following ischemia or excitotoxic injury in the brain, and may play a role in neuronal and endothelial cell death induced by protein aggregates (Tsirka 1995; Chen 1997; Yepes 2008). Furthermore, following traumatic brain-injury-induced protein aggregation, excess tPA-mediated plg activation is detrimental, inducing inflammatory responses (Samson *et al.* 2009). Further work to examine whether the degradation of amorphous aggregates by plm inhibits or promotes the formation of toxic protein species will be addressed in Chapter 5.

A2AP is the main physiologic plm inhibitor in mammalian plasma, and like PAI-1 and PAI-2, is a serpin. It inhibits plm very rapidly by forming an inactive 1:1 stoichiometric complex with plm (Collen 1976; Collen and Wiman 1978; Lijnen 1982). In a manner similar to plm bound to fibrin, insoluble protein aggregates were found to shield plm from inhibition by A2AP, while soluble protein aggregates did not (Figure 4.15). A2AP inhibited plm bound to insoluble aggregates of both Ovo and SOD Agg. by approximately 13 – 15% while plm bound to soluble aggregates was inhibited by 60 – 67%. Inhibition by A2AP requires the presence of a free active site and free lysine-binding sites in plg/plm, inaccessible when plg/plm is bound to substrates such as fibrin (Collen 1976; Collen and Wiman 1978; Lijnen 1982). The shielding effects are thought to localise the activity of plm to specific regions of the extracellular environment, to avoid inappropriate proteolysis (Longstaff and Gaffney 1991). This would allow plm to be formed at the surface of large insoluble protein aggregates and to effectively degrade them into smaller protein fragments - the biological effects of these

plm-generated fragments are poorly understood and investigations of this are reported in Chapter 5.

The plg activation system and thus production of active plm is tightly controlled. Free circulating plm bound to a substrate such as fibrin is readily inhibited by A2AP, and tPA is inhibited by PAI-1 and/or PAI-2 (Lijnen 1982). Previous studies have shown that partial proteolysis of denatured proteins and Alzheimer's disease-associated amyloid fibrils by active plm, further enhanced (or was required for) subsequent plg activation, probably by exposing additional lysine residues to interact with tPA and plg (Table 4.1) (Machovich and Owen 1997; Kranenburg *et al.* 2002). Additionally, partial proteolysis by other circulating proteases such as carboxypeptidases B and N have been shown to further increase fibrin clot dissolution by plm, due to modification of clot super structure to improve plg activation rates and the steric access of plm to the substrate (Kovacs *et al.* 2014). Partial proteolysis by plm of aggregated Ovo, SOD or IgG proteins was not required for the plg activation demonstrated in this chapter (Figure 4.7 onwards). However *in vivo*, limited proteolysis by free active plm (or other proteases) may enhance the removal of extracellular aggregates by providing new binding sites for tPA and plg.

Intracellularly, protective proteases are key elements of protein quality control pathways that are upregulated in response to various protein folding stresses, preventing the accumulation and aggregation of misfolded proteins which can be cytotoxic (Goldberg 2003). Interestingly, the plg activation system has been shown to alleviate Aβ toxicity in Alzheimer's disease by degrading extracellular deposits of amyloid fibrils (Tucker *et al.* 2000). Misfolded proteins have also been found to activate Factor XII, leaving to kallikrein formation independent of coagulation (Maas *et al.* 2008). Other proteases belonging to the high temperature requirement A (e.g. HtrA1) family of serine proteases, which are involved in protein quality control and cell fate, are able to bind to and degrade misfolded proteins (Truebestein *et al.* 2011), and are cytoprotective, by clearing tau neurofibrillary tangles and plaques associated with dementia (Tennstaedt *et al.* 2012). However, a genetic mutation in the promoter sequence of *HtrA1* which increases expression of HtrA1, is considered a risk factor in cases of age-related macular degeneration (Yang *et al.* 2010; Yang *et al.* 2010), resulting in increased expression and abnormal cleavage of both the ECs CLU and A2M (An *et al.* 2010). Collectively, these data suggest that the plg activation system and other extracellular

proteases are involved in the dissolution of insoluble extracellular protein aggregates and are likely to form part of a larger extracellular proteostasis network.

In conclusion, native proteins unfold and aggregate due to stresses, creating a mixture of soluble and insoluble aggregates. tPA and plg can colocalise on the surface of amorphously aggregated proteins via their affinity for lysine-residue binding. Plm activity is shielded from inhibition by A2AP when bound to insoluble aggregates. This would then allow for plm to be formed at the surface of and degrade amorphous aggregates (this final aspect is dealt with in Chapter 5). These findings are consistent with a system in which proteases and chaperones act together as key synergistic mechanisms in extracellular proteostasis, to degrade and clear extracellular pathologic protein deposits and inhibit the development of age-related protein misfolding diseases. A corollary is that once amorphous aggregates have undergone proteolytic degradation (in the absence of PAI-1or -2), smaller soluble fragments of protein that are released from the aggregates are cleared by binding to circulating extracellular chaperones and subsequent receptor-mediated endocytosis. This hypothesis is examined in more detail in Chapter 5.

CHAPTER 5 : PLASMIN DEGRADES PROTEIN AGGREGATES TO GENERATE CYTOTOXIC PROTEIN FRAGMENTS WHICH INTERACT WITH ECs

5.1 INTRODUCTION

5.1.1 Protein Aggregation and Cytotoxicity

All protein deposition diseases involve the appearance of non-native proteins which aggregate to form insoluble protein deposits with one another and other proteostasis-associated proteins, such as ECs (Dobson 1999; Yerbury *et al.* 2005; Wyatt 2009). Disease pathologies can appear when the complex network of protein quality control mechanisms, including chaperones and proteolytic systems that evolved to maintain proteostasis, are overcome (Soti and Csermely 2003; Morimoto 2006; Gidalevitza *et al.* 2010). The pathophysiology of protein deposition diseases can differ with respect to the identity of the aggregating protein, the structure of the aggregate, the location of the insoluble deposits and the cell type(s) affected. The way in which protein aggregates impart their cytotoxic effects is not entirely understood. Aggregates may accumulate and deposit within intra or extracellular environments and cause pathologies by either physically disrupting tissue function (e.g. senile plaques) or via the cellular toxicity of soluble oligomeric aggregates or proteolytic fragments from their degradation (Dobson 2001; Walsh *et al.* 2002; Caughey 2003; Chiti and Dobson 2006; Herczenik and Gebbink 2008; Guo 2009). Numerous pathological downstream effects are stimulated in cells, such as Ca^{2+} mobilisation (Demuro *et al.* 2005), induction of ER stress (Breckenridge *et al.* 2003; Rao *et al.* 2006), and generation of reactive oxygen species (ROS); if these effects are severe enough, cell death may result (Ankarcrona *et al.* 1995; Bonfoco *et al.* 1995; Stefani and Dobson 2003; Emerit *et al.* 2004). In addition to their direct toxic effects, aggregated proteins can also indirectly promote damaging pathologies through excessive inflammatory responses, activation of tPA, and the processing of Aβ-bound neuroendocrine factors, which can inhibit neurotransmitter release (Casserly and Topol 2004; Kranenburg *et al.* 2005; Herczenik and Gebbink 2008).

5.1.2 tPA-Mediated Plasminogen Activation System and Disease States

Plm generated by tPA-mediated plg activation is capable of degrading ECM proteins such as laminin and activating metalloprotease precursors, which can potentiate proteolysis of basement membranes and extracellular matrix proteins, induce cytolysis and trigger inflammatory responses (Vassalli 1991; Chen and Strickland 1997; Cuzner 1999), as well as degrade essential components of the complement system and immunoglobulins, resulting in the release of chemotactic fragments (Lachmann *et al.* 1982; Schaiff and Eisenberg 1997). For additional information on tPA and the plg activation system see Chapter 1, section 1.4.

Various neuropathological conditions such as thrombolytic stroke are thought to involve excitotoxic damage to the brain (Lipton and Rosenberg 1994). tPA is required for neuronal death in adult mice which have undergone excitotoxic insults. In contrast, infusion with PAI-1 protects from neuronal death (Tsirka 1995). Studies have found that following ischemic injury (such as in stroke) tPA is upregulated resulting in increased permeability of the blood brain barrier and increased expression and activity of matrix metalloproteinases (MMP) (Aoki 2002; Kidwell 2008; Yepes 2008). Interestingly, the ECs A2M and CLU are inhibitors of MMPs in tissue fluids. A2M:MMP complexes are cleared via LRP-mediated endocytosis (Egeblad 2002), while clusterin is a negative regulator of membrane type MMP-6 produced by neutrophils and brain tumors (Matsuda 2003) and has been shown to bind to and inhibit the activity of both intra- and extracellular MMP-9 in epithelial cells (Jeong *et al.* 2012). By forming a high molecular weight complex with MT6-MMP and inhibiting the enzymatic activity of MMP-9, CLU appears to regulate neutrophil function, protect host tissue from MMP-6 and similarly protect epithelial barriers from MMP-9-mediated degradation.

Amorphously aggregated proteins as well as amyloid fibrils are able to activate tPA, and in turn enhance plasminogen activation (Tucker *et al.* 2000; Kranenburg *et al.* 2002; Samson *et al.* 2009; Gebbink 2011). Samson *et al.* (2009) showed that injured cells release extracellular protein aggregates - staining with thiazine red R and Congo red suggested that these aggregates consisted in part of amyloid fibrils, but may consist of a mixture of various types of protein aggregates. These aggregates were able to induce the tPA-mediated formation of plasmin (plm); the active plm was then able to degrade the protein aggregates to facilitate their removal. In contrast, the continued release of aggregates may lead to deleterious effects by inducing an excess of plm (Samson *et al.* 2009; Samson *et al.* 2012). It has been shown

that plm is able to protect cells by degrading both non-aggregated Aβ and cytotoxic Aβ fibrils found in Alzheimer's disease (Tucker *et al.* 2000). tPA is overexpressed in amyloid-rich areas in the brain of patients with Alzheimer's disease and may mediate neurotoxicity via extracellular regulated kinase 1/2 activation (Medina *et al.* 2005). The ability of active plm to degrade amorphous aggregates has yet to be characterised.

Plm has been shown to indirectly detrimentally affect cells by generating cytotoxic plm-generated protein fragments (PGPFs) from fibrin (Guo *et al.* 2009). Guo *et al.* showed that cellular internalisation of fibrin fragment central E-domain (FnE) by caveolin-1 mediated endocytosis inhibits mitochondrial function and induces apoptosis in trophoblast-derived BeWo cells, endothelial cells from umbilical vein or pulmonary aorta, and placental trophoblast cells and was dependent on the activation of caspases 3 and 9. The mechanisms of toxicity are likely to apply to other cell types including vascular endothelial cells and may contribute to negative side effects of tPA treatment in stroke victims (Longstaff *et al.* 2008). The plasma concentration of fibrin-derived PGPFs is greatly augmented in patients with thrombotic disorders such as venous thromboembolism or myocardial infarction, disseminated intravascular coagulation, infection, certain types of leukaemia, and other pathologies (Francis and Marder 1987; Cesarman-Maus and Hajjar 2005; Mosesson 2005). PGPFs derived from either amorphous or fibrillar protein aggregates have not been analysed for their effects on cells.

The degradation of fibrin by plm is vital for the maintenance of haemostasis, yet despite the apparent toxicity of the fragments produced, biological functions are not impaired under normal conditions. This suggests the existence of mechanisms which protect cells from toxicity during the plm mediated degradation of proteins. Thus, the tPA system can have both beneficial and detrimental actions. It can aid in the degradation of amyloid fibrils or potentially cause tissue damage by releasing cytotoxic fibrin-derived PGPFs. It is currently unknown whether ECs bind to PGPFs and mediate their disposal, thereby protecting bystander cells from their cytotoxicity.

The aims of the work described in this chapter were to investigate:

1. Whether plm can degrade amorphous aggregates to generate PGPFs
2. If the resulting amorphous aggregate-derived PGPFs have any effects on cells
3. How PGPFs bind to and are disposed of by cells
4. If ECs can inhibit or alter the effects of PGPFs on cells.

5.2 METHODS

5.2.1 Plasmin digestion of amorphous protein aggregates

Native proteins were filter sterilised and aggregated under conditions established in section 4.2.5 to produce amorphously aggregated Ovo, SOD and ox. IgG. Samples taken from protein aggregation assays were centrifuged at 15,000 x *g* for 15 min at 4˚C, and diluted in PBS to 1 mg/mL in a total volume of 100 µL. Plm (Haematologic Technologies, Inc.) was added to aggregates at a final concentration of 100 mU in 120 µL total volume and incubated overnight at 37˚C with shaking. Native protein samples were also digested with plm under the same conditions, to be used in later experiments as a control when assaying the biological effects of PGPFs derived from aggregated proteins. Insoluble, undigested material was removed by centrifugation at 15,000 x *g* for 15 min at 4˚C. The supernatant was pooled and the concentration of soluble PGPFs was determined by BCA assay (section 2.3).

5.2.1.1 Tris-tricine SDS-PAGE

Insoluble protein aggregates and soluble PGPFs derived therefrom were then analysed by 12% resolving Tris-tricine SDS-PAGE under reducing conditions and stained with Coomassie Blue Stain. Samples containing approximately 20 µg of total protein were prepared by mixing an equivalent volume of sample with that of NOVEX 2X Tricine-SDS sample buffer (0.9 M Tris-HCl, pH 8.45, 25% (v/v) glycerol, 8% (w/v) SDS, 0.015% (w/v) Coomassie Blue G) and 1% (v/v) 2-mercaptoethanol. The samples were then heated for 5 min in a 100˚C heating block before being loaded onto the gel which was prepared as per methods outlined in section 2.7 (SDS-PAGE) with several exceptions. Gels were prepared by layering a 4% stacking gel atop a 12% resolving gel layer. The resolving gel layer was buffered using a final concentration of 187 mM Tris-base at pH 8.45, while the stacking gel layer was buffered using 94 mM Tris-base at pH 8.45. Both gel layers contained 0.1% (w/v) SDS, 0.03% (w/v) ammonium persulfate and were polymerised by adding 20 µL of TEMED. The reservoir was filled with Tris-tricine running buffer (0.1 M Tris-base, 0.1 M tricine, 0.1% (w/v) SDS) and electrophoresis carried out at constant voltage at 125 V for 120 min or until the dye front reached the bottom of the gel.

5.2.1.2 Measure of residual plasmin activity in PGPF preparations

Soluble PGPFs derived from Ovo aggregates were dialysed using a Slide-A-Lyzer™ MINI dialysis device (3.5 kDa MWCO; Thermo Fisher) against ice-cold HBST and analysed for Plm activity by measuring changes in absorbance from the breakdown of SPEC-PL, in a 96-well polystyrene microplate at a total volume of 60 µL/well. Plm activity of PGPFs samples were compared to active Plm stored at -20˚C prior to assay (positive control), and Plm incubated alone under the same conditions and time period used to produce PGPFs (treatment control), which were diluted to a final concentration of 100 mU of Plm in ice-cold HBST. The reaction was initiated by adding 10 µL of an ice-cold 3.5 mM stock of SPEC-PL to a final concentration of 0.5 mM per well. Absorbance at 405 nm (A_{405}) was measured on a Spectramax Plus 382 spectrophotometer (Molecular Devices) for 240 min at 37˚C with measurements taken at 30 s cycles with 3 s of shaking between cycles. Plm activities were plotted as the change in A_{405} against time and analysed as described previously for plg activation assays in section 4.2.10.

5.2.3 Chaperone interaction sandwich ELISA assays

Plates (384 well) were coated with shaking for 1 h at 37˚C with 30 uL per well of 10 µg/mL G7 anti-CLU monoclonal antibody or mouse anti-human A2M monoclonal antibody or isotype control antibody (mouse IgG1 kappa antibody). All incubation and wash steps were performed with shaking unless otherwise indicated. Between incubation steps, plates were washed 6 times for 5 min each with PBS containing 0.1% (v/v) Tx-100 (Tx-100/PBS) followed by an additional 6 washes with PBS. Wells were then blocked with 50 uL per well of 1% HDC/PBS for 1 h at 37˚C. Prior to their addition to wells, samples were prepared by incubating biotinylated PGPFs (50 µg/mL) in the presence or absence of 20 µg/mL of chaperone (CLU or A2M) or BSA (as a non-chaperone control protein) in 1% BSA/0.1% Tx-100/PBS, pH 7.4 for 1 h at 37˚C. Biotinylated aggregated proteins, native protein and PGPFs derived from native protein were also incubated with chaperone as described. Following blocking, 30 µL per well of the various protein samples were added and incubated as before. Plates were then washed and incubated for 30 min at 37˚C with 30 uL per well of a mixture of 2.5 µg/mL each of streptavidin and biotinylated HRP in 1% HDC/PBS. Finally, the plates were washed and colour developed with the addition of 30 µL per well of 2.5 mg/mL OPD in phosphate-buffer containing citric acid (50 mM dibasic sodium phosphate, 25 mM citric acid,

pH 5.0) for 5 min at room temperature and the reaction halted with the addition of 30 µL of 1M HCl per well. Absorbance was then measured at 490 nm using a Spectramax Plus 382 plate reader (Molecular Devices). Absorbances from wells coated with isotype control antibody were subtracted from corresponding wells coated with G7 anti-CLU and anti-A2M antibodies.

5.2.4 bisANS fluorescence assays

bisANS assays were performed as described in section 3.2.5, however, samples of aggregated proteins, native protein and PGPFs derived therefrom were diluted in PBS to give a final concentration of 200 µg/mL and compared to an equal mass concentration of native-protein-derived PGPFs. As before, BSA (5 µM) in PBS was used as a positive control for exposed hydrophobicity.

5.2.5 Measurement of intracellular reactive oxygen species levels

EOC 13.31 and SVEC4-10 cells were grown and maintained in 24-well tissue culture plates (Greiner Bio-One; section 2.1). Prior to adding to cells, samples of undigested amorphously aggregated and native forms of Ovo, IgG and G93A SOD, and PGPFs derived from digestion of both aggregates and native proteins (section 5.2.1), were incubated in the presence or absence of CLU or A2M or BSA (as a non-chaperone control protein) at a equivalent mass ratio (w/v) of 1:1 sample to chaperone, in PBS for 1 h at 37°C with gentle shaking. These were then incubated with cells at a final concentration of 100 µg/mL for 1 h at 37˚C. Cells were then incubated with 30 µM dihydrorhodamine 123 (DHR; Sigma-Aldrich) for a further hour before washing in PBS, harvesting with trypsin/EDTA, and resuspending in PBS containing 1% (w/v) BSA. DHR-associated mean fluorescence intensity was measured by flow cytometry (excitation at 488 nm, emission collected at 515 ± 10 nm) (section 2.8).

5.2.6 Cell viability assays

Native proteins were filter sterilised and aggregated as described in section 4.2.5 to produce amorphously aggregated Ovo, SOD and IgG. Sterile native or aggregated proteins were then digested with sterile filtered plasmin (as described in section 5.2.1) to yield PGPFs. Samples of aggregates, native proteins and PGPFs derived from the digestion of both, were then pre-incubated in the presence or absence of CLU or A2M or BSA (as a non-chaperone control

protein) (section 5.2.5) before incubating with EOC 13.31 and SVEC4-10 cells (section 2.1) at a final concentration of 200 µg/mL for 24 – 90 h (depending on individual assay requirements) at 37°C and 5% (v/v) CO_2. Cell viability was measured by real time Sytox Green assay and 3-(4,5-dimethylthiazol-2-yl)-5-(3-carboxymethoxyphenyl)-2-(4-sulfophenyl) -2H-tetrazolium (MTS) assay. Real time Sytox Green assay was performed by incubating cells with 1 µM SYTOX Green viability dye (Life Technologies) and measuring the development of SYTOX Green-associated fluorescence over 90 h by time-resolved epifluorescence microscopy (excitation at 440 – 480 nm, emission at 504 – 544 nm), as well as phase contrast cell imaging (Nikon 4X objective). Images were collected at 2 h intervals using an Incucyte ZOOM epifluorescence live-cell imaging system (Essen Bioscience) and analysed using Incucyte ZOOM software v2015A. MTS assay was performed after 24 h incubation with samples, using a "CellTiter 96 AQ_{ueous} One Solution Cell Proliferation Assay Kit" (Promega) by adding 20 µl/well of the MTS reagent and incubating for 2 h at 37°C to allow the coloured formazan product to develop. Absorbance was then measured at 490 nm using a Spectramax Plus 382 plate reader (Molecular Devices).

5.2.7 Confocal microscopy of mitochondrial membrane polarisation

EOC 13.31 and SVEC4-10 cells (section 2.1) were incubated for 24 h at 37°C and 5% (v/v) CO_2 with or without 200 µg/mL of PGPFs derived from the digestion of protein aggregates; in some cases, before adding to the cells, the PGPFs had been pre-incubated with CLU or A2M or BSA (section 5.2.6). The ability of PGPFs to induce changes in mitochondrial membrane potential ($\Delta\Psi_{mit}$) were measured using confocal microscopy by incubating with 100 nM MitoTracker Deep Red chloromethyl-X-rosamine (CMXRos; Molecular Probes) for 20 min at 37˚C in DMEM/F12 growth medium. Prior to the addition of CMXRos, in some cases 20 µM carbonyl cyanide m-chlorophenyl hydrazone (CCCP) was incubated with cells for 1 h at 37˚C, as a positive control for the loss of $\Delta\Psi_{MIT}$. CMXRos-associated fluorescence was collected using 543 nm excitation and an emission window set at 580-640 nm, on a Leica SP5 inverted confocal microscope (Leica Microsystems). Images were analysed using Leica LAS AF "Lite".

5.2.8 Confocal microscopy of cellular PGPF uptake

Still image and real time confocal microscopy was used to examine how PGPFs are internalised, measure rates of internalisation and observe whether PGPFs are directed to

lysosomal compartments for degradation. Cells were harvested and grown overnight in 8 chambered µ-slides (Ibidi) using conditions described in section 2.3. CF-488-labelled protein aggregate-derived PGPFs (PGPFs^{488}) were prepared as described in sections 2.5 and 5.2.1. 75 nM Lysotracker Deep Red (Molecular Probes) and 20 µg/mL PGPFs^{488} were added to the chambered slide. In some experiments, protein-free unreacted CF-488 label (pooled from gel filtration purifications; section 2.3) served as a negative control for internalisation. Type F immersion fluid (Leica Microsystems) was then applied to the bottom of the slide and quickly transferred to the confocal microscope stage. Using the xyt function to acquire data, regions of interests were imaged, and the microscope was set to record images at 5 min intervals for 180 min. At least 6 regions of interest per well were imaged. Within experiments, treatments were performed in duplicate for each type of PGPFs^{488}; individual experiments were performed at least three times. Cells were selected based on whether the ROI would remain in the confocal field of view during the entire time course and to minimize fluctuations in fluorescence based on z-axis shift. PGPFs^{488}-associated fluorescence was collected using excitation at 488 nm and an emission window set at 510 – 530 nm. Lysotracker-associated fluorescence was collected using excitation at 543 nm and an emission window set at 580-640 nm, using a Leica SP5 inverted confocal microscope (Leica, Sydney). All data was acquired using Leica LAS AF software. Images of PGPF internalisation and rates of uptake were analysed using a combination of Leica LAS AF "Lite" and GraphPad Prism 5. Colocalisation data was analysed with ImageJ 1.49a (National Institute of Health, USA) using the plugin "Manders' coefficients" [formerly Image Correlator Plus; developed by Tony Collins, Wayne Rasband and Kevin Baler, Wright Cell Imaging Facility, Toronto, Canada (2005)] to derive Pearson's correlation coefficient and Mander's overlap coefficient (Manders *et al.* 1993).

5.2.9 Cell-surface binding assays

5.2.9.1 Effects of ECs on cell-surface binding of labelled PGPFs

EOC-13 and SVEC4-10 cells (section 2.1) were harvested by dissociation using StemPro Accutase (Life Technologies) (which does not cleave cell-surface markers, such as receptors) and resuspended in ice-cold 1% BSA/PBS/0.1% NaN_3 (BSA/PBS/Az). Prior to adding to cells, CLU or A2M were incubated with gentle shaking for 1 h at 37°C with PGPFs^{488} (prepared as described in sections 2.5 and 5.2.1) at a mass ratio (w/v) of 1:1 PGPFs^{488} to chaperone in PBS (section 5.2.5). These were then incubated with cells at a final

concentration of 20 µg/mL for 30 min in ice-cold BSA/PBS/Az, before washing and resuspending cells in the same buffer. PGPF-associated mean fluorescence intensity was measured by flow cytometry (excitation at 488 nm, emission collected at 515 ± 20 nm) (section 2.8).

5.2.9.2 Inhibition of cell-surface PGPF binding to EOC-13 and SVEC4-10 cells

Similar experiments to those described in 5.2.9.1 were carried out to assess the effects of inhibition of cell-surface receptors and endocytic mechanisms on the binding of $PGPFs^{488}$ to cells. Cells were incubated for 30 min with ice-cold BSA/PBS/Az in the presence or absence of inhibitor (Table 5.1) prior to washing and resuspension in the same buffer and incubation conditions in the presence or absence of 20 µg/mL of $PGPFs^{488}$. The cells were next washed and resuspended with ice-cold BSA/PBS/Az and PGPF-associated mean fluorescence intensity measured by flow cytometry (section 2.8).

Table 5.1 Panel of inhibitors of cell surface receptors and endocytosis mechanisms.

Inhibitor	Action	Conc. used
Receptor-associated Protein (RAP)	Inhibition of Low-density Lipoprotein Receptor-related Protein	0.5 mg/mL
Lipopolysaccharide	Competitive Antagonist of TLR Binding	0.5 µg/mL
Anti-TLR-2 Antibody	Inhibition of TLR-2	0.1 mg/mL
Polyinosinic Acid	Inhibition of TLR-3	5 µg/mL
Anti-TLR-4 Antibody	Inhibition of TLR-4	0.1 mg/mL
Mannan	Competitive Antagonist of Mannose Receptor	0.5 µg/mL
CD14	Inhibition of CD14 Receptor	1 µg/mL
Methyl-β-cyclodextrin	Inhibition of Lipid Raft Formation	6.6 mg/mL
Fucoidan	Non-specific Inhibition of Scavenger Receptors	0.3 mg/mL
5-(N-ethyl-N-isopropyl)-amiloride (EIPA)	Inhibition of Macropinocytosis	30 µg/mL

Used in experiments outlined in section 5.2.9.2.

5.2.10 Statistical analysis

Data presented in the results was analysed using a one-way ANOVA and a Bonferroni multiple comparison post-test using GraphPad Prism v5.0, unless stated otherwise. The extent of significance of differences between samples is denoted by asterixes shown on the graphs (*$p<0.05$, **$p<0.01$ and ***$p<0.001$). Confocal microscopy image data was analysed for colocalisation (section 5.2.8) with ImageJ 1.49a using the plugin "Manders' coefficients" to derive Pearson's correlation (Pr) coefficient and Mander's overlap coefficient (Mr) from two 8 or 16-bit monochromatic images (Manders *et al.* 1993). Pearson's correlation coefficient is one of the standard procedures in pattern recognition for matching one image with another and can be used to describe the degree of overlap between two patterns. In many forms of correlation analysis the values for Pearson's will range from -1 to +1. In the case of images, a perfect correlation gives a value of +1; perfect exclusion however does not give a value of -1. Low (close to zero) and negative values for Pearson's correlation coefficient for fluorescence images can be difficult to interpret (Manders *et al.* 1993). However, a value close to 1 does indicate reliable colocalisation, but does not take into account differences in mean fluorescence intensities for the two fluorescence channels being analysed (Manders *et al.* 1993). Mander's coefficient does not suffer from this limitation as it can be determined even when signal intensities between two fluorescence channels differ strongly. However, unlike Pearson's coefficient, for Mander's overlap coefficient the number of objects in both channels of the image has to be more or less equal. Therefore, both values are usually reported together. Mander's overlap coefficient is proportional to the amount of fluorescence of the colocalising pixels or voxels in each colour channel. Values range from 0 to 1, expressing the fraction of intensity in a channel that is located in pixels where there is above zero (or threshold) intensity in the other colour channel (Manders *et al.* 1993).

5.3 RESULTS

5.3.1 Plasmin digestion of amorphous aggregates

Aggregates are known to have inflammatory and cytotoxic effects *in vivo* and amyloid fibrils are known to enhance tPA-mediated plm formation. However, it was previously unclear whether amorphous protein aggregates can stimulate tPA-mediated plm activation, or whether plm can degrade amorphous protein aggregates. Furthermore, the effects of PGPFs derived from amorphous protein aggregates on cells is unknown. Native proteins were induced to aggregate amorphously as in Chapter 4 (section 4.2.5), digested with plm to generate soluble PGPFs, which were then purified (section 5.2.1), and analysed by Tris-tricine SDS-PAGE (section 5.2.1.1). The sizes of soluble PGPFs derived from aggregated proteins were compared using Tris-tricine SDS-PAGE to whole (undigested) protein aggregates (Figure 5.1). Native proteins were also digested with plm under the same conditions as amorphous aggregates (not shown), to test the cytotoxic effects of various PGPFs in later cell-based experiments (section 5.3.5).

Most of the aggregated SOD, Ovo and ox. IgG was very large, too large to enter the SDS-PAGE gel matrix completely and accumulated at the top of the resolving gel. Thus, the apparent molecular weight was not able to be interpolated from protein standards of known molecular weights using this method. Digestion with plasmin generated PGPFs of varying sizes. The digestion of aggregated: (i) SOD yielded PGPFs ranging from 15 – 200 kDa in size, which appeared as a "smear" with no visually distinct bands, (ii) Ovo yielded PGPFs of between 88 – 164 kDa in size, and other visually indistinct, smeared bands less than 75 kDa in size, (iii) ox. IgG yielded PGPFs of between 150 – 200 kDa in size and above, and three minor bands at 41, 44 and 48 kDa. Autolysis of plm resulting from prolonged incubation (> 2 h at neutral pH) in aqueous solution should yield fragments of heavy chain (~ 63 kDa) and light chain (~ 26.5 kDa) (Wu *et al.* 1987), however, these bands are not easily visually resolved from those detected in PGPF preparations.

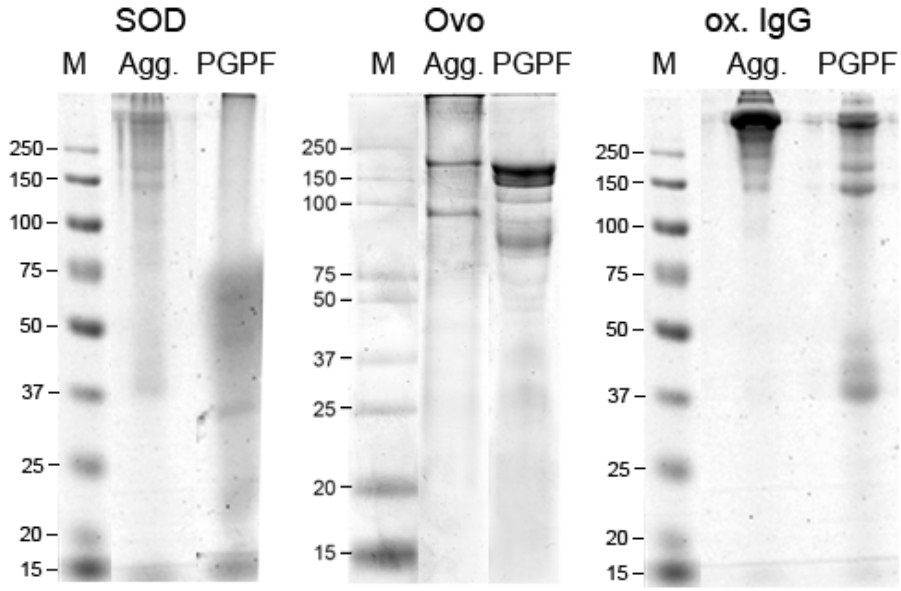

Figure 5.1 Images of Tris-tricine SDS-PAGE analyses of plm digests of amorphous protein aggregates. Samples of amorphously aggregated SOD, Ovo and ox. IgG taken from *in vitro* aggregation assays were diluted in PBS and incubated with or without 100 mU plm overnight at 37˚C to yield PGPFs and undigested aggregates (Agg.) respectively, as indicated. Samples were then analysed under reducing conditions on 12% Tris-tricine gels. Molecular weights of protein standards are indicated in kDa (M; Fermentas).

Prior to testing the biological effects of PGPFs on cultured cells, PGPF preparations were analysed for their residual plm activity to determine whether this could contribute to any measured cytotoxicity. Soluble PGPFs derived from Ovo aggregates were analysed for residual plm activity by measuring changes in absorbance from the breakdown of SPEC-PL. The initial rate of reaction (or velocity) was calculated from the gradient of the change in A_{405} versus t^2 using GraphPad Prism v5 (section 5.2.1.2). The plm activity of PGPFs samples was compared to active plm stored at -20˚C prior to assay (positive control), and Plm incubated alone under the same conditions and time period used to produce PGPFs (treatment control). The residual plm activity of freshly prepared PGPF samples was 1 ± 0.01 $\mu A_{405}.min^{-2}$ (Figure 5.2). This was significantly less than both the active plm positive control and plm treatment control, which demonstrated activities of 5810 ± 235 and 46 ± 1 $\mu A_{405}.min^{-2}$. The very low levels of residual plm activity in PGPF samples is insufficient to affect cells directly (Tucker *et al.* 2000), and thus any cell responses subsequently measured will be attributable to the PGPFs themselves.

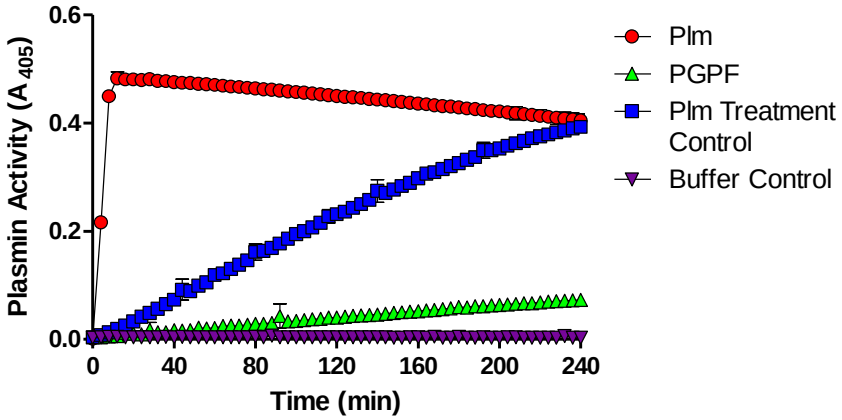

Figure 5.2 Residual plasmin activity of plasmin-generated protein fragments. Ovo aggregate-derived PGPFs (PGPF) were produced as described (section 5.2.1) and assayed for residual Plm activity, together with Plm incubated alone under the same conditions used to produce PGPFs (Plm Treatment Control), Plm stored at -20˚C prior to assay (Plm; as a positive control), and HBST containing SPEC-PL in the absence of Plm (Buffer Control). Data points represent the mean ± SD (n=3) of triplicate measurements of a single experiment, and the results shown are representative of three separate experiments.

5.3.2 Binding of extracellular chaperones to PGPFs

Given their general role in disposing of hydrophobic damaged proteins, the possibility that CLU and A2M also bind to PGPFs appeared worthy of investigation. As a first step, both CLU and A2M were assayed in sandwich ELISA for their ability to bind to undigested and plm digested forms of both aggregated and native client proteins (Figure 5.3). CLU and A2M were separately pre-incubated with biotinylated PGPFs, before they were incubated in plates containing an EC-specific capture antibody; any EC-bound biotinylated PGPFs or proteins were detected using a streptavidin-HRP conjugate. These assays detected significant binding of CLU to all three amorphous protein aggregates, which were structurally characterised (section 4.1) as a mixture of various sized oligomers and larger insoluble protein aggregates, and PGPFs derived from aggregates of SOD, Ovo and IgG. Negligible binding of CLU was detected to native PGPFs and background controls. The level of binding detected of CLU to undigested protein aggregates of SOD and ox. IgG was greater than to their corresponding PGPFs. Unsurprisingly, CLU bound significantly to Ovo and IgG aggregates and native IgG, known binding partners for CLU (Wilson and Easterbrook-Smith 1992; Humphreys *et al.*

1999). While there was significant binding of CLU to native Ovo but not to PGPFs derived from native Ovo and controls, this was substantially lower than the binding of CLU to either Ovo aggregates or Ovo aggregate-derived PGPFs. This suggests that the regions of native Ovo to which CLU binds may be destroyed by plm digestion during the formation of native PGPFs. In addition, while the binding of CLU to PGPFs derived from aggregates of IgG was significantly less than CLU binding to IgG aggregates and native IgG, it was still significantly higher than the binding of CLU to native IgG PGPFs and controls.

A2M also bound significantly to all three amorphous protein aggregates and PGPFs derived from aggregates of SOD, Ovo and ox. IgG. The level of binding of A2M detected to undigested protein aggregates of SOD and Ovo was greater than to their corresponding PGPFs. There was negligible binding of A2M to native proteins or their corresponding PGPFs. The above data demonstrates that in addition to amorphous aggregates, ECs specifically bind to aggregate-derived PGPFs.

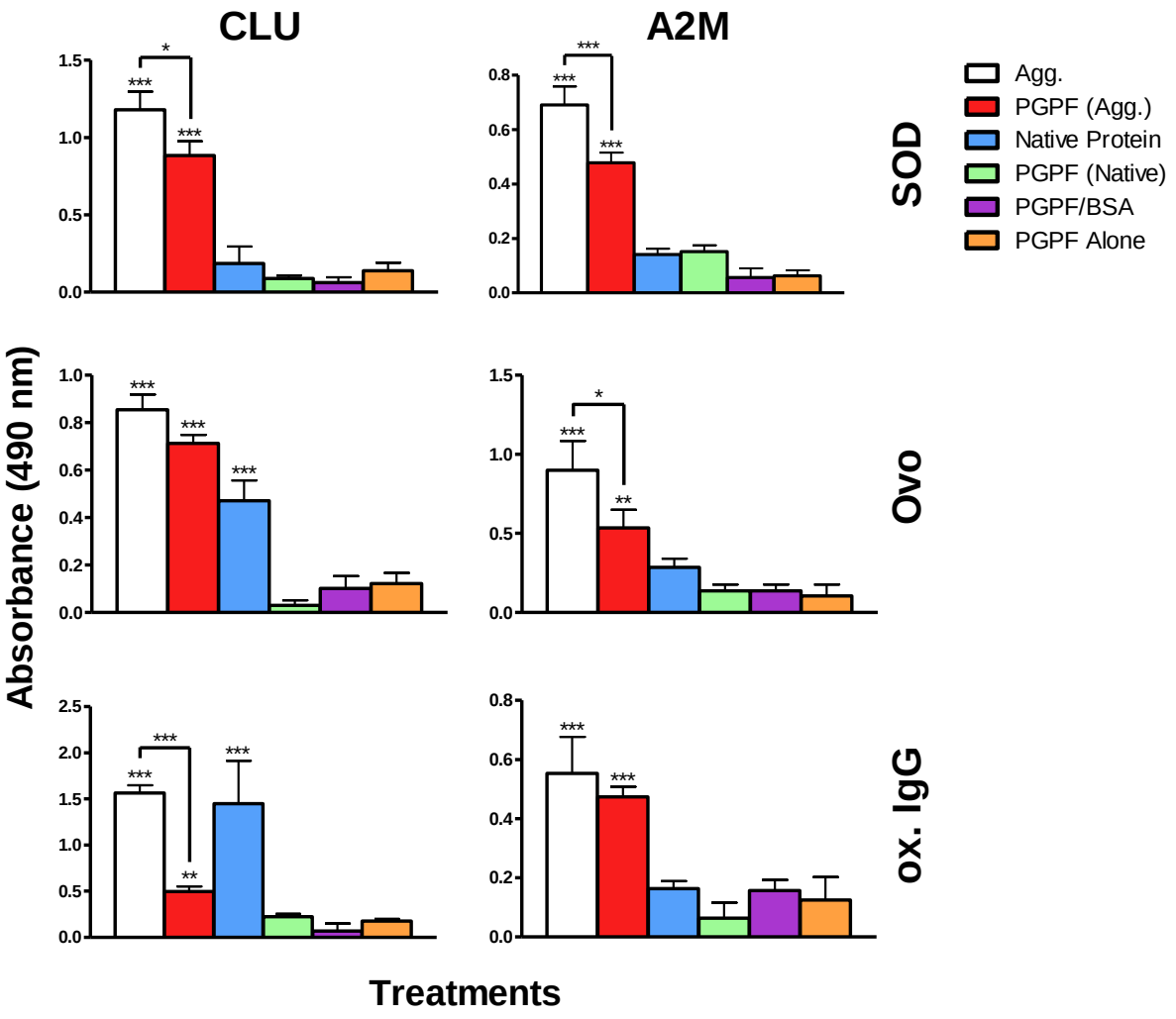

Figure 5.3 CLU and A2M bind to aggregates of SOD, Ovo and ox. IgG and their corresponding PGPFs. Sandwich ELISA tested the binding of extracellular chaperones CLU and A2M to biotinylated aggregated proteins (Agg.) and to aggregate-derived PGPFs (PGPF Agg.). Biotinylated native protein and native protein-derived PGPFs (PGPF Native) were also incubated with chaperones as described. As controls, ELISA plates were incubated with biotinylated PGPF Agg. alone and BSA was used as a non-chaperone control protein (PGPF/BSA). Absorbances from wells coated with isotype control antibody were subtracted from corresponding wells coated with G7 anti-CLU and anti-A2M antibodies. Bars represent the mean ± SD (n=9) of data from three separate experiments (in individual experiments, measurements were performed in triplicate). Asterixes placed immediately above error bars indicate that the sample is significantly different from values for PGPF native, PGPF/BSA and PGPF alone. Asterixes above horizontal brackets indicate a significant difference between the bracketed samples. * ($p<0.05$), ** ($p<0.01$), *** ($p<0.001$).

5.3.3 Aggregates and their PGPFs have greater exposed hydrophobicity than the corresponding native proteins

To investigate whether the specific binding of ECs to aggregates and their PGPFs might be due to hydrophobic interactions, the aggregates and derived PGPFs were analysed for exposed hydrophobicity using a bisANS fluorescence assay (5.2.4). BSA was included as a positive control for bisANS fluorescence. In all cases, aggregates and their corresponding PGPFs had significantly higher bisANS fluorescence than wells containing only bisANS in buffer (i.e. no protein) (Figure 5.4). Relative to bisANS in buffer, the increases in fluorescence were 2.7 ± 0.1 fold for SOD aggregates, 2.1 ± 0.0 fold for SOD aggregate-derived PGPFs; 3.5 ± 0.5 fold for Ovo aggregates, 2.7 ± 0.1 fold for Ovo aggregate-derived PGPFs; and 6.2 ± 0.4 fold for ox. IgG aggregates, 3.2 ± 0.0 fold for ox. IgG aggregate-derived PGPFs. Additionally, amorphous protein aggregates gave a significantly greater bisANS fluorescence than the PGPFs derived from them. The fluorescence of wells containing native SOD or Ovo, or ox.IgG, and their respective PGPFs was not significantly greater than background levels (bisANS in buffer).

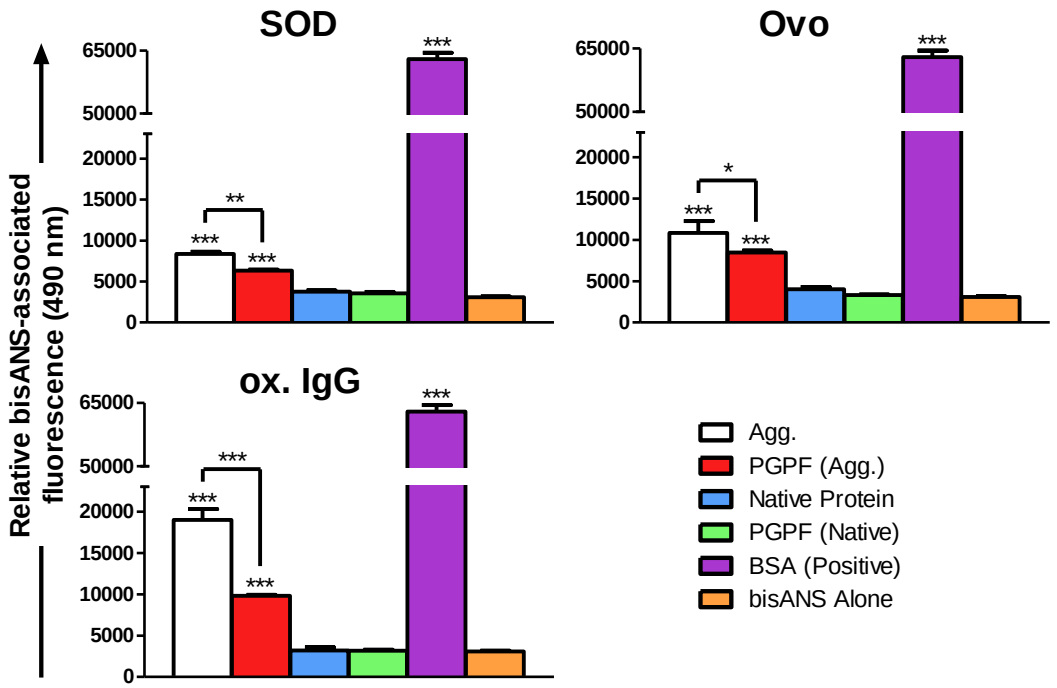

Figure 5.4 Aggregates and aggregate-derived PGPFs have increased hydrophobicity relative to native proteins. bisANS-associated fluorescence was used to measure exposed hydrophobicity for samples of aggregated protein (Agg.), aggregate-derived PGPFs (PGPF Agg.) and native protein diluted to 200 µg/mL in PBS. This was compared to native protein-derived PGPFs (PGPF Native) and bisANS alone. BSA at 5 µM in PBS was used as a positive control. Bars represent the mean ± SD measurements of six replicates (n=6). Asterixes above error bars denote a significant difference from values for PGPF Native and bisANS alone; asterixes above a bracket indicate a significant difference between the bracketed treatments; * ($p<0.05$) ** ($p<0.001$), *** ($p<0.001$).

5.3.4 Effect of chaperones on ROS formation in aggregate and PGPF treated cells

Oxidative stress, including increased ROS formation, is a common feature of cells exposed to several acute and chronic pathologies associated with the deposition of protein aggregates resulting from disregulation of proteostasis machinery (Davies and Delsignore 1987; Berlett and Stadtman 1997; Finkel and Holbrook 2000; Grune *et al.* 2004). This includes Alzheimer's disease (Tabner *et al.* 2010), amyotrophic lateral sclerosis (Okado-Matsumoto and Fridovich 2002), atherosclerosis (Devaraj and Jialal 1996), diabetes (Borcea *et al.* 1999), and Parkinson's disease (Maguire-Zeiss *et al.* 2005). ROS formation can either be indicative of toxic insult or itself lead to premature cell death in various disease states (Lipton and Rosenberg 1994; Bonfoco *et al.* 1995). Furthermore, ROS can exacerbate protein misfolding

and may lead to worsening pathology, as implicated for mutant SOD in amyotrophic lateral sclerosis (Rakhit *et al.* 2002), α-synuclein in Parkinson's disease (Guo and Scarlata 2013), and IgG in rheumatoid arthritis (Uesugi *et al.* 2000).

Clustered populations of activated microglia surrounding extracellular deposits of protein aggregates and neuritic plaques are hallmarks of neurodegenerative diseases including Alzheimer's disease, Parkinson's disease and amyotrophic lateral sclerosis and are likely to contribute to the mechanisms of neuronal damage and cognitive loss (Giulian 1999; Gao *et al.* 2003; West *et al.* 2004). EOC 13.31 cells were selected as a representative microglial-like cell line as they possess the ability to secrete many cytokines, and generate reactive oxygen/nitrogen species (Stansley *et al.* 2012) when incubated with either 1 – 40 or 1 – 42 form of Alzheimer's disease-associated β-amyloid ($A\beta_{40}$ or $A\beta_{42}$) (Ii *et al.* 1996; Manzano-Leon *et al.* 2006) or extracellular aggregates of SOD (Roberts *et al.* 2013). In addition, Aβ-induced ROS has been demonstrated to impair the function of scavenger receptor-mediated endocytosis in EOC 13.31 cells; this may also occur for microglia *in vivo* and could potentially contribute to the lack of Aβ clearance in Alzheimer's disease (Manzano-Leon *et al.* 2006).

As mentioned previously, fibrin-derived PGPFs have been shown to bind to and induce caspase-dependent apoptosis in endothelial cell types from various sources (Guo *et al.* 2009). Fibrin cytotoxicity may occur in other cell types. Endothelial cells are vital for the maintenance of fibrinolysis and haemostasis through the release of tPA *in vivo* (Levin 1983; Levin *et al.* 1997; Mosesson 2005). In addition, endothelial cells take up extracellular Aβ peptide and release ROS by the action of NADPH oxidases on their cell surface (Babior 2000; Moldovan *et al.* 2006). They also have the ability to produce intracellular ROS and undergo ROS-mediated cell death in response to oxidatively-modified proteins, such as amyloid-like oxidized low density lipoprotein in atherosclerosis (Ciolino and Levine 1997; Stewart *et al.* 2005; Zmijewski *et al.* 2005). SVEC4-10 cells were selected as a representative endothelial-like cell line as it retains morphological and functional characteristics of normal endothelial cells (O'Connell and Edidin 1990), is able to generate ROS in response to toxic insult (ethanol) (Qian *et al.* 2007) and has been used to measure the uptake of Aβ peptide (Kandimalla *et al.* 2009).

The oxidation of dihydrorhodamine 123 (DHR) to the fluorescent product rhodamine can be used to measure the production of many different reactive oxygen and nitrogen species in cellular systems (Henderson and Chappell 1993; Hempel *et al.* 1999; Winterbourn 2014), including HOCl, $ONOO^-$ and its breakdown products (Wardman 2008). Generation of fluorescent rhodamine is triggered in response to $NO^{\bullet}$ and $O_2^{\bullet-}$, mediated by oxidants ($NO_2^{\bullet}$ and $OH^{\bullet}$) formed from the rapid and spontaneous decomposition of $ONOO^-$ (Jourd'heuil *et al.* 2001). While protein aggregates found in extracellular protein deposition diseases have been shown to induce ROS formation, the ability of PGPFs to do so is unknown. To ascertain whether PGPFs could induce the formation of intracellular ROS in a similar manner to aggregated proteins, cells were incubated in the presence of whole protein aggregates or PGPFs and intracellular ROS subsequently measured with DHR (Figure 5.5). Subsequent experiments involved measuring ROS with or without prior incubation with CLU and A2M, and additional non-chaperone (BSA) and native protein controls (Figure 5.6 – 5.8).

In two separate experiments, both amorphous aggregates and aggregate-derived PGPFs were found to illicit the transient production of ROS in cells (Figure 5.5). ROS was rapidly generated within 1 h following incubation with either aggregate or PGPF, and seen to further rise in intensity at 2 h in both cell lines in the presence of PGPFs generated from aggregates of Ovo or ox. IgG, before gradually diminishing over time. In the presence of PGPFs from SOD aggregates, ROS further increased at 2 h in EOC 13.31 but decreased in SVEC4-10 cells before diminishing over time as for the other PGPFs. The one hour time point was selected for use in further experiments to test whether the addition of chaperones could suppress ROS formation.

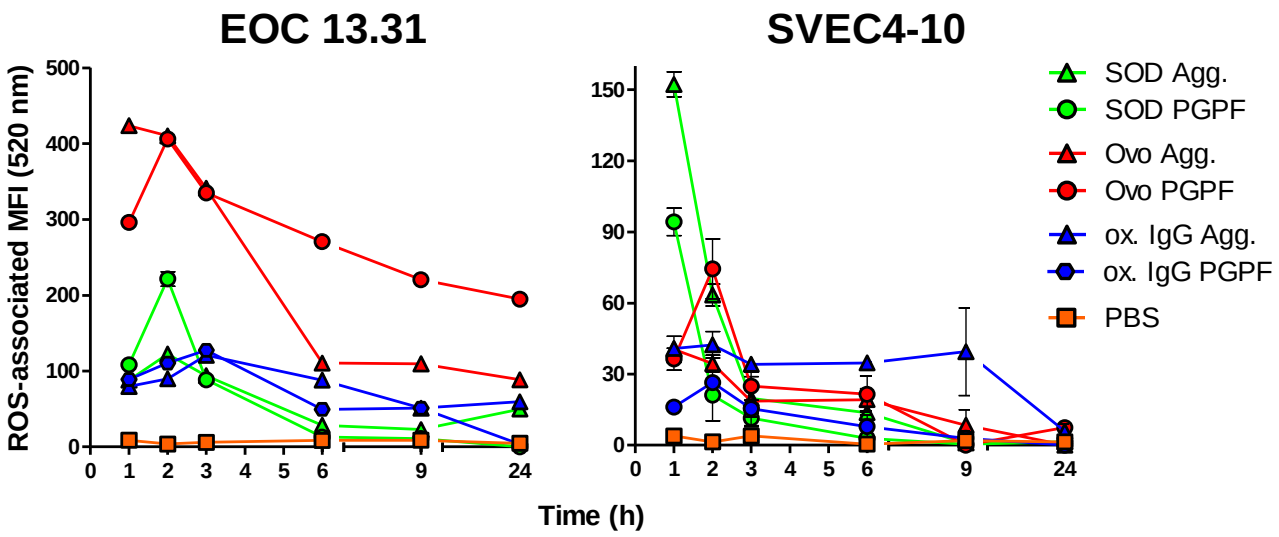

Figure 5.5 Incubation of EOC 13.31 and SVEC4-10 cells with aggregates and aggregate-derived PGPFs results in transiently increased intracellular ROS. Whole amorphous aggregates (Agg.) or aggregate-derived PGPF (prepared as per section 5.2.1) at a final concentration of 100 µg/mL, or PBS control, were incubated with EOC 13.31 or SVEC4-10 cells. Cells were then incubated with 30 µM DHR 1 h prior to flow cytometric analysis. Cells were washed and ROS-associated MFI was measured by flow cytometry. Dead cells stained with propidium iodide were electronically excluded from the analyses. Results are displayed as ROS-associated MFI ± SD (n=9) and represent pooled data from three independent experiments.

The effects of ECs on aggregate/PGPFs-associated formation of ROS were conducted in separate experiments performed at different times for each parent protein used to form aggregates and their corresponding PGPFs (Figure 5.6 SOD; Figure 5.7 Ovo; Figure 5.8 IgG). In experiments testing the effects of SOD agg. and PGPFs on EOC 13.31 cells, relative to PBS control, ROS levels were increased by treatment with both SOD agg. (Figure 5.6 A ~86%, B ~ 87%) and the corresponding PGPFs (Figure 5.6 A ~35%, B ~39%). Similar effects were seen on SVEC4-10 cells in which ROS levels were also increased by treatment with SOD agg. (Figure 5.6 C ~26%, D ~59%) and the corresponding PGPFs (Figure 5.6 C ~9%, D ~19%). Similarly, Ovo agg. and the derived PGPFs induced increased ROS levels in both (i) EOC 13.31 cells (Ovo agg. induced increases, Figure 5.7 A ~48%, B ~63%; PGPF induced increases, Figure 5.7 A ~37 %, B ~19%) and (ii) SVEC4-10 cells (Ovo agg. induced increases, Figure 5.7 C ~52%, D ~52%; PGPF induced increases, Figure 5.7 C ~39%, D ~42%). In EOC 13.31 cells, ROS levels were also increased by treatment with ox. IgG agg.

(Figure 5.8 A ~29%, B ~59%) and the corresponding PGPFs (Figure 5.8 A ~23 %, B ~27%). In contrast, in one set of experiments with SVEC4-10 cells, treatment with either ox. IgG agg. or the corresponding PGPFs failed to induce any significant change in ROS levels (Figure 5.8 C). However, in a separate set of experiments with SVEC4-10 cells, ox. IgG agg. and the derived PGPFs induced small increases in ROS levels (Figure 5.8 D, ~9% and ~5%, respectively). In all the above experiments, treatment with the native proteins did not significantly affect ROS levels in either cell line. Furthermore, in all cases, BSA had no significant effect on ROS levels induced by the aggregates/PGPFs (Figures 5.6 – 5.8).

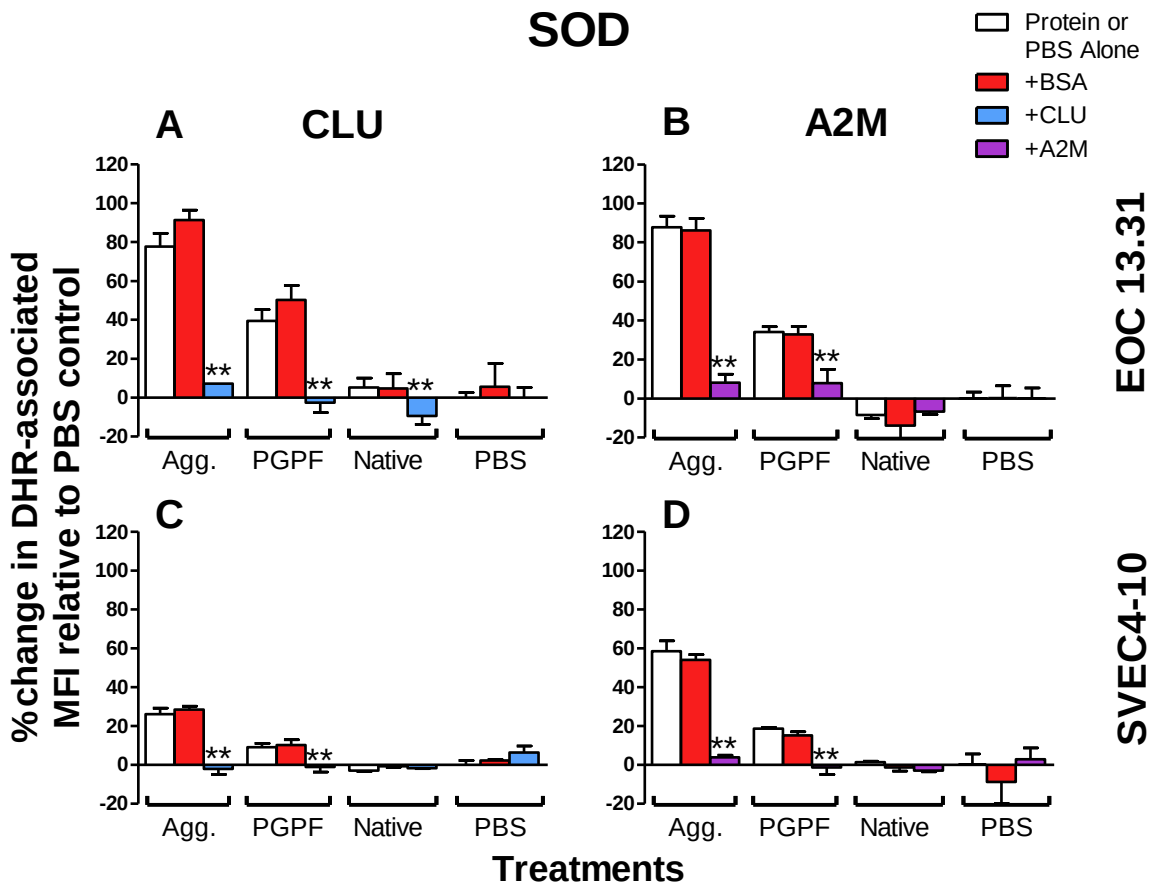

Figure 5.6 Effect of pre-incubation of CLU and A2M with aggregated SOD and corresponding PGPFs on induced ROS levels in EOC-13.31 and SVEC4-10 cells. Whole SOD aggregates (Agg.), SOD aggregate-derived PGPF, native SOD (Native) or PBS alone were incubated in the absence or presence of CLU or A2M or BSA (non-chaperone control protein) for 1 hour at 37˚C prior to addition to cells. Proteins were added to a final concentration of 100 µg/mL and additions are indicated by labelled brackets below the x-axis. Cells were then treated with 30 µM DHR for 1 h, 37˚C. Cells were washed and DHR-associated MFI was measured by flow cytometry. Dead cells stained with propidium iodide were electronically excluded from the analyses. Results are displayed as the mean percentage increase in DHR fluorescence relative to PBS control treated cells; data plotted are means ± SD (n=9) and represent pooled data from three separate experiments (in each experiment measurements were performed in triplicate). Asterixes above error bars denote a significant difference between that treatment (in the presence of chaperone) and the corresponding treatment (in the absence of chaperone); ** ($p<0.01$), * ($p<0.05$).

For both cell lines, pre-incubation of SOD aggregates/PGPFs with CLU significantly decreased ROS levels compared to SOD aggregates/PGPFs ($p<0.01$) in the absence of chaperone (aggregates/PGPFs alone) (Figure 5.6 A,C). For EOC 13.31 cells, pre-incubation of CLU with aggregates/PGPFs prior to their addition to cells inhibited their ability to induce elevated levels of ROS by ~ 67% (SOD agg.) and ~ 48% (SOD agg. PGPF) relative (Figure 5.6 A). For SVEC4-10 cells, the corresponding level of inhibition effected by CLU was essentially 100% for both SOD agg. and SOD agg. PGPF (Figure 5.6 C). A2M was similarly able to inhibit aggregate/PGPF-induced increases in ROS. For both cell lines, pre-incubation of SOD aggregates/PGPFs with A2M significantly decreased ROS levels compared to SOD aggregates/PGPFs ($p<0.01$) alone (Figure 5.6 B,D). For EOC 13.31 cells, pre-incubation of A2M with aggregates/PGPFs prior to their addition to cells inhibited their ability to induce elevated levels of ROS levels by ~ 91% (SOD agg.) and ~ 77% (SOD agg. PGPF) (Figure 5.6 B). For SVEC4-10 cells, the corresponding level of inhibition effected by A2M was ~ 94% (SOD agg.) and ~ 100% (SOD agg. PGPF) (Figure 5.6 D).

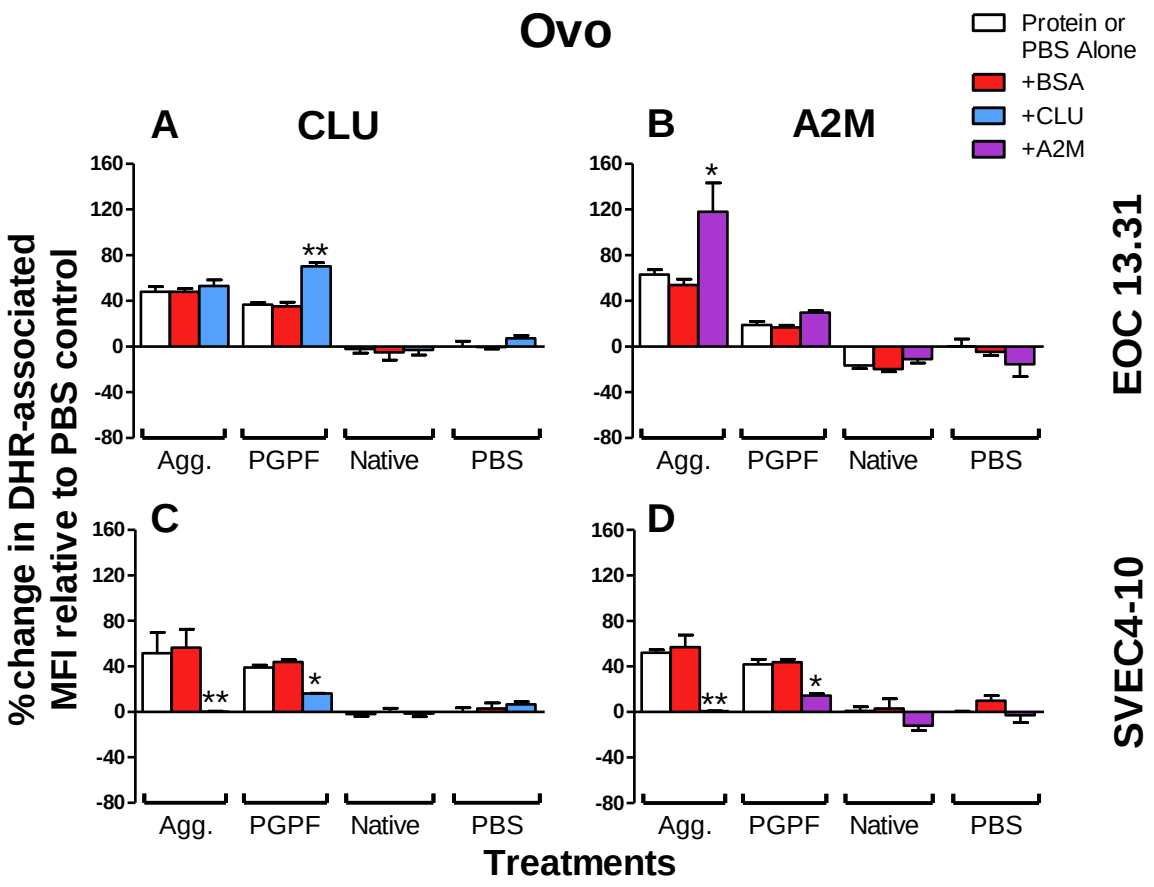

Figure 5.7 Effect of pre-incubation of CLU and A2M with aggregated Ovo and corresponding PGPFs on induced ROS levels in EOC-13.31 and SVEC4-10 cells. Whole Ovo aggregates (Agg.), Ovo aggregate-derived PGPF, native Ovo (Native) or PBS alone were incubated in the absence or presence of CLU or A2M or BSA (non-chaperone control protein) for 1 hour at 37˚C prior to addition to cells. Proteins were added to a final concentration of 100 µg/mL and additions are indicated by labelled brackets below the x-axis. Cells were then treated with 30 µM DHR for 1 h, 37˚C. Cells were washed and DHR-associated MFI was measured by flow cytometry. Dead cells stained with propidium iodide were electronically excluded from the analyses. Results are displayed as the mean percentage increase in DHR fluorescence relative to PBS control treated cells; data plotted are means ± SD (n=9) and represent pooled data from three separate experiments (in each experiment measurements were performed in triplicate). Asterixes above error bars denote a significant difference between that treatment (in the presence of chaperone) and the corresponding treatment (in the absence of chaperone); ** ($p<0.01$), * ($p<0.05$).

Comparing EOC 13.31 and SVEC4-10 cells, pre-incubation of Ovo aggregates/PGPFs with CLU elicited different and opposing effects on the level of ROS (Figure 5.7 A,C). Pre-incubation of CLU with aggregates/PGPFs prior to their addition to EOC 13.31 cells did not alter their ability to induce elevated levels of ROS by Ovo agg. In contrast, in cells treated with Ovo agg. PGPF, pre-incubation with CLU increased levels of ROS by ~ 44% (Figure 5.7 A; $p<0.01$). For SVEC4-10 cells, the corresponding significant levels of inhibition effected by CLU were ~ 100% (Ovo agg.) and ~ 29% (Ovo agg. PGPF) (Figure 5.7 C; $p<0.05$). As for CLU, when comparing EOC 13.31 and SVEC4-10 cells, pre-incubation of Ovo aggregates/PGPFs with A2M elicited different and opposing effects on the level of induced ROS, depending on the cell type (Figure 5.7 B,D). For EOC 13.31 cells, pre-incubation of A2M with Ovo Agg. prior to their addition to cells significantly increased its ability to induce elevated levels of ROS by ~ 17% (Figure 5.7 B; $p<0.05$). In contrast, A2M had no effect on the level of ROS induced by Ovo Agg. derived PGPFs (Figure 5.7 B). For SVEC4-10 cells, the corresponding level of inhibition effected by CLU was ~ 100% (Ovo agg.; $p<0.01$) and ~ 48% (Ovo agg. PGPF; $p<0.05$) (Figure 5.7 D).

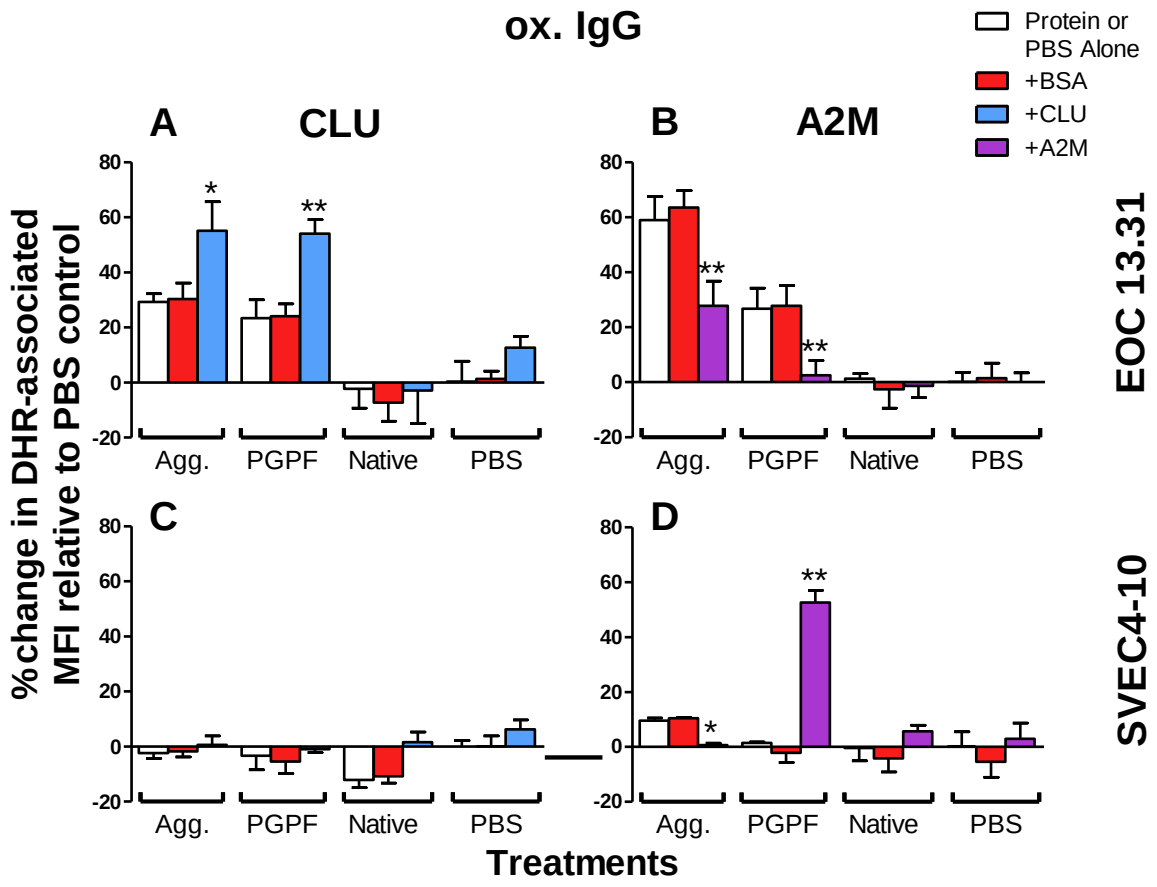

Figure 5.8 Effect of pre-incubation of CLU and A2M with aggregated ox. IgG and corresponding PGPFs on induced ROS levels in EOC-13.31 and SVEC4-10 cells. Whole ox. IgG aggregates (Agg.), ox. IgG aggregate-derived PGPF, native IgG (Native) or PBS alone control were incubated in the absence or presence of CLU or A2M or BSA (non-chaperone control protein) for 1 hour at 37˚C prior to addition to cells. Proteins were added to a final concentration of 100 µg/mL and treatments are indicated by labelled brackets below the x-axis. Cells were then treated with 30 µM DHR for 1 h, 37˚C. Cells were washed and DHR-associated MFI was measured by flow cytometry. Dead cells stained with propidium iodide were electronically excluded from the analyses. Results are displayed as the mean percentage increase in DHR fluorescence relative to PBS control treated cells; data plotted are means ± SD (n=9) and represent pooled data from three separate experiments (in each experiment measurements were performed in triplicate). Asterixes above error bars denote a significant difference between that treatment (in the presence of chaperone) and the corresponding treatment (in the absence of chaperone); ** ($p<0.01$), * ($p<0.05$).

For EOC 13.31 cells, pre-incubation of ox. IgG aggregates/PGPFs with CLU significantly increased induced ROS levels compared to ox. IgG agg. and ox. IgG PGPF alone (Figure 5.8 A). Pre-incubation with CLU increased the ability of ox. IgG agg. and the derived PGPFs to induce elevated levels of ROS by ~ 68% and ~ 117%, respectively (Figure 5.8 A). Pre-incubation with A2M had the opposite effect to CLU on the induction of ROS in EOC 13.31 cells by ox. IgG aggregates/PGPFs. Pre-incubation of A2M with aggregates/PGPFs significantly inhibited their subsequent ability to induce ROS by ~ 52% (ox. IgG agg.) and ~ 90% (ox. IgG agg. PGPF) (Figure 5.8 A). As mentioned before, ox. IgG agg. and the corresponding PGPFs generally induced very limited ROS production in SVEC4-10 cells. Pre-incubation of CLU with these protein species before adding to SVEC4-10 cells had no significant effect on induced ROS levels (Figure 5.8 C). In contrast, pre-incubation of A2M with ox. IgG aggregates/PGPFs did significantly affect induced ROS levels (Figure 5.8 D). A2M effectively abolished the small amount of ROS induced by ox. IgG agg. but substantively increased (by many-fold) ROS induced by ox. IgG PGPF (Figure 5.8 D).

5.3.4 Effect of chaperones on the cytotoxicity of protein aggregates and PGPFs

Cell death by either apoptosis or necrosis, which are distinct from one another, can involve the formation of ROS (Fink and Cookson 2005; Kroemer *et al.* 2009) which if severe enough may end in cell death (Fleury *et al.* 2002; Emerit *et al.* 2004). The extent and type of cell death depends on the intensity of the insult (Bonfoco *et al.* 1995) and cell death signalling via mitochondrial mediated caspase-dependent and independent pathways (Ankarcrona *et al.* 1995; McManus *et al.* 2014). It is not known whether PGPFs derived from amorphously aggregated proteins can harm cells, or whether chaperones can ameliorate any cytotoxic effects. Nucleic acid stain (Sytox Green) and cell proliferation (MTS) assays were used to analyse the potential of amorphously aggregated proteins and their PGPFs to induce cell-death in EOC 13.31 and SVEC4-10 cells, and whether the presence of ECs ameliorated their cytotoxic effects. In both EOC 13.31 and SVEC4-10 cells, protein aggregates and their corresponding PGPFs were found to exert significant cytoxicity as indicated by an increase in Sytox green fluorescence (compared to PBS control; $p<0.05$); similar to the positive control etoposide (Figure 5.9). Native Ovo and IgG lacked any significant cytotoxicity towards either cell line. Relative to the PBS control, native SOD significantly decreased Sytox green-fluorescence after 48 h ($p<0.05$), suggesting that prolonged incubation of SOD with EOC

13.31 and SVEC4-10 has a positive effect on cell viability. This may be due to an antioxidant action of SOD (Dhanasekaran *et al.* 2004).

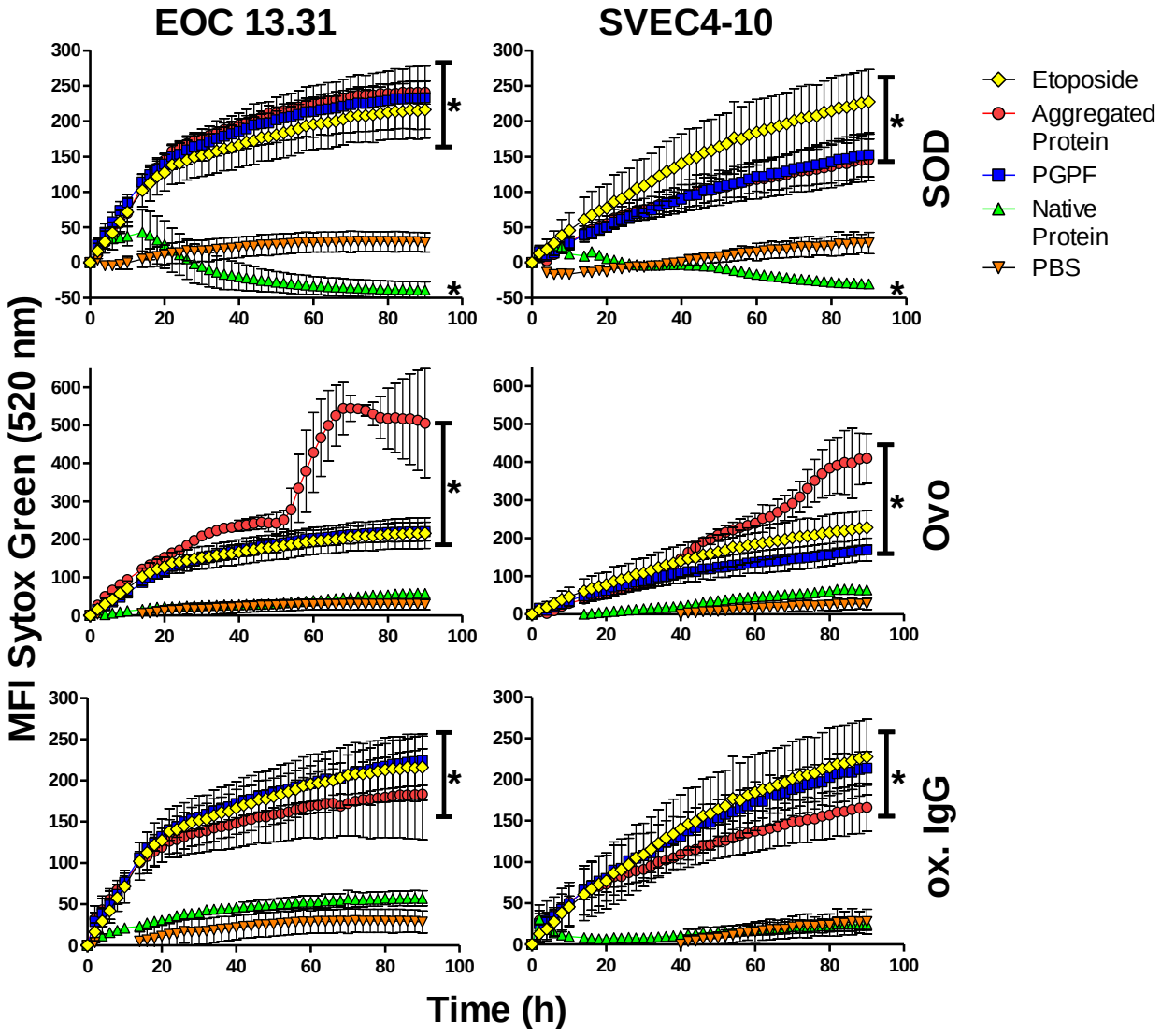

Figure 5.9 Amorphous protein aggregates and derived PGPFs induced cell death in EOC-13.31 and SVEC4-10 cells. Proteins were incubated with EOC 13.31 and SVEC4-10 cells at a final concentration of 200 µg/mL at 37°C for 90 h. Real time Sytox green assay was performed by incubation with 1 µM SYTOX Green viability dye (Life Technologies) and measuring the development of SYTOX Green-associated fluorescence in live cultured cells for 90 h by time-resolved epifluorescence microscopy. Results displayed as SYTOX green-associated mean fluorescence intensity ± SD (n=6), and the data shown is pooled from three independent experiments. Vertical brackets marked with an asterix denote a significant difference between the bracketed treatments and the PBS control; * ($p<0.05$).

MTS assays are used to measure the amount of metabolically active and hence viable cells. For both cell types, as in Sytox-green assays, aggregate-derived PGPFs exerted significant toxicity (Figure 5.10; $p < 0.001$). For both cell types, pre-incubation of PGPFs derived from SOD/Ovo/ox. IgG aggregates with CLU or A2M (but not BSA) prior to their addition to cells significantly reduced PGPF-induced cytotoxicity (Figure 5.10; $p < 0.001$). Native proteins and their corresponding PGPFs, and the non-chaperone control protein BSA, had no significant effect on the viability of either cell type.

Relative to PBS control, SOD agg. PGPFs reduced the viability of EOC 13.31 cells by ~ 72% and the viability of SVEC4-10 cells by ~ 45%. Pre-incubation of CLU or A2M with SOD agg. PGPF prior to their addition to cells, completely inhibited their cytotoxicity against both cell types (Figure 5.10). In the case of SVEC4-10 cells, this treatment actually increased the number of viable cells above that of the PBS control (Figure 5.10). Ovo agg. PGPFs reduced the viability of EOC 13.31 cells by ~ 44% and in SVEC4-10 cells by ~ 55%. Pre-incubation of CLU or A2M with SOD agg. PGPF prior to their addition to EOC13.31 cells, reduced the cytotoxicity of the PGPFs by ~ 82% % and ~ 79%, respectively (Figure 5.10). The corresponding levels of inhibition of PGPF-induced cytotoxicity for SVEC4-10 cells were ~ 90% and ~ 84% for CLU and A2M, respectively (Figure 5.10). Lastly, ox. IgG agg. PGPFs reduced the viability of EOC 13.31 cells by ~ 44% and in SVEC4-10 cells by ~ 30%. Pre-incubation of CLU or A2M with ox. IgG agg. PGPF prior to their addition to EOC 13.31 cells inhibited PGPF-induced cytotoxicity by ~ 82% % and ~ 100%, respectively (Figure 5.10). In SVEC4-10 cells, pre-incubation of ox. IgG aggregate derived PGPFs with CLU completely protected against cytotoxicity and actually increased viable cell numbers to ~ 124% of the PBS control; corresponding treatment with A2M reduced PGPF-associated toxicity by ~ 88% (Figure 5.10).

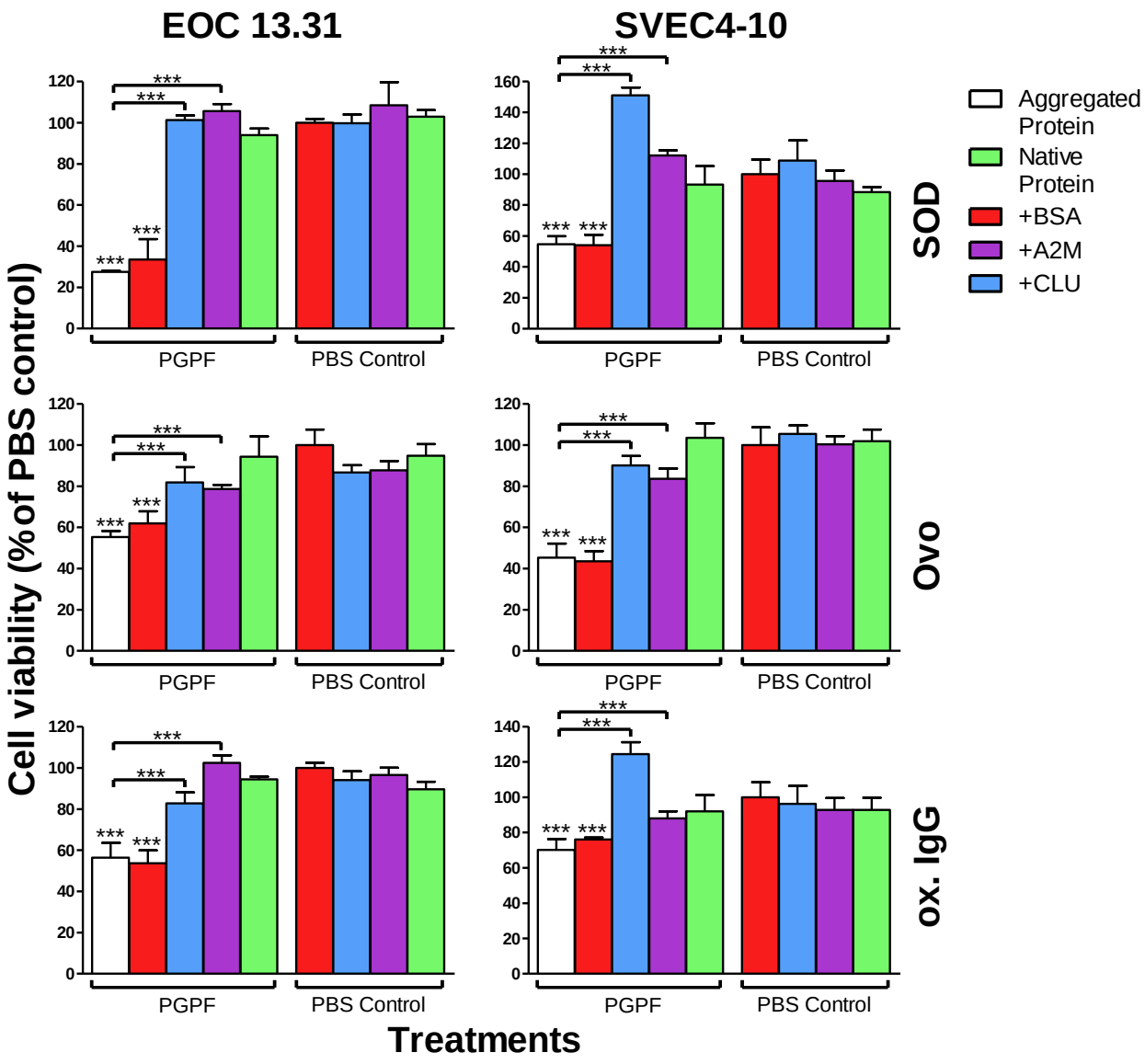

Figure 5.10 Effect of CLU and A2M on the cytotoxicity of amorphous protein aggregates and PGPFs derived from them. Sterile samples of aggregates, native proteins and PGPFs derived from the digestion of both were prepared as described in section 5.2.1. Samples were then pre-incubated in the presence or absence of CLU or A2M or BSA (non-chaperone control protein) for 1 h at 37˚C before incubating with EOC 13.31 and SVEC4-10 cells at a final concentration of 200 µg/mL at 37°C for 24 h. The identity of treatments is indicated by labelled brackets below the x-axis. The MTS assay was performed as described in section 5.2.6. Results are plotted as a percentage of the A_{490} for PBS control wells. Individual data points are means ± SD (n=9), and the data shown is pooled from three independent experiments done in triplicate. Asterixes placed immediately above error bars indicate that the sample is significantly different to the corresponding PBS control; asterixes above horizontal brackets indicate a significant difference between the indicated treatment in the presence versus absence of chaperone; *** ($p<0.001$).

5.3.5 Protein aggregates and PGPFs induce loss of mitochondrial membrane potential

While ROS formation can be indicative of either apoptosis or necrosis, the rapid dissipation of mitochondrial membrane potential ($\Delta\Psi_{MIT}$) following cytotoxic insult can be indicative of apoptosis (Zamzami *et al.* 1995; Fleury *et al.* 2002; Kroemer *et al.* 2009). To examine the mode of cell death induced by protein aggregates and PGPFs, ox. IgG aggregates, their corresponding PGPFs or native IgG-derived PGPFs were incubated with EOC 13.31 and SVEC4-10 cells while measuring $\Delta\Psi_{MIT}$ over time. As controls, cells were also separately incubated with CCCP (to induce loss of $\Delta\Psi_{MIT}$) and etoposide (to induce apoptosis).

In two separate experiments, both CCCP and etoposide significantly and rapidly dissipated $\Delta\Psi_{MIT}$ over time, relative to the PBS control (Figure 5.11; $p<0.001$). Both ox. IgG aggregates and aggregate-derived PGPFs induced significant loss of $\Delta\Psi_{MIT}$ in both EOC 13.31 and SVEC4-10 within 3 h ($p<0.001$). Native IgG PGPFs had no significant effect on $\Delta\Psi_{MIT}$ during the duration of the experiment. Confocal transmission images showed cells exhibiting a gradual change in morphology known as “rounding up” suggestive of apoptosis (not shown). Taken together, the rapid loss of $\Delta\Psi_{MIT}$ and morphological changes suggest that the cytotoxicity of ox. IgG PGPF may induce apoptosis, although more evidence is needed to conclusively state this.

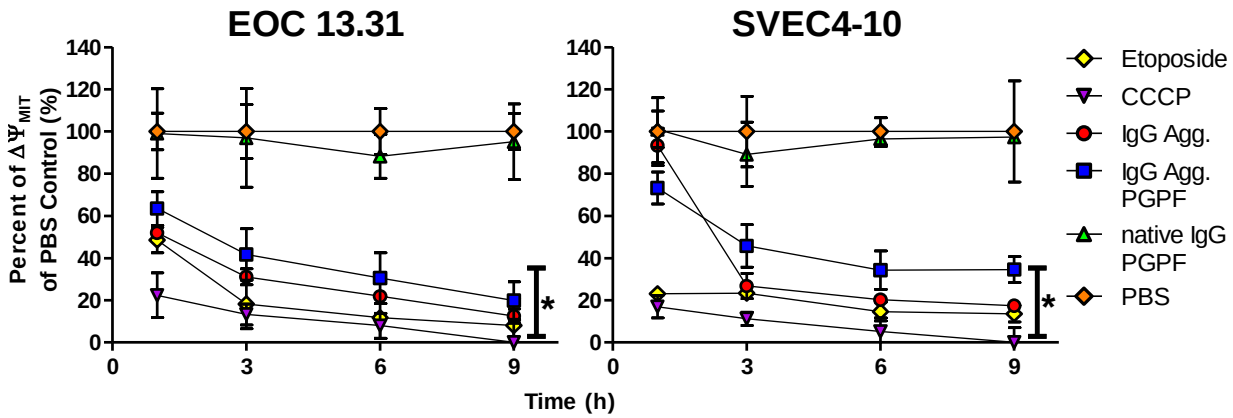

Figure 5.11 Ox. IgG aggregates and derived PGPFs induced loss of mitochondrial mitochondrial potential in EOC-13.31 and SVEC4-10 cells. Samples of 200 µg/mL ox. IgG aggregates or PGPFs derived from ox. IgG aggregates, or native IgG, were incubated for 9 h with EOC 13.31 and SVEC4-10 cells which were continuously imaged by time resolved confocal microscopy. Changes in mitochondrial membrane potential ($\Delta\Psi_{MIT}$) were measured as described in section 5.2.7. As positive controls, cells were incubated with CCCP to induce loss of $\Delta\Psi_{MIT,}$ and etoposide to induce apoptosis. Images were analysed using Leica LAS AF "Lite" and results are displayed as the percent of $\Delta\Psi_{MIT}$ of PBS control ± SD (n=6), and the data shown are pooled from three independent experiments. Vertical brackets marked with an asterix denote a significant difference between the bracketed treatments versus the PBS control; *** ($p<0.001$).

5.3.6 Cell surface-binding and internalisation of labelled PGPFs^{488}

5.3.6.1 PGPFs^{488} are internalised rapidly and co-localise with lysosomes

Live-cell imaging is a powerful technique - it allows the monitoring of cell-based events that are normally difficult to measure using fixed time points, such as the internalisation of proteins and their trafficking to cellular compartments. PGPFs were labelled with CF-488 (PGPFs^{488}) and purified by SEC. PGPFs^{488} were then incubated with cells which were subsequently imaged using confocal microscopy. PGPFs were internalised into the cytoplasm and dendritic-like projections but not the nucleus of: astrocyte-like (AST-1), microglial-like (EOC 13.31), motor neuron-like (NSC-34) and endothelial-like (SVEC4-10) cells, and purified human polymorphonuclear neutrophils (PMN) (Figure 5.12). Having identified that Ovo agg. PGPFs^{488} are internalised into several cell types, in subsequent experiments the internalisation of labelled PGPFs derived from SOD, Ovo and ox. IgG aggregates was studied in greater detail using two cell lines, EOC 13.31 and SVEC4-10.

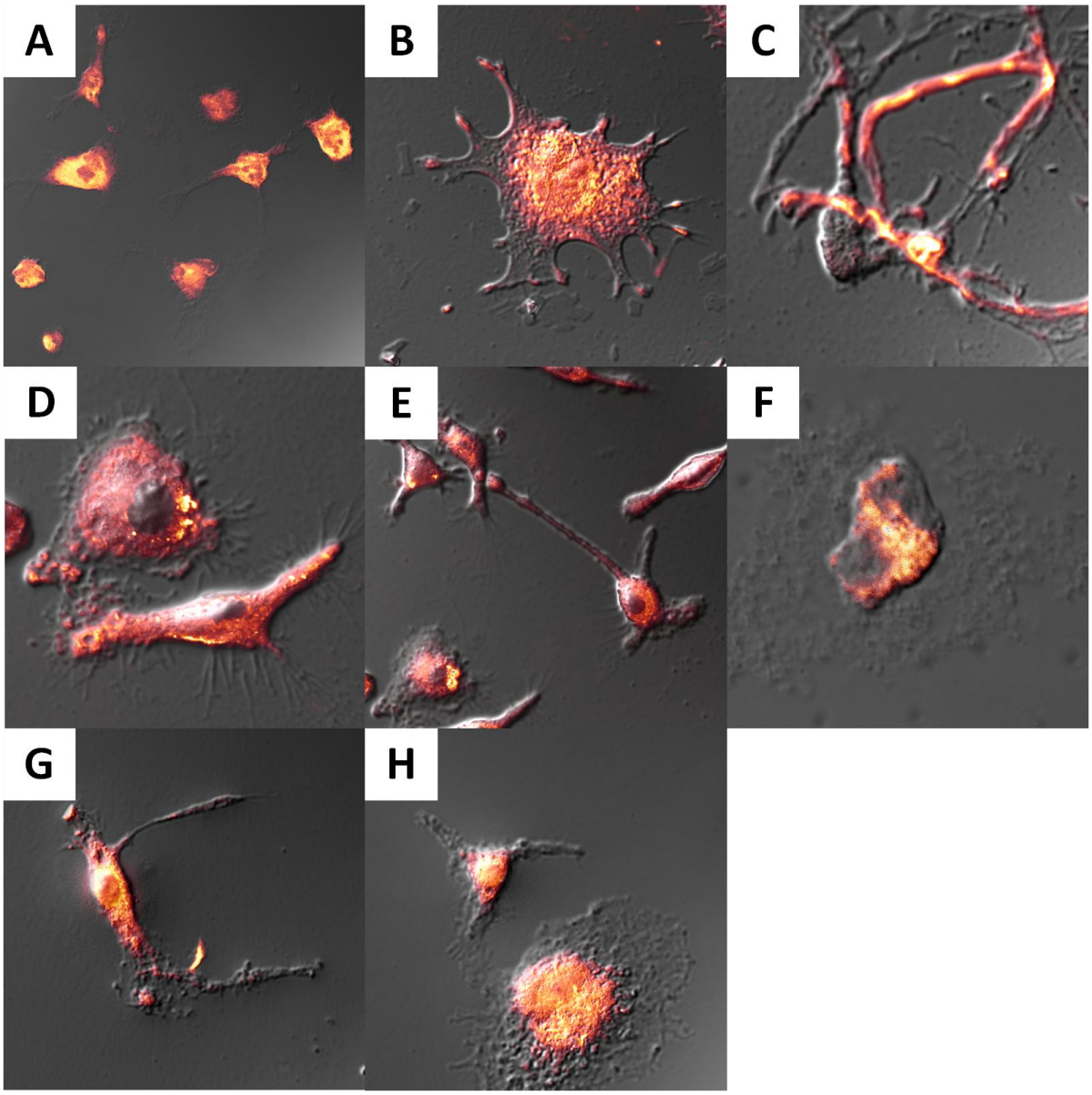

Figure 5.12 Representative confocal microscopy images of the internalisation of fluorescently labelled Ovo aggregate-derived PGPFs488 into cells. A range of cell-types grown on cover slips were incubated with Ovo aggregate-derived PGPFs^{488} for 1 h and imaged using confocal microscopy. PGPFs^{488} were internalised into all cell-types assayed, including astrocyte-like (AST-1; A), microglial-like (EOC 13.31; B – C), motor neuron-like (NSC-34; D – E), purified human polymorphonuclear neutrophils (PMN; F), and endothelial-like (SVEC4-10; G – H) cells. Free CF-488 label served as a negative control for internalisation (5.2.8). No visible internalisation of the negative control was observed.

Using image analysis including Pearson's correlation coefficient and Mander's overlap coefficient (for a description of statistical analysis method used to derive correlation coefficients, see section 5.2.10), PGPFs were found to significantly co-localise with lysosomes (Figure 5.13). Overlayed confocal images show intracellular $PGPF^{488}$-associated fluorescence overlapping with that of Lysotracker staining in EOC 13.31 and SVEC4-10 cells. This suggests that PGPFs are being shuttled to lysosomes after being internalised. In both EOC-13 and SVEC4-10 cells, $PGPFs^{488}$ were rapidly internalised within 15 min into the intracellular space and subsequently shuttled to lysosomes (Figure 5.14). The rates of internalisation of aggregate-derived PGPFs differed between both the parent protein aggregate used to generate the PGPFs as well as the cell type. In EOC-13 cells, the rates of internalisation of ox. IgG $PGPFs^{488}$ were significantly higher than that of PGPFs derived from aggregates of either SOD or Ovo. In contrast, in SVEC4-10 cells, the rate of internalisation of Ovo aggregate derived $PGPF^{488}$ was significantly higher than the rates of uptake of $PGPFs^{488}$ derived from aggregates of either SOD or oxidized IgG. Generally, the rate of $PGPFs^{488}$ internalisation was significantly higher in EOC-13.31 cells than in SVEC4-10 cells.

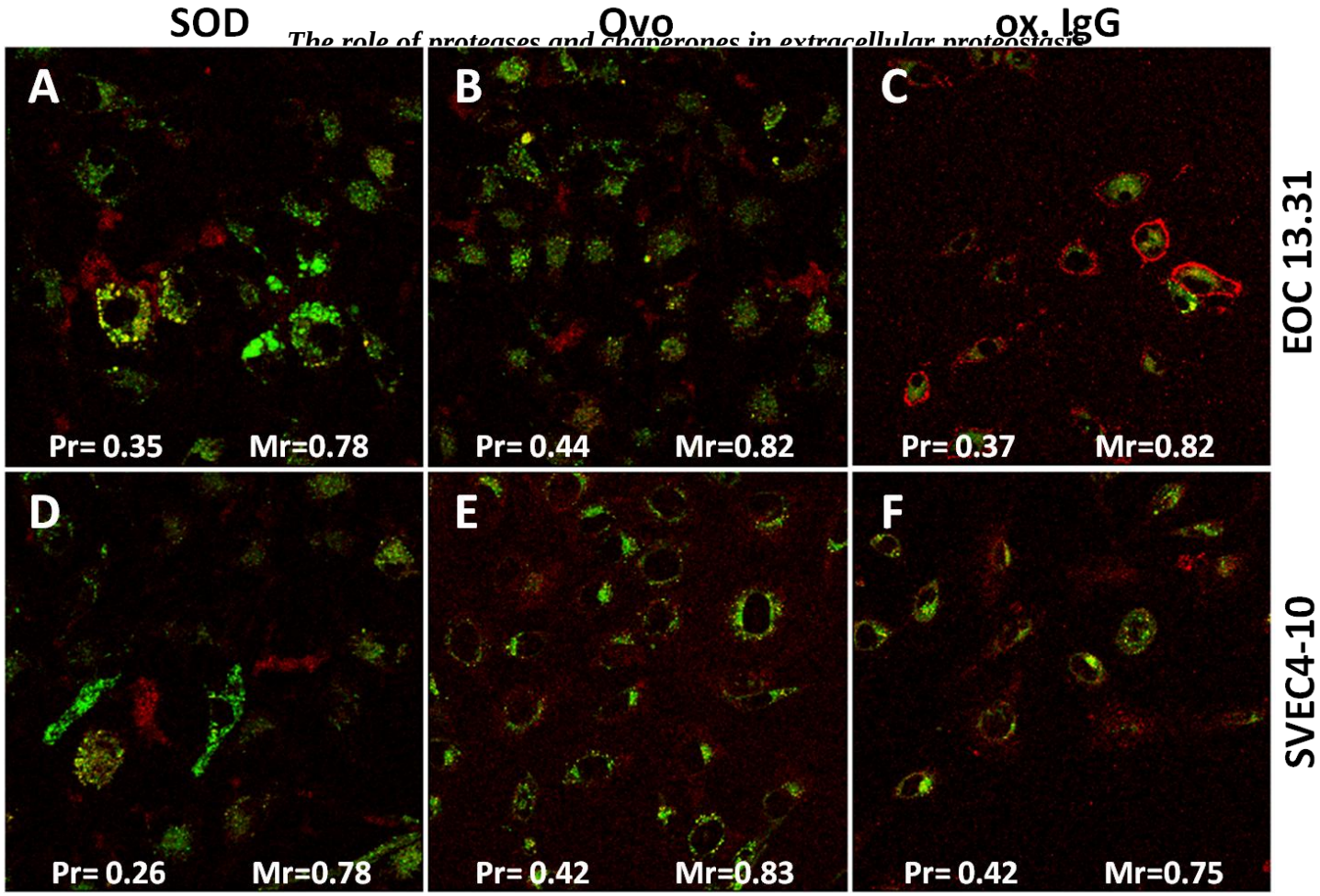

Figure 5.13 Representative confocal microscopy images of the internalisation of fluorescently labelled aggregate-derived PGPFs into the lysosomes of EOC 13.31 and SVEC4-10 cells. 75 nM Lysotracker Deep Red (Molecular Probes) and 20 µ/mL $PGPFs^{488}$ were added to EOC 13.31 (A – C) and SVEC4-10 (D – F) cells (section 5.2.8). Images are representative of regions of interest taken at 30 min of a 3 h time course imaged by time-resolved confocal microscopy. $PGPFs^{488}$ (red fluorescence) derived from aggregates of SOD (A, D), Ovo (B, E), and ox. IgG (C, F) were overlayed with lysosomes (green fluorescence). The extent of colocalisation was analysed with ImageJ using the plugin "colocalization finder" to derive Pearson's correlation coefficient (Pr) ranging from -1 to +1 and Mander's overlap coefficient (Mr) ranging from 0 to 1 (correlation statistical analysis; section 5.2.10).

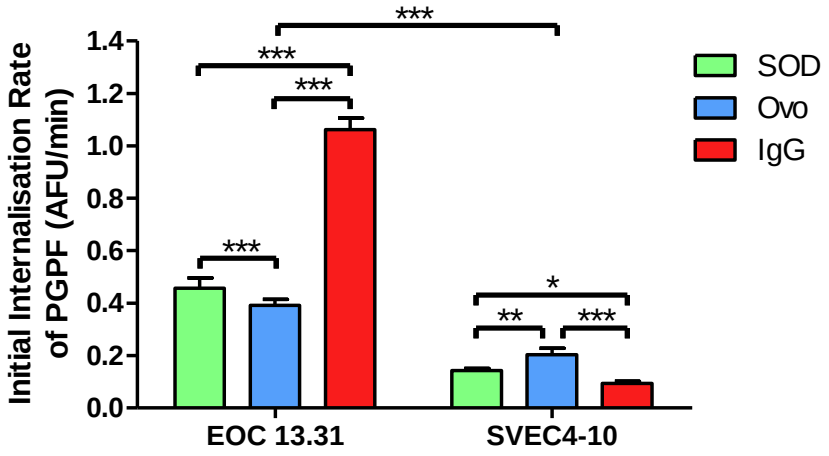

Figure 5.14 Internalisation rates of aggregate-derived PGPFs into EOC-13.31 and SVEC4-10 cells. Initial rate of uptake was calculated using a linear regression of arbitrary fluorescence units versus time in minutes (AFU/min). This was calculated over 180 min of recorded internalisation, which was based on the increase in $PGPF^{488}$ fluorescence into an intracellular, circular region of interest (ROI) over the recorded period (section 5.2.8). Results represent the mean initial rate of fluorescence uptake of at least 6 regions of interest imaged per well and is expressed as AFU/min ± SD (n=6). For each type of $PGPFs^{488}$, measurements were performed in duplicate and each experiment was performed at least three times. Asterixes above horizontal brackets indicate a significant difference in the rates of internalisation for different $PGPF^{488}$ between the bracketed samples; * $p<0.05$, ** $p<0.01$, *** $p<0.001$.

5.3.6.2 Binding of $PGPFs^{488}$ to the surface of cells is via multiple mechanisms and is affected by the presence of chaperones

As a first step to examine if pre-incubation of PGPFs affects their binding to the cell-surface, and which receptors or endocytic mechanism(s) might be involved, EOC 13.31 and SVEC4-10 cells were incubated with labelled PGPFs that had been pre-incubated (or not) with ECs. The incubations were performed for 30 min on ice in the presence of 0.1% (w/v) sodium azide (to stop internalisation of the PGPFs) and the level of cell bound $PGPFs^{488}$ was then quantified by flow cytometry.

In the absence of ECs, PGPFs bound to both EOC-13.31 and SVEC4-10 cells (Figure 5.15). Generally more $PGPF^{488}$ bound to EOC-13.31 than to SVEC4-10 cells. Neither A2M or CLU

had any significant effect on the binding of SOD aggregate derived $PGPF^{488}$ to either EOC-13.31 or SVEC4-10 cells (Figure 5.15). In contrast, A2M significantly inhibited the binding of Ovo aggregate derived $PGPF^{488}$ to EOC-13.31 and SVEC4-10 cells by ~ 24% and ~ 35%, respectively. Corresponding values for the inhibition of binding produced by CLU were ~ 30% and ~ 34%, respectively. A2M and CLU also significantly decreased cell-surface binding of ox. IgG derived PGPFs to SVEC4-10 cells relative to the corresponding controls by ~ 43% and ~ 59%, respectively. In contrast, relative to the corresponding control, A2M significantly increased the binding of these same PGPFs to EOC-13.31 cells by ~ 37%. Pre-incubation with CLU increased cell-surface binding of ox. IgG PGPF to EOC 13.31 cells by ~ 12%.

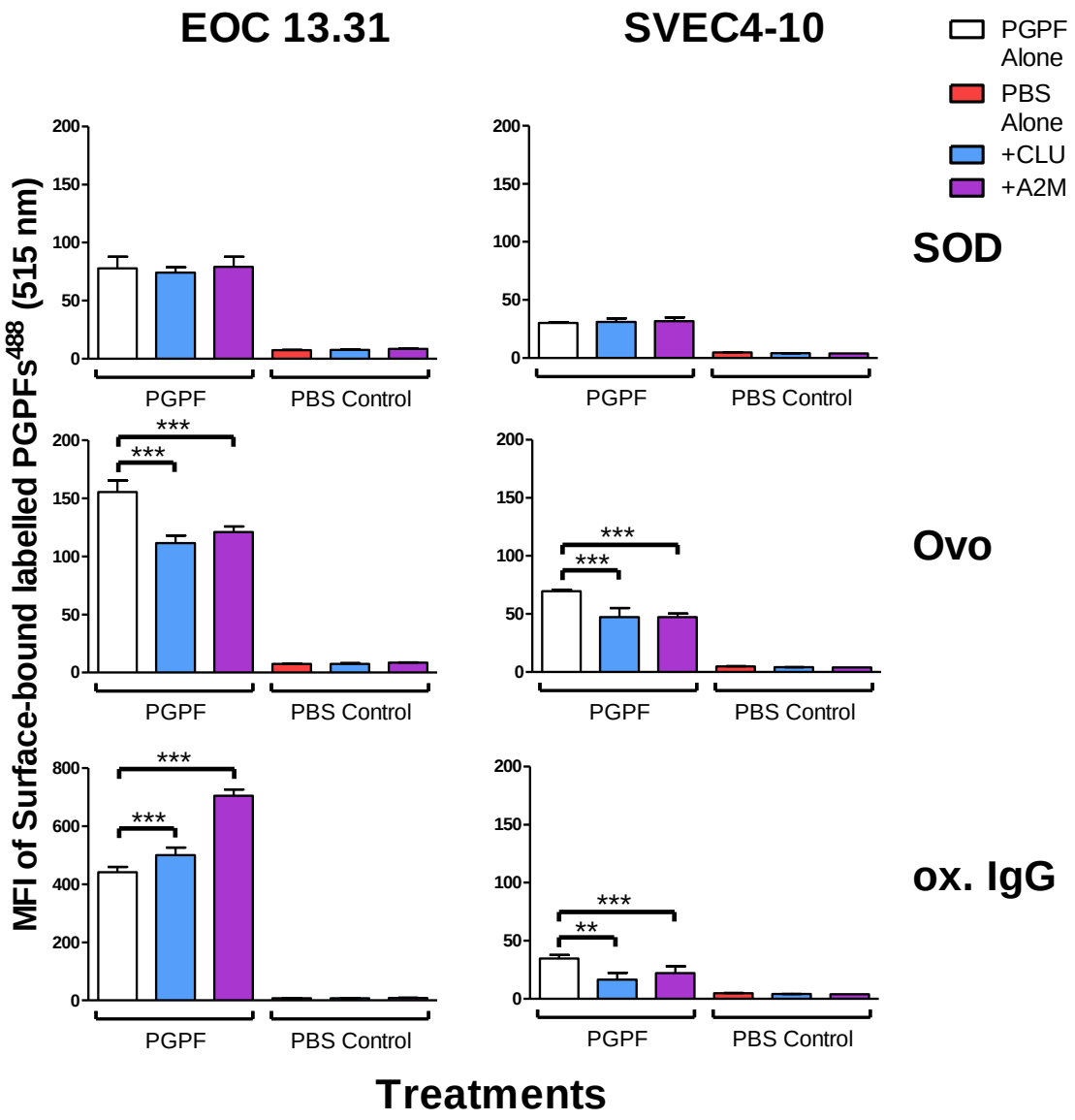

Figure 5.15 Effect of CLU and A2M on the binding of aggregate-derived PGPF to the surface of EOC-13.31 and SVEC4-10 cells. Prior to adding to cells, PGPFs^{488} were incubated with or without CLU or A2M (section 5.2.9.1). Cells were then incubated in the presence (PGPF) or absence (PBS Control) of PGPFs^{488} at a final concentration of 20 µg/mL for 30 min in ice-cold BSA/PBS/Az. Cells were washed in the same buffer and MFI measured by flow cytometry. Dead cells stained with propidium iodide were electronically excluded from the analyses. Results are displayed as the MFI ± SD (n=9) of three independent experiments performed in triplicate. Asterixes above horizontal bars indicate a significant difference between the indicated treatments compared to cells in the absence of chaperones (PGPF Alone); ** ($p<0.001$), *** ($p<0.001$).

Next, a panel of inhibitors was selected based on broad-specificity for multiple receptors and endocytic mechanisms as well as more specific antagonists for receptors of an immune-cell origin (section 5.2.8.1; Table 5.1). The results indicate that the receptors and mechanism(s) by which aggregate-derived PGPFs bind to the surface of cells varies with both the PGPFs source as well as cell type used (Table 5.2). EIPA, LPS and MethBCD significantly inhibited the binding of SOD aggregate derived $PGPF^{488}$ to EOC 13.31 cells. Thus, this binding appears to be mediated in part by toll-like receptors and lipid rafts, and internalisation by macropinocytosis. Macropinocytosis was not expected to occur under experimental conditions, as they were conducted at 4˚C, regardless a significant reduction in $PGPF^{488}$-associated fluorescence was observed. In the case of Ovo aggregate derived $PGPF^{488}$, significant inhibition of binding to EOC-13.31 cells was obtained by GST-RAP, LPS, MethBCD and mannan, implicating the involvement of LDL family of receptors, toll-like receptors, mannose receptor, and lipid rafts. Lastly, the binding of ox. IgG derived $PGPF^{488}$ to EOC-13.31 cells was significantly inhibited by anti-TLR2 and anti-CD14 antibodies, fucoidan and PolyI, implicating toll-like receptors (TLR) 2 and 3, CD14, and scavenger receptors in the binding. CD14 is a pattern recognition receptor with a hydrophobic binding pocket (Kelley *et al.* 2013), found either in a secreted soluble form or anchored on the surface of immune cells (Jersmann 2005). CD14 acts as to deliver lipoproteins to TLR1 and TLR2 (soluble form) and as a co-receptor for the detection of bacterial LPS by forming a ternary complex with the Toll-like receptor TLR 4 and MD-2 (anchored form) (Jersmann 2005; Ranoa *et al.* 2013). In the case of SVEC4-10 cells, the only significant instances of inhibition measured were MethBCD on the binding of SOD aggregate derived $PGPF^{488}$, and fucoidan, on the binding of ox. IgG derived $PGPF^{488}$, implicating lipid rafts and scavenger receptors respectively.

Table 5.2 Summary of the effects of specific inhibitors on the binding of labelled PGPFs488 derived from aggregated SOD, Ovo and ox. IgG to the surface of EOC-13.31 and SVEC4-10 cells.

Cell Line	PGPF	anti-TLR-2 Ab	PolyI (TLR-3)	anti-TLR-4 Ab	LPS (pan-TLR)	anti-CD14 Ab	EIPA	Fucoidan	Mannan	M-β-CD	RAP
EOC-13.31	SOD	-	-	-	57.5±7.8	-	20.2±9.2	-	-	37.3±5.8	-
	Ovo	-	-	-	21.5±7.4	-	-	-	19.2±5.2	25.7±0.1	46.9±7.9
	ox. IgG	16.6±6.3	21.1±6.9	-	-	41.6±8.7	-	89.2±0.3	-	-	-
SVEC4-10	SOD	-	-	-	-	-	-	-	-	23.3±7.2	-
	Ovo	-	-	-	-	-	-	-	-	-	-
	ox. IgG	-	-	-	-	-	-	28.7±9.0	-	-	-

Cells were incubated in the absence or presence of inhibitor (section 5.2.9.2) for 30 min in ice-cold BSA/PBS/Az, followed by incubation in the same buffer and temperature for a further 30 min in the presence or absence of 20 µg/mL $PGPFs^{488}$. Cells were washed and MFI measured by flow cytometry. Results are displayed as the MFI ± SD (n=9) of three independent experiments performed in triplicate for each separate inhibitor. Horizontal dashes denote that no significant inhibition was measured.

5.4 DISCUSSION

5.4.1 Proteolytic degradation of amorphous aggregates by the plg activation system

In the CNS, both neurons and microglial cells express tPA (Salles and Strickland 2002), plg (Tsirka *et al.* 1997), PAI-1 (Masos and Miskin 1997), PAI-2 (Akiyama *et al.* 1993; Dietzmann *et al.* 2000), and neuroserpin (Teesalu *et al.* 2004; Yepes and Lawrence 2004; Melchor and Strickland 2005). tPA is secreted from neurons and microglia following aggregate-induced excitotoxic injury, such as in Alzheimer's disease and spongiform encephalopathies (Fischer *et al.* 2000; Siao and Tsirka 2002; Siao 2003) and has been shown to bind to and become activated by structural components of amyloid fibrils, which acted as both a co-factor and substrate (Kranenburg *et al.* 2002; Gebbink *et al.* 2009). The ability of amorphously structured aggregates (but not native proteins) to significantly enhance tPA-mediated plg activation was demonstrated in Chapter 4. This activated form of tPA then cleaves plg into the active serine protease plm which can degrade protein aggregates into PGPFs (Figure 5.1).

Plm was found to degrade amorphous aggregates efficiently; for example, after 8 h of reaction time, 100 mU plm would generate 3.13 mg/mL of soluble PGPFs of varying sizes from 4 mg/ml of SOD aggregate (determined using BCA assay (section 2.3); not shown) (Figure 5.1 and 5.2). This activity is similar to that reported for *in vitro* plm degradation of aggregated Aβ (Tucker *et al.* 2000). Concentrations of plm used to generate PGPFs from amorphous aggregates were half that reported for plg in plasma (1.6 – 2 µM) (Cederholm-Williams 1981; Kwaan 1992). The resting cerebrospinal fluid concentrations for plg are reported to be much lower than plasma concentrations (3 – 15 nM) (Mezzapesa *et al.* 2014), this however appears sufficient to allow the degradation of Aβ peptide in mice (Melchor *et al.* 2003). Additionally, the concentration of plg in CSF is further increased during breakdown of the BBB (Mezzapesa *et al.* 2014). Disruption of the BBB can be mediated by (i) plasmin, (ii) endothelial cell activation (Gonzalez-Villalobos *et al.* 2006; Gonzalez-Velasquez *et al.* 2011), or (iii) endothelial cell death induced by fibrin-derived PGPFs (Guo *et al.* 2009).

Interestingly, impaired BBB integrity is observed in Alzheimer's disease (Yamada 2000; Jellinger 2002). Sub-toxic concentrations of less than 10 µM (43 µg/mL) of soluble oligomeric Aβ aggregates can activate endothelial cells (HBMVEC cells) by inducing nuclear

factor-κB activation, and lead to the breakdown of tight junctions and the BBB and allow infiltration/transmigration of monocytes (Gonzalez-Velasquez and Moss 2008; Gonzalez-Velasquez *et al.* 2011). It is possible that endothelial activation may result from other protein aggregates and PGPFs which could allow for infiltration of plg and the recruitment of monocytes through the permeabilised BBB. This series of events would intensify both tPA-mediated plg activation and inflammatory pathology.

5.4.2 Binding of extracellular chaperones to aggregates and PGPFs

CLU and A2M are expressed by a wide variety of cells; CLU expression is up-regulated in response to a variety of stresses, while A2M is present at high levels in extracellular fluids (Wyatt *et al.* 2013). Both are found co-localised with aggregates at sites of extracellular deposition in numerous diseases (Dabbs *et al.* 2013). CLU and A2M were shown to bind to both amorphous aggregates and their corresponding PGPFs (Figure 5.3). These interactions are consistent with a model hypothesised by Wyatt *et al.* in which extracellular proteases and ECs cooperate to maintain extracellular proteostasis by synergistically facilitating the degradation of aggregates and their subsequent disposal (Wyatt *et al.* 2013). In addition, since CLU and A2M bind to aggregates/PGPFs of both SOD (amyotrophic lateral sclerosis) and IgG (corneal dystrophy, multiple myeloma and rheumatoid arthritis), the involvement of ECs in these diseases should be further investigated.

Native A2M and A2M:protease complexes have been shown to inhibit the aggregation of proteins (Chapter 3) (French *et al.* 2008; Wyatt *et al.* 2013). However, A2M:(Trp or Plm) complexes would be cleared quickly *in vivo*, thus A2M:protease complexes were not tested for their ability to bind to PGPFs. Around sites of existing extracellular amorphous aggregates, plm is likely to be in an active state, assisting with proteolysis; at the same locations A2M is likely to inhibit plm by forming complexes with it, thereby restricting "bystander" damage to extracellular proteins by excessive levels of plm. There may, however, be instances where A2M already bound to PGPFs could become activated by protease, thereby increasing the rate of PGPF removal by LRP via receptor-mediated endocytosis.

Amorphous protein aggregates and the PGPFs derived from them have greater exposed hydrophobicity than the corresponding native proteins (Figure 5.4). This increase in exposed

hydrophobicity correlates with increased binding of ECs to aggregates/PGPFs (Figure 5.3 and 5.4). However, one notable exception to this is the greater binding of CLU to native IgG than to PGPFs from IgG aggregates. This is not entirely unexpected, as in addition to binding to exposed hydrophobicity, CLU is known to bind to the Fab and Fc fragments of both native and heat-aggregated human IgG (Wilson and Easterbrook-Smith 1992). These native binding sites may be destroyed by plm digestion during the formation of the PGPFs. ECs are known to bind to misfolded proteins by interacting with regions of exposed hydrophobicity (Humphreys *et al.* 1999; Poon *et al.* 2000; Yerbury *et al.* 2005; Yerbury *et al.* 2007; French *et al.* 2008); this represents the most likely mechanism to account for why ECs preferentially bind to aggregate-derived PGPFs but not to native protein-derived PGPFs. The interaction between ECs and PGPFs may facilitate removal of the latter from the extracellular space and, in conjunction with plg activation and the subsequent proteolytic degradation of protein aggregates, may constitute an important part of the overall proteostasis quality control machinery.

5.4.3 The effects of PGPFs on microglial and endothelial cells

5.4.3.1 In the absence of ECs

Proteolytic fragments liberated by plasmin degradation of amorphous aggregates (PGPFs) were shown to bind to the surface of cells by various mechanisms and receptors and become internalised into lysosomal compartments. Furthermore, in EOC 13.31 and SVEC4-10 cells, PGPFs increased the levels of ROS (Figure 5.5 – 5.8), were cytotoxic (Figure 5.9 and 5.10), and induced loss of $\Delta\Psi_{MIT}$ (Figure 5.11). For three different proteins, aggregates and PGPFs prepared from these, but not the corresponding native proteins or PGPFs prepared directly from those, exerted cytotoxicity towards both microglial and endothelial cell lines which was preceded by a large increase in ROS formation (Figure 5.4 – 5.8). Moreover, PGPFs from both SOD and Ovo aggregates induced significantly less ROS formation than undigested aggregates, while there was no significant difference in the level of induced ROS formation between ox. IgG aggregates and their PGPFs (Figure 5.5 – 5.7). As mentioned previously, ROS has deleterious effects on cells and can elicit cell death signalling pathways. The induction of intracellular ROS production had a rapid onset but was transient, decreasing over time (Figure 5.4), and was followed by cell death (Figure 5.8) indicating triggering of either apoptosis or necrosis cell-death pathways (Lipton and Rosenberg 1994; Bonfoco *et al.* 1995; Fleury *et al.* 2002; Fink and Cookson 2005).

Similar to the effects of fibrin-derived PGPFs on endothelial cells (Guo *et al.* 2009), ox. IgG-derived PGPFs most likely induced cell death via apoptosis, including activation of intrinsic mitochondrial pathways, indicated by the loss of mitochondrial membrane potential and the formation of ROS (Figure 5.10) (Zamzami *et al.* 1995; Fleury *et al.* 2002; Fink and Cookson 2005; Kroemer *et al.* 2009). The fact that PGPFs derived from amorphous aggregates, but not those derived from the corresponding native proteins, induce cell death suggests that the cytotoxic effects are mediated by a conformational or structural feature inherent to the aggregates rather than any specific amino acid sequence. Amorphous aggregates are often regarded as generally non-toxic to cells, despite their occurrence in many PDDs (Chapter 1, Table 1.1). Results presented in this thesis, however, demonstrate that amorphous aggregates of SOD, Ovo and ox. IgG can induce the formation of ROS and are cytotoxic (Figure 5.4 – 5.9).

It should be noted that several PDDs such as Parkinson's disease, dementia (Parkinson's disease-related), Huntington's disease, and ALS, are associated with non-classical modes of cell death including excitotoxicity (Lipton and Rosenberg 1994; Ankarcrona *et al.* 1995; Bonfoco *et al.* 1995; Lau and Tymianski 2010) and lysosomal membrane permeabilisation (Zhang *et al.* 2009; Freeman *et al.* 2013). Excitotoxicity and lysosomal permeabilisation are both associated with ROS formation and mitochondrial dysfunction and cells may adopt either an apoptotic or necrotic appearance, with or without caspase activation, depending on the situation (i.e. influenced by the intensity of insult).

Confocal imaging suggests that PGPFs were internalised mainly into lysosomal compartments as well as into the cytoplasm (Figure 5.12). Disposal of PGPFs by lysosomal degradation is insufficient to prevent the cytotoxicity measured by SYTOX (Figure 5.8) and MTS assays (Figure 5.9). The appearance of PGPFs in both lysosomes and within the cytoplasm suggests that either sufficient amounts are being internalised into the cytoplasm via non-classical endocytotic mechanisms to induce cytotoxicity, or PGPFs may be able to disrupt lysosomal vesicles and thereby impart cytotoxicity.

5.4.3.2 In the presence of ECs

For both microglial and endothelial cells, pre-incubation of protein species with CLU and A2M significantly and dramatically reduced ROS formation induced by SOD aggregates and PGPFs derived from them (Figure 5.6). Similarly, in endothelial cells, CLU and A2M inhibited ROS formation induced by Ovo aggregates and the corresponding PGPFs (Figure 5.7), and A2M inhibited ROS formation induced by ox. IgG aggregates and the corresponding PGPFs (Figure 5.8). In microglial cells, however, opposing effects were seen - pre-incubation of protein species with CLU and A2M both increased ROS formation when cells were exposed to Ovo aggregates and their corresponding PGPFs (Figure 5.7), and CLU increased ROS formation when cells were exposed to ox. IgG aggregates and PGPFs derived from these (Figure 5.8). It remains controversial whether microglial cells have beneficial or detrimental functions in various neuropathological conditions. Low level activation of microglia has been shown to initiate neuroprotective mechanisms such as phagocytosis of tissue debris and damaged cells (Streit *et al.* 2005). It has also been observed that in Alzheimer's disease microglia play an important role in the clearance of cytotoxic Aβ aggregates via phagocytosis (Neumann *et al.* 2009). In addition, activation of microglia may assist in the clearance of protein aggregates and PGPFs, by increasing the expression of LRP (Marzolo *et al.* 2000) and scavenger receptors (Weiner and Frenkel 2006). Increased expression of LRP has been shown to facilitate clearance of A2M:Aβ (Narita *et al.* 1997) and other A2M:client complexes (French *et al.* 2008), while scavenger receptors have been shown to bind to ox. IgG PGPFs (Table 5.2), and facilitate the clearance of soluble HMW complexes of CLU:client protein complexes by CD14+ monocytes (Wyatt *et al.* 2011). Therefore, ECs may assist in the disposal of PGPFs by activating microglia (evidenced as a ROS burst) to stimulate them to clear protein aggregates, PGPFs, and cellular debris much in the same way as monocytes.

There is no simple relationship between the effect of ECs on the binding of PGPFs and the subsequent induced ROS formation (Figure 5.15). For example, ECs decrease cell-surface binding of Ovo aggregate PGPFs to both cell types, and decrease ROS formation in EOC 13.31 cells, but increase ROS formation in SVEC4-10 cells (Figure 5.8). Furthermore, how ECs affected ROS formation in relation to cell-surface binding in the same cell line depended on the chaperone being used. For example, both CLU and A2M increased cell-surface binding of ox. IgG aggregate PGPFs to EOC 13.31 cells, however, ROS formation was increased when incubated with CLU but decreased when incubated with A2M (Figure 5.9). However, these differences may relate to differences in the types of receptors expressed by

microglia versus endothelial cells, and thus differences in subsequent signalling pathways elicited. Interestingly, the binding of SOD PGPFs to the cell-surface is not affected by pre-incubation with ECs (Figure 5.15), despite the fact that the ECs dramatically decreased ROS formation (Figure 5.6) and cytotoxicity (Figure 5.10). In MTS assays, a straightforward pattern was observed. Pre-incubation of ECs with amorphous protein aggregates and aggregate-derived PGPFs suppressed their cytotoxicity towards both microglial and endothelial cells completely, and in some cases appeared to promote cell proliferation significantly above that of the PBS control (Figure 5.8), indicating that ECs provide general protection against these cytotoxic protein species.

It appears that the ability of extracellular protein aggregates to mediate activation of plm and the subsequent release of toxic PGPFs passes unnoticed in routine proteostasis. This suggests the existence of mechanisms to protect cells from PGPF toxicity during plm-mediated degradation of protein aggregates. This may include the involvement of ECs which, as shown earlier, are able to bind to aggregate-derived PGPFs (Figure 5.3). The results also suggest that in the treatment of ALS and rheumatoid arthritis, and potentially other degenerative PDDs, increased levels of ECs *in vivo* could provide a therapeutic benefit.

5.4.4 The dichotomy of the action of plm-mediated release of PGPFs in a biological context

The activity of plm resulting from activation by protein aggregates can be either beneficial or detrimental, depending on circumstances. Similarly, PGPF-induced ROS formation or cell death may be beneficial or detrimental in different contexts.

5.4.4.1 The bad

Amorphous aggregates can serve as a cofactor for tPA-mediated plm formation (Chapter 4), contributing to neurotoxicity by attacking ECM and cell surface proteins, in a manner analogous to how tPA-induced plm formation has been suggested to contribute to neuronal loss in ischemia or excitotoxicity (Chen and Strickland 1997; Tsirka *et al.* 1997; Medina *et al.* 2005). Cellular internalisation of fibrin fragment central E-domain by caveolin-1 mediated endocytosis inhibits mitochondrial function and elicits caspase-mediated apoptosis in placental trophoblast cells (Guo *et al.* 2009). Plasma concentrations of fibrin-derived PGPFs

is greatly augmented in patients with thrombotic disorders such as venous thromboembolism or myocardial infarction, disseminated intravascular coagulation, infection, certain types of leukemia, and other pathologies such as diabetic retinopathy (Cederholm-Williams *et al.* 1981; Francis and Marder 1987; Cesarman-Maus and Hajjar 2005; Mosesson 2005). Similarly, localised plm-mediated degradation and release of PGPFs may accompany the deposition of extracellular amorphous protein aggregates.

The cytotoxicity imparted by protein aggregates in degenerative PDDs has previously been largely attributed to cytotoxic protein oligomers or large insoluble aggregates causing direct damage to cells/tissues (Stefani and Dobson 2003; Chiti and Dobson 2006). The release of cytotoxic PGPFs from extracellular deposits of amorphously aggregated protein may represent a novel physiologically relevant mechanism which, in conjunction with decreased availability or absence of chaperones (such as when they are sequestered by aggregates (Okado-Matsumoto and Fridovich 2002; Narayan *et al.* 2012)), could contribute to inflammation and other pathologies associated with disease.

5.4.4.1 The good

As mentioned previously, amorphous aggregates and their corresponding PGPFs induced ROS formation in cells (Figure 5.4 – 5.8). ROS formation may be beneficial in the phagocytic removal of unhealthy cells. Phagocytes can also internalise protein aggregates directly and degrade them, aided by ROS. Additionally, it is thought that apoptosis induced by fibrin-derived PGPFs may be beneficial by aiding in clearing damaged cells from injury sites, but have deleterious cytotoxic effects when produced excessively, such as in acute lung injury and chronic lung disease (Sio *et al*., 2003; Gando *et al*., 2004; Guo *et al*., 2009). More generally, the interaction of the plm activation system with ECs may allow the body to clear insoluble extracellular protein deposits resulting from disease by firstly digesting them into smaller soluble fragments (PGPFs) and then with the aid of the ECs neutralise their toxicity and dispose of them via cell uptake and lysosomal degradation (Wyatt *et al.* 2013). Without this co-ordinated system, the body would be left with a static protein mass, potentially disrupting tissues and sequestering chaperones.

5.4.5 PGPFs-mediated inflammatory responses triggered by cell-surface binding

The ability of soluble and insoluble protein aggregates to promote excessive and damaging/cytotoxic inflammatory responses was briefly mentioned above. This is potentiated via the activation of microglia or neutrophils; this is evident for SOD, αSyn and IgG aggregates in ALS, Parkinson's disease and rheumatoid arthritis respectively (Robinson *et al.* 1993; Zhang *et al.* 2005; Roberts *et al.* 2013). PGPFs were found to bind to cells by a variety of different mechanisms including via lipid rafts, and toll-like and scavenger receptors (Table 5.2). Similar binding interactions have been reported previously for undigested aggregates of Aβ (Verdier *et al.* 2004) and SOD (Roberts *et al.* 2013).

Toll-like, CD14 and scavenger receptors are known as pattern recognition receptors, and have been shown to bind to and facilitate the clearance of a broad variety of protein aggregates in Alzheimer's disease, age-related macular degeneration and ALS. Binding induces signalling pathways which subsequently invoke inflammatory responses in these diseases by the activation of cells such as microglia (Coller and Paulnock 2001; Herczenik *et al.* 2007; Jana *et al.* 2008; Liu *et al.* 2008; Kaarniranta and Salminen 2009; Liu *et al.* 2009; Roberts *et al.* 2013). Activated microglia can damage neurons by secreting pro-inflammatory cytokines such as TNF-α, IL-1β, and reactive oxygen/nitrogen species. Production of these same species by monocytes, macrophages and neutrophils (Colton and Gilbert 1987; Stansley *et al.* 2012) can in neurons mediate cell death (Boje and Arora 1992; Blasko *et al.* 2004; Kitazawa *et al.* 2004; Walker and Lue 2005; Sastre *et al.* 2006), stimulate Aβ production (Blasko *et al.* 2004), and induce tau hyperphosphorylation (Kitazawa *et al.* 2004).

The binding to microglial cells of PGPFs derived from aggregates of three different proteins, is mediated in part by pattern recognition receptors (Table 5.2) which are known to activate microglial cells, and specifically signalling pathways to stimulate ROS generation and inflammatory cytokine production (Coller and Paulnock 2001; Lue *et al.* 2001; Roberts *et al.* 2013). Thus, PGPFs may contribute to the neuroinflammatory pathology witnessed in numerous PDDs. There are many reports describing the anti-inflammatory properties of CLU and A2M and their effects on the immune system (van Gool *et al.* 1990; Kurdowska *et al.* 2000; McLaughlin *et al.* 2000; Navab *et al.* 2005). Some of their immunomodulatory properties have been attributed to their ability to bind exposed hydrophobic residues (LaMarre *et al.* 1991; Tschopp *et al.* 1993; Mathew *et al.* 2003). Again, this may be another context in which ECs could be beneficial to modulate the effects of PGPFs *in vivo*.

5.4.6 Conclusion

Current therapies for PDDs are largely limited to treatments to ameliorate the symptoms of disease rather than directly address the underlying causes. Pre-emptive treatments to avoid the onset of disease are so far yet to be realised. Progress will be reliant upon advances in understanding of the cellular and molecular processes that underpin disease onset and progression. Results presented in this Chapter suggest a novel mechanism by which both extracellular proteases and chaperones may work cooperatively *in vivo*. In this model tPA-mediated plm activity efficiently degrades large insoluble amorphous aggregates into soluble, yet toxic PGPFs which are then bound by ECs to facilitate their removal and subsequent degradation by cells to maintain proteostasis. Clearly, the advances reported in this Chapter are a promising first step which may lead to confirmation of the operation of these processes *in vivo* and, ultimately, to the development of effective therapeutic strategies to combat serious degenerative PDDs.

CHAPTER 6 : CONCLUSIONS

Aging is characterised by a progressive loss of physiological integrity, impaired function and increased vulnerability to death. This deterioration is the primary risk factor for major human pathologies, including cancer, diabetes, and cardiovascular and neurodegenerative disorders (Lopez-Otin *et al.* 2013). Age-related pathologies such as Alzheimer's disease, Parkinson's disease, cataracts and many other protein deposition diseases (> 40) involve the common features of abnormal and chronic expression of misfolded or aggregated proteins, and their inappropriate deposition, either intra- or extracellularly, in the brain or other tissues specific to the disease (Dobson 2003; Wyatt *et al.* 2013). Proteins have evolved their structure to maximise function and have an inherent tendency to aggregate (Dobson 2003; Stefani and Dobson 2003; Bucciantini *et al.* 2004). Furthermore, endogenous and exogenous stresses (e.g. mutations, extremes of pH or temperature) can cause the unfolding of proteins or impair proper post-translational folding, leading to the surface exposure of hydrophobic residues on protein molecules. Failure to refold or degrade unfolded proteins can result in their aggregation to form either structured fibrils or unstructured amorphous aggregates. The aggregation process can generate toxic protein oligomers and/or insoluble deposits which can disrupt tissue and organ function (Dobson 2003; Wyatt *et al.* 2013).

In addition to their direct toxic effects, aggregated proteins can also indirectly promote inflammatory responses and the processing of neuroendocrine factors (Casserly and Topol 2004; Kranenburg *et al.* 2005). This has made it necessary for organisms to evolve a variety of defences against misfolded or abnormal proteins. All organisms utilise an array of quality control mechanisms that act to preserve the conformation, concentration and correct sub-compartmentalisation of their proteomes, collectively termed the proteostasis network (Balch *et al.* 2008; Hutt *et al.* 2009). This network is critical for organismal viability, and when operating correctly maintains the solubility and function of the entire proteome in both intra- and extracellular environments, responding to stresses as they arise (Balch *et al.* 2008; Powers *et al.* 2009). As a consequence of aging, however, protein quality control systems malfunction and the ability of the body to defend itself against a variety of serious protein deposition diseases is decreased. In particular, intracellular chaperone and proteasome systems show reduced expression and activity and, unsurprisingly, higher levels of misfolded and aggregated proteins result (Esser *et al.* 2004; Morimoto 2008; Powers *et al.* 2009; Koga *et al.* 2011; Cook *et al.* 2012).

Intracellular proteases and chaperones work together to maintain protein fold and solubility, inhibit aggregation and clear intracellular protein aggregates (Ross and Poirier 2005). In contrast, the corresponding extracellular mechanisms are much less well understood (Dobson 2003; Wyatt *et al.* 2013). An earlier proposed model of how extracellular proteostasis may function (Figure 6.1) put forward the hypothesis that levels of extracellular misfolded proteins are controlled by (i) binding of still soluble misfolded proteins to cell-surface pattern recognition receptors and subsequent internalisation and degradation, and (ii) interactions with ECs (for example, CLU and A2M) which by binding to the misfolded client protein molecules maintain their solubility and facilitate their clearance by receptor-mediated endocytosis (Wyatt *et al.* 2011). Building upon this model, this thesis has attempted to further characterise quality control mechanisms that contribute to extracellular proteostasis.

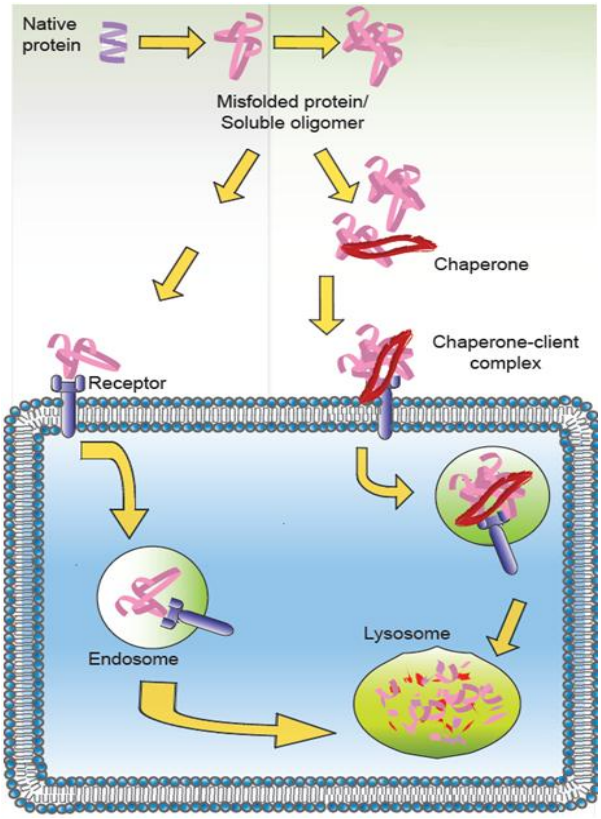

Figure 6.1 Hypothetical model of extracellular proteostasis. When present at low levels, soluble misfolded proteins or oligomers can be cleared by direct binding to cell surface receptors and subsequent uptake and lysosomal degradation. When present at higher levels (favouring more extensive protein aggregation and deposition), the same species may form stable soluble complexes with extracellular chaperones. This acts to neutralise the toxicity of protein oligomers, and keep the species soluble so that they can be efficiently cleared by cell surface receptors and subsequently degraded. Adapted from Dabbs, R. A. *et al.* (2010)

A2M is a broad-spectrum inhibitor of extracellular proteases with a unique mode of action that functions in haemostatic and inflammatory reactions (Harpel 1973; Imber 1981; LaMarre *et al.* 1991). Native tetrameric A2M has also been shown to bind to misfolded proteins and inhibit the amorphous and fibrillar aggregation of client proteins, as well as become

subsequently proteolytically activated forming A2M:protease complexes which expose LRP-binding sites (French *et al.* 2008). A2M is found in the plasma and CSF of healthy humans mainly as a tetramer in a range of 2.8 – 5.6 μM (Gourine *et al.* 2002). However, in different animal species A2M can exist as tetrameric, dimeric and monomeric forms, all of which can function as protease inhibitors (Sottrup-Jensen 1989). In humans, under physiological conditions 4-5% of the extracellular A2M pool is in the form of circulating disufide-linked dimers (Ozawa *et al.* 2011). A2M dimers have been found to be dissociated by oxidative compounds secreted by leukocytes (hypohalous acids) (Reddy *et al.* 1989; Reddy *et al.* 1994) and by neutrophils and microglia (OCl^-) (Wyatt *et al.* 2014). Increased oxidative modification (carbonylation) of A2M has been shown in the plasma of patients with rheumatoid arthritis (accompanied by a two-fold higher expression of A2M) (Wu and Pizzo 2001) and Alzheimer's disease (Cocciolo *et al.* 2012). SDS- and OCl^--dissociated dimers of A2M inhibit fibrillar protein aggregation (Ozawa *et al.* 2011; Wyatt *et al.* 2014). In humans, A2M monomers in plasma have been identified as a clinical biomarker in patients with diabetes at a range of 1 – 1.7 μM (Takada *et al.* 2013) and increased ~2-fold relative to healthy controls in cardiac hypertrophy (Rajamanickam *et al.* 1998), myocardial infarction in diabetes, (Annapoorani *et al.* 2006), and cardiac diseases (Rathinavel *et al.* 2005; Ramasamy *et al.* 2006). In addition, A2M monomers can be generated extracellularly *in vivo* by thioredoxin (Larsson *et al.* 1988), which is secreted by lymphocytes in response to oxidative stress and inflammation (Kondo *et al.* 2004; Nakamura *et al.* 2006).

In the current study, native tetrameric A2M was dissociated by mild reductive or physiologically-relevant oxidative (redox) stress to form A2M monomers and dimers, respectively. A2M species can inhibit aggregation by binding to misfolded and fibrillar and amorphously aggregating proteins via hydrophobic interactions, thereby facilitating their removal via LRP receptor-mediated endocytosis. The ability of A2M dimers and monomers to inhibit protein aggregation was more potent than that of the native A2M tetramer. The level of chaperone activity of A2M dimers/monomers also correlates with the level of surface-exposed hydrophobicity. Altogether, the ability of dimers and monomers to be generated *in vivo*, their presence in diseased patients, together with the observation that misfolded proteins are a hallmark of these same diseases, suggests that dimers/monomers may function as physiologically relevant ECs. A2M activated with either Trp or Plm prior to incubation with misfolding client proteins, was shown to potently inhibit the stress-induced

aggregation of a variety of proteins; this activity was more potent than that of native A2M. In addition, A2M:Trp and A2M:Plm complexes were able to partially degrade some aggregating client proteins, however, due to the exposure of LRP-binding sites these are likely to be cleared by cell-surface receptors within minutes (Gliemann *et al.* 1985; Roche and Pizzo 1987; Roche and Pizzo 1988), and thus the residual protease activity of the complexes is unlikely to be physiologically relevant. Protease-activation of A2M after the formation of soluble A2M:client complexes has been shown to expedite disposal by LRP, and may facilitate clearance of misfolded client proteins via LRP in diseases which involve extracellular protein aggregation and increased extracellular protease secretion such as in arthritis (Abbink *et al.* 1991) and diabetic retinopathy (Sanchez *et al.* 2007). Furthermore, the binding of A2M:protease complexes induces increased expression and secretion of (i) tPA (Fischer *et al.* 2000; Siao and Tsirka 2002; Siao 2003) and A2M (Hughes *et al.* 1998; Lauer *et al.* 2001) from microglia, and (ii) plg and A2M from mononuclear cells (Zhabin *et al.* 1995). These interactions provide a feed-forward mechanism to co-localise chaperones and proteases at sites of protein aggregation, which act together to facilitate return of the system to normal healthy proteostasis. Collectively, the results presented here show that the chaperone activity of A2M can be changed in response to a variety of conditions related to diseases, such as reductive/oxidative stress, inflammation, and increased protease secretion.

tPA is an essential mediator of cell death following ischemia or excitotoxic injury in the brain, and may play a role in neuronal and endothelial cell death induced by aggregates (Tsirka 1995; Chen 1997; Yepes 2008). Additionally, the fact that excitotoxicity is found in PDDs and other neurological disorders concurrent with ROS formation and mitochondrial dysfunction, and that tPA is required for excitotoxic neuronal death, suggests a link between aggregate-induced tPA activation and extracellular protein aggregates. tPA was previously shown to bind to structural components of fibrillar protein aggregates (Kranenburg *et al.* 2002; Samson *et al.* 2009). Fibrillar protein aggregates formed after cellular injury can serve as a cofactor for tPA and plg to enhance the generation of plm, which in turn facilitates the removal of unhealthy and nonviable cells (Samson *et al.* 2009; Samson *et al.* 2012). In addition, plm can degrade fibrillar protein aggregates, akin to the dissolution of fibrin-clots (Tucker *et al.* 2000; Melchor *et al.* 2003; Gebbink *et al.* 2009). These studies however, did not measure whether amorphous aggregates could induce tPA-mediated plg activation nor the effects on cells of plasmin-generated protein fragments (PGPFs) derived from protein aggregates. The degradation of fibrin by plasmin is vital for the maintenance of haemostasis,

yet despite the apparent toxicity of the PGPFs produced (Guo *et al.* 2009), biological functions are not impaired under normal conditions. This suggests the existence of mechanisms which protect cells from toxicity during the plasmin mediated degradation of proteins. $A\beta_{42}$ promotes upregulation of the tPA/plg proteolytic system, which can degrade both native and amyloid fibrils of Aβ, reducing the load of amyloid plaques *in vivo* with no associated toxicity to cells (Tucker 2000; Tucker *et al.* 2000; Melchor *et al.* 2003; Lee *et al.* 2007). Thus the plg activation system may also play an important role in extracellular proteostasis, and this was examined further in this thesis.

In the current study, native SOD, Ovo and IgG were exposed to stresses to induce their amorphous aggregation. This created a mixture of soluble and insoluble protein aggregates. tPA and plg were shown to co-localise on the surface of amorphously aggregated proteins via their binding to lysine residues. It was also shown that when bound to insoluble protein aggregates, active plm was shielded from inhibition by A2AP. These findings are consistent with a model in which active plm formed at the surface of amorphous protein aggregates could remain persistently active and progressively degrade the aggregate. The action of plm on amorphous protein aggregates was shown to release smaller soluble fragments of protein (PGPFs). PGPFs were bound and internalised (via different mechanisms) to both endothelial and microglial cells, and were subsequently trafficked to lysosomes in both cell types. When incubated with cells, PGPFs generated from different types of protein aggregates all elicited ROS formation and cytotoxicity. ECs were able to bind to PGPFs, significantly ameliorating their negative effects on cells. In addition, ECs had differential effects on the binding of PGPFs to cells, depending on the combination of individual protein and cell type, probably reflecting differences in the repertoire of surface receptors expressed by the different cell types. CLU and A2M each have known specific cell surface receptors that recognise and internalise them in complex with ligands for subsequent lysosomal degradation (Hammad *et al.* 1997; Shibata *et al.* 2000). More detailed analysis of the interactions between ECs and the tPA system, and the toxicity and fate of the resulting chaperone:PGPFs complexes, will provide a better understanding of the mechanisms of extracellular proteostasis.

In summary, findings presented in this thesis suggest a novel system in which proteases and circulating ECs act together as key synergistic agents in extracellular proteostasis; together they mediate the progressive degradation and safe clearance of large insoluble protein deposits. We hypothesise that extracellular amorphous protein aggregates, amyloid fibrils, and fibrin can all act as substrates and activators for tPA, and that ECs such as CLU and A2M bind to cytotoxic PGPFs generated by proteolytic breakdown of the aggregates to facilitate their clearance and ultimate degradation. These actions will collectively inhibit the development of age-related protein misfolding diseases (Figure 6.2). This model is consistent with the idea that in healthy individuals extracellular proteostasis operates to provide efficient clearance of toxic protein species (Yerbury *et al.* 2005; Wilson *et al.* 2008). As mentioned previously, the likelihood of onset of PDDs increases with age and is thought to coincide with a reduction in the ability of protein quality control systems to maintain proteostasis, allowing pathophysiological deposits of extracellular protein aggregates to form. This may have implications in Alzheimer's disease where plm has been shown to degrade and clear extracellular amyloid deposits (Tucker *et al.* 2000).

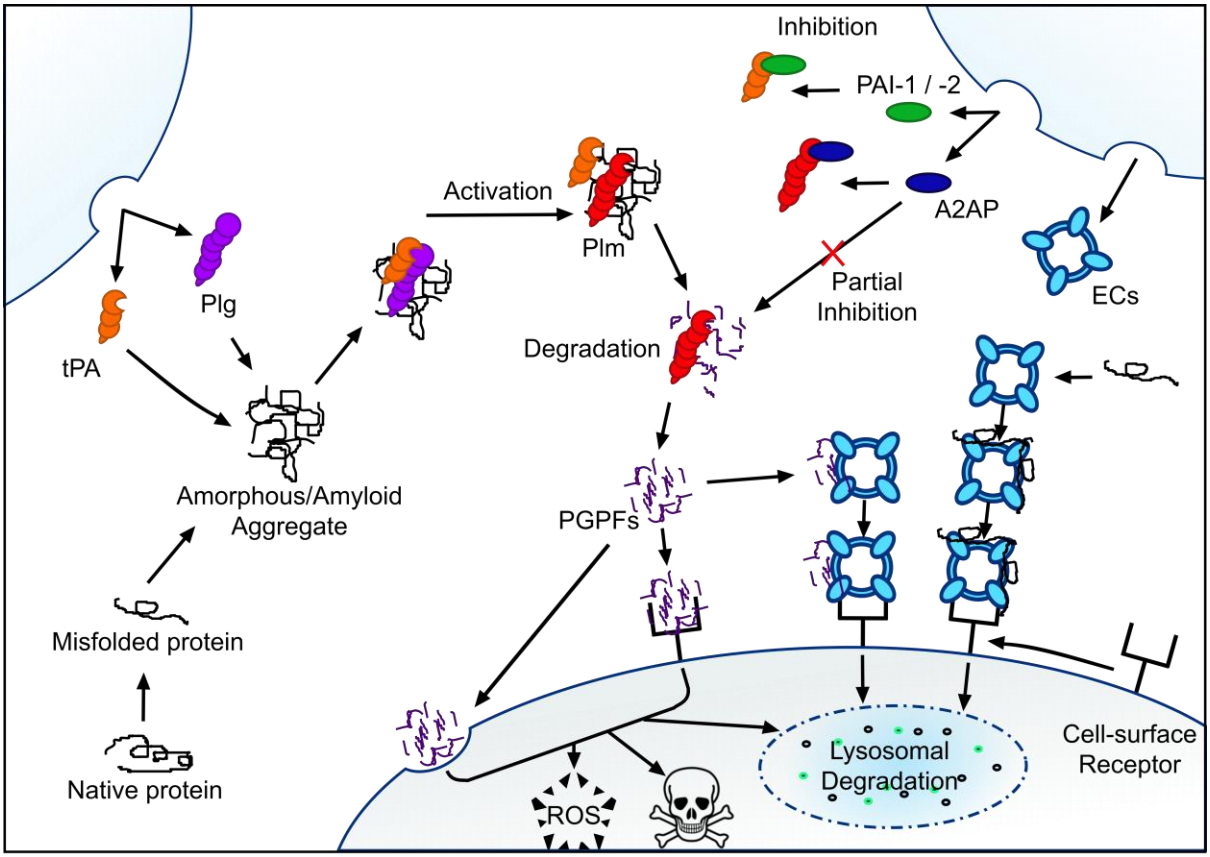

Figure 6.2 Hypothetical model of an extracellular proteostasis mechanism involving the cooperation of extracellular proteases and chaperones. Stress conditions induce native proteins to misfold and expose hydrophobic residues. ECs can bind to misfolded proteins and dispose of them by internalisation via receptor-mediated endocytosis and lysosomal degradation. However, amorphous or amyloid fibril structured aggregates can form, as a mixed population of soluble and larger insoluble aggregates. Both soluble and insoluble aggregates then serve as a cofactor for tPA and Plg. tPA-mediated activation is partially inhibited by PAI-1 and PAI-2. tPA induces activation of Plg into the serine protease Plm which can then degrade aggregated proteins into PGPFs. Free Plm is readily inhibited by A2AP, however Plm bound to insoluble amorphously aggregated proteins is protected from inhibition. PGPFs are released into the extracellular space and can either bind to (i) cell-surface receptors, followed by receptor-mediated endocytosis (RME) and trafficking to lysosomes for degradation; they can also induce the formation of reactive oxygen species (ROS) and cytotoxicity (skull), (ii) ECs and subsequently be internalised by RME and degraded in lysosomes. The binding of ECs to PGPFs protects against ROS (in some cases) and cytotoxicity.

The levels of expression of plasminogen activator inhibitor-1 and -2 (PAI-1 / PAI-2) have been shown to increase in tissues and plasma with age and cellular senescence (Kumar *et al.* 1993; West *et al.* 1996; Eren *et al.* 2014). PAI-2 expression is also markedly increased in the vascular endothelium, granulosa cells and in microglial cells of patients with Alzheimer's disease (Akiyama *et al.* 1993; Dear and Medcalf 1995). The inhibition of tPA-mediated plg activation by PAI-1 / PAI-2 may result in an age-dependent decrease in the efficiency of clearance of extracellular protein deposits. The expression of PAI-1 also increases following inflammatory responses (Festa *et al.* 2002; Levi *et al.* 2003). PDDs are associated with inflammation and activation of the complement system; protein aggregates themselves have been shown to promote excessive and damaging/cytotoxic inflammatory responses (Papp *et al.* 2003; Tabner *et al.* 2005), which results in the release of oxidants, proteinases, and cytokines (Casserly and Topol 2004). This is potentiated via the activation of microglia or neutrophils, and is evident for aggregates of SOD, αSyn and IgG in ALS, Parkinson's disease and rheumatoid arthritis, respectively (Robinson *et al.* 1993; Zhang *et al.* 2005; Roberts *et al.* 2013). In these disease states, A2M may become chaperone-activated, triggered by, for example, oxidation-induced dissociation into dimers, or by interaction with proteases. In the disease state, however, this activation is insufficient to prevent pathology.

PGPFs may also activate endothelial and microglial cells to compromise BBB integrity and exacerbate inflammatory responses, respectively. This was demonstrated by their ability to significantly increase ROS formation, which can trigger cytokine release via endothelial and microglial activation. It is possible that endothelial and microglial activation may occur for other aggregates and PGPFs derived thereof, such as those from amyloid fibrils in Alzheimer's disease where the recruitment of monocytes through permeabilised BBB accompanies an intensified inflammatory pathology (Yamada 2000; Kaur *et al.* 2001; Nagele *et al.* 2004; Gonzalez-Velasquez *et al.* 2008).

The extracellular proteostasis field is in its infancy, but in time will provide important insights into the mechanisms underlying extracellular PDDs. However, much work is required before that point is reached. In particular, research demonstrating that the processes described here occur *in vivo* are necessary. In addition, further research into other possible components of the quality control system is required. Further work would also involve identifying the mechanisms and signalling pathways by which PGPFs are cytotoxic and more importantly, how the binding of ECs to PGPFs ameliorates their cytotoxicity when incubated

with cells. It would also be worthwhile establishing whether PGPFs do induce the activation and release of cytokines and PAI-1 / PAI-2 from endothelial and microglial cells and the receptors that recognise ECs bound to PGPFs. This will need to be followed by important work determining the role of the proposed extracellular proteostasis mechanisms in specific diseases which are associated with either amyloid fibrils or amorphous protein aggregates.

Increased knowledge of these mechanisms could lead to the development of new therapies to treat serious PDDs and other age-related diseases such as Alzheimer's disease, amyotrophic lateral sclerosis, and rheumatoid arthritis. Current therapeutic strategies involve (i) native protein replacement (Balch *et al.* 2008), (ii) abrogating the aggregation of proteins using small molecules of either naturally occurring or synthetic origin termed "chemical and peptidic chaperones" (Wyatt *et al.* 2009), which can act by either steric hindrance of protein-protein interaction (Fulop *et al.* 2004; Gibson and Murphy 2006), shielding regions of exposed hydophobicity (Baskakov and Bolen 1998) or, in the case of amyloid fibrillogenesis, minimising structural changes leading to β-sheet formation (Soto *et al.* 1998), and (iii) mesenchymal stem cell therapy, which decreases apoptosis and promotes endogenous cell growth (Joyce *et al.* 2010). However, these approaches suffer from inadequate delivery methods and inefficient targeting of cells/tissues of interest (Balch *et al.* 2008). For example, most chemical and peptidic chaperones cannot cross the BBB to correctly treat neurodegenerative diseases (Wyatt *et al.* 2009). Small molecules termed "proteostasis regulators" which manipulate signalling pathways and/or the transcription and translation of elements of the protein quality control machinery show promise in developing future therapies for the treatment of PDDs (Balch *et al.* 2008). For example, one strategy using RNA interference directed against the proteostasis regulator *age-1* induced an increase in chaperone expression levels and conferred protection from polyQ cytotoxicity (Morley *et al.* 2002). In a similar manner, potential future strategies could include bolstering existing proteostasis systems by manipulating the expression levels or activity of the plg activation system, or ECs and/or their receptors. Conceivably, these changes could enhance the body's own existing systems to safely degrade and clear disease-associated insoluble protein aggregates.

The findings of the National Institute of Neurological Disorders and Stroke (No authors listed, 1995) and the European Cooperative Acute Stroke Study (Hacke 1995) showed that intravenously administered recombinant tPA for the treatment of acute ischemic stroke after 3

hours of stroke onset resulted in poor recovery outcomes and enhanced tissue damage. It has been noted that fibrin deposition on the surface of placental cells was associated with apoptosis which could be prevented by inhibiting fibrinolysis, suggesting that cell death was caused by the degradation of products of fibrin (Isermann 2003). The toxicity of PGPFs derived from the degradation of fibrin may contribute to the negative side effects associated with tPA treatment in stroke victims (Guo *et al.* 2009). The potential of ECs to interact with PGPFs and aid in their clearance could lead to new stroke therapy that combines the use of tPA and ECs to effectively degrade a clot and dispose of cytotoxic PGPFs.

REFERENCES

"- Tissue plasminogen activator for acute ischemic stroke. The National Institute of Neurological Disorders and Stroke rt-PA Stroke Study Group." - N Engl J Med. 1995 Dec 14;333(24):1581-7.(- 0028-4793 (Print)): T - ppublish.

Abbink, J. J., A. M. Kamp, et al. (1991). "Predominant role of neutrophils in the inactivation of alpha 2-macroglobulin in arthritic joints." Arthritis Rheum **34**(9): 1139-1150.

Adachi, T., J. Wang, et al. (2000). "Age-related change of plasma extracellular-superoxide dismutase." Clin Chim Acta **290**(2): 169-178.

Akiyama, H., K. Ikeda, et al. (1993). "Microglia express the type 2 plasminogen activator inhibitor in the brain of control subjects and patients with Alzheimer's disease." Neurosci Lett **164**(1-2): 233-235.

Akiyama, H., Ikeda, K., Kondo, H., Kato, M. and McGeer, P.L. (1993). "Microglia express the type 2 plasminogen activator inhibitor in the brain of control subjects and patients with Alzheimer's diseases. ." Neuroscience Letters **164**: 233-235.

Alessi, M. C., I. Juhan-Vague, et al. (1991). "Molecular forms of plasminogen activator inhibitor-1 (PAI-1) and tissue-type plasminogen activator (t-PA) in human plasma." Thromb Res **62**(4): 275-285.

An, E., S. Sen, et al. (2010). "Identification of novel substrates for the serine protease HTRA1 in the human RPE secretome." Invest Ophthalmol Vis Sci **51**(7): 3379-3386.

Andreasen, P. A., R. Egelund, et al. (2000). "The plasminogen activation system in tumor growth, invasion, and metastasis." Cell Mol Life Sci **57**(1): 25-40.

Ankarcrona, M., J. M. Dypbukt, et al. (1995). "Glutamate-induced neuronal death: a succession of necrosis or apoptosis depending on mitochondrial function." Neuron **15**(4): 961-973.

Annapoorani, P., P. S. Dhandapany, et al. (2006). "Cardiac isoform of alpha-2 macroglobulin--a new biomarker for myocardial infarcted diabetic patients." Atherosclerosis **186**(1): 173-176.

Anonick, P. K., B. Wolf, et al. (1990). "Regulation of plasmin, miniplasmin, and streptokinase-plasmin complex by alpha 2-antiplasmin, alpha 2-macroglobulin, and antithrombin III in the presence of heparin." Thromb Res **59**(3): 449-462.

Antzutkin, O. N., Balbach, J.J., Leapman, R.D., Rizzo, N.W., Reed, J. and Tycko, R. (2000). "Multiple quantum solid-state NMR indicates a parallel, not antiparallel, organization of β-sheets in Alzheimer's β-amyloid fibrils. ." Proceedings of the National Academy of Sciences of the United States of America **97**: 13045-13050.

Aoki, T., Sumii, T., Mori, T., Wang, X. and Lo, E.H. (2002). "Blood-Brain Disruption and Matrix Metalloproteinase-9 Expression During Reperfusion Injury: Mechanical Versus Embolic Focal Ischemia in Spontaneously Hypertensive Rats." Stroke **33** 2711-2717.

Arvan, P., M. G. Rossmann, et al. (2002). "Secretory pathway quality control operating in golgi, plasmalemmal, and endosomal systems." Traffic **3**: 771-780.

Ashcom, J. D., Tiller, S.E., Dickerson, K., Cravens, J.L., Argraves, W.S. and Strickland, D.K. (1990). "The Human α2-Macroglobulin Receptor: Identification of A 420-kD Cell Surface Glycoprotein Specific for The Activated Conformation of α2-Macroglobulin." The Journal of Cell Biology **110**: 1041-1048.

Aucouturier, P., M. Bauwens, et al. (1993). "Monoclonal Ig L chain and L chain V domain fragment crystallization in myeloma-associated Fanconi's syndrome." J Immunol **150**(8 Pt 1): 3561-3568.

Aucouturier, P., A. A. Khamlichi, et al. (1993). "Brief report: heavy-chain deposition disease." N Engl J Med **329**(19): 1389-1393.

Babior, B. M. (2000). "The NADPH oxidase of endothelial cells." IUBMB Life **50**(4-5): 267-269.
Balch, W. E., R. I. Morimoto, et al. (2008). "Adapting proteostasis for disease intervention." Science **319**(5865): 916-919.
Baldwin, R. L. (1994). "Matching speed and stability." Nature **368**: 183-184.
Banks, R. E., S. W. Evans, et al. (1991). "Alpha 2 macroglobulin state in acute pancreatitis. Raised values of alpha 2 macroglobulin-protease complexes in severe and mild attacks." Gut **32**(4): 430-434.
Banks, R. E., S. W. Evans, et al. (1990). "Measurement of the 'fast' or complexed form of alpha 2 macroglobulin in biological fluids using a sandwich enzyme immunoassay." J Immunol Methods **126**(1): 13-20.
Barral, J. M., Broadley, S.A., Schaffar, G. and Hartl, F.U. (2004). "Roles of molecular chaperones in protein misfolding diseases." Seminars in Cell & Developmental Biology **15**: 17-29.
Barrett, A. J., M. A. Brown, et al. (1979). "The electrophoretically 'slow' and 'fast' forms of the alpha 2-macroglobulin molecule." Biochem J **181**(2): 401-418.
Barrett, A. J. and P. M. Starkey (1973). "The interaction of alpha 2-macroglobulin with proteinases. Characteristics and specificity of the reaction, and a hypothesis concerning its molecular mechanism." Biochem J **133**(4): 709-724.
Barrett, A. J. and P. M. Starkey (1973). "The interaction of alpha 2-macroglobulin with proteinases. Characteristics and specificity of the reaction, and a hypothesis concerning its molecular mechanism." The Biochemical Journal **133**: 709-724.
Baskakov, I. and D. W. Bolen (1998). "Forcing thermodynamically unfolded proteins to fold." J Biol Chem **273**(9): 4831-4834.
Beissinger, M. and J. Buchner (1998). "How chaperones fold proteins." Biol Chem **379**(3): 245-259.
Bell, R. D., A. P. Sagare, et al. (2007). "Transport pathways for clearance of human Alzheimer's amyloid beta-peptide and apolipoproteins E and J in the mouse central nervous system." J Cereb Blood Flow Metab **27**(5): 909-918.
Bergt, C., G. Marsche, et al. (2001). "Human neutrophils employ the myeloperoxidase/hydrogen peroxide/chloride system to oxidatively damage apolipoprotein A-I." Eur J Biochem **268**(12): 3523-3531.
Berlett, B. S. and E. R. Stadtman (1997). "Protein oxidation in aging, disease and oxidative stress." The Journal of Biological Chemistry **272**(33): 20313-20316.
Bieth, J. G., M. Tourbez-Perrin, et al. (1981). "Inhibition of alpha 2-macroglobulin-bound trypsin by soybean trypsin inhibitor." J Biol Chem **256**(15): 7954-7957.
Binder, R. J., S. K. Kumar, et al. (2002). "Naturally Formed or Artificially Reconstituted Non-Covalent Alpha2-Macroglobulin-Peptide Complexes Elicit Cd91-Dependent Cellular Immunity." Cancer Immunity **2**: 16.
Birkenmeier, G., L. Carlsson-Bostedt, et al. (1989). "Differences in hydrophobic properties for human alpha 2-macroglobulin and pregnancy zone protein as studied by affinity phase partitioning." Eur J Biochem **183**(2): 239-243.
Blasko, I., M. Stampfer-Kountchev, et al. (2004). "How chronic inflammation can affect the brain and support the development of Alzheimer's disease in old age: the role of microglia and astrocytes." Aging Cell **3**(4): 169-176.
Bleyer, A. J., T. C. Hart, et al. (2005). "Clinico-pathologic findings in medullary cystic kidney disease type 2." Pediatr Nephrol **20**(6): 824-827.
Bodas, M., T. Min, et al. (2010). "Early-age-related changes in proteostasis augment immunopathogenesis of sepsis and acute lung injury." PLoS One **5**(11): e15480.

Boje, K. M. and P. K. Arora (1992). "Microglial-produced nitric oxide and reactive nitrogen oxides mediate neuronal cell death." Brain Res **587**(2): 250-256.

Bonfoco, E., D. Krainc, et al. (1995). "Apoptosis and necrosis: two distinct events induced, respectively, by mild and intense insults with N-methyl-D-aspartate or nitric oxide/superoxide in cortical cell cultures." Proc Natl Acad Sci U S A **92**(16): 7162-7166.

Borcea, V., J. Nourooz-Zadeh, et al. (1999). "alpha-Lipoic acid decreases oxidative stress even in diabetic patients with poor glycemic control and albuminuria." Free Radic Biol Med **26**(11-12): 1495-1500.

Bouma, B., L. M. Kroon-Batenburg, et al. (2003). "Glycation induces formation of amyloid cross-beta structure in albumin." J Biol Chem **278**(43): 41810-41819.

Breckenridge, D. G., M. Germain, et al. (2003). "Regulation of apoptosis by endoplasmic reticulum pathways." Oncogene **22**(53): 8608-8618.

Brodsky, J. L. and A. A. Mc Cracken (1999). "ER protein quality control and proteasome-mediated protein degradation." Cell and Developmental Biology **10**: 507-513.

Bucciantini, M., G. Calloni, et al. (2004). "Pre-fibrillar amyloid protein aggregates share common features of cytotoxicity." The Journal of Biological Chemistry **279**(30): 31374-31382.

Buchner, J. (1996). "Supervising the fold: functional principles of molecular chaperones." Journal of the Federation of American Societies for Experimental Biology **10**: 10-19.

Buss, I. H., R. Senthilmohan, et al. (2003). "3-Chlorotyrosine as a marker of protein damage by myeloperoxidase in tracheal aspirates from preterm infants: association with adverse respiratory outcome." Pediatr Res **53**(3): 455-462.

Calero, M., A. Rostagno, et al. (2000). "Apolipoprotein J (clusterin) and Alzheimer's disease." Microscopy Research and Technique **50**(4): 305-315.

Carver, J. A., A. Rekas, et al. (2003). "Small heat-shock proteins and clusterin: intra- and extracellular molecular chaperones with a common mechanism of action and function." IUBMB Life **55**(12): 661-668.

Casserly, I. and E. Topol (2004). "Convergence of atherosclerosis and Alzheimer's disease: inflammation, cholesterol, and misfolded proteins." Lancet **363**(9415): 1139-1146.

Castellino, F. J. and V. A. Ploplis (2005). "Structure and function of the plasminogen/plasmin system." Thromb Haemost **93**(4): 647-654.

Caughey, B. a. L., P.T. (2003). "PROTOFIBRILS, PORES, FIBRILS, AND NEURODEGENERATION: Separating the Responsible Protein Aggregates from The Innocent Bystanders." Annual Review of Neuroscience **26**: 267-298.

Cederholm-Williams, S. A. (1981). "Concentration of plasminogen and antiplasmin in plasma and serum." J Clin Pathol **34**(9): 979-981.

Cederholm-Williams, S. A., T. L. Dornan, et al. (1981). "The metabolism of fibrinogen and plasminogen related to diabetic retinopathy in man." Eur J Clin Invest **11**(2 Suppl 1): 133-138.

Cesarman-Maus, G. and K. A. Hajjar (2005). "Molecular mechanisms of fibrinolysis." Br J Haematol **129**(3): 307-321.

Chakravarthy, U., J. Evans, et al. (2010). "Age related macular degeneration." BMJ **340**: c981.

Chen, L., V. Shick, et al. (1997). "Laminin E8 alveolarization site: heparin sensitivity, cell surface receptors, and role in cell spreading." Am J Physiol **272**(3 Pt 1): L494-503.

Chen, Z. a. S., S. (1997). "Neuronal Death in the Hippocampus Is Promoted by Plasmin-Catalyzed Degradation of Laminin." Cell **91**: 917-925.

Chen, Z. L. and S. Strickland (1997). "Neuronal death in the hippocampus is promoted by plasmin-catalyzed degradation of laminin." Cell **91**(7): 917-925.

Cheung, M. S., Garcia, A.E. and Onuchic, J. (2002). "Protein folding mediated by salvation: Water expulsion and formation of the hydrophobic core after the structural collapse." Proceedings of the National Academy of Sciences of the United States of America **99**: 685-690.
Chiti, F. and C. M. Dobson (2006). "Protein misfolding, functional amyloid, and human disease." Ann Rev Biochem **75**: 333-366.
Chiti, F., M. Stefani, et al. (2003). "Rationalization of the effects of mutations on peptide and protein aggregation rates." Nature **424**(6950): 805-808.
Chiti, F., Webster, P., Taddei, N., Clark, A., Stefani, M., Ramponi, G., Dobson, C.M. (1999). "Designing conditions for in vitro formation of amyloid protofilaments and fibrils." Proceedings of the National Academy of Sciences of the United States of America **96**: 3590-3594.
Christensen, U. and L. Molgaard (1992). "Positive co-operative binding at two weak lysine-binding sites governs the Glu-plasminogen conformational change." Biochem J **285 (Pt 2)**: 419-425.
Christensen, U. and L. Sottrup-Jensen (1984). "Mechanism of alpha 2-macroglobulin-proteinase interactions. Studies with trypsin and plasmin." Biochemistry **23**(26): 6619-6626.
Ciolino, H. P. and R. L. Levine (1997). "Modification of proteins in endothelial cell death during oxidative stress." Free Radic Biol Med **22**(7): 1277-1282.
Clemmensen, I. and R. B. Andersen (1982). "The fibrinolytic system and its relation to inflammatory diseases." Semin Arthritis Rheum **11**(4): 390-398.
Cocciolo, A., F. Di Domenico, et al. (2012). "Decreased expression and increased oxidation of plasma haptoglobin in Alzheimer disease: Insights from redox proteomics." Free Radic Biol Med **53**(10): 1868-1876.
Cochran, B. J., L. P. Gunawardhana, et al. (2009). "The CD-loop of PAI-2 (SERPINB2) is redundant in the targeting, inhibition and clearance of cell surface uPA activity." BMC Biotechnol **9**: 43.
Collen, D. (1976). "Identification and some properties of a new fast-reacting plasmin inhibitor in human plasma." Eur J Biochem **69**(1): 209-216.
Collen, D. and B. Wiman (1978). "Fast-acting plasmin inhibitor in human plasma." Blood **51**(4): 563-569.
Coller, S. P. and D. M. Paulnock (2001). "Signaling pathways initiated in macrophages after engagement of type A scavenger receptors." J Leukoc Biol **70**(1): 142-148.
Colton, C. A. and D. L. Gilbert (1987). "Production of superoxide anions by a CNS macrophage, the microglia." FEBS Lett **223**(2): 284-288.
Cook, C., C. Stetler, et al. (2012). "Disruption of protein quality control in Parkinson's disease." Cold Spring Harb Perspect Med **2**(5): a009423.
Crookston, K. P., D. J. Webb, et al. (1994). "Classification of alpha 2-macroglobulin-cytokine interactions based on affinity of noncovalent association in solution under apparent equilibrium conditions." J Biol Chem **269**(2): 1533-1540.
Csermely, P. (1997). "Proteins, RNAs and chaperones in enzyme evolution: a folding perspective." Trends Biochem Sci **22**(5): 147-149.
Csermely, P. (1999). "Chaperone-percolator model: a possible molecular mechanism of Anfinsen-cage-type chaperones." Bioessays **21**(11): 959-965.
Csermely, P., Sőti, C., Kalmar, E., Papp, E., Pato, B., Vermes, A. and Sreedhar, A.S. (2003). "Molecular Chaperones, evolution and medicine." The Journal of Molecular Structure **666-667**: 373-380.

Cummings, H. S., S. V. Pizzo, et al. (1984). "Effect of methylamine and plasmin on the conformation of human alpha 2-macroglobulin as revealed by differential scanning calorimetric analysis." Biophys J **45**(4): 721-724.

Cuzner, M. L. a. O., G. (1999). "Plasminogen activators and matrix metalloproteases, mediators of extracellular proteolysis in inflammatory demyelination of the central nervous system." Journal of Neuroimmunology **94**: 1-14.

Dabbs, R. A., A. R. Wyatt, et al. (2013). "Extracellular chaperones." Top Curr Chem **328**: 241-268.

Dano, K., Behrendt, N., Hoyer-Hansen, G., Johnsen, M., Lund, L.R., Ploug, M. and Romer, J. (2005). "Plasminogen activation and cancer." Journal of Thrombosis and Haemostasis **93**: 676-681.

Dasgupta, A., J. Zheng, et al. (2013). "Increased carbonylation, protein aggregation and apoptosis in the spinal cord of mice with experimental autoimmune encephalomyelitis." ASN Neuro **5**(1): e00111.

David, M. A. and M. Tayebi (2014). "Detection of protein aggregates in brain and cerebrospinal fluid derived from multiple sclerosis patients." Front Neurol **5**: 251.

Davies, K. J. A. and M. E. Delsignore (1987). "Protein damage and degradation by oxygen radicals." The Journal of Biological Chemistry **262**(20): 9908-9913.

de Boer, J. P., A. A. Creasey, et al. (1993). "Alpha-2-macroglobulin functions as an inhibitor of fibrinolytic, clotting, and neutrophilic proteinases in sepsis: studies using a baboon model." Infect Immun **61**(12): 5035-5043.

Dear, A. E. and R. L. Medcalf (1995). "The cellular and molecular biology of plasminogen activator inhibitor type-2." Fibrinolysis **9**(6): 321-330.

DeMattos, R. B., J. R. Cirrito, et al. (2004). "ApoE and clusterin cooperatively suppress Abeta levels and deposition: evidence that ApoE regulates extracellular Abeta metabolism in vivo." Neuron **41**(2): 193-202.

Demuro, A., E. Mina, et al. (2005). "Calcium dysregulation and membrane disruption as a ubiquitous neurotoxic mechanism of soluble amyloid oligomers." J Biol Chem **280**(17): 17294-17300.

Devaraj, S. and I. Jialal (1996). "Oxidized low-density lipoprtoein in atherosclerosis." Int J Clin Lab Res **26**(3): 178-184.

Dhanasekaran, A., S. Kotamraju, et al. (2004). "Supplementation of endothelial cells with mitochondria-targeted antioxidants inhibit peroxide-induced mitochondrial iron uptake, oxidative damage, and apoptosis." J Biol Chem **279**(36): 37575-37587.

Dietzmann, K., P. von Bossanyi, et al. (2000). "Expression of the plasminogen activator system and the inhibitors PAI-1 and PAI-2 in posttraumatic lesions of the CNS and brain injuries following dramatic circulatory arrests: an immunohistochemical study." Pathol Res Pract **196**(1): 15-21.

Dinner, A. R., A. Sali, et al. (2000). "Understanding protein folding via free-energy surfaces from theory and experiment." Trends in Biochemical Sciences **25**: 331-339.

Dobson, C. M. (1999). " Protein misfolding, evolution and disease." Trends in Biochemical Sciences **24**: 329-332.

Dobson, C. M. (2001). "The structural basis of protein folding and its links with human disease." Philosophical Transactions of the Royal Society B **325**: 133-145.

Dobson, C. M. (2003). "Protein folding and misfolding." Nature **426**: 884-890.

Dobson, C. M. a. K., M. (1999). "The fundamentals of protein folding: bringing together theory and experiment." Current Opinion in Structural Biology **9**: 92-101.

Du, Y., K. R. Bales, et al. (1998). "Alpha2-macroglobulin attenuates beta-amyloid peptide 1-40 fibril formation and associated neurotoxicity of cultured fetal rat cortical neurons." J Neurochem **70**(3): 1182-1188.

Egeblad, M. a. W., Z. (2002). "New functions for the matrix metalloproteinases in cancer progression." Nature reviews **2**: 161-174.
Emerit, J., M. Edeas, et al. (2004). "Neurodegenerative diseases and oxidative stress." Biomed Pharmacother **58**(1): 39-46.
Eren, M., A. E. Boe, et al. (2014). "PAI-1-regulated extracellular proteolysis governs senescence and survival in Klotho mice." Proc Natl Acad Sci U S A **111**(19): 7090-7095.
Esser, C., S. Alberti, et al. (2004). "Cooperation of molecular chaperones with the ubiquitin/proteasome system." Biochim Biophys Acta **1695**(1-3): 171-188.
Fabrizi, C., R. Businaro, et al. (2001). "Role of alpha2-macroglobulin in regulating amyloid -protein neurotoxicity: protective or detrimental factor?" Journal of Neurochemistry **78**: 406-412.
Farias, M., 3rd, M. W. Gorman, et al. (2005). "Plasma ATP during exercise: possible role in regulation of coronary blood flow." Am J Physiol Heart Circ Physiol **288**(4): H1586-1590.
Feige, J. J., A. Negoescu, et al. (1996). "Alpha 2-macroglobulin: a binding protein for transforming growth factor-beta and various cytokines." Horm Res **45**(3-5): 227-232.
Feldman, S. R., S. L. Gonias, et al. (1985). "Model of alpha 2-macroglobulin structure and function." Proc Natl Acad Sci U S A **82**(17): 5700-5704.
Fersht, A. R. (2000). "Transition-state structure as a unifying basis in protein-folding mechanisms: Contact order, chain topology, stability, and the extended nucleus mechanism." Proceedings of the National Academy of Sciences of the United States of America **97**: 1525-1529.
Festa, A., R. D'Agostino, Jr., et al. (2002). "Elevated levels of acute-phase proteins and plasminogen activator inhibitor-1 predict the development of type 2 diabetes: the insulin resistance atherosclerosis study." Diabetes **51**(4): 1131-1137.
Fink, A. (1999). "Chaperone-Mediated Protein Folding." Physiological Reviews **79** 425-449.
Fink, S. L. and B. T. Cookson (2005). "Apoptosis, pyroptosis, and necrosis: mechanistic description of dead and dying eukaryotic cells." Infect Immun **73**(4): 1907-1916.
Finkel, T. and N. J. Holbrook (2000). "Oxidants, oxidative stress and the biology of aging." Nature **408**: 239-247.
Fischer, M. B., C. Roeckl, et al. (2000). "Binding of disease-associated prion protein to plasminogen." Nature **408**(6811): 479-483.
Fleury, C., B. Mignotte, et al. (2002). "Mitochondrial reactive oxygen species in cell death signaling." Biochimie **84**(2-3): 131-141.
Fleury, V. and E. Angles-Cano (1991). "Characterization of the binding of plasminogen to fibrin surfaces: the role of carboxy-terminal lysines." Biochemistry **30**(30): 7630-7638.
Francis, C. W. and V. J. Marder (1987). "Physiologic regulation and pathologic disorders of fibrinolysis." Hum Pathol **18**(3): 263-274.
Freeman, D., R. Cedillos, et al. (2013). "Alpha-synuclein induces lysosomal rupture and cathepsin dependent reactive oxygen species following endocytosis." PLoS One **8**(4): e62143.
French, K., J. J. Yerbury, et al. (2008). "Protease activation of alpha2-macroglobulin modulates a chaperone-like broad specificity." Biochemistry **47**: 1176-1185.
Frydman, J. (2001). "Folding of newly translated proteins in vivo: the role of molecular chaperones." Annu Rev Biochem **70**: 603-647.
Fulop, L., M. Zarandi, et al. (2004). "Beta-amyloid-derived pentapeptide RIIGLa inhibits Abeta(1-42) aggregation and toxicity." Biochem Biophys Res Commun **324**(1): 64-69.

Furukawa, Y., K. Kaneko, et al. (2013). "Intracellular seeded aggregation of mutant Cu,Zn-superoxide dismutase associated with amyotrophic lateral sclerosis." FEBS Lett **587**(16): 2500-2505.

Galantai, R., K. Modos, et al. (2006). "Structural basis of the cofactor function of denatured albumin in plasminogen activation by tissue-type plasminogen activator." Biochem Biophys Res Commun **341**(3): 736-741.

Galantai, R., K. Modos, et al. (2006). "Structural basis of the cofactor function of denatured albumin in plasminogen activation by tissue-type plasminogen activator." Biochem, Biophys. Res. Comm. **341**(3): 736-741.

Galliano, M. F., E. Toulza, et al. (2006). "A novel protease inhibitor of the alpha2-macroglobulin family expressed in the human epidermis." J Biol Chem **281**(9): 5780-5789.

Gando, S., T. Kameue, et al. (2004). "Systemic inflammation and disseminated intravascular coagulation in early stage of ALI and ARDS: role of neutrophil and endothelial activation." Inflammation **28**(4): 237-244.

Ganrot, P. O. (1966). "Determination of alpha-2-macroglobulin as trypsin-protein esterase." Clin Chim Acta **14**(4): 493-501.

Gao, H. M., B. Liu, et al. (2003). "Novel anti-inflammatory therapy for Parkinson's disease." Trends Pharmacol Sci **24**(8): 395-401.

Garg, S. K., V. Vitvitsky, et al. (2011). "Astrocytic redox remodeling by amyloid beta peptide." Antioxid Redox Signal **14**(12): 2385-2397.

Gebbink, M., B. Bouma, et al. (2009). "Fibrinolysis, coagulation and inflammation (new roles for old factors)." FEBS Letters **583**: 2691-2699.

Gebbink, M., B. Bouma, et al. (2009). "Physiological responses to protein aggregates: Fibrinolysis, coagulation and inflammation (new roles for old factors)." FEBS Letters **583**(16): 2691-2699.

Gebbink, M. F. (2011). "Tissue-type plasminogen activator-mediated plasminogen activation and contact activation, implications in and beyond haemostasis." J Thromb Haemost **9 Suppl 1**: 174-181.

Gebbink, M. F. B. G., Bouma, B., Maas, C. and Bouma, B.N. (2009). "Physiological responses to protein aggregates: Fibrinolysis, coagulation and inflammation (new roles for old factors)." Federation of European Biochemical Societies Letters **583**: 2691-2699.

Gejyo, F., T. Yamada, et al. (1985). "A new form of amyloid protein associated with chronic hemodialysis was identified as beta 2-microglobulin." Biochem Biophys Res Commun **129**(3): 701-706.

Gendreau, K. L. and G. F. Hall (2013). "Tangles, Toxicity, and Tau Secretion in AD - New Approaches to a Vexing Problem." Front Neurol **4**: 160.

Gibson, T. J. and R. M. Murphy (2006). "Inhibition of insulin fibrillogenesis with targeted peptides." Protein Sci **15**(5): 1133-1141.

Gidalevitza, T., E. A. Kikisa, et al. (2010). "A cellular perspective on conformational disease: the role of genetic background and proteostasis networks." Current Opinion in Structural Biology **20**(1): 23-32.

Giffard, R. G., L. Xu, et al. (2004). "Chaperones, protein aggregation, and brain protection from hypoxic/ischemic injury." J Exp Biol **207**(Pt 18): 3213-3220.

Gilabert, J., A. Estelles, et al. (1995). "Fibrinolytic system and reproductive process with special reference to fibrinolytic failure in pre-eclampsia." Hum Reprod **10 Suppl 2**: 121-131.

Giulian, D. (1999). "Microglia and the immune pathology of Alzheimer disease." Am J Hum Genet **65**(1): 13-18.

Gliemann, J., O. Davidsen, et al. (1985). "Uptake of rat and human alpha 2-macroglobulin-trypsin complexes into rat and human cells." FEBS Lett **188**(2): 352-356.
Goers, J., S. E. Permyakov, et al. (2002). "Conformational prerequisites for alpha-lactalbumin fibrillation." Biochemistry **41**(41): 12546-12551.
Goldberg, A. L. (2003). "Protein degradation and protection against misfolded or damaged proteins." Nature **426**(6968): 895-899.
Gonias, S. L., J. LaMarre, et al. (1994). "Alpha 2-macroglobulin and the alpha 2-macroglobulin receptor/LRP. A growth regulatory axis." Ann N Y Acad Sci **737**: 273-290.
Gonias, S. L., L. B. Marshall, et al. (1993). "Electron microscopy studies of alpha 2-macroglobulin subunit association after limited reduction with dithiothreitol." Arch Biochem Biophys **302**(1): 42-48.
Gonias, S. L. and S. V. Pizzo (1983). "Reaction of human alpha 2-macroglobulin half-molecules with plasmin as a probe of protease binding site structure." Biochemistry **22**(21): 4933-4940.
Gonzalez-Velasquez, F., J. W. Reed, et al. (2011). "Activation of brain endothelium by soluble aggregates of the amyloid-beta protein involves nuclear factor-kappaB." Curr Alzheimer Res **8**(1): 81-94.
Gonzalez-Velasquez, F. J., J. A. Kotarek, et al. (2008). "Soluble aggregates of the amyloid-beta protein selectively stimulate permeability in human brain microvascular endothelial monolayers." J Neurochem **107**(2): 466-477.
Gonzalez-Velasquez, F. J. and M. A. Moss (2008). "Soluble aggregates of the amyloid-beta protein activate endothelial monolayers for adhesion and subsequent transmigration of monocyte cells." J Neurochem **104**(2): 500-513.
Gonzalez-Villalobos, R., R. B. Klassen, et al. (2006). "Megalin binds and internalizes angiotensin-(1-7)." American Journal of Physiology - Renal Physiology **290**(5): F1270-F1275.
Gourine, A. V., V. N. Gourine, et al. (2002). "Role of alpha(2)-macroglobulin in fever and cytokine responses induced by lipopolysaccharide in mice." Am J Physiol Regul Integr Comp Physiol **283**(1): R218-226.
Green, P. S., A. J. Mendez, et al. (2004). "Neuronal expression of myeloperoxidase is increased in Alzheimer's disease." J Neurochem **90**(3): 724-733.
Greenbaum, E. A., C. L. Graves, et al. (2005). "The E46K mutation in alpha-synuclein increases amyloid fibril formation." J Biol Chem **280**(9): 7800-7807.
Grune, T., T. Jung, et al. (2004). "Decreased proteolysis caused by protein aggregates, inclusion bodies, plaques, lipofuscin, ceroid, and 'aggresomes' during oxidative stress, aging, and disease." Int J Biochem Cell Biol **36**(12): 2519-2530.
Gunnarsson, M., T. Stigbrand, et al. (2000). "Aberrant forms of alpha(2)-macroglobulin purified from patients with multiple sclerosis." Clin Chim Acta **295**(1-2): 27-40.
Guo, Y., Hernandez, I., Isermann, B., Kang, T., Medved, L., Sood, R., Kerschen, E.J., Holyst, T., Mosesson, M.W. and Weiler, H. (2009). "Caveolin-1-dependent apoptosis induced by fibrin degradation products." Blood **113**: 4431-4439.
Guo, Y. and S. Scarlata (2013). "A loss in cellular protein partners promotes alpha-synuclein aggregation in cells resulting from oxidative stress." Biochemistry **52**(22): 3913-3920.
Guo, Y. H., I. Hernandez, et al. (2009). "Caveolin-1-dependent apoptosis induced by fibrin degradation products." Blood **113**(18): 4431-4439.
Hacke, W., Kaste, M., Fieschi, C., Toni, D., Lesaffre, E., von Kummer, R., Boysen, G., Bluhmki, E., Hoxer, G., Mahagne, N. and Hennerici, M. (1995). "Intravenous Thrombolysis with Recombinant Tissue Plasminogen Activator for Acute

Hemispheric Stroke. The European Cooperative Acute Stroke Study (ECASS). ." The Journal of the American Medical Association **274** 1017-1025.
Hammad, S. M., S. Ranganathan, et al. (1997). "Interaction of Apolipoprotein J-Amyloid B-peptide Complex with Low Density Lipoprotein Receptor-Related Protein-2/Megalin." The Journal of Biological Chemistry **272**(30): 18644-18649.
Hampton, M. B., A. J. Kettle, et al. (1998). "Inside the neutrophil phagosome: oxidants, myeloperoxidase, and bacterial killing." Blood **92**(9): 3007-3017.
Harpel, P. C. (1973). "Studies on human plasma α2-Macroglobulin-enzyme interactions." The Journal of Experimental medicine **138**: 508-521.
Harpel, P. C., M. B. Hayes, et al. (1979). "Heat-induced fragmentation of human alpha 2-macroglobulin." J Biol Chem **254**(17): 8669-8678.
Harpel, P. C., R. Sullivan, et al. (1989). "Binding and activation of plasminogen on immobilized immunoglobulin G. Identification of the plasmin-derived Fab as the plasminogen-binding fragment." J Biol Chem **264**(1): 616-624.
Hartl, F. U. and M. Hayer-Hartl (2002). "Molecular chaperones in the cytosol: from nascent chain to folded protein. (Review: protein folding)." Science **295**(1852-1857).
Hassan, R., P. Claudia, et al. (2011). "Large Proteins Have a Great Tendency to Aggregate but a Low Propensity to Form Amyloid Fibrils." PLoS One **6**(1): e16075.
Hazell, L. J., J. J. van den Berg, et al. (1994). "Oxidation of low-density lipoprotein by hypochlorite causes aggregation that is mediated by modification of lysine residues rather than lipid oxidation." Biochem J **302 (Pt 1)**: 297-304.
Heegaard, C. W., P. A. Andreasen, et al. (1997). "Binding of plasminogen and tissue-type plasminogen activator to dimeric αs2-casein accelerates plasmin generation." Fibrinolysis and Proteolysis **11**(1): 29-36.
Hempel, S. L., G. R. Buettner, et al. (1999). "Dihydrofluorescein diacetate is superior for detecting intracellular oxidants: comparison with 2',7'-dichlorodihydrofluorescein diacetate, 5(and 6)-carboxy-2',7'-dichlorodihydrofluorescein diacetate, and dihydrorhodamine 123." Free Radic Biol Med **27**(1-2): 146-159.
Henderson, L. M. and J. B. Chappell (1993). "Dihydrorhodamine 123: a fluorescent probe for superoxide generation?" Eur J Biochem **217**(3): 973-980.
Herczenik, E., B. Bouma, et al. (2007). "Activation of human platelets by misfolded proteins." Arteriosclerosis Thrombosis and Vascular Biology **27**(7): 1657-1665.
Herczenik, E. and M. F. B. G. Gebbink (2008). "Molecular and cellular aspects of protein misfolding and disease." The FASEB Journal **22**: 2115-2133.
Hjerten, S. (1962). "Chromatographic separation according to size of macromolecules and cell particles on columns of agarose suspensions." Arch Biochem Biophys **99**: 466-475.
Ho, M. R., Y. C. Lou, et al. (2006). "Human pancreatitis-associated protein forms fibrillar aggregates with a native-like conformation." J Biol Chem **281**(44): 33566-33576.
Hofmann, J. P., P. Denner, et al. (2013). "Cell-to-cell propagation of infectious cytosolic protein aggregates." Proc Natl Acad Sci U S A **110**(15): 5951-5956.
Holmes, B. B. and M. I. Diamond (2012). "Cellular mechanisms of protein aggregate propagation." Curr Opin Neurol **25**(6): 721-726.
Hong, E., Davidson, A.R. and Kaider, C.A. (1996). "A Pathway for Targeting Soluble Misfolded Proteins to the Yeast Vacuole." The Journal of Cell Biology **135**: 623-633.
Hoover, G. J., N. Menhart, et al. (1993). "Amino acids of the recombinant kringle 1 domain of human plasminogen that stabilize its interaction with omega-amino acids." Biochemistry **32**(41): 10936-10943.
Hoppener, J. W., M. G. Nieuwenhuis, et al. (2000). "[Islet amyloid and diabetes mellitus type 2]." Ned Tijdschr Geneeskd **144**(42): 1995-2000.

Howell, J. B., T. Beck, et al. (1983). "Interaction of alpha 2-macroglobulin with trypsin, chymotrypsin, plasmin, and papain." Arch Biochem Biophys **221**(1): 261-270.
Hughes, S. R., O. Khorkova, et al. (1998). "Alpha2-macroglobulin associates with beta-amyloid peptide and prevents fibril formation." Proceedings of the National Academy of Sciences of the United States of America **95**: 3275-3280.
Humphreys, D. T., J. A. Carver, et al. (1999). "Clusterin has chaperone-like activity similar to that of small heat shock proteins." J Biol Chem **274**(11): 6875-6881.
Humphreys, D. T., J. A. Carver, et al. (1999). "Clusterin has chaperone-like activity similar to that of small heat shock proteins." The Journal of Biological Chemistry **274**(11): 6875-6881.
Hutt, D. M., E. T. Powers, et al. (2009). "The proteostasis boundary in misfolding diseases of membrane traffic." FEBS Lett **583**(16): 2639-2646.
Ii, M., M. Sunamoto, et al. (1996). "beta-Amyloid protein-dependent nitric oxide production from microglial cells and neurotoxicity." Brain Res **720**(1-2): 93-100.
Imber, M. J. a. P., S.V. (1981). "Clearance and Binding of Two Electrophoretic "Fast" Forms of Human α2-Macroglobulin." The Journal of Biological Chemistry **256** 8134-8139.
Indyk, J. A., Chen, Z.L., Tsirka, S.E. and Strickland, S. (2003). "Laminin chain expression suggests that laminin-10 is a major isoform in the mouse hippocampus and is degraded by the tissue plasminogen activator/plasmin protease cascade during excitotoxic injury." Neuroscience Letters **116**: 359-371.
Isermann, B., R. Sood, et al. (2003). "The thrombomodulin-protein C system is essential for the maintenance of pregnancy." Nat Med **9**(3): 331-337.
Isermann, B., Sood, R., Pawlinski, R., Zogg, M., Kalloway, S., Degen, J.L., Mackman, N. and Weiler, H. (2003). "The thrombomodulin-protein C system is essential for the maintenance of pregnancy." Nature Medicine **9**: 331-337.
Jana, M., C. A. Palencia, et al. (2008). "Fibrillar amyloid-beta peptides activate microglia via TLR2: implications for Alzheimer's disease." J Immunol **181**(10): 7254-7262.
Jellinger, K. A. (2002). "Alzheimer disease and cerebrovascular pathology: an update." J Neural Transm **109**(5-6): 813-836.
Jensen, P. E. and L. Sottrup-Jensen (1986). "Primary structure of human alpha 2-macroglobulin. Complete disulfide bridge assignment and localization of two interchain bridges in the dimeric proteinase binding unit." J Biol Chem **261**(34): 15863-15869.
Jeong, S., D. R. Ledee, et al. (2012). "Interaction of clusterin and matrix metalloproteinase-9 and its implication for epithelial homeostasis and inflammation." Am J Pathol **180**(5): 2028-2039.
Jersmann, H. P. (2005). "Time to abandon dogma: CD14 is expressed by non-myeloid lineage cells." Immunol Cell Biol **83**(5): 462-467.
Joh, K., S. Aizawa, et al. (1990). "Microlamellar structures in lobular glomerulonephritis associated with monoclonal IgG lambda paraproteinemia. A case report and review of the literature." Acta Pathol Jpn **40**(12): 913-921.
Jourd'heuil, D., F. L. Jourd'heuil, et al. (2001). "Reaction of superoxide and nitric oxide with peroxynitrite. Implications for peroxynitrite-mediated oxidation reactions in vivo." J Biol Chem **276**(31): 28799-28805.
Joyce, N., G. Annett, et al. (2010). "Mesenchymal stem cells for the treatment of neurodegenerative disease." Regen Med **5**(6): 933-946.
Kaarniranta, K. and A. Salminen (2009). "Age-related macular degeneration: activation of innate immunity system via pattern recognition receptors." J Mol Med (Berl) **87**(2): 117-123.

Kandimalla, K. K., O. G. Scott, et al. (2009). "Mechanism of neuronal versus endothelial cell uptake of Alzheimer's disease amyloid beta protein." PLoS One **4**(2): e4627.
Kannan, S., V. R. Muthusamy, et al. (2013). "Nrf2 deficiency prevents reductive stress-induced hypertrophic cardiomyopathy." Cardiovasc Res **100**(1): 63-73.
Kaufman, R. J., Scheuner, D., Schroder, M., Shen, X., Lee, K., Liu, C.Y. and Arnold, S.M. (2002). "The Unfolded Protein Response in Nutrient Sensing and Differentiation." Nature **3**: 411-421.
Kaur, C., A. J. Hao, et al. (2001). "Origin of microglia." Microsc Res Tech **54**(1): 2-9.
Kelley, S. L., T. Lukk, et al. (2013). "The crystal structure of human soluble CD14 reveals a bent solenoid with a hydrophobic amino-terminal pocket." J Immunol **190**(3): 1304-1311.
Khamlichi, A. A., P. Aucouturier, et al. (1995). "Structure of abnormal heavy chains in human heavy-chain-deposition disease." Eur J Biochem **229**(1): 54-60.
Khamlichi, A. A., A. Rocca, et al. (1995). "Role of light chain variable region in myeloma with light chain deposition disease: evidence from an experimental model." Blood **86**(10): 3655-3659.
Kidwell, C. S., Latour, L., Saver, J.L., Alger, J.R., Starkman, S., Duckwiler, G., Jahan, R. and Vinuela, S. (2008). "Thrombolytic Toxicity: Blood Brain Barrier Disruption in Human Ischemic Stroke." Cerebrovascular Diseases **25**: 338-343.
Kitazawa, M., T. R. Yamasaki, et al. (2004). "Microglia as a potential bridge between the amyloid beta-peptide and tau." Ann N Y Acad Sci **1035**: 85-103.
Kitching, A. R., S. R. Holdsworth, et al. (1997). "Plasminogen and plasminogen activators protect against renal injury in crescentic glomerulonephritis." J Exp Med **185**(5): 963-968.
Koenig, W. and R. S. Rosenson (2002). "Acute-phase reactants and coronary heart disease." Semin Vasc Med **2**(4): 417-428.
Koga, H., S. Kaushik, et al. (2011). "Protein homeostasis and aging: The importance of exquisite quality control." Ageing Res Rev **10**(2): 205-215.
Kolodziej, S. J., H. U. Klueppelberg, et al. (1998). "Three-dimensional structure of the human plasmin alpha2-macroglobulin complex." J Struct Biol **123**(2): 124-133.
Kondo, N., Y. Ishii, et al. (2004). "Redox-sensing release of human thioredoxin from T lymphocytes with negative feedback loops." J Immunol **172**(1): 442-448.
Kopito, R. R. (2000). "Aggresomes, inclusion bodies and protein aggregation." Trends Cell Biol **10**(12): 524-530.
Kovacs, A., L. Szabo, et al. (2014). "Ambivalent roles of carboxypeptidase B in the lytic susceptibility of fibrin." Thromb Res **133**(1): 80-87.
Kranenburg, O., B. Bouma, et al. (2002). "Tissue-type plasminogen activator is a multiligand cross-beta structure receptor." Curr Biol **12**(21): 1833-1839.
Kranenburg, O., B. Bouma, et al. (2002). "Tissue-type plasminogen activator is a multiligand cross-β structure receptor." Current Biology **12**(21): 1833-1839.
Kranenburg, O., Y. Y. J. Gent, et al. (2005). "Amyloid-beta-stimulated plasminogen activation by tissue-type plasminogen activator results in processing of neuroendocrine factors." Neuroscience **131**(4): 877-886.
Krishna, M. M. G., Lin, Y. and Englander, W. (2004). "Protein Misfolding: Optional Barriers, Misfolded Intermediates, and Pathway Heterogeneity." Journal of Molecular Biology **343**: 1095-1109.
Kroemer, G., L. Galluzzi, et al. (2009). "Classification of cell death: recommendations of the Nomenclature Committee on Cell Death 2009." Cell Death Differ **16**(1): 3-11.
Kumar, S., J. M. Vinci, et al. (1993). "Expression of interleukin-1 alpha and beta in early passage fibroblasts from aging individuals." Exp Gerontol **28**(6): 505-513.

Kumita, J. R., S. Poon, et al. (2007). "The extracellular chaperone clusterin potentially inhibits amyloid formation by interacting with prefibrillar species." Journal of Molecular Biology **369**(1): 157-167.
Kurdowska, A., N. Fujisawa, et al. (2000). "Specific binding of IL-8 to rabbit alpha-macroglobulin modulates IL-8 function in the lung." Inflamm Res **49**(11): 591-599.
Kwaan, H. C. (1992). "The plasminogen-plasmin system in malignancy." Cancer Metastasis Rev **11**(3-4): 291-311.
Lachmann, P. J., M. K. Pangburn, et al. (1982). "Breakdown of C3 after complement activation. Identification of a new fragment C3g, using monoclonal antibodies." J Exp Med **156**(1): 205-216.
Laemmli, U. K. (1970). "Cleavage of structural proteins during the assembly of the head of bacteriophage T4." Nature **227**(5259): 680-685.
LaMarre, J., G. K. Wollenberg, et al. (1991). "Cytokine binding and clearance properties of proteinase-activated alpha 2-macroglobulins." Lab Invest **65**(1): 3-14.
LaMarre, J., G. K. Wollenberg, et al. (1991). "Reaction of alpha 2-macroglobulin with plasmin increases binding of transforming growth factors-beta 1 and beta 2." Biochim Biophys Acta **1091**(2): 197-204.
Larsson, L. J., A. Holmgren, et al. (1988). "Subunits of human alpha 2-macroglobulin produced by specific reduction of interchain disulfide bonds with thioredoxin." Biochemistry **27**(3): 983-991.
Lau, A. and M. Tymianski (2010). "Glutamate receptors, neurotoxicity and neurodegeneration." Pflugers Arch **460**(2): 525-542.
Lauer, D., A. Reichenbach, et al. (2001). "Alpha 2-macroglobulin-mediated degradation of amyloid beta 1--42: a mechanism to enhance amyloid beta catabolism." Experimental Neurology **169**(2): 385-392.
Law, R. H., T. Caradoc-Davies, et al. (2012). "The X-ray crystal structure of full-length human plasminogen." Cell Rep **1**(3): 185-190.
Lee, H. J., S. Patel, et al. (2005). "Intravesicular localization and exocytosis of alpha-synuclein and its aggregates." J Neurosci **25**(25): 6016-6024.
Lee, J. Y., H. S. Kweon, et al. (2007). "Upregulation of tPA/plasminogen proteolytic system in the periphery of amyloid deposits in the Tg2576 mouse model of Alzheimer's disease." Neurosci Lett **423**(1): 82-87.
Leung, K. C., J. A. Byatt, et al. (1987). "Poly-D-lysine dependent inactivation of tissue plasminogen activator by a class PAI-2 inhibitor (minactivin)." Thromb Res **46**(6): 767-777.
Leung, K. C., J. A. Byatt, et al. (1987). "The resistance of fibrin-stimulated tissue plasminogen activator to inactivation by a class PAI-2 inhibitor (minactivin)." Thromb Res **46**(6): 755-766.
Levi, M., M. J. Schultz, et al. (2003). "Bronchoalveolar coagulation and fibrinolysis in endotoxemia and pneumonia." Crit Care Med **31**(4 Suppl): S238-242.
Levin, E. G. (1983). "Latent tissue plasminogen activator produced by human endothelial cells in culture: evidence for an enzyme-inhibitor complex." Proc Natl Acad Sci U S A **80**(22): 6804-6808.
Levin, E. G., L. Santell, et al. (1997). "The expression of endothelial tissue plasminogen activator in vivo: a function defined by vessel size and anatomic location." J Cell Sci **110 (Pt 2)**: 139-148.
Lijnen, H. R., M. Maes, et al. (1982). "Kinetics of the inhibition of plasmin in acidified human plasma." Thromb Haemost **48**(3): 257-259.
Lijnen, H. R. a. C., D. (1982). "Interaction of plasminogen activators and inhibitors with plasminogen and fibrin." Seminars in Thrombosis and Hemostasis **8**: 2-10.

Lindberg, M. (2004). Protein folding studies of human superoxide dismutase and ALS associated mutants, Umeå University.
Linding, R., J. Schymkowitz, et al. (2004). "A comparative study of the relationship between protein structure and beta-aggregation in globular and intrinsically disordered proteins." J Mol Biol **342**(1): 345-353.
Lipton, S. A. and P. A. Rosenberg (1994). "Excitatory amino acids as a final common pathway for neurologic disorders." N Engl J Med **330**(9): 613-622.
Liu, Y., W. Hao, et al. (2009). "Expression of amyotrophic lateral sclerosis-linked SOD1 mutant increases the neurotoxic potential of microglia via TLR2." J Biol Chem **284**(6): 3691-3699.
Liu, Y., H. Yu, et al. (2008). "TLRs are important inflammatory factors in atherosclerosis and may be a therapeutic target." Medical Hypothesis **70**(2): 314-316.
Lobov, S. and M. Ranson (2011). "Molecular competition between plasminogen activator inhibitors type -1 and -2 for urokinase: Implications for cellular proteolysis and adhesion in cancer." Cancer Lett **303**(2): 118-127.
Longstaff, C. and P. J. Gaffney (1991). "Serpin-serine protease binding kinetics: alpha 2-antiplasmin as a model inhibitor." Biochemistry **30**(4): 979-986.
Longstaff, C., S. Williams, et al. (2008). "Fibrin binding and the regulation of plasminogen activators during thrombolytic therapy." Cardiovasc Hematol Agents Med Chem **6**(3): 212-223.
Lopez-Otin, C., M. A. Blasco, et al. (2013). "The hallmarks of aging." Cell **153**(6): 1194-1217.
Lue, L. F., D. G. Walker, et al. (2001). "Modeling microglial activation in Alzheimer's disease with human postmortem microglial cultures." Neurobiol Aging **22**(6): 945-956.
Ma, J. H., J. J. Wang, et al. (2014). "The unfolded protein response and diabetic retinopathy." J Diabetes Res **2014**: 160140.
Maas, C., J. W. Govers-Riemslag, et al. (2008). "Misfolded proteins activate factor XII in humans, leading to kallikrein formation without initiating coagulation." J Clin Invest **118**(9): 3208-3218.
Maas, C., B. Schiks, et al. (2008). "Identification of fibronectin type I domains as amyloid-binding modules on tissue-type plasminogen activator and three homologs." Amyloid-Journal of Protein Folding Disorders **15**(3): 166-180.
Machovich, R. and W. G. Owen (1997). "Denatured proteins as cofactors for plasminogen activation." Arch Biochem Biophys **344**(2): 343-349.
Machovich, R. and W. G. Owen (1997). "Denatured proteins as cofactors for plasminogen activation." Archives of Biochemistry and Biophysics **344**(2): 343-349.
Maguire-Zeiss, K. A., D. W. Short, et al. (2005). "Synuclein, dopamine and oxidative stress: co-conspirators in Parkinson's disease?" Brain Res Mol Brain Res **134**(1): 18-23.
Malle, E., C. Woenckhaus, et al. (1997). "Immunological evidence for hypochlorite-modified proteins in human kidney." Am J Pathol **150**(2): 603-615.
Manders, E. M. M., F. J. Verbeek, et al. (1993). "Measurement of co-localization of objects in dual-colour confocal images." Journal of Microscopy **169**(3): 375-382.
Manzano-Leon, N., B. Delgado-Coello, et al. (2006). "Beta-adaptin: key molecule for microglial scavenger receptor function under oxidative stress." Biochem Biophys Res Commun **351**(3): 588-594.
Margineanu, I. and V. Ghetie (1981). "A selective model of plasma protein catabolism." Journal of Theoretical Biology **90**: 101-110.

Marrero, A., S. Duquerroy, et al. (2012). "The crystal structure of human alpha2-macroglobulin reveals a unique molecular cage." Angew Chem Int Ed Engl **51**(14): 3340-3344.
Marsh, R., Corey, R.B. and Pauling, L. (1955). " An investigation of the structure of silk fibrin." Biochemica et Biophysica Acta **16**: 1-34.
Marx, J., Hudry-Clergeon, G., Capet-Antonini, F. and Bernard, L. (1979). "Laser Raman spectroscopy study of bovine fibrinogen and fibrin." Biochimica et Biophysica Acta **578**: 107-115.
Marzolo, M. P., R. von Bernhardi, et al. (2000). "Expression of alpha(2)-macroglobulin receptor/low density lipoprotein receptor-related protein (LRP) in rat microglial cells." J Neurosci Res **60**(3): 401-411.
Masos, T. and R. Miskin (1997). "mRNAs encoding urokinase-type plasminogen activator and plasminogen activator inhibitor-1 are elevated in the mouse brain following kainate-mediated excitation." Brain Res Mol Brain Res **47**(1-2): 157-169.
Mathew, S., S. Arandjelovic, et al. (2003). "Characterization of the interaction between alpha2-macroglobulin and fibroblast growth factor-2: the role of hydrophobic interactions." Biochem J **374**(Pt 1): 123-129.
Mathias, M. (2007). "Understanding haemostasis." Pediatrics and Child Health **17**: 317-321.
Matsuda, A., Yoshifumi, I., Koshikawa, N., Akizawas, T. and Yana, I. (2003). "Clusterin, an Abundant Serum Factor, Is a Possible Negative Regulator of MT6-MMP/MMP-25 Produced by Neutrophils." The Journal of Biological Chemistry **278**: 36350-36357.
Matthews, J. B. (1983). "The immunoglobulin nature of Russell bodies." Br J Exp Pathol **64**(3): 331-335.
McAlpine, C. S., A. J. Bowes, et al. (2010). "Diabetes, hyperglycemia and accelerated atherosclerosis: evidence supporting a role for endoplasmic reticulum (ER) stress signaling." Cardiovasc Hematol Disord Drug Targets **10**(2): 151-157.
McLaughlin, L., G. Zhu, et al. (2000). "Apolipoprotein J/clusterin limits the severity of murine autoimmune myocarditis." The Journal of Clinical Investigation **106**: 1105-1113.
McManus, M. J., M. P. Murphy, et al. (2014). "Mitochondria-derived reactive oxygen species mediate caspase-dependent and -independent neuronal deaths." Mol Cell Neurosci **63**: 13-23.
Medcalf, R. L. (2011). "Plasminogen activator inhibitor type 2: still an enigmatic serpin but a model for gene regulation." Methods Enzymol **499**: 105-134.
Medina, M. G., M. D. Ledesma, et al. (2005). "Tissue plasminogen activator mediates amyloid-induced neurotoxicity via Erk1/2 activation." EMBO J **24**(9): 1706-1716.
Melchor, J. P., R. Pawlak, et al. (2003). "The tissue plasminogen activator-plasminogen proteolytic cascade accelerates amyloid-beta (Abeta) degradation and inhibits Abeta-induced neurodegeneration." J Neurosci **23**(26): 8867-8871.
Melchor, J. P. and S. Strickland (2005). "Tissue plasminogen activator in central nervous system physiology and pathology." Thromb Haemost **93**(4): 655-660.
Menhart, N., G. J. Hoover, et al. (1995). "Roles of individual kringle domains in the functioning of positive and negative effectors of human plasminogen activation." Biochemistry **34**(5): 1482-1488.
Mettenburg, J. M., D. J. Webb, et al. (2002). "Distinct binding sites in the structure of alpha 2-macroglobulin mediate the interaction with beta-amyloid peptide and growth factors." J Biol Chem **277**(15): 13338-13345.
Mezzapesa, A., C. Orset, et al. (2014). "Plasminogen in cerebrospinal fluid originates from circulating blood." J Neuroinflammation **11**: 154.

Milosavljevic, T. S., M. V. Petrovic, et al. (2002). "DNA binding activity of C/EBPbeta and C/EBPdelta for the rat alpha2-macroglobulin gene promoter is regulated in an acute-phase dependent manner." Biochemistry (Mosc) **67**(8): 918-926.

Minton, A. P. (2000). "Protein folding: Thickening the broth." Current Biology **10**(3): R97-R99.

Moldovan, L., K. Mythreye, et al. (2006). "Reactive oxygen species in vascular endothelial cell motility. Roles of NAD(P)H oxidase and Rac1." Cardiovasc Res **71**(2): 236-246.

Moncino, M. D., P. A. Roche, et al. (1991). "Characterization of human alpha 2-macroglobulin monomers obtained by reduction with dithiothreitol." Biochemistry **30**(6): 1545-1551.

Moreno, A., J. Mas-Oliva, et al. (2000). "Turbidity as a useful optical parameter to predict protein crystallization by dynamic light scattering." Journal of Molecular Structure **519**(1–3): 243-256.

Morimoto, M. (2006). "Stress, Aging, and Neurodegenerative Disease." The New England Journal of Medicine **355**: 2254-2255.

Morimoto, R. I. (2008). "Proteotoxic stress and inducible chaperone networks in neurodegenerative disease and aging." Genes Dev **22**(11): 1427-1438.

Morley, J. F., H. R. Brignull, et al. (2002). "The threshold for polyglutamine-expansion protein aggregation and cellular toxicity is dynamic and influenced by aging in Caenorhabditis elegans." Proc Natl Acad Sci U S A **99**(16): 10417-10422.

Mosesson, M. W. (2005). "Fibrinogen and fibrin structure and functions." J Thromb Haemost **3**(8): 1894-1904.

Munch, C., J. O'Brien, et al. (2011). "Prion-like propagation of mutant superoxide dismutase-1 misfolding in neuronal cells." Proc Natl Acad Sci U S A **108**(9): 3548-3553.

Nagele, R. G., J. Wegiel, et al. (2004). "Contribution of glial cells to the development of amyloid plaques in Alzheimer's disease." Neurobiol Aging **25**(5): 663-674.

Nakamura, H., H. Masutani, et al. (2006). "Extracellular thioredoxin and thioredoxin-binding protein 2 in control of cancer." Semin Cancer Biol **16**(6): 444-451.

Narayan, P., S. Meehan, et al. (2012). "Amyloid-beta oligomers are sequestered by both intracellular and extracellular chaperones." Biochemistry **51**(46): 9270-9276.

Nardai, G., T. Korcsmaros, et al. (2003). "Reduction of the endoplasmic reticulum accompanies the oxidative damage of diabetes mellitus." Biofactors **17**(1-4): 259-267.

Narita, M., D. M. Holtzman, et al. (1997). "Alpha2-macroglobulin complexes with and mediates the endocytosis of beta-amyloid peptide via cell surface low-density lipoprotein receptor-related protein." J Neurochem **69**(5): 1904-1911.

Narita, M., Moltzman, D.M., Schwartz, A.L. and Bu, G. (1997). "α2-Macroglobulin Complexes with and Mediates the Endocytosis of β-Amyloid Peptide via Cell Surface Low-Density Lipoprotein Receptor-Related Protein." Journal of Neurochemistry **69**: 1904-1911.

Navab, M., G. M. Anantharamaiah, et al. (2005). "An Oral ApoJ Peptide Renders HDL Antiinflammatory in Mice and Monkeys and Dramatically Reduces Atherosclerosis in Apolipoprotein E–Null Mice." Arteriosclerosis, Thrombosis and Vascular Biology **25**: 1932-1937.

Neumann, H., M. R. Kotter, et al. (2009). "Debris clearance by microglia: an essential link between degeneration and regeneration." Brain **132**(Pt 2): 288-295.

Nilsen, S. L., M. Prorok, et al. (1999). "Enhancement through mutagenesis of the binding of the isolated kringle 2 domain of human plasminogen to omega-amino acid ligands and to an internal sequence of a Streptococcal surface protein." J Biol Chem **274**(32): 22380-22386.

Norton, J. A., Stein, P. and Brennan, M. (1981). "Whole Body Protein Synthesis and Turnover in Normal Man and Malnourished Patients with and without Known Cancer." Annals of Surgery **194**: 123-128.
O'Connell, K. A. and M. Edidin (1990). "A mouse lymphoid endothelial cell line immortalized by simian virus 40 binds lymphocytes and retains functional characteristics of normal endothelial cells." J Immunol **144**(2): 521-525.
Okado-Matsumoto, A. and I. Fridovich (2002). "Amyotrophic lateral sclerosis: a proposed mechanism." Proc Natl Acad Sci U S A **99**(13): 9010-9014.
Ozawa, D., K. Hasegawa, et al. (2011). "Inhibition of beta2-microglobulin amyloid fibril formation by alpha2-macroglobulin." J Biol Chem **286**(11): 9668-9676.
Papp, E., G. Nardai, et al. (2003). "Molecular chaperones, stress proteins and redox homeostasis." Biofactors **17**(1-4): 249-257.
Papp, E., P. Szaraz, et al. (2006). "Changes of endoplasmic reticulum chaperone complexes, redox state, and impaired protein disulfide reductase activity in misfolding alpha1-antitrypsin transgenic mice." FASEB J **20**(7): 1018-1020.
Pestel, J., J. P. Dessaint, et al. (1984). "Macrophage triggering by aggregated immunoglobulins. II. Comparison of IgE and IgG aggregates or immune complexes." Clin Exp Immunol **57**(2): 404-412.
Ponting, C. P., J. M. Marshall, et al. (1992). "Plasminogen: a structural review." Blood Coagul Fibrinolysis **3**(5): 605-614.
Poon, S., S. B. Easterbrook-Smith, et al. (2000). "Clusterin is an ATP-independent chaperone with very broad substrate specificity that stabilizes stressed proteins in a folding-competent state." Biochemistry **39**(51): 15953-15960.
Poon, S., M. S. Rybchyn, et al. (2002). "Mildly acidic pH activates the extracellular molecular chaperone clusterin." J Biol Chem **277**(42): 39532-39540.
Poon, S., M. S. Rybchyn, et al. (2000). "Clusterin is an ATP-independent chaperone with a very broad substrate specificity that stabilizes stressed proteins in a folding-competent state." Biochemistry **39**: 15953-15960.
Powers, E. T., R. I. Morimoto, et al. (2009). "Biological and chemical approaches to diseases of proteostasis deficiency." Annu Rev Biochem **78**: 959-991.
Qian, Y., J. Luo, et al. (2007). "Hydrogen peroxide formation and actin filament reorganization by Cdc42 are essential for ethanol-induced in vitro angiogenesis." Nihon Arukoru Yakubutsu Igakkai Zasshi **42**(6): 605-609.
Qiu, Z., D. K. Strickland, et al. (1999). "Alpha 2-macroglobulin enhances the clearance of endogenous soluble beta-amyloid peptide via low-density lipoprotein receptor-related protein in cortical neurons." Journal of Neurochemistry **73**: 1393–1398.
Radcliffe, R. (1983). "A critical role of lysine residues in the stimulation of tissue plasminogen activator by denatured proteins and fibrin clots." Biochim Biophys Acta **743**(3): 422-430.
Radcliffe, R. and T. Heinze (1981). "Stimulation of tissue plasminogen activator by denatured proteins and fibrin clots: a possible additional role for plasminogen activator?" Arch Biochem Biophys **211**(2): 750-761.
Radcliffe, R. a. H., T. (1981). "Stimulation of tissue plasminogen activator by denatured proteins and fibrin clots: A possible additional role for plasminogen activator?" Archives of Biochemistry and Biophysics **211**: 750-761.
Rajamanickam, C., S. Sakthivel, et al. (1998). "A novel serum protein of molecular weight 182 kDa: a molecular marker for an early detection of increased left ventricular mass in patients with cardiac hypertrophy." J Cardiovasc Risk **5**(5-6): 335-338.

Rajasekaran, N. S., P. Connell, et al. (2007). "Human alpha B-crystallin mutation causes oxido-reductive stress and protein aggregation cardiomyopathy in mice." Cell **130**(3): 427-439.

Rakhit, R., P. Cunningham, et al. (2002). "Oxidation-induced misfolding and aggregation of superoxide dismutase and its implications for amyotrophic lateral sclerosis." J Biol Chem **277**(49): 47551-47556.

Ramasamy, S., R. Omnath, et al. (2006). "Cardiac isoform of alpha 2 macroglobulin, an early diagnostic marker for cardiac manifestations in AIDS patients." AIDS **20**(15): 1979-1981.

Rampoldi, L., G. Caridi, et al. (2003). "Allelism of MCKD, FJHN and GCKD caused by impairment of uromodulin export dynamics." Hum Mol Genet **12**(24): 3369-3384.

Ranoa, D. R., S. L. Kelley, et al. (2013). "Human lipopolysaccharide-binding protein (LBP) and CD14 independently deliver triacylated lipoproteins to Toll-like receptor 1 (TLR1) and TLR2 and enhance formation of the ternary signaling complex." J Biol Chem **288**(14): 9729-9741.

Rao, R. V., K. Niazi, et al. (2006). "Coupling endoplasmic reticulum stress to the cell-death program: a novel HSP90-independent role for the small chaperone protein p23." Cell Death Differ **13**(3): 415-425.

Rathinavel, A., P. S. Dhandapany, et al. (2005). "Cardiac isoform of alpha-2 macroglobulin as a novel diagnostic marker for cardiac diseases." Eur J Cardiovasc Prev Rehabil **12**(6): 601-603.

Reddy, V. Y., P. E. Desorchers, et al. (1994). "Oxidative dissociation of human alpha 2-macroglobulin tetramers into dysfunctional dimers." J Biol Chem **269**(6): 4683-4691.

Reddy, V. Y., S. V. Pizzo, et al. (1989). "Functional inactivation and structural disruption of human alpha 2-macroglobulin by neutrophils and eosinophils." J Biol Chem **264**(23): 13801-13809.

Reuning, U., Magdolen, V., Wilhelm, O., Fisher, K., Lutz, V., Graeff, H. and Schmitt, M. (1998). " Multifunctional potential of the plasminogen activation system in tumor invasion and metastasis (review)." International Journal of Oncology **13**: 893-906.

Roberts, K., R. Zeineddine, et al. (2013). "Extracellular aggregated Cu/Zn superoxide dismutase activates microglia to give a cytotoxic phenotype." Glia **61**(3): 409-419.

Robinson, J. J., F. Watson, et al. (1993). "Activation of neutrophils by soluble and insoluble immunoglobulin aggregates from synovial fluid of patients with rheumatoid arthritis." Ann Rheum Dis **52**(5): 347-353.

Roche, P. A. and S. V. Pizzo (1987). "Characterization of alpha 2-macroglobulin-plasmin complexes: complete subunit cleavage alters receptor recognition in vivo and in vitro." Biochemistry **26**(2): 486-491.

Roche, P. A. and S. V. Pizzo (1988). "Analysis of thiolester bond cleavage-dependent conformational changes in binary alpha 2-macroglobulin-proteinase complexes." Arch Biochem Biophys **267**(1): 285-293.

Roche, P. A., G. S. Salvesen, et al. (1988). "Symmetry of the inhibitory unit of human alpha 2-macroglobulin." Biochemistry **27**(20): 7876-7881.

Rosenberg, M. E., R. Girton, et al. (2002). "Apolipoprotein J/clusterin prevents a progressive glomerulopathy of aging." Mol Cell Biol **22**(6): 1893-1902.

Rosenberg, M. E., R. Girton, et al. (2002). "Apolipoprotein J/clusterin prevents progressive glomerulopathy of aging." Molecular Cell Biology **22**: 1893-1902.

Ross, C. A. and M. A. Poirier (2005). "Opinion: What is the role of protein aggregation in neurodegeneration?" Nat Rev Mol Cell Biol **6**(11): 891-898.

Rubenstein, D. S., I. B. Thogersen, et al. (1993). "Identification of monomeric alpha-macroglobulin proteinase inhibitors in birds, reptiles, amphibians and mammals, and

purification and characterization of a monomeric alpha-macroglobulin proteinase inhibitor from the American bullfrog Rana catesbeiana." Biochem J **290 (Pt 1)**: 85-95.
Salles, F. J. and S. Strickland (2002). "Localization and regulation of the tissue plasminogen activator-plasmin system in the hippocampus." J Neurosci **22**(6): 2125-2134.
Samson, A. L., R. J. Borg, et al. (2009). "A nonfibrin macromolecular cofactor for tPA-mediated plasmin generation following cellular injury." Blood **114**(9): 1937-1946.
Samson, A. L., A. S. Knaupp, et al. (2012). "Nucleocytoplasmic coagulation: an injury-induced aggregation event that disulfide crosslinks proteins and facilitates their removal by plasmin." Cell Rep **2**(4): 889-901.
Sanchez, M. C., J. D. Luna, et al. (2007). "Effect of retinal laser photocoagulation on the activity of metalloproteinases and the alpha(2)-macroglobulin proteolytic state in the vitreous of eyes with proliferative diabetic retinopathy." Exp Eye Res **85**(5): 644-650.
Sastre, M., T. Klockgether, et al. (2006). "Contribution of inflammatory processes to Alzheimer's disease: molecular mechanisms." Int J Dev Neurosci **24**(2-3): 167-176.
Saunders, R., B. J. Dyce, et al. (1971). "The separation of alpha-2 macroglobulin into five components with differing electrophoretic and enzyme-binding properties." J Clin Invest **50**(11): 2376-2383.
Schaiff, W. T. and P. R. Eisenberg (1997). "Direct induction of complement activation by pharmacologic activation of plasminogen." Coron Artery Dis **8**(1): 9-18.
Schiesser, M., D. Bimmler, et al. (2001). "Conformational changes of pancreatitis-associated protein (PAP) activated by trypsin lead to insoluble protein aggregates." Pancreas **22**(2): 186-192.
Schreiber, G., G. Howlett, et al. (1982). "The acute phase response of plasma protein synthesis during experimental inflammation." J Biol Chem **257**(17): 10271-10277.
Schubert, U., Anton, L.C., Gibbs, J., Norbury, C.C., Yewdell, J.W. and Bennink, J.R. (2000). "Rapid degeneration of a large fraction of newly synthesised proteins by proteasomes." Nature **404**: 770-774.
Senior, J., C. Delgado, et al. (1991). "Influence of surface hydrophobicity of liposomes on their interaction with plasma protein and clearance from the circulation: studies with poly(ethylene glycol)-coated vesicles." Biochimica Biophys Acta **1062**: 77-82.
Shamu, C. E. (1998). "Splicing: HACking into the unfolded-protein response." Current Biology **8**: R121-R123.
Shanbhag, V. P., T. Stigbrand, et al. (1996). "The conformational state of human alpha 2-macroglobulin influences its dissociation into half-molecules by sodium thiocyanate." Arch Biochem Biophys **333**(1): 35-41.
Shibata, M., S. Yamada, et al. (2000). "Clearance of Alzheimer's amyloid-ss(1-40) peptide

from brain by LDL receptor–related protein-1

at the blood-brain barrier." Journal of Clinical Investigation **106**: 1489-1499.
Shultz, L. D., D. R. Coman, et al. (1987). "Development of plasmacytoid cells with Russell bodies in autoimmune "viable motheaten" mice." Am J Pathol **127**(1): 38-50.
Siao, C., Fernandez, S.R. and Tsirka, S.E. (2003). "Cell Type-Specific Roles for Tissue Plasminogen Activator Released by Neurons or Microglia after Excitotoxic Injury." The Journal of Neuroscience **23**: 3234-3242.
Siao, C. J. and S. E. Tsirka (2002). "Extracellular proteases and neuronal cell death." Cell Mol Biol (Noisy-le-grand) **48**(2): 151-161.
Sipe, J. D. (1994). "Amyloidosis." Critical Review of Clinical Laboratory Science **31**: 325-354.

Sixt, S. U. and B. Dahlmann (2008). "Extracellular, circulating proteasomes and ubiquitin - incidence and relevance." Biochim Biophys Acta **1782**(12): 817-823.

Sjoberg, B., S. Pap, et al. (1992). "Temperature dependence of the kinetics of the urea-induced dissociation of human plasma alpha 2-macroglobulin into half-molecules. A minimum rate at 15 degrees C indicates hydrophobic interaction between the subunits." J Mol Biol **225**(2): 551-556.

Song, H. K. and S. W. Suh (1998). "Kunitz-type soybean trypsin inhibitor revisited: refined structure of its complex with porcine trypsin reveals an insight into the interaction between a homologous inhibitor from Erythrina caffra and tissue-type plasminogen activator." J Mol Biol **275**(2): 347-363.

Soti, C. and P. Csermely (2003). "Aging and molecular chaperones." Exp Gerontol **38**(10): 1037-1040.

Soto, C., E. M. Sigurdsson, et al. (1998). "Beta-sheet breaker peptides inhibit fibrillogenesis in a rat brain model of amyloidosis: implications for Alzheimer's therapy." Nat Med **4**(7): 822-826.

Sottrup-Jensen, L. (1989). "Alpha-macroglobulins: structure shape and mechanism of proteinase complex formation." The Journal of Biological Chemistry **264**: 11539-11542.

Squier, T. C. (2001). "Oxidative stress and protein aggregation during biological aging." Exp Gerontol **36**(9): 1539-1550.

Stamp, L. K., I. Khalilova, et al. (2012). "Myeloperoxidase and oxidative stress in rheumatoid arthritis." Rheumatology (Oxford) **51**(10): 1796-1803.

Stansley, B., J. Post, et al. (2012). "A comparative review of cell culture systems for the study of microglial biology in Alzheimer's disease." J Neuroinflammation **9**: 115.

Stefani, M. and C. M. Dobson (2003). "Protein aggregation and aggregate toxicity: new insights into protein folding, misfolding diseases and biological evolution." Journal of Molecular Medicine **81**: 678-699.

Steinbeck, M. J., L. J. Nesti, et al. (2007). "Myeloperoxidase and chlorinated peptides in osteoarthritis: potential biomarkers of the disease." J Orthop Res **25**(9): 1128-1135.

Stewart, C. R., A. A. Tseng, et al. (2005). "Oxidation of low-density lipoproteins induces amyloid-like structures that are recognized by macrophages." Biochemistry **44**(25): 9108-9116.

Stirling, P. C., Lundin, V.F. and Leroux, M.R. (2003). "Getting a grip on non-native proteins." European Molecular Biology Organization Reports **4**: 565-570.

Stoffels, J. M., J. C. de Jonge, et al. (2013). "Fibronectin aggregation in multiple sclerosis lesions impairs remyelination." Brain **136**(Pt 1): 116-131.

Stranks, S. D., H. Ecroyd, et al. (2009). "Model for amorphous aggregation processes." Phys Rev E Stat Nonlin Soft Matter Phys **80**(5 Pt 1): 051907.

Streit, W. J., J. R. Conde, et al. (2005). "Role of microglia in the central nervous system's immune response." Neurol Res **27**(7): 685-691.

Suenson, E. and L. C. Petersen (1986). "Fibrin and plasminogen structures essential to stimulation of plasmin formation by tissue-type plasminogen activator." Biochimica et Biophysica Acta (BBA) - Protein Structure and Molecular Enzymology **870**(3): 510-519.

Sutton, R., M. E. Keohane, et al. (1994). "Plasminogen activator inhibitor-1 in the cerebrospinal fluid as an index of neurological disease." Blood Coagul Fibrinolysis **5**(2): 167-171.

Swash, M. (2013). "How does ALS spread between neurones in the CNS?" J Neurol Neurosurg Psychiatry **84**(1): 116-117.

Tabner, B. J., O. M. El-Agnaf, et al. (2005). "Protein aggregation, metals and oxidative stress in neurodegenerative diseases." Biochem Soc Trans **33**(Pt 5): 1082-1086.
Tabner, B. J., J. Mayes, et al. (2010). "Hypothesis: soluble abeta oligomers in association with redox-active metal ions are the optimal generators of reactive oxygen species in Alzheimer's disease." Int J Alzheimers Dis **2011**: 546380.
Tabrizi, P., Wang, L., Seeds, N., McComb, J.G., Yamada, S., Griffin, J.H., Carmeliet, P., Weiss, M.H. and Zlokovic, B.V. (1999). "Tissue Plasminogen Activator (tPA) Deficiency Exacerbates Cerebrovascular Fibrin Deposition and Brain Injury in a Murine Stroke Model: Studies In tPA-Deficient Mice and Wild-Type Mice on a Matched Genetic Background." Arteriosclerosis, Thrombosis, and Vascular Biology **19**: 2801-2806.
Takada, T., Y. Kodera, et al. (2013). "Serum monomeric alpha2-macroglobulin as a clinical biomarker in diabetes." Atherosclerosis **228**(1): 270-276.
Tan, J. M. M., Wong, E.S.P. and Lim, K. (2009). "Protein Misfolding and Aggregation in Parkinson's Disease." Antioxidants and Redox Signaling **11**: 2119-2134.
Taylor, J. P., Hardy, J. and Fischbeck, K.H. (2002). "Toxic Proteins in Neurodegenerative Disease." Science **296**: 1991-1995.
Teesalu, T., A. Kulla, et al. (2004). "Tissue plasminogen activator and neuroserpin are widely expressed in the human central nervous system." Thromb Haemost **92**(2): 358-368.
Tennstaedt, A., S. Popsel, et al. (2012). "Human high temperature requirement serine protease A1 (HTRA1) degrades tau protein aggregates." J Biol Chem **287**(25): 20931-20941.
Truebestein, L., A. Tennstaedt, et al. (2011). "Substrate-induced remodeling of the active site regulates human HTRA1 activity." Nat Struct Mol Biol **18**(3): 386-388.
Truscott, R. J. (2005). "Age-related nuclear cataract-oxidation is the key." Exp Eye Res **80**(5): 709-725.
Tschopp, J., A. Chonn, et al. (1993). "Clusterin, the human apolipoprotein and complement Inhibitor, binds to complement C7, C8beta, and the b Domain of C9." The Journal of Immunology **151**(4): 2159-2165.
Tsirka, S., Gualandris, A., Amaral, D.G. and Strickland, S. (1995). "Excitotoxin-induced neuronal degeneration and seizure are mediated by tissue Plasminogen activator." Nature **377**: 340-344.
Tsirka, S. E., A. D. Rogove, et al. (1997). "An extracellular proteolytic cascade promotes neuronal degeneration in the mouse hippocampus." J Neurosci **17**(2): 543-552.
Tsujimura, A., K. Taguchi, et al. (2014). "Lysosomal enzyme cathepsin B enhances the aggregate forming activity of exogenous alpha-synuclein fibrils." Neurobiol Dis **73C**: 244-253.
Tucker, H. M., Kihiko-Ehmann, M., Wright, S., Rydel, R.E. and Estus, S. (2000). "Tissue Plasminogen Activator Requires Plasminogen to Modulate Amyloid-β Neurotoxicity and Deposition." Journal of Neurochemistry **75**: 2172-2177.
Tucker, H. M., M. Kihiko, et al. (2000). "The plasmin system is induced by and degrades amyloid-beta aggregates." J Neurosci **20**(11): 3937-3946.
Uesugi, M., K. Yoshida, et al. (2000). "Inflammatory properties of IgG modified by oxygen radicals and peroxynitrite." J Immunol **165**(11): 6532-6537.
Urano, T., Y. Takada, et al. (1991). "Stimulation of the amidolytic activity of single chain tissue-type plasminogen activator by fibrinogen degradation products: possible fibrin binding sites on single chain tissue-type plasminogen activator molecule." Biochimica et Biophysica Acta (BBA) - Protein Structure and Molecular Enzymology **1077**(3): 245-252.

van Gool, J., H. van Vugt, et al. (1990). "Alpha 2-macroglobulin and fibrinogen modulate inflammatory edema in man." Inflammation **14**(3): 275-283.

van Zonneveld, A., Veerman, H. and Pannekoek, H. (1986). "On the Interaction of the Finger and the Kringle-2 Domain of Tissue-type Plasminogen Activator with Fibrin." The Journal of Biological Chemistry **261**: 14214-14218.

Vassalli, J., Sappino, A. and Belin, D. (1991). "The Plasminogen Activator/Plasmin System." The Journal of Clinical Investigation **88**: 1067-1072.

Verdier, Y., M. Zarandi, et al. (2004). "Amyloid beta-peptide interactions with neuronal and glial cell plasma membrane: binding sites and implications for Alzheimer's disease." J Pept Sci **10**(5): 229-248.

Vidair, C., R. Huang, and S. Doxsey (1996). "Heat shock causes protein aggregation and reduced protein solubility at the centrosome and other cytoplasmic locations." International Journal of Hyperthermia **12**: 681-695.

Vlasova, II, A. V. Sokolov, et al. (2011). "[Myeloperoxidase-induced biodegradation of single-walled carbon nanotubes is mediated by hypochlorite]." Bioorg Khim **37**(4): 510-521.

Walker, D. G. and L. F. Lue (2005). "Investigations with cultured human microglia on pathogenic mechanisms of Alzheimer's disease and other neurodegenerative diseases." J Neurosci Res **81**(3): 412-425.

Walsh, D. M., I. Klyubin, et al. (2002). "Naturally Secreated Oligomers of Amyloid B Protein Potently Inhibited Hippocampal Long-Term Potentiation in vivo." Nature **416**: 535-539.

Wang, J., G. Xu, et al. (2002). "High molecular weight complexes of mutant superoxide dismutase 1: age-dependent and tissue-specific accumulation." Neurobiol Dis **9**(2): 139-148.

Wardman, P. (2008). "Methods to measure the reactivity of peroxynitrite-derived oxidants toward reduced fluoresceins and rhodamines." Methods Enzymol **441**: 261-282.

Weiner, H. L. and D. Frenkel (2006). "Immunology and immunotherapy of Alzheimer's disease." Nat Rev Immunol **6**(5): 404-416.

Weiss, S. J. (1989). "Tissue destruction by neutrophils." N Engl J Med **320**(6): 365-376.

West, M., M. Mhatre, et al. (2004). "The arachidonic acid 5-lipoxygenase inhibitor nordihydroguaiaretic acid inhibits tumor necrosis factor alpha activation of microglia and extends survival of G93A-SOD1 transgenic mice." J Neurochem **91**(1): 133-143.

West, M. D., J. W. Shay, et al. (1996). "Altered expression of plasminogen activator and plasminogen activator inhibitor during cellular senescence." Exp Gerontol **31**(1-2): 175-193.

White, R., A. Janoff, et al. (1980). "Secretion of Alpha-2-macroglobulin by human alveolar macrophages." Lung **158**(1): 9-14.

Wilson, M., J. Yerbury, et al. (2008). "Potential roles of abundant extracellular chaperones in the control of amyloid formation and toxicity." Molecular Biosystems **4**: 42-52.

Wilson, M. R. and S. B. Easterbrook-Smith (1992). "Clusterin binds by a multivalent mechanism to the Fc and Fab regions of IgG." Biochimica et Biophysica Acta **1159**: 319-326.

Wilson, M. R., J. Yerbury, et al. (2008). Extracellular chaperones and amyloids. Heat Shock Proteins and the Brain: Implications for Neurodegenerative Diseases and Neuroprotection. A. Asea and I. Brown, Springer Science**:** 283-315.

Wiman, B. and P. Wallen (1977). "The specific interaction between plasminogen and fibrin. A physiological role of the lysine binding site in plasminogen." Thromb Res **10**(2): 213-222.

Winterbourn, C. C. (2014). "The challenges of using fluorescent probes to detect and quantify specific reactive oxygen species in living cells." Biochim Biophys Acta **1840**(2): 730-738.
Wu, H. L., G. Y. Shi, et al. (1987). "Preparation and purification of microplasmin." Proc Natl Acad Sci U S A **84**(23): 8292-8295.
Wu, S. M. and S. V. Pizzo (2001). "alpha(2)-Macroglobulin from rheumatoid arthritis synovial fluid: functional analysis defines a role for oxidation in inflammation." Arch Biochem Biophys **391**(1): 119-126.
Wyatt, A., J. Yerbury, S. Poon, and M. Wilson (2009). "Novel therapeutic targets in protein deposition diseases." Current Medicinal Chemistry **16**: 2855-2866.
Wyatt, A., J. Yerbury, et al. (2010). "Discovery of a novel system for extracellular proteostasis." submitted to Nature.
Wyatt, A., J. Yerbury, et al. (2009). "Novel therapeutic targets in protein deposition diseases." Current Medicinal Chemistry **16**: 2855-2866.
Wyatt, A., J. Yerbury, et al. (2009). "Novel therapeutic targets in protein deposition diseases." Current Medicinal Chemistry **16**: 2855-2866.
Wyatt, A. R., P. Constantinescu, et al. (2013). "Protease-activated alpha-2-macroglobulin can inhibit amyloid formation via two distinct mechanisms." FEBS Lett **587**(5): 398-403.
Wyatt, A. R., J. R. Kumita, et al. (2014). "Hypochlorite-induced structural modifications enhance the chaperone activity of human alpha2-macroglobulin." Proc Natl Acad Sci U S A **111**(20): E2081-2090.
Wyatt, A. R., J. J. Yerbury, et al. (2011). "Clusterin facilitates in vivo clearance of extracellular misfolded proteins." Cell Mol Life Sci **68**(23): 3919-3931.
Wyatt, A. R., J. J. Yerbury, et al. (2013). "Extracellular chaperones and proteostasis." Annu Rev Biochem **82**: 295-322.
Wyatt, A. R., J. J. Yerbury, et al. (2009). "Structural characterization of clusterin-chaperone client protein complexes." J Biol Chem **284**(33): 21920-21927.
Wyatt, A. R., J. J. Yerbury, et al. (2009). "Structural characterization of clusterin-client protein complexes." The Journal of Biological Chemistry **284**(33): 21920-21927.
Wyatt, A. R., N. W. Zammit, et al. (2013). "Acute phase proteins are major clients for the chaperone action of alpha(2)-macroglobulin in human plasma." Cell Stress Chaperones **18**(2): 161-170.
Yamada, M. (2000). "Cerebral amyloid angiopathy: an overview." Neuropathology **20**(1): 8-22.
Yamamoto, K., K. Takeshita, et al. (2005). "Aging and plasminogen activator inhibitor-1 (PAI-1) regulation: implication in the pathogenesis of thrombotic disorders in the elderly." Cardiovasc Res **66**(2): 276-285.
Yang, W. Y. and M. Gruebele (2003). "Folding at the speed limit." Nature **423**: 193-197.
Yang, X., J. Hu, et al. (2010). "Polymorphisms in CFH, HTRA1 and CX3CR1 confer risk to exudative age-related macular degeneration in Han Chinese." Br J Ophthalmol **94**(9): 1211-1214.
Yang, Z., Z. Tong, et al. (2010). "Genetic and functional dissection of HTRA1 and LOC387715 in age-related macular degeneration." PLoS Genet **6**(2): e1000836.
Yepes, M. and D. A. Lawrence (2004). "New functions for an old enzyme: nonhemostatic roles for tissue-type plasminogen activator in the central nervous system." Exp Biol Med (Maywood) **229**(11): 1097-1104.
Yepes, M., Roussel, B.D., Ali, C. and Vivien, D. (2008). "Tissue-type plasminogen activator in the ischemic brain: more than a thrombolytic." Trends in Neurosciences **32**: 48-55.

Yerbury, J. J., J. R. Kumita, et al. (2009). "Alpha 2 macroglobulin and haptoglobin supress amyloid formation by interacting with prefibrillar protien species." The Journal of Biological Chemistry **284**(7): 4246-4254.

Yerbury, J. J., Kumita, J.R., Meehan, S., Dobson, C.M. and Wilson, M.R. (2009). "α2-Macroglobulin and Haptoglobulin Supress Amyloid Formation by Interacting with Prefibrillar Protein Species." The Journal of Biological Chemistry **284**: 4246-4254.

Yerbury, J. J., S. Poon, et al. (2007). "The extracellular chaperone clusterin influences amyloid formation and toxicity by interacting with pre-fibrillar structures." The FASEB Journal **21**: 2312-2322.

Yerbury, J. J., M. S. Rybchyn, et al. (2005). "The acute phase protein haptoglobin is a mammalian extracellular chaperone with an action similar to clusterin." Biochemistry **44**: 10914-10925.

Yerbury, J. J., E. M. Stewart, et al. (2005). "Quality control of protein folding in extracellular space." European Molecular Biology Organization Reports **6**(12): 1131-1136.

Zammit, N. (2009). "“Investigating the function of alpha-2-macroglobulin as a molecular chaperone”." Honours thesis, School of Biological Sciences, University of Wollongong.

Zamzami, N., P. Marchetti, et al. (1995). "Sequential reduction of mitochondrial transmembrane potential and generation of reactive oxygen species in early programmed cell death." J Exp Med **182**(2): 367-377.

Zhabin, S. G. and N. A. Zorin (1995). "[Concentration of plasmin complexes with alpha-2-macroglobulin and alpha-2-antiplasmin in blood plasma and serum]." Klin Lab Diagn(4): 43-44.

Zhabin, S. G., N. A. Zorin, et al. (1995). "[The effect of plasmin and its complexes with alpha 2-antiplasmin and alpha 2-macroglobulin on secretion of proteinase and plasminogen inhibitors from peripheral mononuclear cells]." Vopr Med Khim **41**(3): 34-37.

Zhang, L., R. Sheng, et al. (2009). "The lysosome and neurodegenerative diseases." Acta Biochim Biophys Sin (Shanghai) **41**(6): 437-445.

Zhang, S. J., M. Zou, et al. (2009). "Nuclear calcium signaling controls expression of a large gene pool: identification of a gene program for acquired neuroprotection induced by synaptic activity." PLoS Genet **5**(8): e1000604.

Zhang, W., T. Wang, et al. (2005). "Aggregated alpha-synuclein activates microglia: a process leading to disease progression in Parkinson's disease." FASEB J **19**(6): 533-542.

Zmijewski, J. W., D. R. Moellering, et al. (2005). "Oxidized LDL induces mitochondrially associated reactive oxygen/nitrogen species formation in endothelial cells." Am J Physiol Heart Circ Physiol **289**(2): H852-861.

Zoeger, A., M. Blau, et al. (2006). "Circulating proteasomes are functional and have a subtype pattern distinct from 20S proteasomes in major blood cells." Clin Chem **52**(11): 2079-2086.